การประยุกต์ข้อมูลธรณีฟิสิกส์ทางอากาศและข้อมูลการรับรู้ระยะไกลเพื่อการตีความสภาพทางธรณีวิทยาในพื้นที่จังหวัดน่าน-อุตรดิตถ์ ภาคเหนือของประเทศไทย

นางสาววิวรรณ ฤทธิสิทธิ์

วิทยานิพนธ์นี้เป็นส่วนหนึ่งของการศึกษาตามหลักสูตรปริญญาวิทยาศาสตรมหาบัณฑิต
สาขาวิชาธรณีวิทยา ภาควิชาธรณีวิทยา
คณะวิทยาศาสตร์ จุฬาลงกรณ์มหาวิทยาลัย
ปีการศึกษา 2554

APPLICATION OF AIRBORNE GEOPHYSICAL AND REMOTE SENSING DATA TO THE INTERPRETATION OF GEOLOGIC SETTING IN NAN-UTTARADIT AREA, NORTHERN THAILAND

Miss Rawiwan Rittisit

A Thesis Submitted in Partial Fulfillment of the Requirements

for the Degree of Master of Science Program in Geology

Department of Geology

Faculty of Science

Chulalongkorn University

Academic Year 2011

Thesis Title	APPLICATION OF AIRBORNE GEOPHYSICAL AND REMOTE SENSING DATA TO THE INTERPRETATION OF GEOLOGIC SETTING IN NAN-UTTARADIT AREA, NORTHERN THAILAND
By	Miss Rawiwan Rittisit
Field of Study	Geology
Thesis Advisor	Associate Professor Punya Charusiri, Ph.D.
Thesis Co-advisor	Thanop Thitimakorn, Ph.D.

Accepted by the Faculty of Science, Chulalongkorn University in Partial Fulfillment of the Requirements for the Master's Degree

…….. Dean of the Faculty of Science
(Professor Supot Hannongbua, Dr. rer. nat.)

THESIS COMMITTEE

…….. Chairman
(Associate Professor Montri Choowong, Ph.D.)

…….. Thesis Advisor
(Associate Professor Punya Charusiri, Ph.D.)

…….. Thesis Co-advisor
(Thanop Thitimakorn, Ph.D.)

…….. External Examiner
(Kachentra Neawsuparp, Ph.D.)

รวิวรรณ ฤทธิสิทธิ์ : การประยุกต์ข้อมูลธรณีฟิสิกส์ทางอากาศและข้อมูลการรับรู้ระยะไกลเพื่อตีความสภาพทางธรณีวิทยาในพื้นที่จังหวัดน่าน-อุตรดิตถ์ ภาคเหนือของประเทศไทย. (Application of Airborne Geophysical and Remote Sensing Data to the Interpretation of Geologic Setting in Nan-Uttaradit Area, Northern Thailand) อ. ที่ปรึกษาวิทยานิพนธ์หลัก : รศ.ดร. ปัญญา จารุศิริ , อ.ที่ปรึกษาวิทยานิพนธ์ร่วม ดร. ฐานบ ฐิติมากร 210 หน้า.

การสำรวจธรณีฟิสิกส์ทางอากาศและการแปลความหมายระยะไกลมีจุดประสงค์เพื่ออธิบายโครงสร้างใต้ดินของบริเวณน่าน-อุตรดิตถ์ โดยข้อมูลแม่เหล็กทางอากาศ รวมกับข้อมูลจากการรับรู้ระยะไกล และทำการปรับปรุงข้อมูลด้วยวิธีการ RTP, analytical signal, automatic gain control, vertical derivative, upward และdownward continuation ส่วนข้อมูลกัมมันตรังสีทางอากาศได้มีวิธีการศึกษาโดยวิธีผสมสี และข้อมูลการรับรู้ระยะไกลด้วยวิธีผสมแบนด์และ Principal Component Analysis จากการศึกษาได้มีการจำแนกพื้นที่ศึกษาออกเป็น 3 ส่วน โดยใช้ รูปแบบ รูปทรง และค่าความเข้มของข้อมูล และการแปลความหมายระยะไกล ได้เป็น ส่วนเหนือ กลาง และใต้ ส่วนกลางมีลักษณะการวางตัวโครงสร้างแนวตะวันออกเฉียงเหนือ-ตะวันตกเฉียงใต้ เป็นบริเวณแคบอยู่บริเวณแม่น้ำน่าน ส่วนกลางมีค่าความเป็นแม่เหล็กสูง ความเข้มของกัมมันตรังสีต่ำ ล้อมรอบด้วยบริเวณที่มีความเป็นแม่เหล็กต่ำ ความเข้มของกัมมันตรังสีสูง ส่วนทางเหนือและทางใต้มีการวางตัวในแนวเหนือ-ใต้ แสดงลักษณะความเป็นแม่เหล็กต่ำ และค่าความเข้มของ กัมมันตรังสีกระจัดกระจาย พื้นที่ทางด้านเหนือยังความแตกต่างจากทางใต้ในทางธรณีวิทยาอีกด้วย ส่วนความแตกต่างความเข้มสนามแม่เหล็กในแต่ละพื้นที่ สามารถแบ่งแยกได้เป็น 2 ลักษณะ คือ ลักษณะวงรีที่ถูกดึงยืด พบบริเวณแม่น้ำน่าน วางตัวในแนวตะวันออกเฉียงเหนือ-ตะวันตกเฉียงใต้ มีค่าความเป็นแม่เหล็กสูงแต่ความเข้มของกัมมันตรังสีต่ำ ลักษณะวงกลม พบในบริเวณเหนือสุดของพื้นที่ซึ่งค่าความเป็นแม่เหล็กต่ำ หลังจากการใช้โปรแกรมศึกษาในสามมิติ สามารถระบุการวางตัวของค่าความผิดปกติ แสดงการเอียงเทไปทางตะวันออก จากศิลาวิทยาเคมี และการสำรวจธรณีวิทยาภาคสนามที่มีมาก่อน บ่งบอกว่าตะเข็บธรณีน่าน มีการเกิดในบริเวณหมู่เกาะโค้ง และไม่ได้เกิดจากการชนกันของแผ่นทวีป ซึ่งให้หินสีเข้มและสีเข้มมากที่มีองค์ประกอบของโครเมียน สปิเนลซึ่งจากการศึกษาศิลาวิทยาเคมี พบว่าเกิดจากการมุดตัวของแผ่นมหาสมุทรกับแผ่นมหาสมุทรในทิศตะวันออก ได้แสดงให้เห็นในภาพตัดขวางทางธรณีฟิสิกส์ในการศึกษาครั้งนี้ ดังนั้นจึงเป็นอีกหลักฐานหนึ่งซึ่งยืนยันว่ารอยตะเข็บธรณีน่าน มีความต่อเนื่องไปทางตะวันออกเฉียงเหนือสู่ประเทศลาว

ภาควิชา ธรณีวิทยา ลายมือชื่อนิสิต.....

สาขาวิชา ธรณีวิทยา ลายมือชื่อ อ.ที่ปรึกษาวิทยานิพนธ์หลัก.....

ปีการศึกษา 2554 ลายมือชื่อ อ.ที่ปรึกษาวิทยานิพนธ์ร่วม.....

5172573623 : MAJOR GEOLOGY

KEYWORDS : Airborne Geophysics / Nan Suture / Tectonic / Remote Sensing Data

RAWIWAN RITTISIT : APPLICATION OF AIRBORNE GEOPHYSICAL AND REMOTE SENSING DATA TO THE INTERPRETATION OF GEOLOGIC SETTING IN NAN-UTTARADIT AREA, NORTHERN THAILAND. ADVISOR : ASSOC. PROF PUNYA CHARUSIRI, Ph.D., THANOP THITIMAKORN, Ph.D., 210 pp.

This investigation is aimed to reprocess airborne geophysical and remote sensing data for interpreting subsurface structures in the Nan-Uttaradit area.

Airborne magnetic data in conjunction with remote sensing and EM data have been enhanced using various techniques. This study applies that RTP, ANA, AGC, vertical derivative, upward and downward continuation, for interpretation. Airborne radiometric data processed by Cooking Technique and Remote sensing data by Band Combination and Principle Component Analysis Technique.

Three domains have been identified, namely northern, central and southern domain. The central domain is a significant highly anomalous NE-SW trending narrow zone situating within the Nan River Basin. This domain possesses high magnetic and low radiometric intensities. The central high magnetic domain is enveloped by very low magnetic and high radiometric intensities referred as the north and south domains, both of which orient in the N-S direction and they generally exhibit the low magnetic and various radiometric intensities with the sporadic high magnetic patterns. The northern domain is quite different from the southern domain, suggesting contrast in the geology.

The high magnetic anomalies in each domain have been recognized in 2 patterns, elongate pattern located mainly along the Nan River in the NE-SW direction with high magnetic and low radiometric intensities, and circular pattern located in the northernmost area with low magnetic anomalies zone in southern part area. After using magnetic modeling program to identify polarity of magnetic bodies, their patterns show the well-defined east-dipping direction.

After validation with previous petrochemical and field investigations, it is quite reliable that the Nan suture formed in island-arc system, not by the continental collision setting as previously thought. The occurrence of island arc-type mafic/ultramafic rocks and their associated chromian spinels suggest an eastward ocean-ocean subduction that is consistent with the present geophysical model. Therefore, it is ascertained that the Nan suture zone can be well delineated and definitely extends northeastward to the Lao PDR.

Department : Geology Student's Signature .....

Field of Study : Geology Advisor's Signature .....

Academic Year : 2011 Co-advisor's Signature .....

ACKNOWLEDGEMENTS

Foremost, I would like to express my sincere gratitude to my advisor Prof. Dr. Punya Charusiri for his support of my research study and for his patience, motivation, enthusiasm, and immense knowledge. His guidance helped me in all the time of research and writing of this thesis.

Besides my advisor, I would like to thank my Co-Advisor Dr. Thanop Thitimakorn and the rest of committee for their encouragement, insightful comments, and crucial questions.

My sincere thanks also go to Dr. Kachentra Neawsuparp and Mr. Adichart Paiyarom, who both are the senior geologists for supporting the data and assistance during the processing at Department of Mineral Resources.

This research project has been supported by the Chulalongkorn Research Fund under the title of “Nan Project”.

Last but not the least, I would like to thank my family, my parents, my sister and my beloved grandmother for physical and mental supporting me throughout my life.

CONTENTS

LIST OF TABLE

LIST OF FIGURES

Chapter I Introduction

1.1 General backgrounds

Nan suture is located in northern Thailand between Nan and Uttaradit provinces (Figure 1.1). It is a complex zone with intricate geology and structures. Nan suture is first mentioned by a pioneer Thai geologist (Bunopas, 1981) to be a continent-continent collision between Shan-Thai and Indo-China blocks. Barr and Macdonald (1987) suggested that the Nan-River Suture zone consists of ophiolite suit dominated by ultramafic rocks. The zone formed in back-arc or inter-arc setting in Pre-Permian age. Panjasawatwong (1991) studied chromian spinel in this area and the spinel also indicated arc-related magma which was crystallized from highly refractory melt, probably generated in a suprasubduction zone. Singharajwarapan and Berry (2000) conclude that Nan Suture is a serpentinitic mélange, thrust slice, accretionary complex occurring during Late Permian. They also mentioned that the suture is an oceanic crust subduction with westward dipping.

Department of Mineral Resources (1988) has launched a nationwide airborne geophysical survey (magnetic, radiometric and electromagnetic surveys) and selected five potential areas including Nan-Uttaradit area (Figure 1.2). This survey is target to find anomalies related with the potential areas of mineral resources. The airborne geophysical interpretation is aimed to target potential mineral areas. In this study the purpose of this investigation is to use airborne geophysical data to interpret essential geological structures to clarify the understanding of tectonic settings along the Nan suture zone.

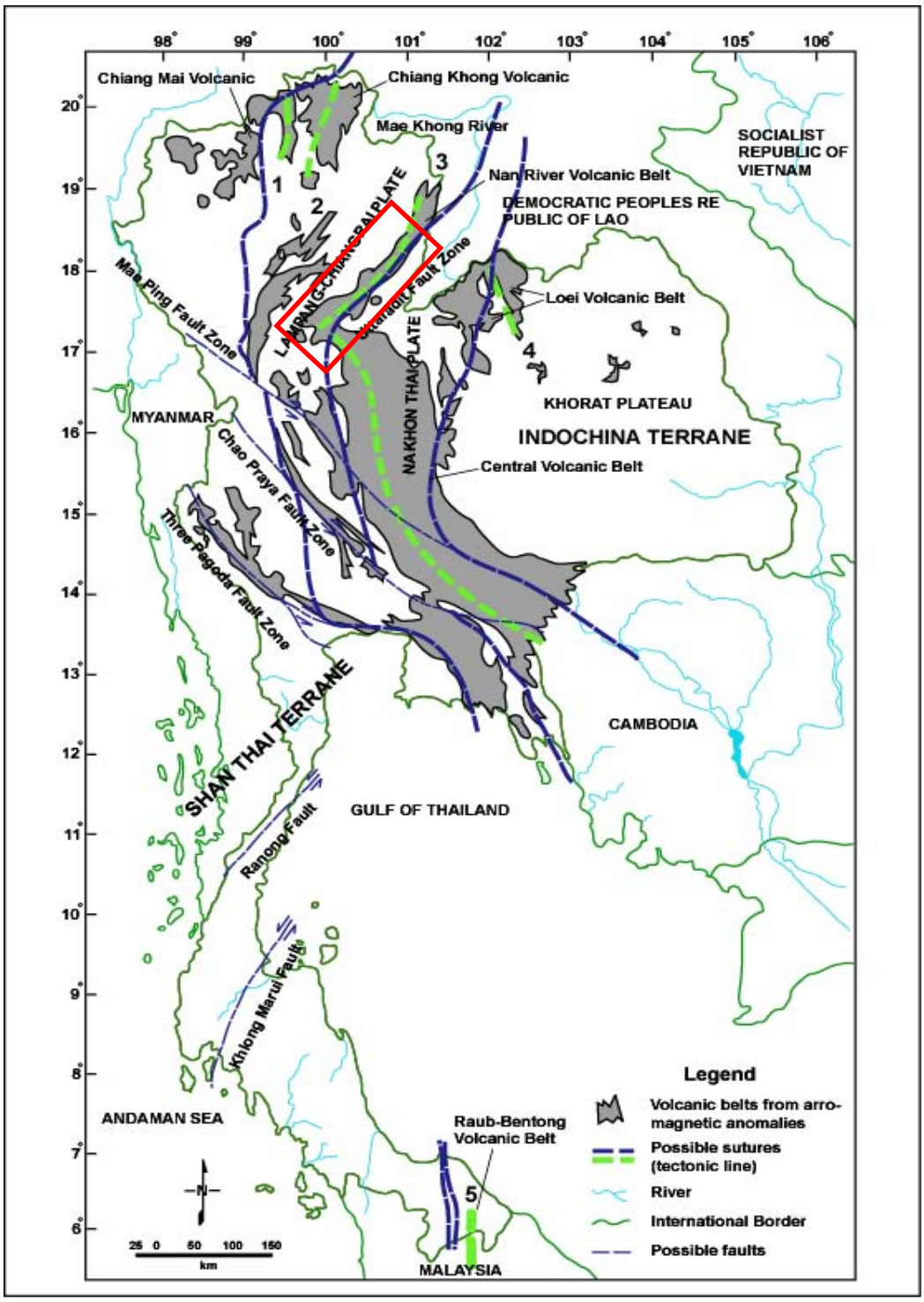

Figure 1.1 Tectonic map showing major tectonic blocks (or plates) and faults in Thailand (Modified after Tulyatid and Charusiri, 1999 and Charusiri et al., 2002).

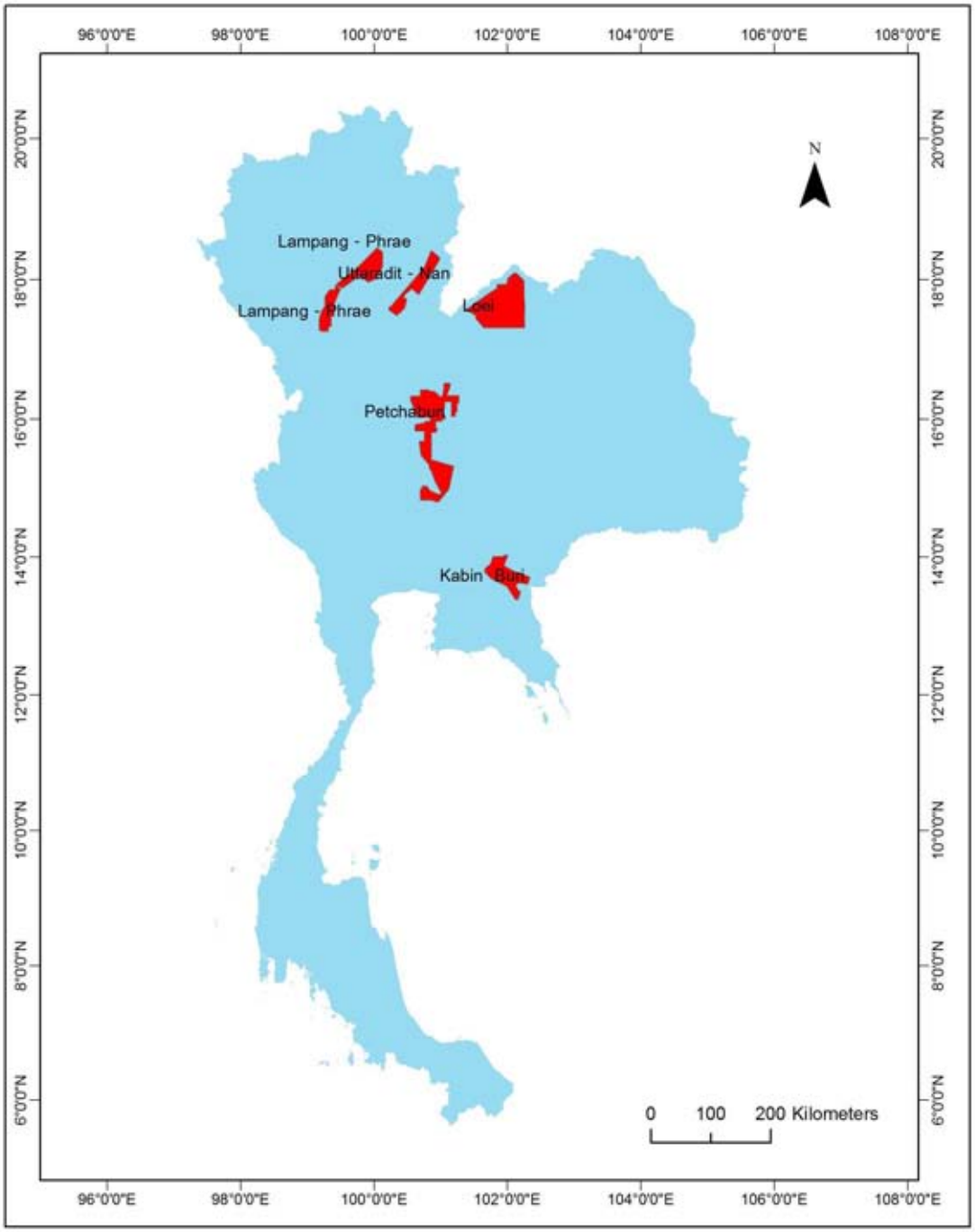

Figure 1.2 Map of Thailand showing 5 selected potential areas after launched nationwide airborne geophysical survey. Noted that the study area covers the so called "Uttaradit-Nan".

1.2 Previous works on the study area

1.2.1 Geology and Tectonic Setting

Nan and Uttaradit provinces are located (from west to east) between Shan Thai plate, Nan suture zone and Indochina plate. Local structures trend in NE-SW direction (Figure 1.1).

Chaodumrong (1994) reports that Nan suture consists of mafic and ultramafic igneous rocks occurred along the Nan River and extends from eastern part of Nan province to Sirikit Dam in Uttaradit province. Nan suture contacts with Paleozoic rocks in the western side and with Mesozoic rocks in the eastern side. Some parts of the Nan suture is covered by Mafic and Ultramafic Igneous rock (Serpentinite) and can be related to Changning-Shuangjiang Suture.

Barr and Macdonald (1987), Hutchison (1988) mention that in Pre-Permian, Shan-Thai plate attached with Gondwana, in Late Permian Shan-Thai plate has move against to Indochina plate, and in Late Triassic both were collided as shown by mafic and ultramafic obduction. After that transgression of the sea in Lampang and Nan basins as evident from the existence of marine and oceanic sediments in this area.

Sukvattananunt and Assavapatchara (1987) studied accretionary complex in the Sirikit Dam area and concluded that the collision during Late Triassic.

Singharajwarapan (1993) determined petrochemistry of basalt and suggested that basalts are formed after collision by intra-volcanism.

Panjasawatwong and Yaowanoiyothin (1993) studied chromian spinel of ultramafic rocks and purposed suprasubduction for the generation of those igneous rocks. Lunwongsa (2004) suggested that chromian spinels in mafic and ultramafic rocks in Nan-Uttaradit area are separated into 2 groups. The first group has been formed in suprasubduction zone and the second group formed in island arc setting.

1.2.2 Airborne Geophysics

Airborne geophysic survey in Nan-Uttaradit area was operated in 1988 by Department of Mineral Resources and Kenting Earth Science International Limited. Magnetic intensity were measured over area 1,740 square kilometer. The purpose is to find potential areas for mineral resources in Nan-Uttaradit provinces. Results show that there are 743 magnetic anomalies, from bed rock conductors, formation conductors, magnetic associated conductors and cultural conductors. But we only interested in 616 anomalies from bed rock conductors and magnetic associated conductors that could be related to mineral resources, targeted to detailed study (Kutthikul, 1988).

After finishing airborne magnetic survey, there are many follow-up field studies to identify what was affected to anomalies and to find potential area for detail study. Two areas of chromite prospects were found in Ban Had Ngew and Ban Huay Phung in Uttaradit province.

Dechawan (1992) operated ground survey exploration by using MaxMin-I EM magnetometer and Induced polarization in Sirikit dam area (Map Sheet 5144-IV). There are some potential areas for chromites, magnesite and talc were encountered in mafic and ultramafic rocks.

Neawsuparp (1997) applied airborne magnetic data with Landsat Thematic map to study relationship between structural geology and mineral occurrences in Uttaradit area nearby Sirikit Dam area.

1.2.3 Mineral Occurrences

Most of previous studies in Nan-Uttaradit area are aimed to find mineral potential areas. Important works are shown below.

Sekthera et al. (1978) studied geochemistry of rocks in southern part of Sirikit dam in Uttaradit province, by collecting stream samples for chemical analysis. They concluded that there are potentials of nickel and chromites

Surinkum and Siripongsatian (1992) made a detailed study of Khao Kee Nok area of Uttaradit province. They found occurrences of graphite deposits in Nan suture

and concluded that the graphite deposits were originated from sedimentary sequences subsequently deformed by contact metamorphism.

Pintawong (1998) studied economic geology which is in Nan-Uttaradit area and found potential of economic minerals (talc) at Ta-Pla, Uttaradit which is located lower part of the Nan River.

Yensabai (2002) mapped mineral potentials at a scale of 1:250,000 and most mineral occurrences are nickel and chromium in the central part of area and some Au-deposit was discovered in the upper part.

From previous mineralization studies, they made use of airborne geophysical data to locate the area of interest and for selecting areas for further detailed study. The interpretations of geophysical data almost aim to find structural anomalies that are spatially related to subsurface mineralization.

1.3 Purpose of study

This study is aimed to apply airborne geophysical data both magnetic data and radiometric data in combination with remote sensing data to analyze tectonic setting in this area. The interpreted data along with previous field and petrochemical investigations are also verified. Maps and sections of the interpreted results are also purposed.

1.4 Location and study area

The study area covers 19,400 sq km of Nan and Uttaradit provinces, northern Thailand location. It is between lat 17˚17” - 19˚33” N and long 99˚57” - 101˚18” E (As shown in Figure 1.3)

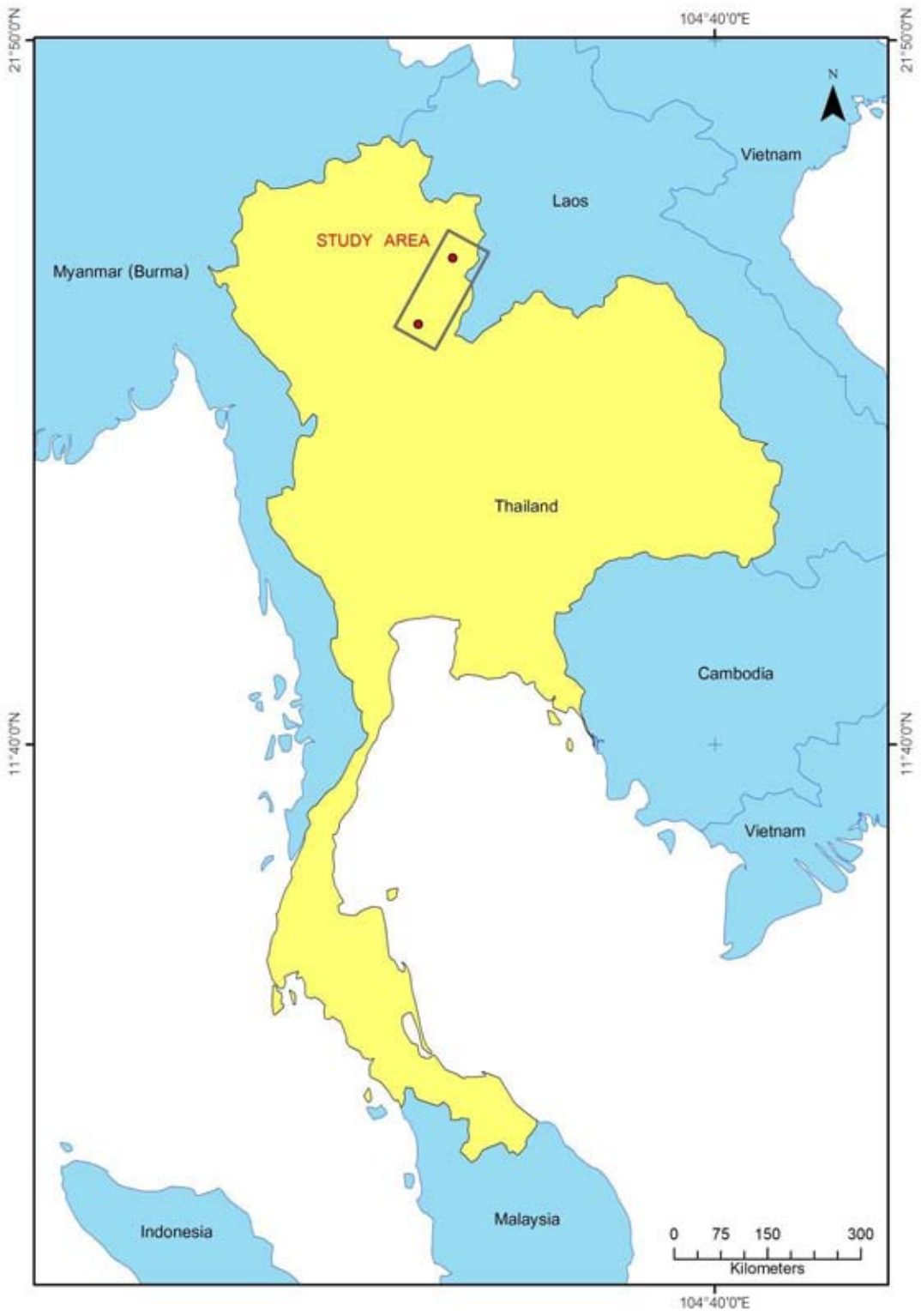

Figure 1.3 Index map of Thailand showing location of the study area in Nan-Uttaradit provinces, Northern Thailand, nearby Laos.

1.5 Methodology

Method of this study is shown as a flow chart (Figure 1.4). There are 7 steps listed below.

1. Literature Reviews

Previous works on geology, geophysics, airborne geophysics, remote sensing, mineral resources and tectonic setting of Nan-Uttaradit and adjacent area were carried out to locate and planning our research.

2. Data Gathering

This research contains several kinds of data, such as airborne geophysical data (both of magnetic and radiometric data) in grid file format which belongs to Department of Mineral Resources, Remote sensing data (Landsat TM5 and SRTM Dem) are in digital forms and can be downloaded directly from United States Geological Survey (USGS) website.

3. Data Processing

Data processing are aimed to improve the quality of data, removing noise and help us focusing on geologic structures by using many filtering techniques. In magnetic data enhancement, reduction to the pole (RTP), analytic signal grids, automatic grain control (AGC), vertical derivative, shaded relief and directional cosine filter constitute major methods. For radiometric data enhancement products, cooking technique is used to create color composite map and ternary maps, which represent potassium, effective uranium and effective thorium. Both of airborne magnetic and airborne radiometric data are reprocessed by computer based program name “Geosoft Oasis Montaj version 6.4.2”. For Landsat TM5 data are processed by “ERDAS IMAGINE version 8.5” and for SRTM DEM data are processing by “ArcMap version 10”. For Magnetic modeling are processing by “Encom Model Vision version 7.0”

4. Interpretation of data

The combined uses of airborne magnetic, airborne radiometric and remote sensing enhanced products have enabled mapping of geologic structures and locate the anomalies zone that can be related to geologic setting of the study area

5. Validation data

It is necessary to verify that the anomalies which interpreted from data processing are correct by using the previous field data and electromagnetic data in the area to support the interpretation.

6. Mapping and Conclusion.

This stage includes integration of all results to create geophysical map and interpretation map by using “Arc Map version 10” program. Focus is made on geologic setting and tectonic setting in this area.

7. Discussion

All results obtained from this study were collected for interpretation to complete the discussion on tectonic setting.

Figure 1.4 Schematic diagram showing sequences of work under this study.

Chapter II Geology of Study area

Bunopas (1978) named “Nan-Uttaradit Geosuture” whereas Barr and Macdonald (1991), and Metcalfe (1997) concluded that Nan-Uttaradit Suture is formed by continental collision of Shan Thai and Indochina continents in Late Triassic. Charusiri (1997) believe that there are one more sutures between two continents (Loei Suture in the east and Chiang Mai suture in the west). They also considered that there was paleotethys developed between Shan Thai and Indochina continents which were terminated in Late Triassic.

The Nan and Uttaradit area is mostly covered by sedimentary rocks of Late Paleozoic to Holocene. The basic concepts of stratigraphy sequences are described in numerous articles. The Geologic map in (Figure 2.1) modified from Geologic map of Thailand scale 1:250,000 of Department of Mineral Resources (2007). There are 32 units of rock as describe below.

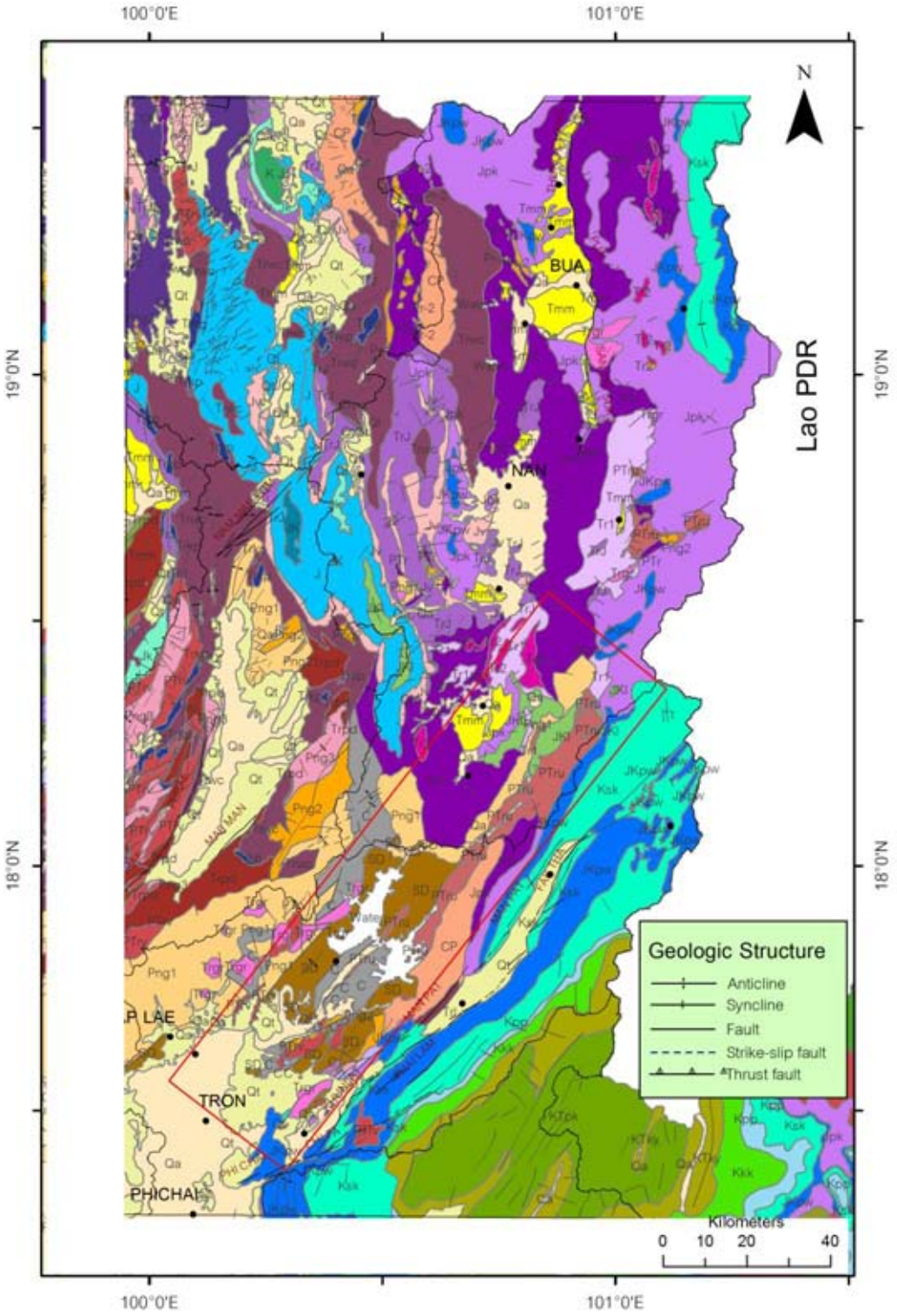

Figure 2.1 Geologic map of the study area (modified from Department of mineral resources, 2007). Noted that the study area are in the red box.

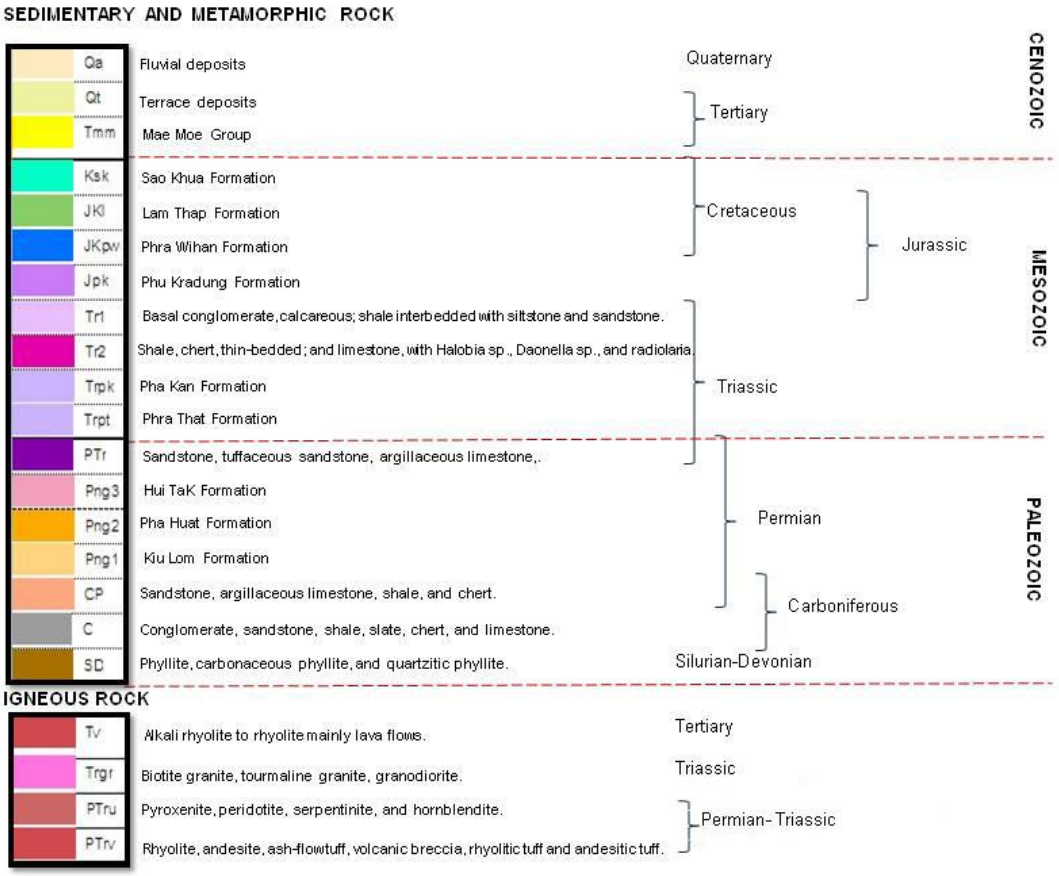

Figure 2.2 Explanation of geologic map of the Nan-Uttaradit area (Department of Mineral Resources, 2007).

2.1 Stratigraphy

The study area mostly covered by sedimentary rocks of Late Paleozoic to Holocene. The sedimentary rocks are herein described in order of ages from the oldest to the youngest below (Based on Charusiri 2006, Figure 2.3).

Pha Som Group

This group is mainly in carboniferous to Permian in age, and covered 40 percent of the study area. The group consists of 6 metamorphic rocks Thanasuthipitak (1978), reported mica-hornblende schist, chlorite-schist, actinolite schist, epidote-quartz schist, muscovite-quartz schist and quartz& quartzitic phyllite/phylite. Petrochemistry of metamorphic rocks suggests low grade metamorphism. Chairungsri (1989) separated phyllite in Tha Pla and Fak Tha areas of Uttaradit into 2 groups, sedimentary phyllite with brown color and volcanic phyllite with green color. Both groups occur in the same trend (NE-SW direction) both are bounded fault contacts with other groups with many folding structure.

Barr & Macdonald (1978) use EMPA analysis and reported blue amphibolites with quartz and epidote. This blue amphiboles shows low grade green schist metamorphism.

Phrae Group

The group consists of Mae Sai Formation, Rong Kwang Formation and Na thanung Formation, age from Carboniferous to Early Triassic and can related to Mae Tha group of Piyasin et al. (1975).

1 Mae Sai Formation, this formation is found in low terrace along the Nan River, particularly at Ban Satern, Ban Pak Hun, Ban Kung Yang, Sirikit Dam and Thapla areas. There are mainly gray sediments, medium grained sandstone with mica, tuff, rhyolitic tuff, andesite, black shale, chert massive interbed with gray shale and low grade metamorphic rock .

2 Rong Kwang Formation occurred as clastic rocks, mainly in Permian age. These rocks are found in Tron, Uttaradit and Khao Kee Nok areas, there are massive limestone with clastic sediment, shale, marble and sandstone.

3 Na Thanung Formation is found in eastern part of Sirikitt Dam, trending in NE-SW direction forwarding to Nan River. This formation mainly consists of andesitic tuff, rhyolite tuff, conglomerate, greywacke with lithic tuff and shale.

Lampang Group

Piyasin (1975) reported that Lampang group is mountain range and cliff trending in NE-SW direction. Charusiri (2006) separated Lampang Group into 2 formations, lower Triassic and upper Triassic.

1 Lower Triassic Formation consists of volcanic and volcaniclastic overlain by limestone of Nam Nan Formation, poorly sorted conglomerate, sandstone, silt and shale. Some part of this formation shows compression of tuffaceous sandstone interbed with argillaceous limestone.

2 Upper Triassic Formation has the approximate thickness of 300 m. The formation is correlated with Hong Hoi Formation which is siltstone, shale and massive limestone.

Nakhon Thai Group

This group occurs in the eastern part of the study area and looks similar to the Khorat Group, both of which consist of alluvial lacustrine sediments from Middle to Late Mesozoic, the group lies unconformably beneath the Lampang group. Charusiri et al. (2006) separated the Nakhon Thai group into 4 formations as listed below from oldest to youngest order.

1 Lower Nakhon Thai Formation, This formation is unconformably contact with Nam Nan Volcanic. The formation can be related with Phu Kradung Formation. It has an average thickness of 200 meters on eastern part and about 100-500 meters

nearby the suture. The formation consists of quartzitic sandstone, white, pink, and gray, large scale cross-bedded, thick-bedded, intercalated conglomeratic sandstone; thin laminations of red siltstone, clay stone with dipping 10 ° in NE direction. Stratigraphy in western part of Nan Suture is same, they also consist of conglomerate, sandstone and shale interbeded, showing fined upward sequence. Drumm et al. (1993) suggested the environment of deposition is braided stream and occurrence in Early Jurassic and source rocks maybe came from volcanic rock.

2 Middle Nakhon Thai Formation, This formation is unconformably contact with lower Nakhon Thai Formation. The formation consists of sandstone, orthoquartzite, Arkose with cross bedding and orientation in NE direction with dipping 50°-70° into NW or SE. Sukwattananun (1984) suggest the environment of deposition is point bar deposit in middle Jurassic age.

3 Upper Nakhon Thai Formation, The formation is found nearby Nan Suture and eastern part of suture consisting of various size of sediments, red-violet sandstone with fracture , mica disseminated, conglomerate and thin layer of shale, silt stone with limestone calcrete. Drumm et al. (1993) suggest the environment of deposition being lacustrine on alluvial plains in semi-arid to arid zone dominated by a fluvial system. Chairungsri (1989) suggested that source rocks derived from metamorphic rocks from an existing of mica, well rounded quartzite shows paleocurrent from NE direction. Dating results show that metamorphic source rock occurred during 300-350 Ma (Late Devonian – Early Carboniferous).

4 Uppermost Nakhon Thai Formation, Lower part of this formation shows in mountain range with NE-SW direction in Cretaceous age. The rocks are characterized by reddish brown to gray sandstone with poorly cementation and few cross beddings in gray sandstone. The formation can be correlated with the Phu Phan Formation of the Khorat Group. The Upper part is in Cretaceous age, reddish brown sandstone with siltstone interbed, show polygonal crack on surface, carbonate or Fe oxide cementing. It can be correlated with Khok Kruat Formation of Khorat Group.

Cenozoic Sediments and Rocks

Cenozoic sediments are found in basin and mostly basins in this area are fault bound basin. There are 6 significant basin found in this area , Wat Bot Basin, Uttaradit Basin, Nam Phi Basin, Saen Khan Basin, Mae Ja Rim Basin and Mae Moh Basin. Cenozoic basins can be separated into 2 units listed below

1 Lower Unit is the Tertiary basin found along Fak Tha area in central part of study are, consist in order from sandstone, siltstone, conglomerate, shale, semi consolidate with poorly cementing, coal seam and clay beds. Tertiary deposits unconformity to the older rock and unconformity to the newer Quaternary deposits.

2 Upper Unit is the Quaternary deposits spreading and clearly found in Nam Pat – Fak Tha Basin, trending NE-SW and dipping in SE direction. Quaternary deposits consist of gravel bed, silt stone, silt clay, laterite interbed with unconsolidated deposits, poorly cementing and friability. This Unit is unconformity with older unit and can be aged from Upper Pleistocene to Lower Holocene.

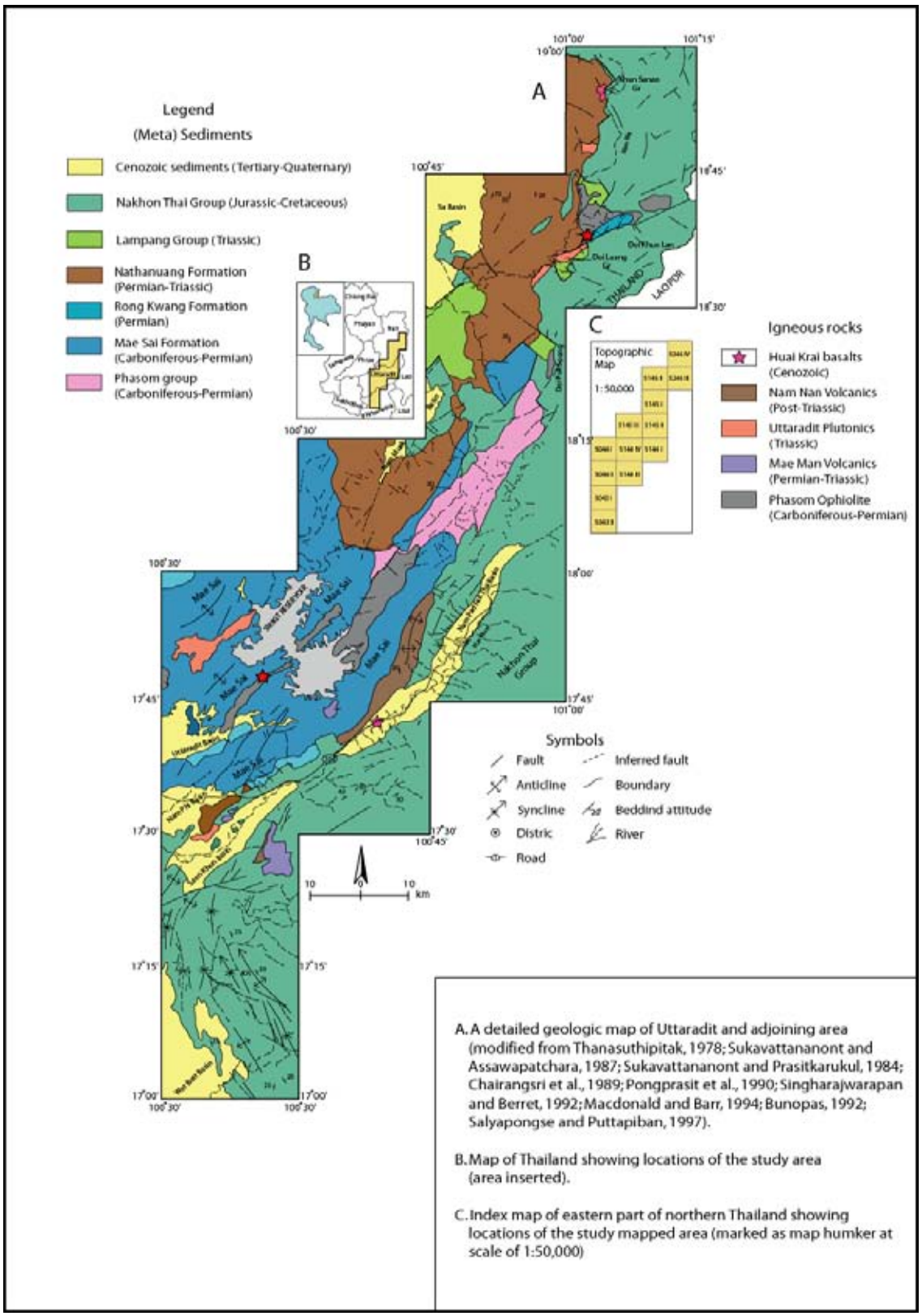

Figure 2.3 Detailed geologic map of the Nan – Uttaradit area (Lunwongsa, 2004). Noted that the study area occupies larger area than the compiled map by Lunwongsa (2004)

2.2 Igneous Rocks

Charusiri et al. (2006) divided igneous rocks into 5 units, from the oldest to the youngest listed below.

1 Pha Som Igneous Rocks, mainly consist of plutonic rocks from ultramafic to mafic rocks and volcanic rock of basalt and andesite, aged from Carboniferous-Permian, covered on regional structure. Mafic to Ultramafic igneous rock of Pha Som Group are found in Khao Sam Sean – Had Ngew, Sirikitt Dam area, Ban Ngom Mod – Huai Luang, Doi Phuk Soong – Phuk Jam Peng and Doi Kaew – Mae Ja Rim area.

2 Mae Man Volcanics can be subdivided into 3 groups below.

2.1 Ban Sean Khun Volcanics comprise intermidiated igneous rocks of andesite in green color. The rocks show sharp contact with Rong Kwang limestone and the clastic rocks of the Nakhon Thai group. Piyasin (1975), summarized that the andesite extrude into sandstone of Nakhon Thai group in Permian to Early Triassic.

2.2 Khao Sam Sean – Had Ngew unit is mainly alkaline basalt, basaltic andesite and andesite in dark green color and porphyritic texture.

2.3 Nam Pad unit is mainly andesite Volcanoes, Intrusion into shale and phyllitic shale of Pha Som Group in Permo-Carboniferous. The unit shows variation in color, texture, and foliation, and some of mica.

3 Nan –Uttaradit Plutonics

Nan – Uttaradit Plutonics have been found in 4 areas in order from north to south part below.

3.1 Nam Phu – Nam Sa Nan are consists of diorite, granodiorite, hornblended diorite, shear surface in E-W direction. Steep slope into the North, fault plane are in NW-SE direction.

3.2 Doi Luang consists of the granites which intruded into shale and sandstone of Na Thanung group. They are granite to granodiorite and diorite.

3.3 Huai Nam Rid – Ban Nam Ree occurs in the western part of Sirikitt Dam. They are stock of granites, hornblended-biotite granite and biotite granite, aged in Permo-Triassic

3.4 Khao Yai and Khao Kee Nok area is mainly granites trending in NE-SW direction, found a stock, veins, dikes through Rong Kwang and Mae Sai Formations, fault contacted with Lampang Group, show silification , pyritization and recrystallization.

4 Nam Nan Volcanics

Nam Nan Volcanics occurred in Post Triassic. They are found in the northern part of area, trend in the NE-SW direction parallel to the Nan River. The volcanic rocks are andesite rhyolite, amigaloidal andesite with vesicular texture and filled void with secondary minerals.

5 Huai Krai Volcanics

The youngest igneous rocks in the area, aged Late Tertiary to Quaternary, are found specific in middle of Nam Pad – Phak Tha Basin. They show obscured contacts to Quaternary sediment. These mostly extrusive igneous rocks show vesicular texture and high weathering.

2.3 Structural Geology

Structural geology in the Nan- Uttaradit area is result of tectonic settings in Late Triassic, Late Cretaceous and Middle Tertiary (Miocene).

1. Folding

Significant folding in this area is a large scale anticline and syncline with axial planes in NE-SW direction. Pha Som Group showed strongly folding because most of are slightly metamorphic rocks.

2. Faulting

Separated fault into 5 groups based on orientation.

1 NE-SW Direction Fault

This Fault set name “Sirikitt Fault”, 150 kilometer long, First movement in Late Triassic, contain of normal and strike slip fault. The significant fault in NE-SW direction is strike slip fault that parallel to Nan River cut in Mae Sai and Pha Som group.

2 N-S Direction Fault

Fault in N-S direction are mainly strike slip fault and dipping west. The significant fault in N-S direction is “Nan Thrust Zone”, 50 kilometer long, located in northern part of area.

3 NW Direction Fault

Fault in NW-SE direction always found in small scale except the northernmost and southernmost of area. The significant fault in NW direction is “Sa-Nam Muap Fault” in northern part, 30 kms long. And “San Ta Kien Fault”, 20 kilometer long in southern part, parallel to fold axis in the area.

4 E/NE Direction Fault

Fault in E to NE direction which is named “Doi Luang Fault”, is 40 kilometer long, and extending to Mae Ja Rim town and cut Nakhon Thai, Doi Klang and Na Tanung group.

5 Cenozoic Fault

Cenozoic faults are largely in NE-SW direction. Mostly they are basin-bounded. The length is about 30 km, the fault occurred in Middle Tertiary to Holocene and can earthquakes in this area.

3. Unconformity

Five unconformities are recognized. They are the unconformity in Nakhon Thai Group over Lampang Group, the unconformity in Mae Sai Group (Carboniferous-Permian) and Nakhon Thai Group (Jurassic), the unconformity in Nakhon Thai over Na Ta Nung Group in Doi Duay Kai area, the unconformity in Nakhon Thai over Na Ta Nung Group in Nam Pang area, and the unconformity in Na Ta Nung Group contact with Nam Pu Granite.

Chapter III Types of Survey Data

It is clear from the previous chapters that geophysical surveys are aimed to record the physical fields, which are imposed by the effects of physical properties and distribution of rocks. These properties are density, magnetism, electrical conductivity and radioactivity.

In applied geophysics, the intention is to trace geology across an area, even where it may not be well exposed. The applicability of geophysics is controlled largely by the correlation between geophysical, geological field and previous investigations. The greater understandings of geological conditions of the interesting Nan-Uttaradit area are help to choose which geophysical methods could be applied, (Reeves, 2005). There are 3 types of data using in this study as described below.

3.1 Documentary data

Previous documentary data in this area can be classified into 3 main categories.

1. Geology and Geologic Structures

Barr and Macdonald (1987) studied Nan river suture zone, northern Thailand. Nan suture consists of ophiolite and ultramafic rocks that formed in back arc and inter arc setting. And Nan suture is a continent-continent collision between Shan Thai and Indosinian cratons in Pre Permian age.

Sukvattananunt and Assavapatchara (1987) investigated and created geologic map of Amphoe Vieng Sa and Ban Nam Muap, scale 1:50,000.

Panjasawatwong and Yaowanoiyothin (1991) studied petrochemical of post-Triassic basalts from the Nan suture, Northern Thailand. Cr-Spinel from this study indicated that are form in supra subduction zone.

Singharajwarapan (1994) studied geologic structure and metamorphism across the Sukhothai fold belt and to test the tectonic models that have been used for geological evolution of this area.

Chaodumrong et al. (1994) studied geologic map (scale 1:50,000) of Nan-Uttaradit area and shown correlation of stratigraphy of AEM area, Nan-Uttaradit.

Lunwongsa (2004) studied petrochemistry of chromian spinel in mafic and ultramafic igneous rocks in Nan-Uttaradit area and the result indicated fore arc and island arc setting.

2. Airborne Geophysic Data

Kuttikun et al. (1988) preliminary studied of airborne geophysics data in Nan-Uttaradit area and found magnetic anomalies 743 points. The anomalies from magnetic associated conductor that should be mineral potential are 616 points. Then Munyou et al. (1991) ground followed up of airborne geophysics data in Nan-Uttaradit area and selected chromite potential at Ban Had Ngew and Ban Huai Phung of Uttaradit area.

Dechavan (1992) reported ground followed up of airborne geophysics data in Nan-Uttaradit area (Sirikit Dam area, map sheet 5144IV) by MaxMin-I EM, Magnetometer and Induced Polarization and found potential area of chromite, magnesite and talc. Subsequently, Neawsuparp (1997) applied Landsat TM and aeromagnetic data for structural interpretation of the Nan suture zone. In the same year, Tulyatid (1997) applied airborne geophysical data to the study of Cenozoic basins in central Thailand. After that Tulyatid and Charusiri (1999) studied ancient tethys in Thailand by nationwide airborne geophysical data. Then Surinkhum (2002) evaluated mineral deposit potential in Nan-Uttaradit suture zone by using geophysical data. Subsequently, Neawsuparp (2004) applied airborne geophysical and remote sensing data to studied structural geology and tectonic setting in Loei area, Northeastern area, Thailand.

3. Mineralization in Nan-Uttaradit Area

Sekthera et al. (1978) studied regional geochemical of Uttaradit area, map sheet NE 47-11, scale 1:250,000. Subsequently, Surinkum and Siripongsatian (1992) reported ground followed up of airborne geophysics data in Khao Khee Nok (KKN) AEM anomaly and found a gigantic graphite deposit in Thailand. Pintawong (1998) studied mineral resources potentials in Nan-Uttaradit area. Later on Yensabai (2002) studied and create mineral resources potentials map, scale 1:250,000, sheet (Changwat Nan).

3.2 Space borne data

3.2.1 Airborne Geophysical Data

Over a past sixty years, a large number of ground and airborne geophysical techniques have been developed to assist in mineral and hydrocarbon exploration (Surinkhum, 2002). Airborne methods are usually the most cost effective tools available for both large regional reconnaissance surveys used as aids in geological mapping and for locating target areas for more detailed follow-up using helicopter borne instruments. Ground techniques are usually most effective when used to test targets discovered by the airborne surveys (Urquhart, 2003).

1. Airborne geophysical survey in Thailand

In 1954, airborne geophysical survey was first developed in Thailand for petroleum exploration in Lower Chao Phraya Basin. Later on in 1959, airborne geophysical survey was developed in Loei, Nakhon Sawan and Chachoengsao province. The survey result was published in USGS Professional Paper number 618 (Brown and others, 1951). And in 1969 airborne geophysical survey was developed for petroleum exploration in upper Chao Phraya basin and Khon Kaen areas. In 1979, Sander Geophysics Company combined airborne magnetic and radiometric surveys in Phu Wiang basin for mineral exploration. Later that in 1984-1988 Kenting Earth Science International Limited (KESIL) of Canada incorporates with Department of Mineral Resources (DMR) through the Mineral Resources Development Project (MRDP) operated nationwide airborne geophysical survey for high-resolution magnetic and high sensibility radiometric. And helicopter-borne electromagnetic surveys were conducted over five selected areas. Nan – Uttaradit is one of the selected area. Table 3.1 below show all details of the airborne geophysical activities operated in Thailand.

Table 3.1 Details of the airborne geophysical activities operated in Thailand (Surinkum, 2002).

DMR = Department of Mineral Resources, Private = Private Company

Flown in	Area	Methods	Organizer	Purpose
1954	Lower Chao Phraya Basin	Magnetic	DMR	Petroleum exploration
1959	Loei	Magnetic& Radiometric	DMR	Mineral investigation
1959	Chachoengsao	Magnetic & Radiometric	DMR	Mineral investigation
1959	Nakhon Sawan	Magnetic & Radiometric	DMR	Mineral investigation
1963	Kanchanaburi	Magnetic	Private	Mineral investigation
1965	Loei (east)	Magnetic	Private	Mineral investigation
1979	Khon Kaen	Magnetic	Private	Petroleum exploration
1979	Upper Chao Phraya Basin	Magnetic	Private	Petroleum exploration
1979	Phu Wiang	Radiometric	DMR	Uranium exploration
1979	Eastern Thailand	Magnetic & Radiometric	DMR	Mineral investigation
1984	Nationwide	Magnetic, Radiometric, VLF-EM& AEM	DMR	Regional mapping & Mineral investigation
1985-1997	Gulf of Thailand	Magnetic	Private	Petroleum exploration
1997	Loei & Petchabun	Magnetic	Private	Gold exploration

2. Airborne Geophysical Data in the study area

2.1 Airborne magnetic data (Aeromagnetic Data)

The aeromagnetic survey, or the so-called Survey A by DMR (2006), was flown by fixed wing aircraft at various altitudes ranging from 300 m MTC (mean terrain clearance) to 2,250 m fixed barometric altitude depending on the relief of the terrain (Figure 3.1). The survey lines direction should be perpendicular to the geological strike and for Thailand is in N-S direction. But magnetic inclination of Thailand are range from -10 to 27 degree, and if flown in E-W direction (perpendicular to the geological strike) when survey line are in magnetic equator (inclination = 0), it can barely see anomalies in that survey line. So, survey A was flown in N-S direction. For data sampling interval in Thailand is setting to 0.25 second and Traverse line is 1,000 m spacing. Control line is flown for checking in E-W direction with spacing of 14,000 m. (Detail of survey specification are listed in Table 3.2)

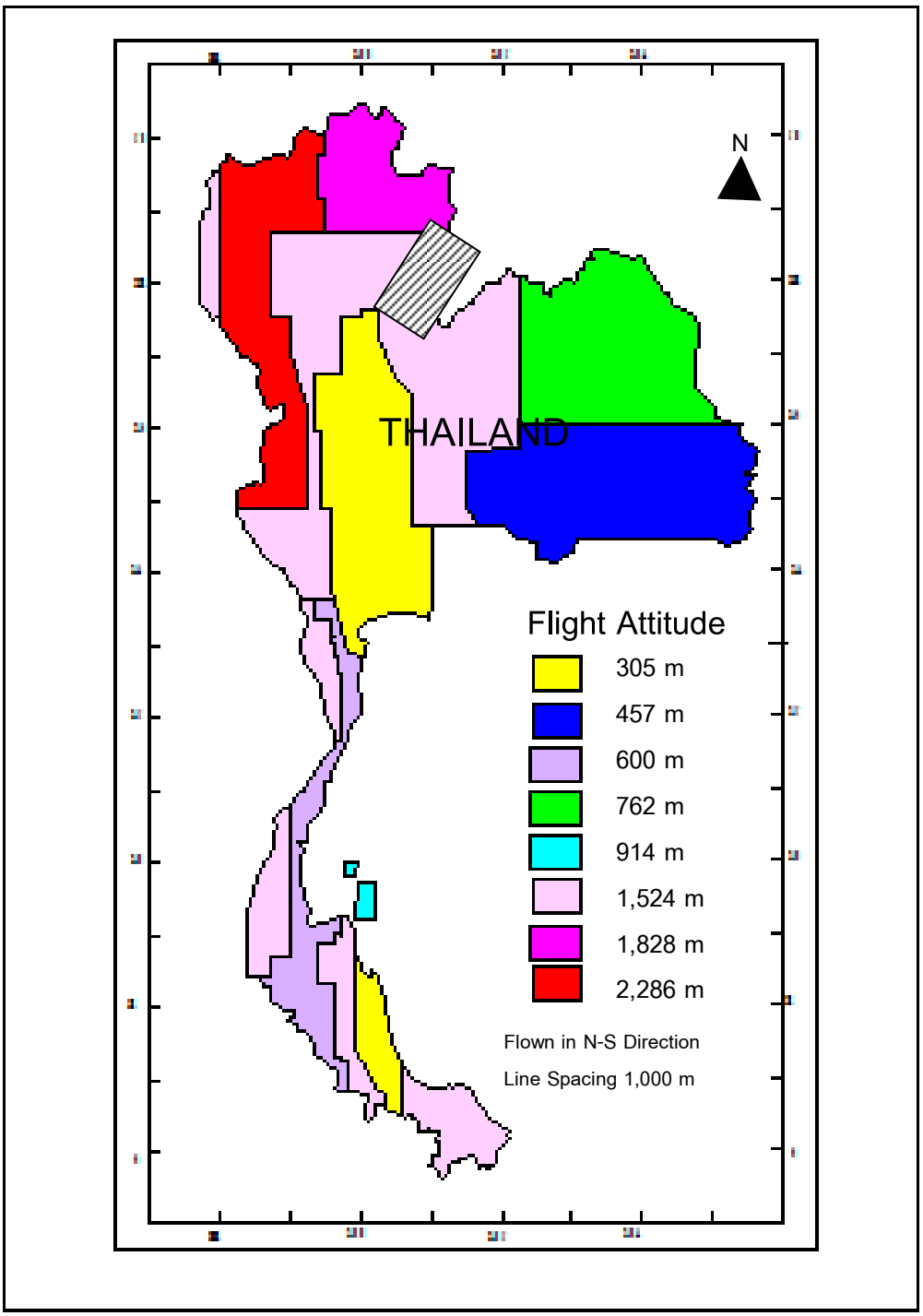

Figure 3.1 Index map of Thailand showing nationwide airborne survey A with specified flight altitude (Modified from Surinkhum, 2002). Noted that the location of the study area is in the striped line box.

Table 3.2 Detail of Airborne Magnetic survey specification (Department of Mineral Resources, 1989)

Categories	Specifications
Traverse line spacing and direction	1 km, N-S
Control line spacing and direction	14 km, E-W
Survey altitudes	Mean terrain clearance in 305m in block of low relief and Flown as fixed barometric altitudes in 457m, 762m, 914m, 1524m, 1828m and 2286 m of several topographic relief.
Data sampling interval	0.25 second = 25 m
Aircraft	2 Cessna 404 Titans (Fixed Wings)
Magnetometer	Varian Optically Pumped Cesium Vapour Noise envelope $\leq$ 0.25 nT, resolution = 0.01 nT
Navigation aids	Tracking camera, Doppler, Barometric and Radar altimeters.
Area of survey flying	440,000 sq.kms.
Total survey flying	439,538 line-km.
Data acquisition period	July 1984 – November 1985

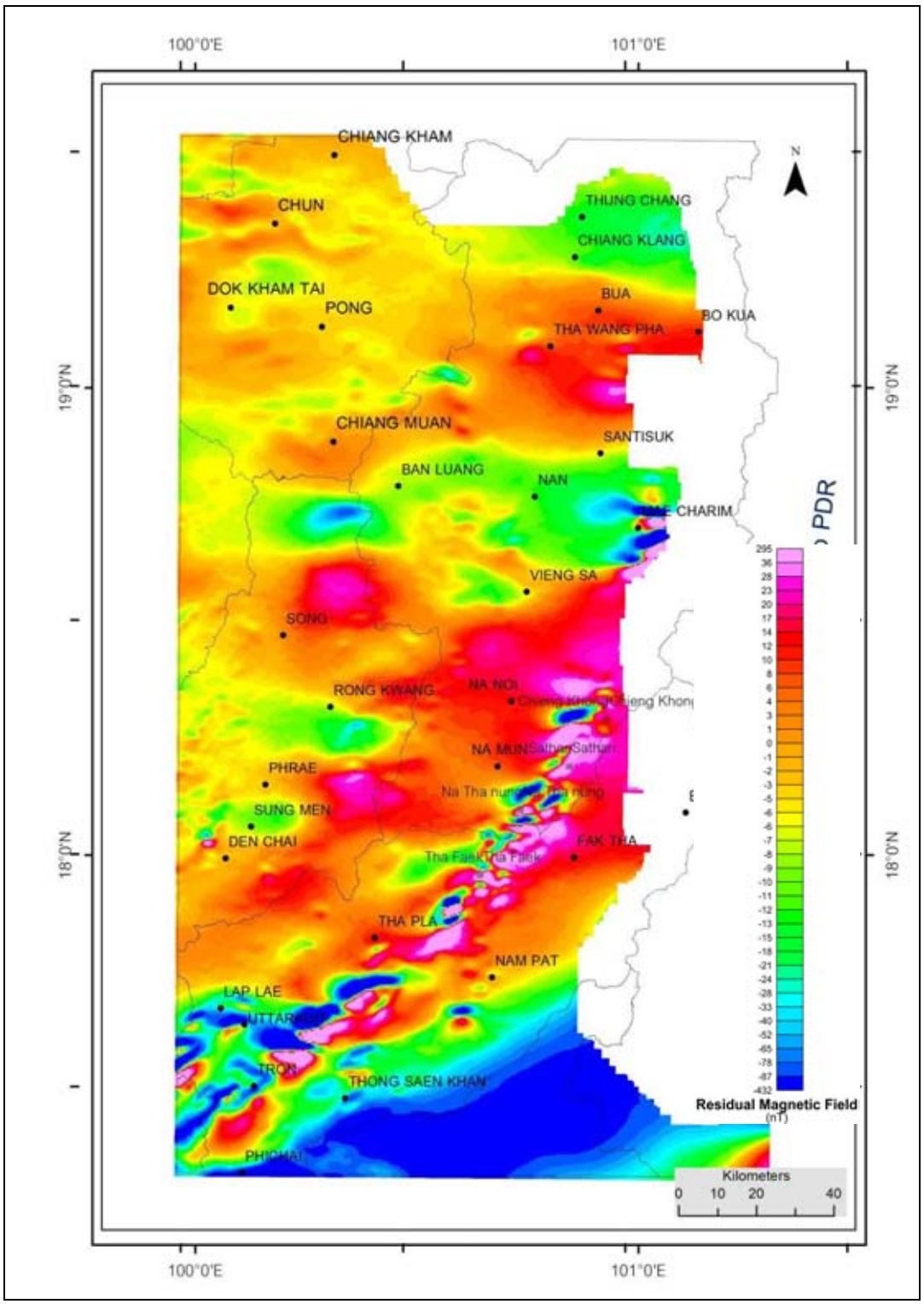

Figure 3.2 Aeromagnetic data (residual field) used in this study for the Nan-Uttaradit provinces, Northern Thailand. Noted that the study area is in Figure 3.1.

2.2 Airborne radiometric data

The radiometric surveys, Survey B and Survey C, were flown at 120 m or 400 ft MTC, with 1, 2 and 5 km line spacing in east-west direction (Figure 3.3). Survey B and Survey C are different by the types of the aircraft used in the surveys. Gamma ray spectrometer has use for recording windows with all energy data. These windows are total count window (Figure 3.4), potassium window (Figure 3.5), uranium window (Figure 3.6) and thorium window (Figure 3.7), for 0.40-2.82 Mev, 1.36-1.56 Mev, 1.66-1.86 Mev and 2.42-2.82 Mev respectively. Ternary map, a superimposed map of potassium, uranium, and thorium elements with different colors assigned, can be used to study theirs correlation (Figure 3.8). Details of survey specification are listed in Table 3.3.

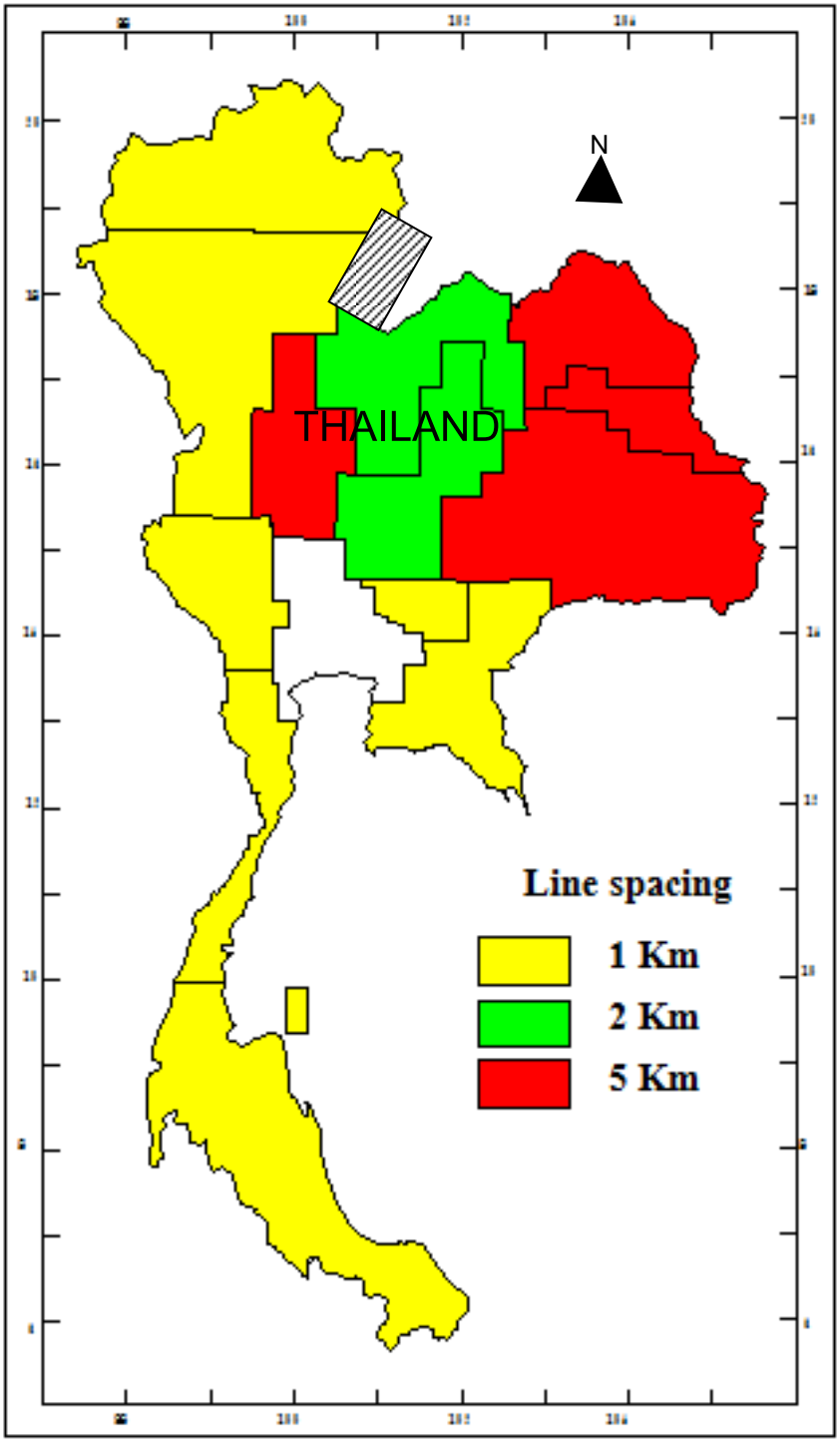

Figure 3.3 Index map of Thailand showing areas flown by airborne survey B and C with specified traverse line spacing, (Surinkhum, 2002). Noted that the location of the study area is in the striped line box.

Table 3.3 Detail of airborne radiometric survey specification (Department of Mineral Resources, 1989)

Categories	Specifications
Traverse line spacing and Direction	1 km, 2 km and 5 km in different blocks, E-W
Control line spacing and Direction	14 km, N-S)control lines were flown only in blocks with 1 km line spacing)
Survey altitudes	122 m, Mean Terrain Clearance.
Data Sampling Interval	1 second = 50 m
Aircraft	Survey B : Britten Norman Islander STOL Survey C : 2 Bell 412 Twin Turbine Helicopters
Gamma Ray Spectrometer	-Detector 50 litters (12 crystals of 4x4x16 cu in), Harshaw NaI(TI) Crystals. -Analogue to Digital Converters Nuclear Data model ND 561 -Spectrometer Interface Kenting Digital Survey system (KDSS-5) -Pulse-Height Analyzer : 256 Channels -Spectrum Stability 0.008 KeV/channel -Detector Resolution < 12% -Dead time Per Pulse < 15 microsec. -4 Data Recording windows regions (energy windows) Total Count Window 0.40-2.82 Mev Potassium Window 1.36-1.56 Mev

Categories	Specifications
Gamma Ray Spectrometer (cont)	Uranium Window 1.66-1.86 Mev Thorium Window 2.42-2.82 Mev
Magnetometer	Geometrics G 813 Proton Precession Noise envelope $\leq$ 1 nT, resolution = 0.25 nT (survey B $\leq$ 8 nT)
Navigation	Tracking camera, Doppler, Barometric and Radar altimeters.
Area of survey flying	430,000 sq.kms.
Total survey flying	Survey B = 68,681 line-km Survey C = 232,709 line-km.
Data acquisition period	Survey B in March 1985, February-May 1986 and November 1986. Survey C in February-May 1985, February 1986-March 1987.

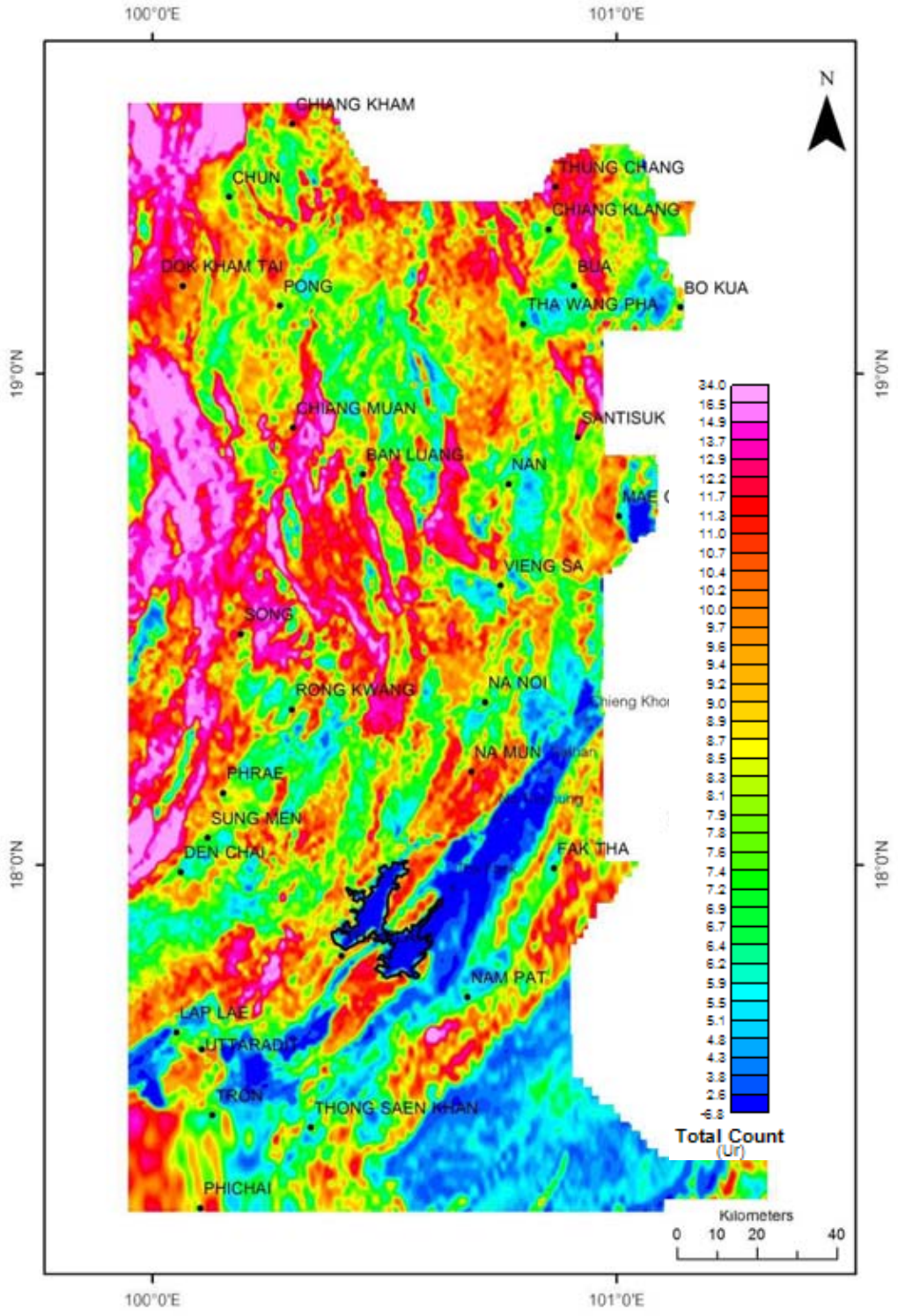

Figure 3.4 Airborne radiometric (Total Count) data used in this study for Nan-Uttaradit provinces, Northern Thailand. Noted that Sirikit reservoir is bound in black.

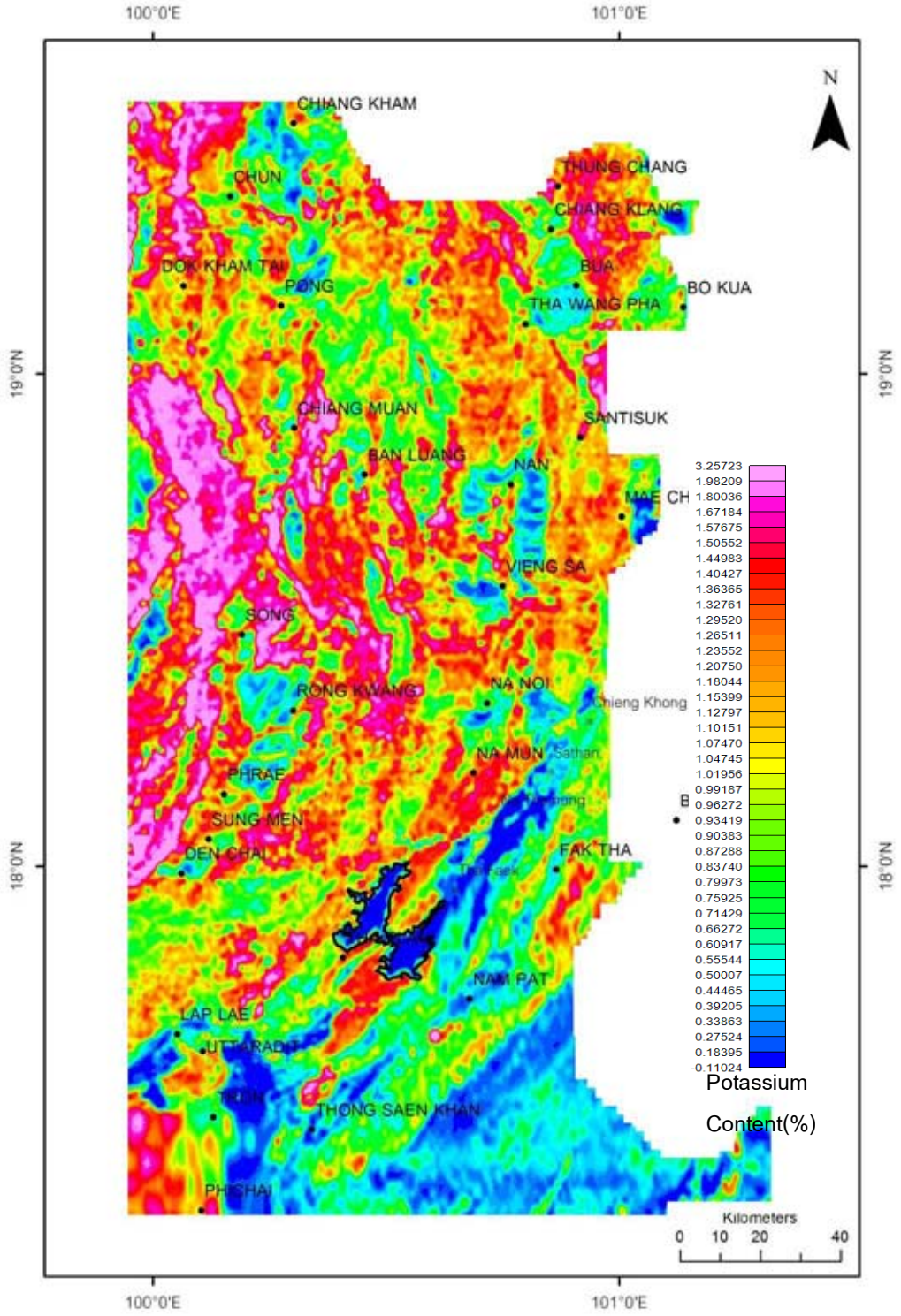

Figure 3.5 Airborne radiometric (Potassium) data used in this study for Nan-Uttaradit provinces, Northern Thailand. Noted that Sirikit reservoir is bound in black.

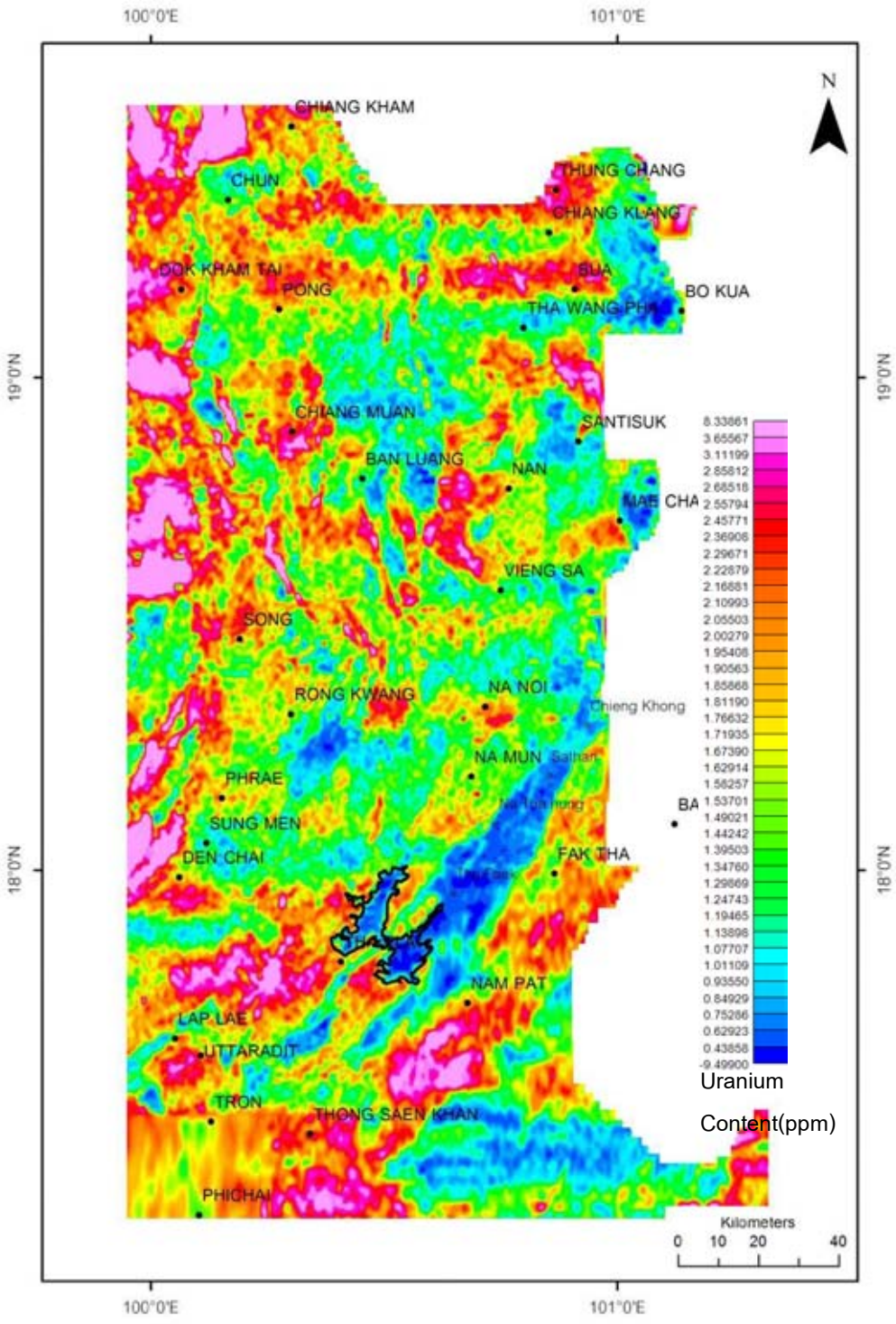

Figure 3.6 Airborne radiometric (Uranium) data used in this study for Nan-Uttaradit provinces, Northern Thailand. Noted that Sirikit reservoir is bound in black.

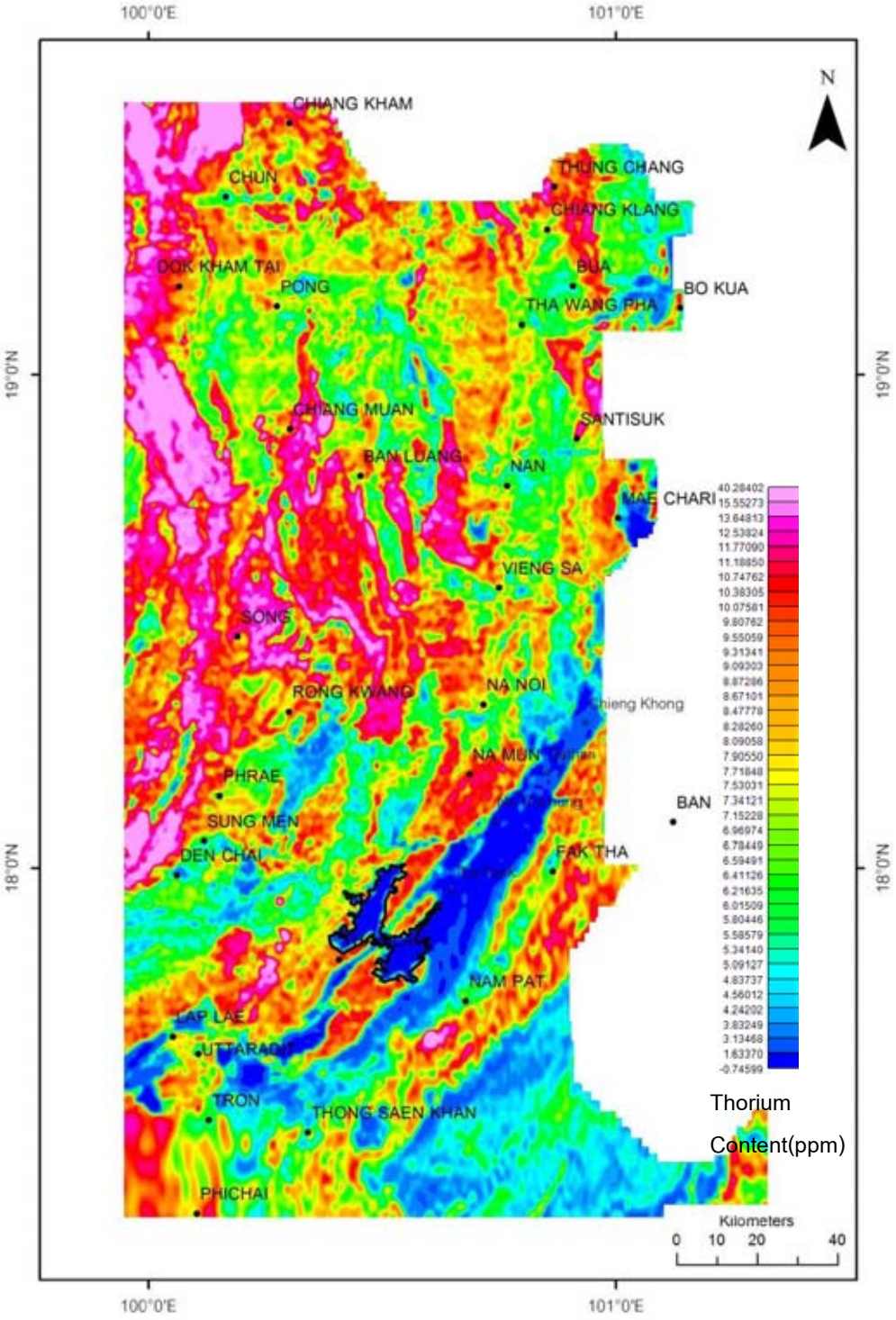

Figure 3.7 Airborne radiometric (Thorium) data used in this study for Nan-Uttaradit provinces, Northern Thailand. Noted that Sirikit reservoir is bound in black.

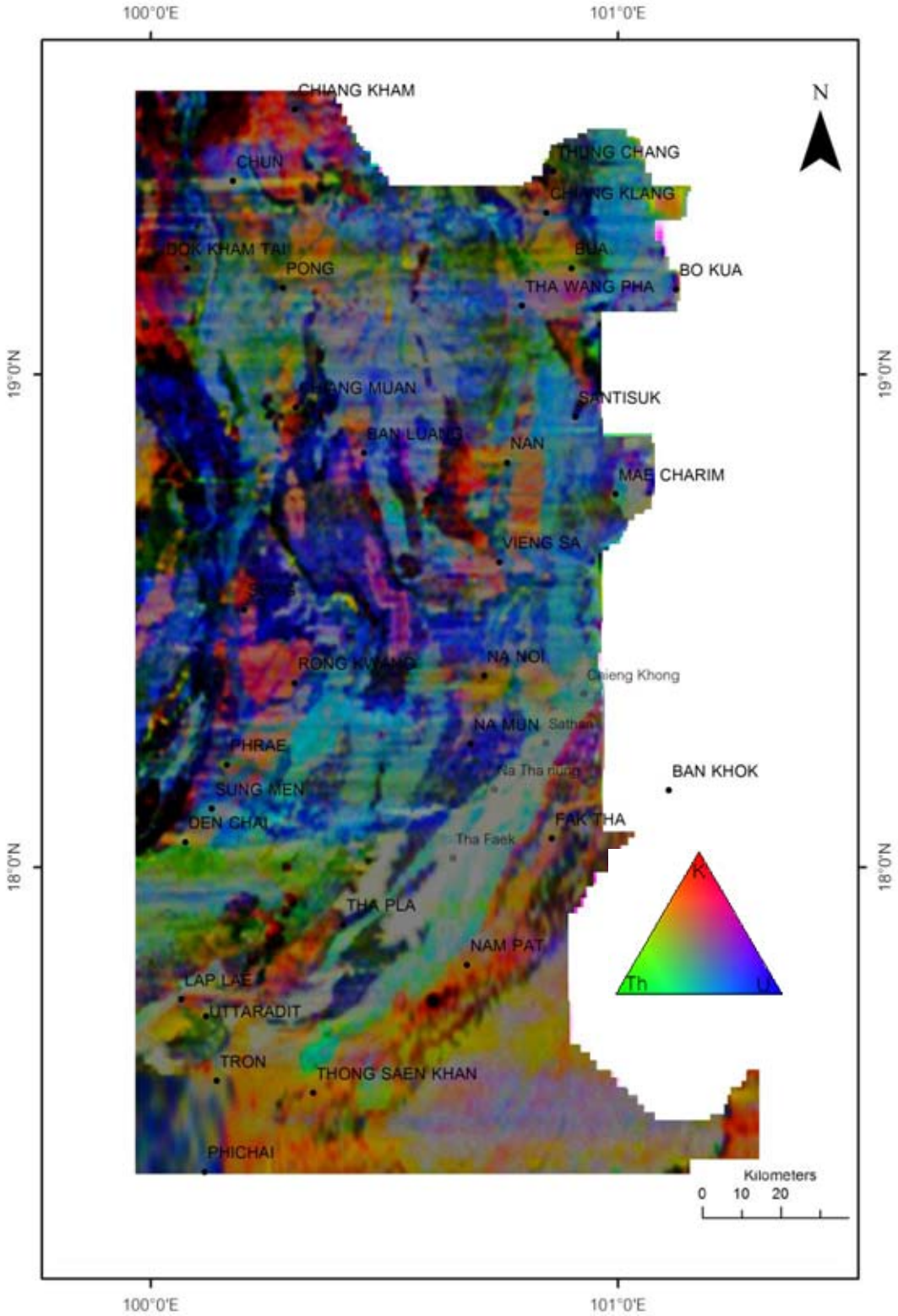

Figure 3.8 Airborne Radiometric (Ternary) data used in this study for Nan-Uttaradit provinces, Northern Thailand.

3.2.2 Remote Sensing Data

Remote sensing is the instrumentation, techniques and methods to observe the Earth's surface at a distance and to interpret the images or numerical values obtained in order to acquire meaningful information of particular objects on earth (Janssen,2004).

1. Landsat Thematic Map

This study made use of remote sensing from the Landsat satellites (TM5) which have been orbiting the earth for over thirty years. Landsat satellites first lunched in 1972, the images data have been available to all countries in the world. There are many application of Landsat images use for study major structure and mineral exploration. At the beginning they made use of Landsat Multispectral Camera (MSS) system, but for today they change to Landsat Thematic Map (TM) system. Thematic Map has high resolutions in 30 meter, recording data in 7 bands between Blue to Middle Infrared. Spectral ranges of TM Landsat in each band are listed below.

Table 3.4 Specifications of Landsat TM5 image data for the study area in Nan-Uttaradit Province Northern Thailand.

Landsat 5 (TM sensor)	Wavelength (micrometers)	Spectral Bands	Resolution (meters)
Band 1	0.45 - 0.52	Blue	30
Band 2	0.52 - 0.60	Green	30
Band 3	0.63 - 0.69	Red	30
Band 4	0.76 - 0.90	Near Infrared	30
Band 5	1.55 - 1.75	Short Wave Infrared	30
Band 6	10.40 - 12.50	Thermal Infrared	120
Band 7	2.08 - 2.35	Short Wave Infrared	30

The individual band images appear as gray scale images. However, they can be combined to form composite images, with a different gray scale image feeding a different color gun (typically a red-green-blue, or RGB combination). There can be applying into many band-color combinations. (NASA Geocover Tutorial, 2000)

1. True Color

Band 1 is displayed in the blue color, band 2 is displayed in the green color, and band 3 is displayed in the red color. The resulting image is fairly close to realistic - as though you took the picture with your camera and were riding in the satellite. But it is also pretty dull - there is little contrast and features in the image are hard to distinguish.

2. False Color

Band 2 is displayed in blue, band 3 is displayed in green, and band 4 is displayed in red. This rendition looks rather strange but it reflects infrared light energy.

In this research, 4 data set from Landsat TM5 from USGS were used for interpret geologic structure in this area.

Table 3.5 Data Set of Landsat TM 5 image data used for the study area in the Nan-Uttaradit area of Northern Thailand.

No.	Path / Row	Date of Acquisition
1	129 / 47	25-12-1993
2	129 / 48	25-12-1993
3	130 / 47	11-01-1989
4	130 / 48	21-12-1989

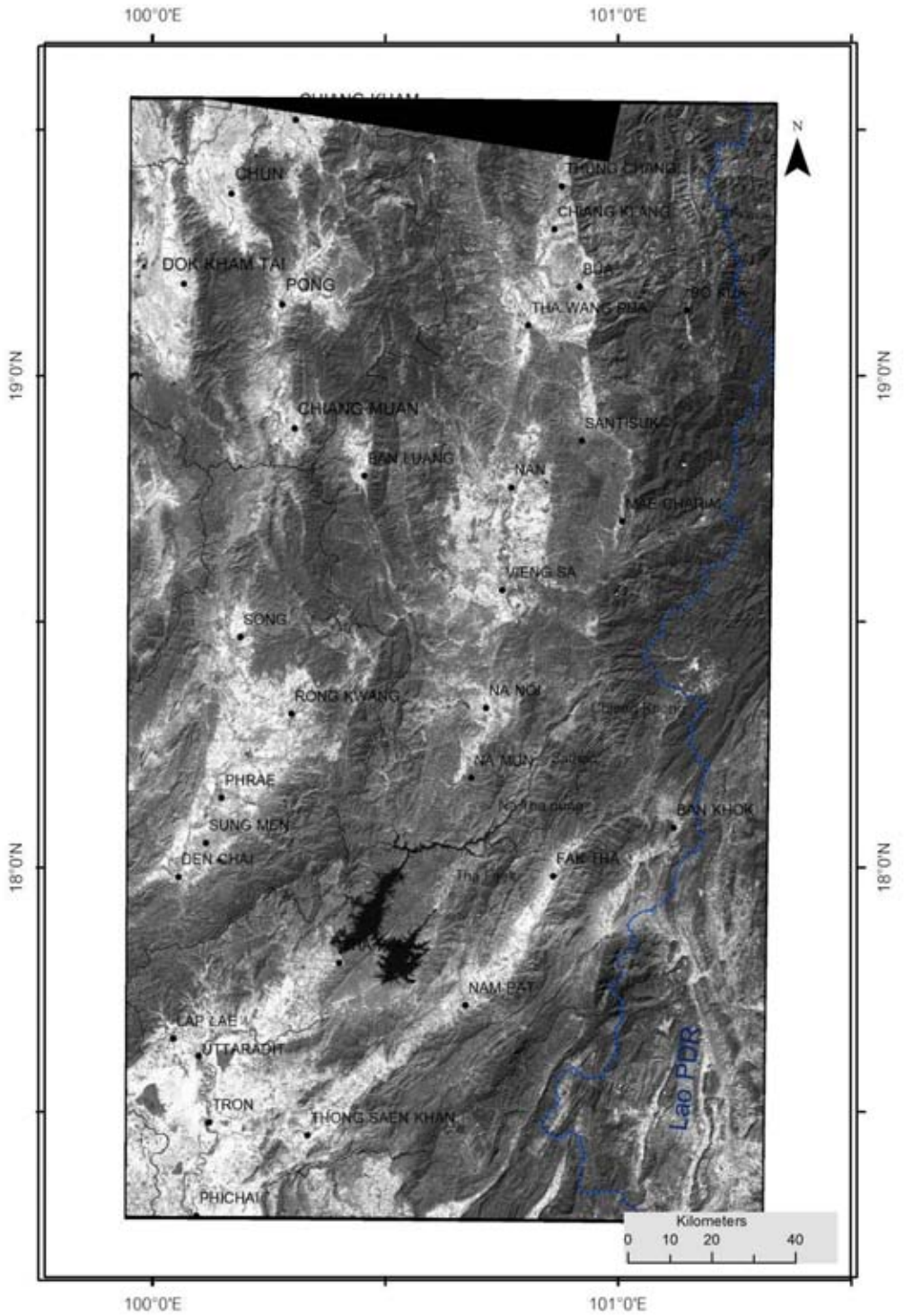

Figure 3.9 Landsat TM5 image map covering the study area in Nan-Uttaradit area, Northern Thailand.

2. The Shuttle Radar Topography Mission (SRTM)

SRTM is a digital topographic data of Earth surface with accuracy of the elevation data is 16 meters. Data Operating had done by National Aeronautics and Space Administration (NASA) in 2000. SRTM data is applied to clarify the Lineament of Study area, combined with other data set. SRTM data in this research are obtained from USGS (Edited by Consultative Group on International Agricultural Research, CGIAR), path 57 row 09, with 90x90 m sample spacing (Figure 3.10).

3.3 Verification data

1. Electromagnetic survey data

Electromagnetic data in this study are from horizontal loop electromagnetic survey (HLEM). The transmitter coils are kept and fixed as a coplanar, when surveying, the coils are moving along traverse line. Over the neutral ground, both inphase and quardrature are zero. Over a conductor, provided a measure of inphase and quardrature and expressed in percent of field intensity at the receiver. This survey method were done by MaxMin I system of Apex of Canada, reading 100 and 150m coil spacing and 8 frequencies (110, 220, 440, 880, 1760, 3520, 7040 qnd 14080 Hz). At each frequency can used at a depth depending on its skin depth (Surinkhum, 2002).

In order to verify the interpreted fault, ground checking is required. Electromagnetic survey is the common technique to locate mineral deposit, fault and fracture zone. If the interpreted lineament is correct, the result can be presented in a similar to EM anomalies.

2. Previous field data

In order to verify the airborne data processing, ground truth survey is required. There are many detailed geologic study in this area. If the processing anomalies are correct, there will be related to type and magnetic properties of rocks existence in field area.

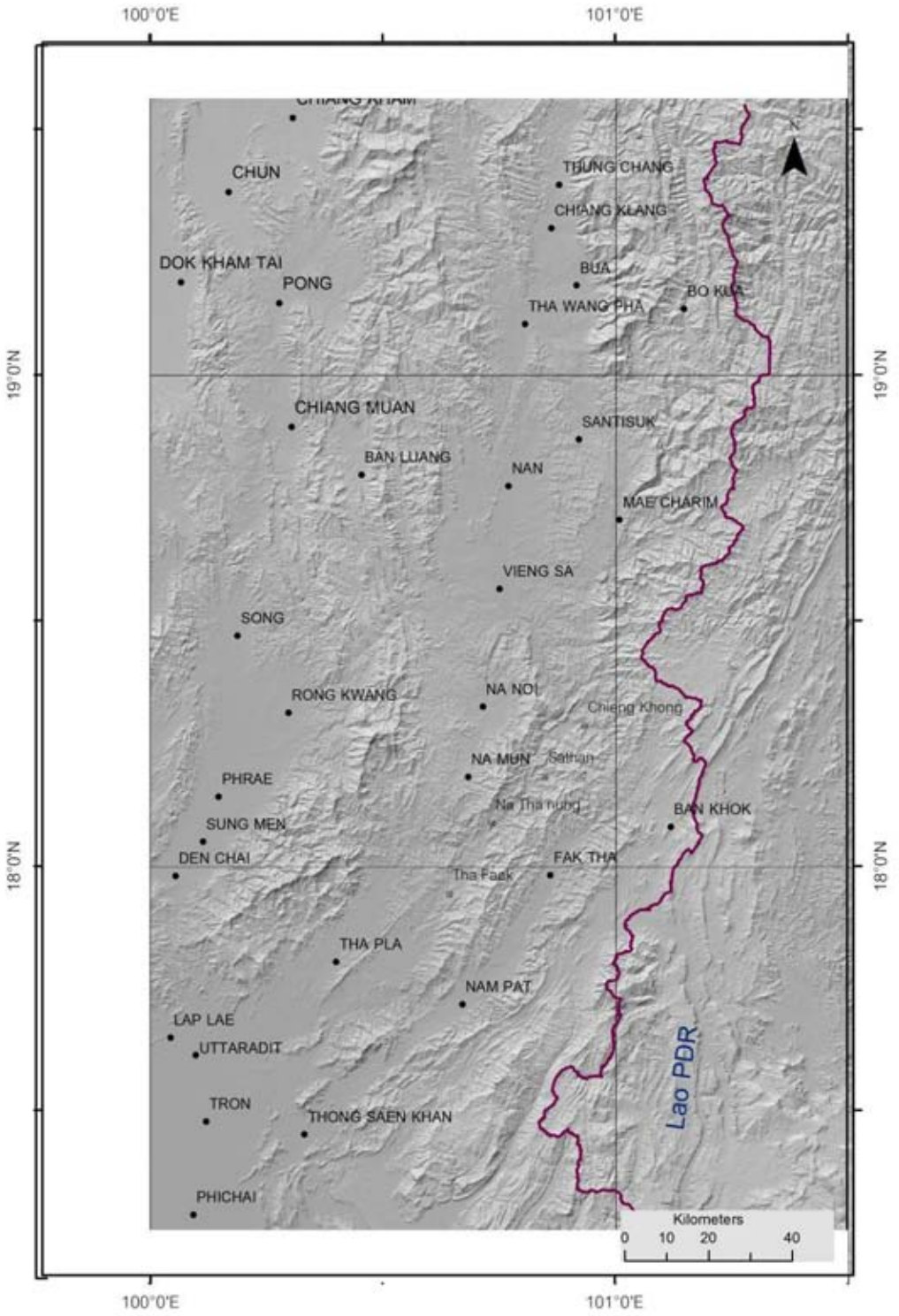

Figure 3.10 SRTM DEM map covering the study area in Nan-Uttaradit area, Northern Thailand.

Chapter IV Methodology

This chapter describes the methodology applied in this study.

4.1 Literature reviews

Literature review is to compile any relevant published and unpublished documents. It is therefore a guide to identify a scope of work and background problems. In this study, previous works are classified into 3 groups, previous geologic study, previous airborne study and previous mineralization study. From the literatures one can comprehend how the airborne geophysics data is applied in the past.

4.2 Airborne Magnetic Method

Airborne magnetic data interpretation of the study area is aimed to analyze anomalies, patterns and variation, correlated with geologic structures obtained from other data to comprehend the geologic and tectonic settings in this area. The sources of airborne magnetic data in this study are based on Nationwide database complied from survey A.

4.2.1 Data Enhancement Methods

Many enhanced techniques are apply to display the magnetic body characteristic (pattern, amplitude, trending and boundary). There are many technique used in this research as listed below.

Reduction to the pole (RTP)

All of magnetic latitude apart from N and S poles, the anomalies are asymmetric and do not corresponded simply with magnetic bodies. These make it hard to delineate the boundaries of the bodies causing the anomalies (Tulyatid, 1993). The reduction to the pole technique is done by recalculates of amplitude and spectra of the original grid, the shape of magnetic anomalies may be symmetric and appear like the positive anomalies located directly above the source at magnetic pole (Inclination angle = ±90°)

which can simplify the interpretation of the data. These can be described by diagram below (Figure 4.1). The study area has inclination 21.7 degree; the reduction to the pole will be effected by data process and will show in the next chapter.

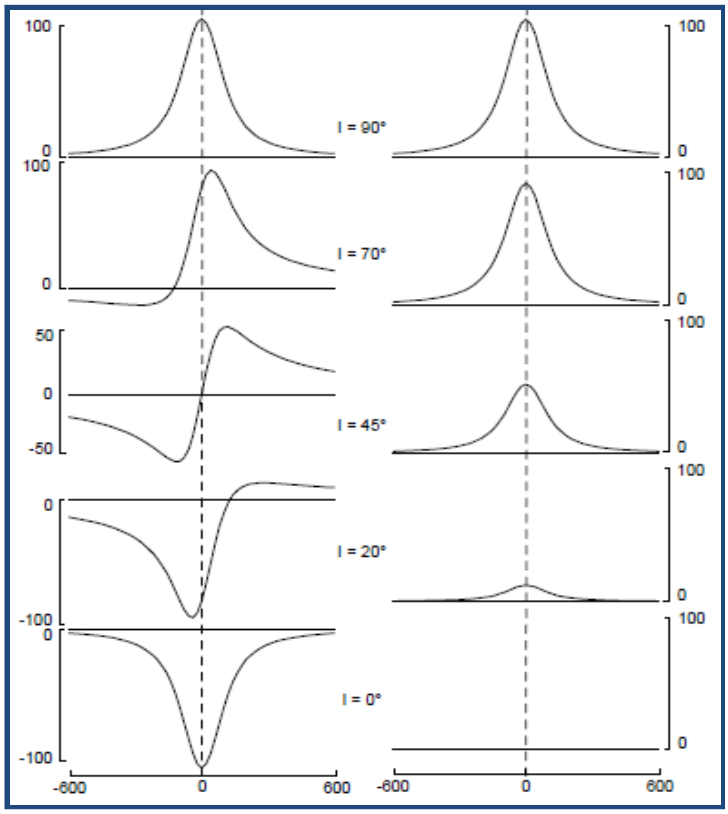

Figure 4.1 Shapes of total magnetic profiles depending on area. On the left side is the magnetic profile at different magnetic inclination and the right side is the profile after correcting to inclination of 90˚ (Macleod, 1993).

The First / Second Vertical Derivatives

The total magnetic field anomaly is broader than causative body, Interference between adjacent bodies are difficult to delineating body boundaries. And the deep but strongly magnetic body can be interfering to the shallow, less magnetic body (Figure 4.2). These can be solve by using Vertical derivative technique, the result anomalies after processing are sharper and posses zero value closed to the boundaries of the body (Tulyatid, 1993).

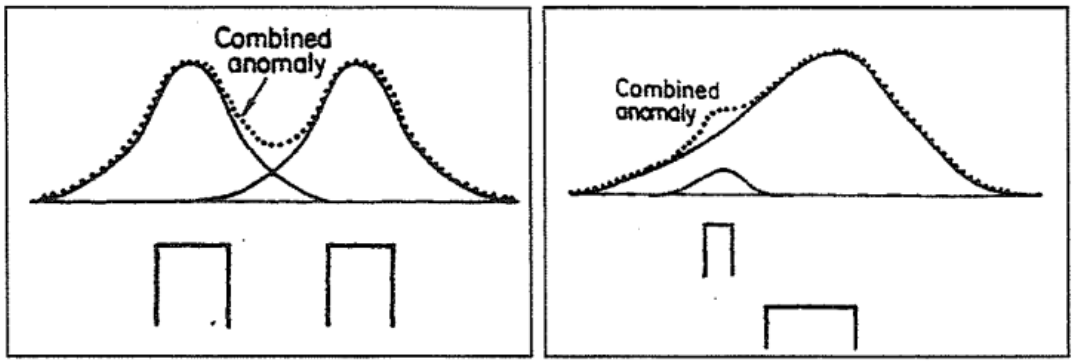

(a) (b)

Figure 4.2 Interpretation of magnetic survey routes

(a) Interference between adjacent magnetic bodies.

(b) Interference between deeply, strong body and shallow, less body (Paterson,1988).

Analytic Signal

The analytic signal is the combination of vertical and horizontal magnetic derivatives. The analytic signal is useful in locating the edge of magnetic source bodies; particularly where remnance are low magnetic latitude complicate interpretation. The analytic signal calculation is immune of the IGRF field, the magnetic anomalies will be properly shifted over the top of the causative bodies (Geosoft, 2003).

Automatic gain control (AGC)

Automatic gain control (AGC) is aimed to remove of amplitude from the data set, to producing an equal emphasis signal of low and high amplitude. AGC is trend to show coherent alignment that can not appear in true amplitude data, usefully for structural mapping.

Upward Continuation

The use of measurements of a field at one elevation, level or surface to determine the values of the field at a higher level. The technique is most often used to reduce scattered measurements to a common level for a simpler interpretation (Schlumberger's Oilfield Glossary, 2012). Upward continuation is considered a “clean”

filter because it produces almost no side effects that may require application of other filters or processes to correct. Because of this, this filter is often used to remove or minimize the effects of shallow sources and noise in grids (Geosoft Manual, 2011).

Downward Continuation

Downward continuation is used to enhance the responses from sources at a depth by effectively bringing the plane of measurement closer to the sources. Noted that it is not theoretically possible to continue through a potential field source. Since short wavelength signal can appear to be from shallow sources, it must be remove to prevent high magnitude and short wavelength noise in the processed data. The energy spectrum is also a good guide for determining the depth to which the data can be continued downward (Geosoft Manual, 2011).

Directional Cosine Filter

The directional cosine filter is very good for removing directional features from a grid. The cosine function makes the filter smooth. The rejection (or pass) notch can be narrowed or widened by setting the degree of the cosine function, so that highly direction features can be isolated (Geosoft Manual, 2011)

4.2.2 Interpretation Method

Many interpretation techniques are applied in this study and aimed to locate and delineate geologic structures in this area. Gunn et al. (1997) define that the methodology of interpretation are purposed to

- Boundary of magnetic units
- Structure dislocation of affecting of morphology of magnetic units
- Depth and attitude of magnetic units
- Superposition of magnetic units, lithologic units
- Chemical change
- Structure synthesis relating distribution of interfered Lithology and structure.

Tulyatid (1993) classified parameters of airborne magnetic data to the interpretation as listed below.

Signature of rocks

Different rock can cause of different response, this called the signature of rock that we can determined by following factors.

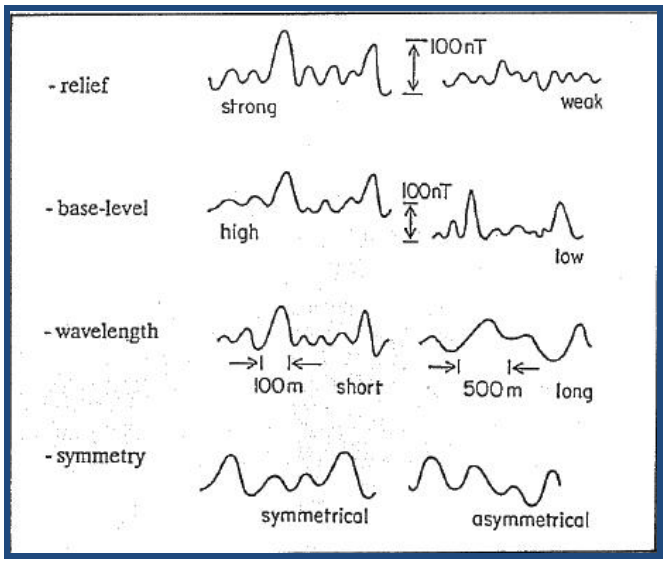

Figure 4.3 Different in wave forms showing signatures of the rocks (Tulyatid, 1993).

Lithologic Interpretation

Magnetite is not rock forming mineral, the spreading of magnetite depended largely on condition of recrystallization, metamorphism, tectonic, and alteration. The summarized data on rock and characteristic of magnetic body are shown in Table 4.1.

Table 4.1 summary of rock and characteristic of magnetic body (Tulyatid, 1993)

Rock	Characteristic of magnetic data
Sedimentary	Low relief and low base level Indistinct linear texture Linear coherent texture
Felsic Volcanic	Variable relief and average base level Linear to partly linear texture Fairly coherent texture Dependent on initial chemistry and metamorphic history
Mafic Volcanic	Variable to strong relief and average base level Linear to partly linear texture Usually coherent texture Very dependent on initial chemistry and metamorphic history
Felsic Intrusive	Variable relief and high base level Post tectonic : rounded to linear texture, often zoned Syn tectonic : granite show low relief, non linear and incoherent texture.
Mafic Intrusive	Variable to strong relief and high base level Post tectonic : rounded, seldom zoned Syn tectonic : texture similar to mafic volcanic
Ultramafic rocks	Strong relief and high base level Linear to fairly coherent texture Banded or zoned depended on serpentinization
Kimberlite	Similar to ultramafic rocks During weathering, alteration made a complex signature Some are non-magnetic

Structural Interpretation

Structural break (contact, fault, shears and unconformity) can be detected from magnetic characteristic as show in Figure 4.4.

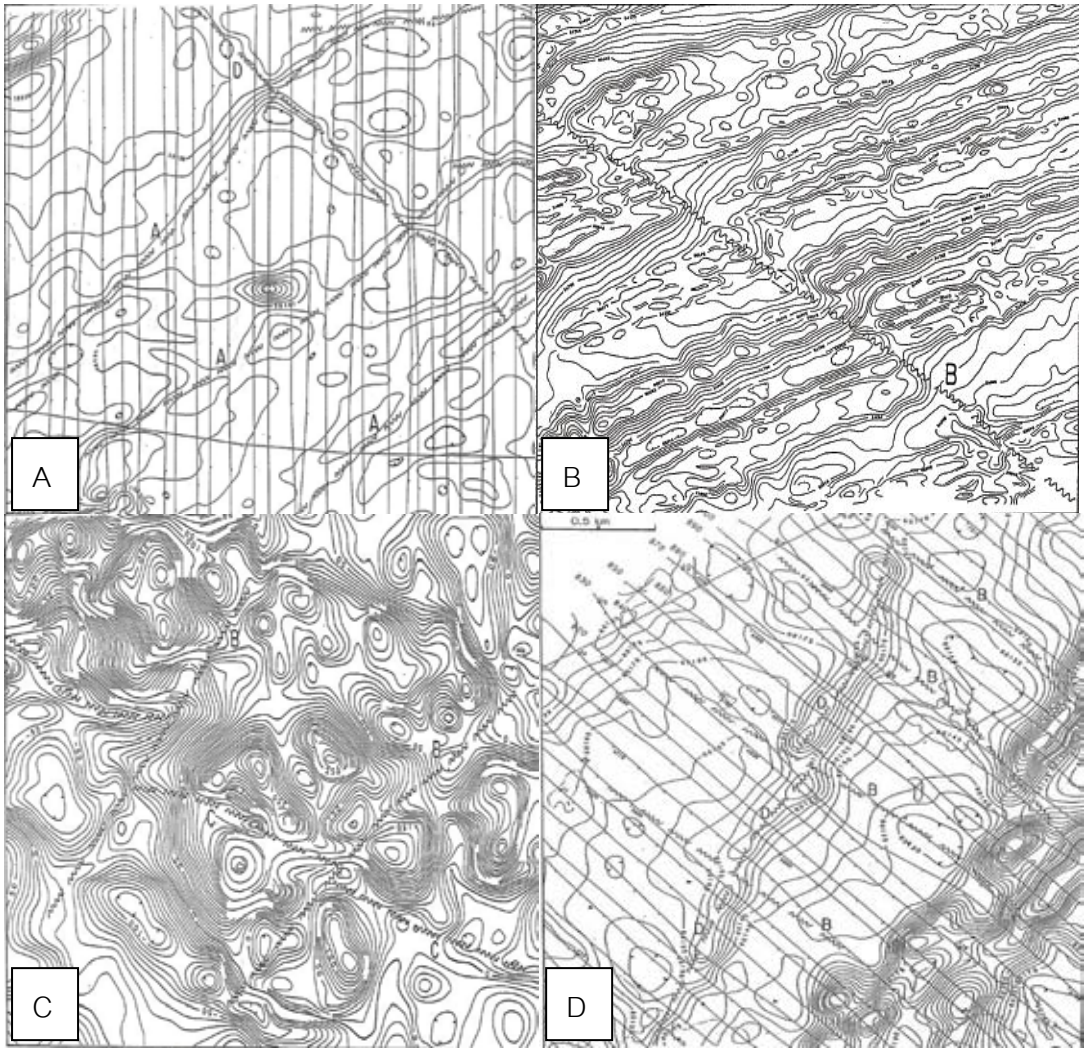

Figure 4.4 Structural interpretation from total intensity map (Peterson, Grant and Watson, 1988) showing

(a) Fault contacts in metavolcanics and igneous intrusive rocks

(b) A wrench fault with left lateral movement in metasedimentary rocks.

(c) Hydrothermal alteration fault zone in basic volcanic igneous rocks cut by cross fault.

(d) Hydrothermal alteration fault zone in metamorphosed volcano sedimentary rocks cut by wrench fault.

4.2.3 Modeling Method

Computer modeling is a tool to create a geological model to explain a geometry of subsurface structure. This research used Model Vision Inversion program to calculate and determined geometry of magnetic body and orientation (Neawsuparp, 2004) divided into 2 parts.

- Linear inversion technique

Linear inversion technique is subdivided observe magnetic field into a geometric bodies and find the magnetization for that shape, until magnetization is match to effect the bodies.

- Non-Linear Inversion technique

Non linear inversion technique is attempted to match between observe and calculated magnetic fields by interacted with unknown parameters and by estimating the parameter to fit the model.

4.3 Airborne Radiometric Method

Radiometric surveys is aimed to detect the natural radioactive emanations from rocks and soils. All detectable radiation come from the natural decay products of only three elements, uranium, thorium, and potassium at the surface of the ground. The radiometric survey is aimed to determine relative amounts of U, Th and K in the surface rocks and soils.

4.3.1 Data Enhancement Method

This study used Cooking technique to determine the intensity of radioactive elements. The red color is assigned to uranium, green and blue are to thorium and potassium respectively. Pairing of U, Th and K are examined to see how they relate to each other and how they are different from the total count.

4.3.2 Interpretation Method

Urquhart (2003) conclude that the interpretation of radiometric surveys are include of

-Changes in the concentration of U, Th and K accompany most major changes in lithology, so the method can be used as a reconnaissance geologic mapping tool in many areas.

-Variations in radioelement concentrations may indicate primary geological processes such as the action of mineralizing solutions or metamorphic processes.

-These variations also characterize secondary geological processes like supergene alteration and leaching.

-Radiometric surveys are capable of directly detecting the presence of uranium.

-This data can also assist in locating some intrusive related mineral deposits.

-Typical radioelement concentrations in earth materials are shown in Table 4.2

Table 4.2 Radioelement concentrations in earth material (Urquhart , 2003).

Rock Class	U (ppm)		Th (ppm)		K(%)	
	Mean	Range	Mean	Range	Mean	Range
Acid Extrusives	4.1	0.8 - 16.4	11.9	1.1 - 41.0	3.1	1.0 - 6.2
Acid Intrusives	4.5	0.1 - 30.0	25.7	0.1 - 253.1	3.4	0.1 - 7.6
Intermediate Extrusives	1.1	0.2 - 2.6	2.4	0.4 - 6.4	1.1	0.01 - 2.5
Intermediate Intrusives	3.2	0.1 - 23.4	12.2	0.4 - 106.0	2.1	0.1 - 6.2
Basic Extrusives	0.8	0.03 - 3.3	2.2	0.05 - 8.8	0.7	0.06 - 2.4
Basic Intrusives	0.8	0.01 - 5.7	2.3	0.03 - 15.0	0.8	0.01 - 2.6
Ultrbasic	0.3	0.0 - 1.6	1.4	0.0 - 7.5	0.3	0.0 - 0.8
Alkali Feldspathoidal Intermediate Extrusives	29.7	1.9 - 62.0	133.9	9.5 - 265.0	6.5	2.0 - 9.0
Alkali Feldspathoidal Intermediate Intrusives	55.8	0.3 - 720.0	132.6	0.4 - 880.0	4.2	1.0 - 9.9
Alkali Feldspathoidal Basic Extrusives	2.4	0.5 - 12.0	8.2	2.1 - 60.0	1.9	0.2 - 6.9
Alkali Feldspathoidal Basic Intrusives	2.3	0.4 - 5.4	8.4	2.8 - 19.6	1.8	0.3 - 4.8
Chemical Sedimentary Rocks*	3.6	0.03 - 26.7	14.9	0.03 - 132.0	0.6	0.02 - 8.4
Carbonates	2.0	0.03 - 18.0	1.3	0.03 - 0.8	0.3	0.01 - 3.5
Detrital Sedimentary Rocks	4.8	0.1 - 80.0	12.4	0.2 - 362.0	1.5	0.01 - 9.7
Metamorphosed Igneous Rocks	4.0	0.1 - 148.5	14.8	0.1 - 104.2	2.5	0.1 - 6.1
Metamorphosed Sedimentary Rocks	3.0	0.1 - 53.4	12.0	0.1 - 91.4	2.1	0.01 - 5.3

4.4 Remote Sensing Method

Two types of remote sensing data have been used - Landsat TM 5 and SRTM DEM data. This study is aimed to obtain the visual interpreted lineaments which indicate the geologic structure at the surface. The combined interpretation of Landsat TM5 and SRTM DEM data were done in order to compare with other data set.

4.4.1 Landsat TM5 Method

The image processing of Landsat TM5 data was done by using 2 enhancements method, band combination and principle component analysis techniques.

The band combination is used to improve the ability of image to identify contrast feature in the study area (mainly to delineate the Cenozoic basin). This study used band combination of 432, 754 and 741 (assigned red, green and blue respectively). This process is complete by Erdas Imagine program (version 8.0).

The principle component analysis (PCA) technique is to compressed information of all bands into a much smaller number and more interpretable than the source data. PCA is applied to the image that has high spatial resolution and a wide range of color that makes the different lithologic units easily discriminated (Amer, 2009). This study used PCA technique to improve data before visual interpreted lineaments by Arc Map program (version 10.0). Trending analysis of lineaments are done by rose diagram using Rock work program (version 15).

4.4.2 SRTM DEM Method

The image processing of SRTM DEM data done by using gray scale image to identify the lineaments.

The gray scale image of hill shade from SRTM DEM data (low area is black, high area is white) is easily to visual interpreted lineaments than color image. The gray scale image has done before visual interpreted lineaments by Arc Map program (version 10.0). Trending analysis of lineaments are done by rose diagram using Rock work program (version 15).

4.5 Verification method

In order to verify the interpreted data, ground truth is required. In this study, interpreted lineaments are verified with ground electromagnetic data and processed magnetic anomalies are verified with field data.

4.5.1 Ground Electromagnetic Verification Method

These ground survey of electromagnetic data is from horizontal loop survey (HLEM). The survey is measured inphase and quardrature of conductive anomalies which related to shear zones and faults. In this study made use of ground EM data by overlay the measured inphase and quardrature onto interpreted lineaments to verified that the lineament is corrected and correspondence with the real fault.

4.5.2 Field Verification Method

These field data are from the present field work and reports of Doi Puk Jum Peng – Doi Pu Lone, Tambon Sri Saket, Amphoe Na Noi, Nan (Munyue et al., 1986). This field data found many evidences of serpentinite and ultramafic rocks that indicate mélange zone. Moreover, they found geologic structure that can indicate the subduction zone and location of serpentinite are correspondence with the magnetic anomalies that processed from our study.

Chapter V Result and Interpretation

5.1 Result and Interpretation of Remote Sensing Data

Two types of remote sensing data were used for identifying structural lineaments in this study, namely Landsat TM5 data and SRTM DEM data. These two data are in rectangular form, so they are useful to visualize and interpret continuation of lineaments, structures and geologic formations together with their extension to western Lao. Several enhancement methods as well as previous geologic maps and EM data were applied to interpret the geologic structures and their lineaments of the Nan-Uttaradit study area. Interpretations of the results are shown in the detail below.

5.1.1 Landsat TM5 Data

To produce optimal multiband images for interpretation, band combination technique is selected in order to describe the workable and efficiently data better than original bands, Principle component analysis of enhancement is selected.

Figure 5.1 shows raw data of Landsat TM5 band 7 in gray scale. White color shows Cenozoic basins which are unclear, pale gray shows the moderate relief area and dark gray shows the high relief area. This data set is Landsat data map sheets 129/47, 129/48, 130/47 and 130/48, covering the Nan-Uttaradit and nearby areas.

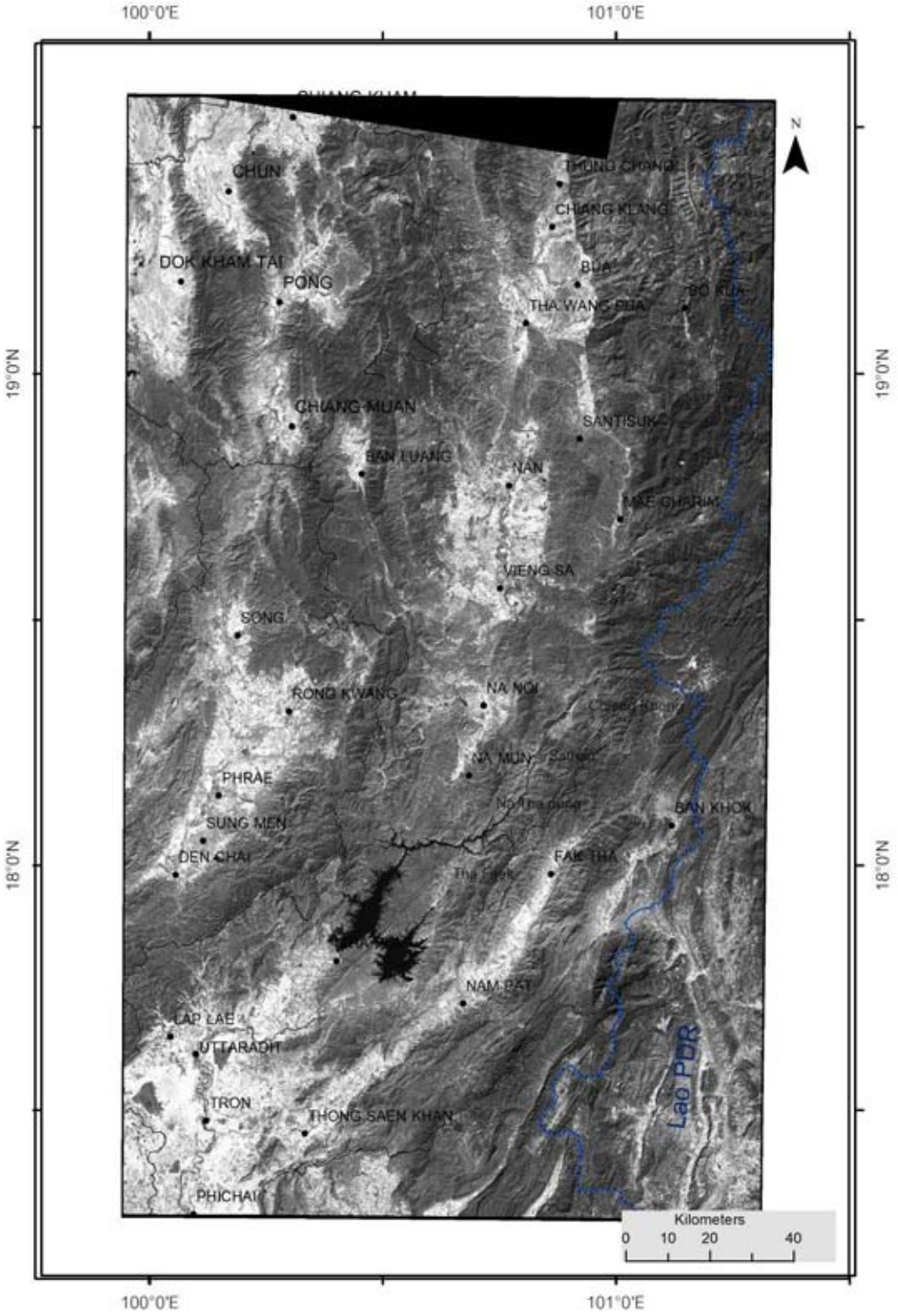

Figure 5.1 Raw data of Landsat TM5 band 7, showing location of the study area in Nan-Uttaradit region. Black color is the Sirikit reservoir.

1. PCA Map

Figure 5.2 shows the Landsat TM5 image data after applying principle component analysis (PCA) technique. This method is aimed to enhance image data to show better scenario of uncorrelated values of different images. The processed image displays hill shade and lineaments of the study area trending in the NE-SW direction. The dark to black color area to the west of Nam Pat and Tha Pla area is Sirikit Reservoir. It is also noted that complex folding and prominent lineations can be seen in the eastern part. There are complex of folding and lineation in the eastern part of lower area, maybe it come from deformation.

2. Band Composite Map

Figures 5.3, 5.4 and 5.5 show Landsat TM5 image data after applying band composite techniques. The initial data of band images are in gray scale but after the enhancement by combining 3 different bands to display better geological features in images.

2.1 Band 741

Figure 5.3a shows the Landsat map with combination of band 7, band 4 and band 1 (assigned band color to red, green, blue, respectively). It is the band combination map without interpretation. Figure 5.3b is the interpretation map shows prominent Cenozoic basins and structural lineaments. Major and important basins, such as Phrae, Na Noi, Vieng Sa, Nan, Pua and Nam Pat Basins, are clearly seen. The high-relief area shown in green color and the apparent lineaments in the eastern area trend in the NE-SW direction, from Thong Saen Khan to Nam Pat to Fak Tha and extending to Lao.

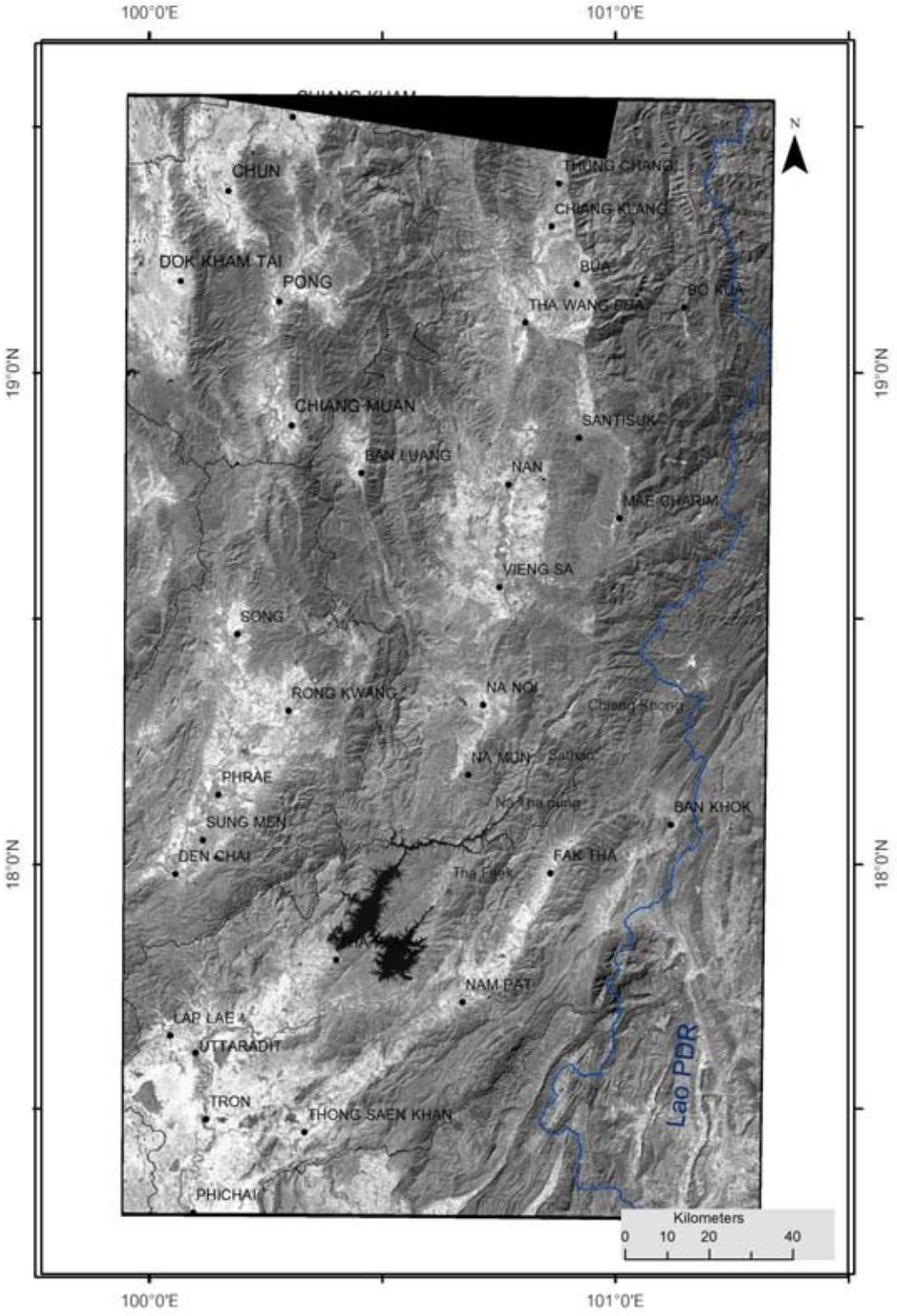

Figure 5.2 Landsat TM5 map of Nan-Uttaradit and nearby region after applying Principle component analysis technique.

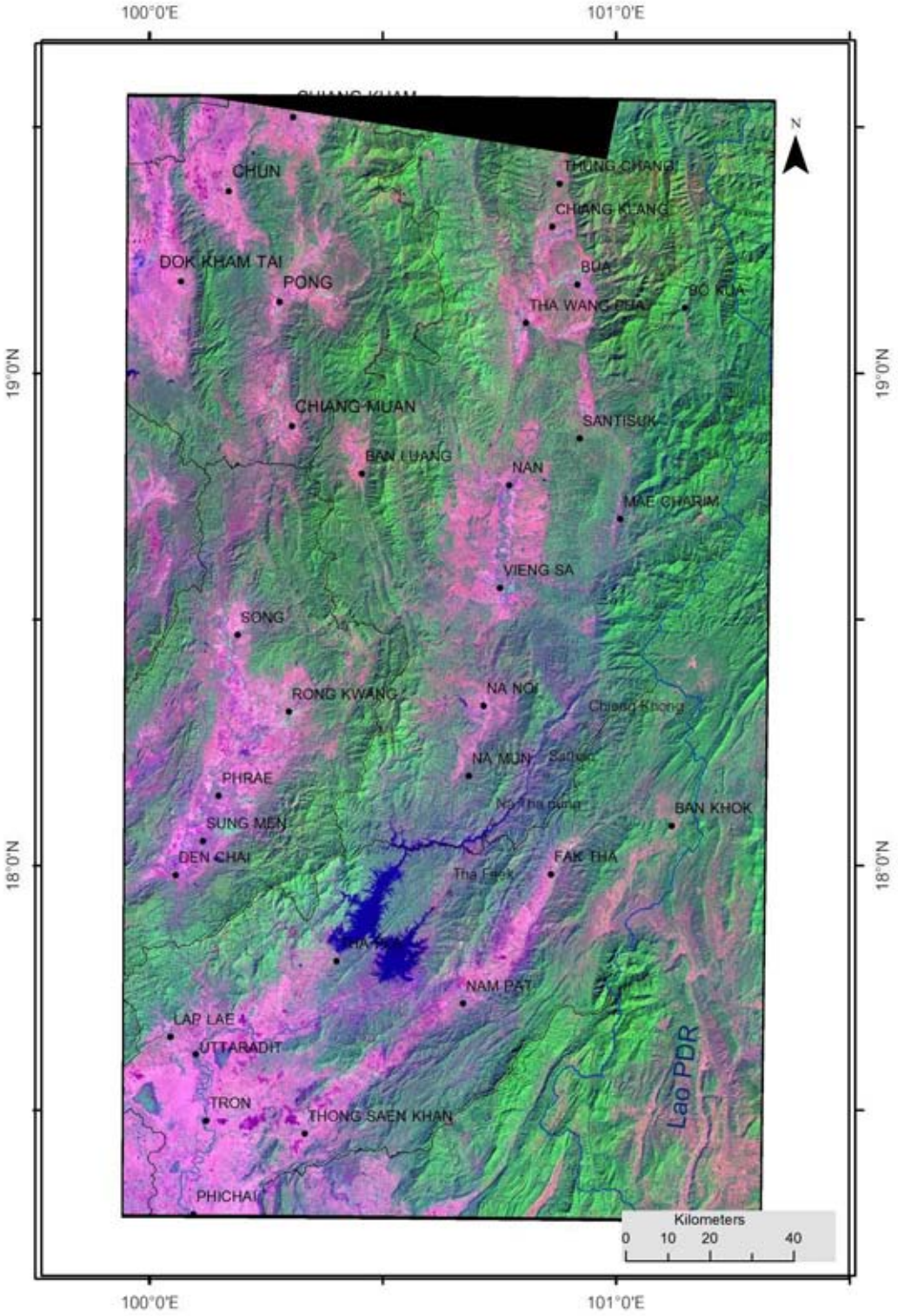

Figure 5.3a Landsat TM5 image data with combination of bands 7, 4 1 (assigned band color to red, green, blue respectively), showing location of the Nan-Uttaradit and nearby areas.

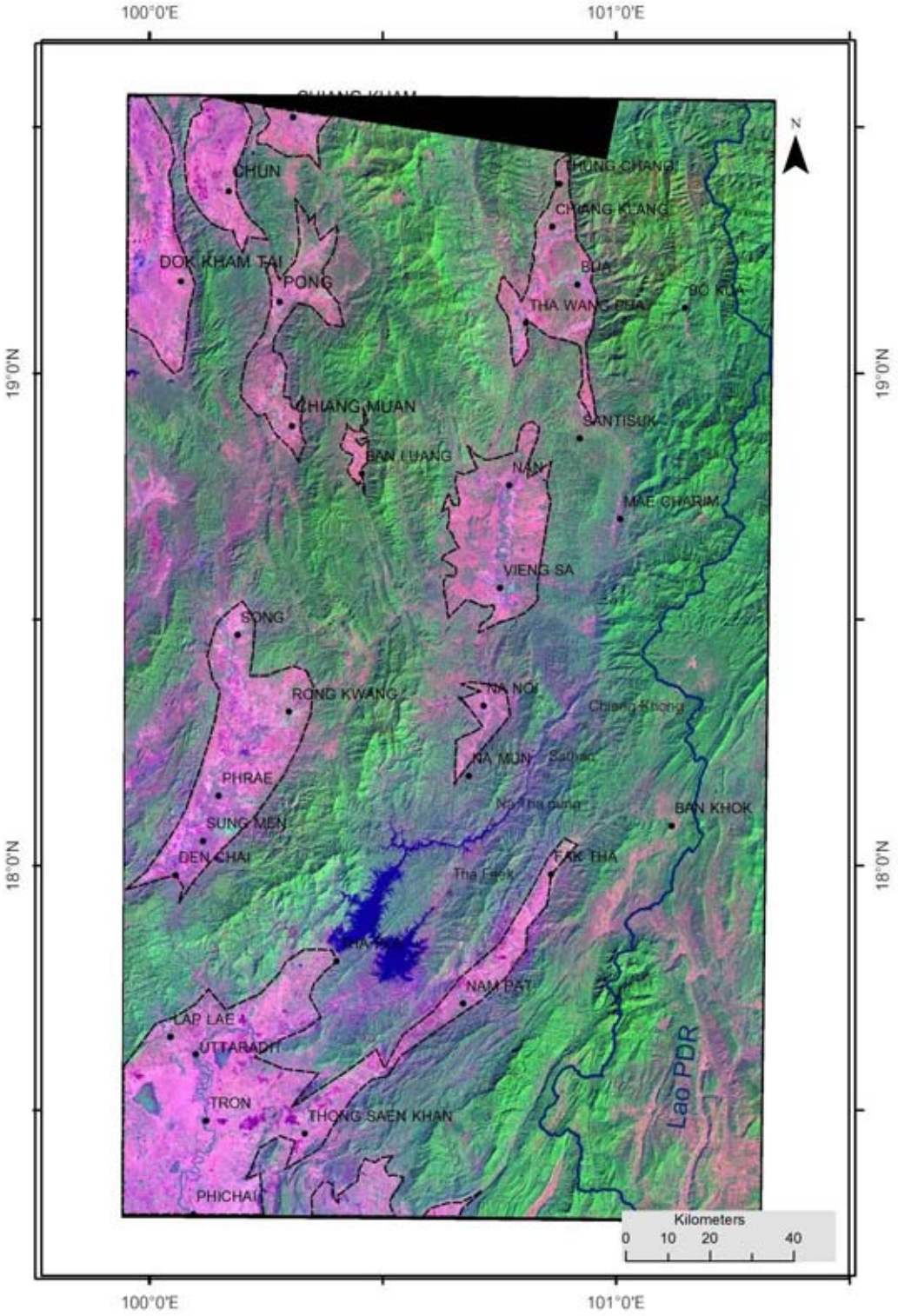

Figure 5.3b Landsat TM5 image data with composite bands 7, 4 1 of the Nan Uttaradit area, showing orientation and distribution of Cenozoic basins (basin boundary in black).

2.2 Band 754

Figure 5.4a is the enhanced Landsat map showing combination of bands 7, 5 and 4 (assigned band color to red, green, blue, respectively). Fig 5.4b is the interpretation map with the high-relief area shown in blue color, apparent lineaments in the eastern area trending in the NE-SW direction, and lineaments clearly extending to Lao in the Ban Khok area. Besides all the Cenozoic basins are also enhanced.

2.3 Band 432

Figure 5.5 shows the enhanced map (a) and the interpretation map (b) with combination of bands 4, 3 and 2 (assigned band color to red, green, blue, respectively). The high-relief area shown in red color whereas the apparent lineaments in the eastern area trending in the NE-SW direction, and forwarding to Lao PDR.

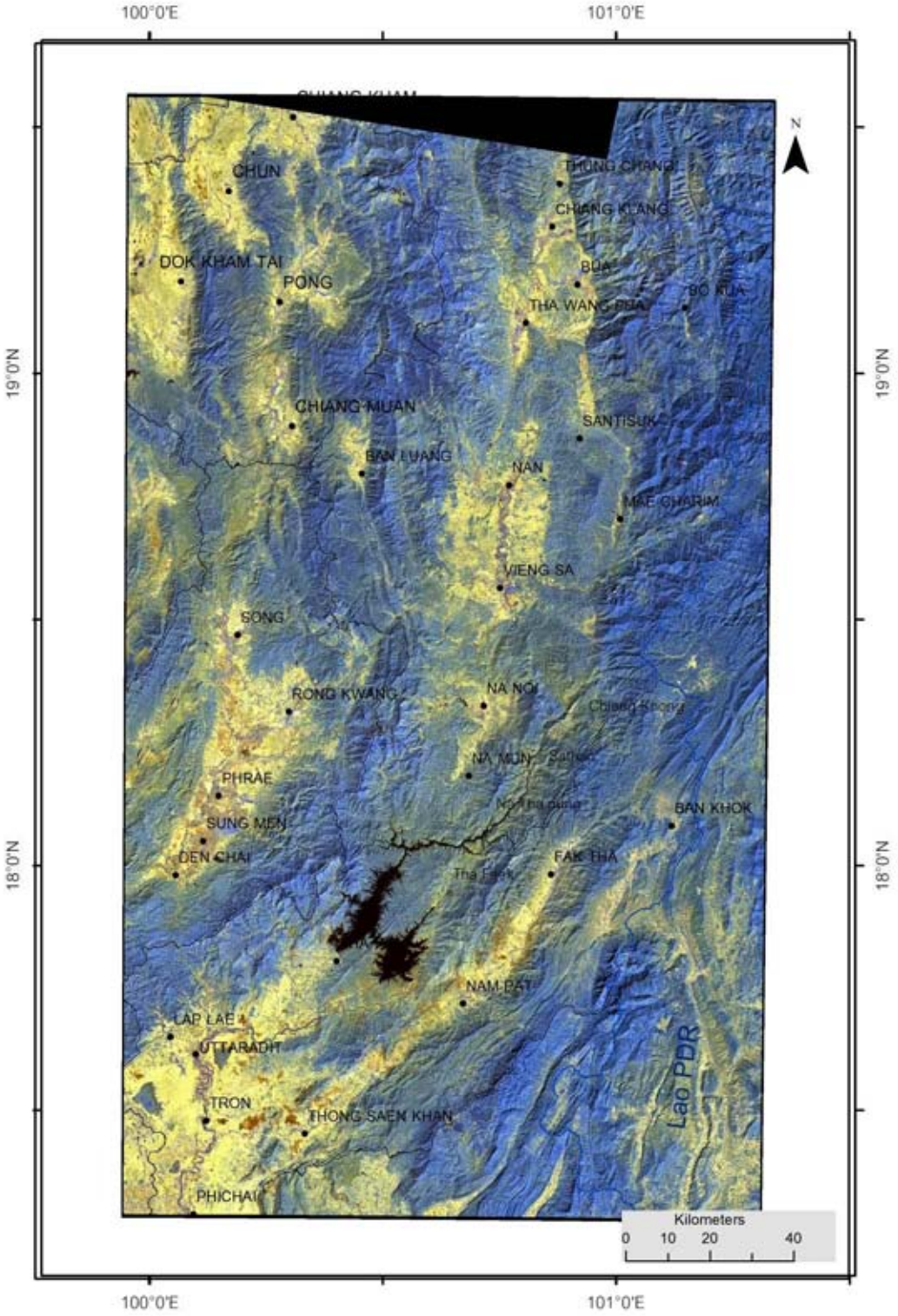

Figure 5.4a Landsat TM5 image data of composite bands 7, 5, 4 (assigned band color to red, green, blue respectively), showing location of the Nan-Uttaradit and nearby areas.

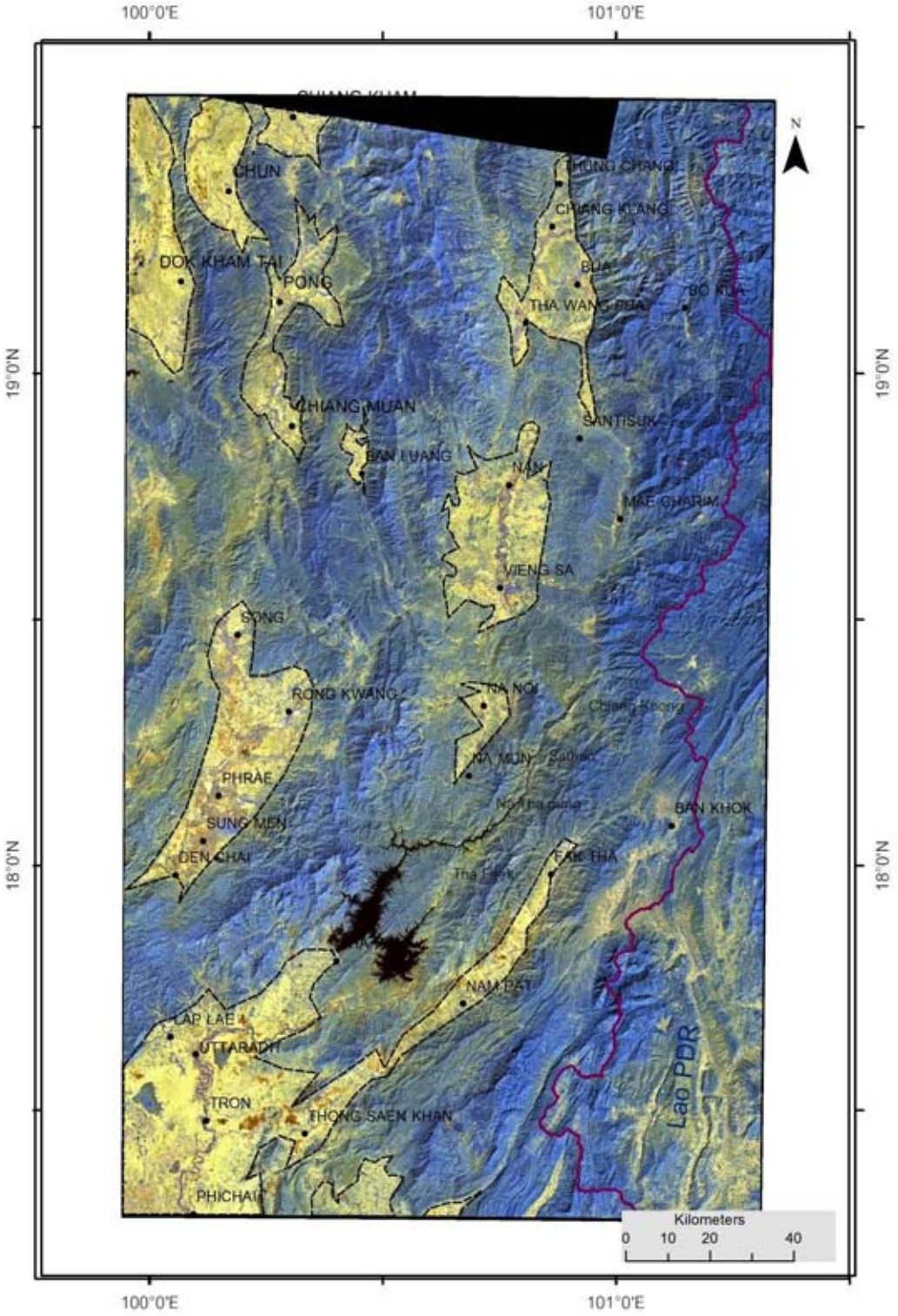

Figure 5.4b Landsat TM5 image data with composite bands 7, 5, 4, showing orientation and distribution of Cenozoic basins (basin boundary in black) in the Nan-Uttaradit and nearby areas.

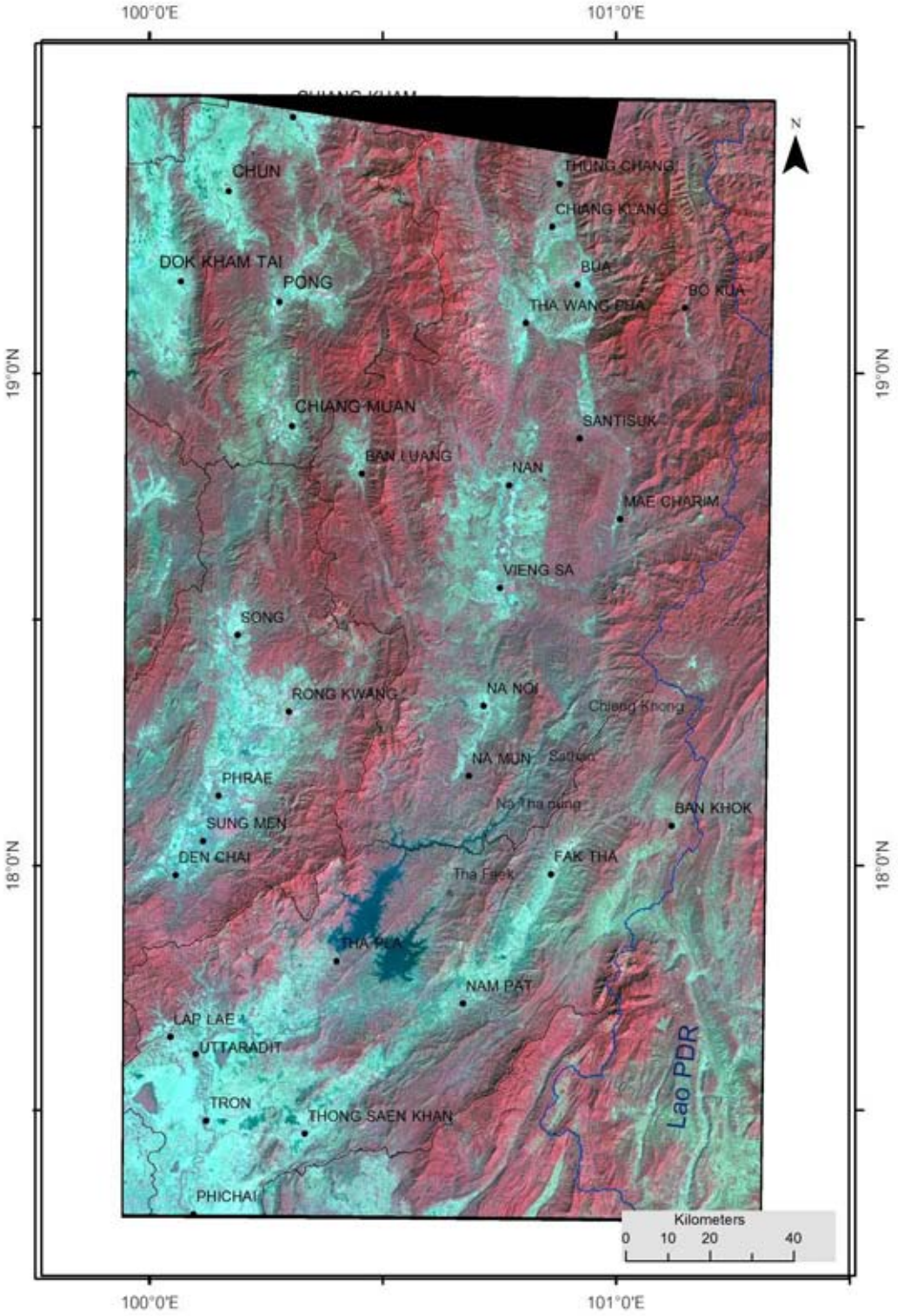

Figure 5.5a Landsat TM5 image data with composite bands 4, 3, 2 (assigned band color to red, green, blue respectively), showing location of the Nan-Uttaradit and nearby areas.

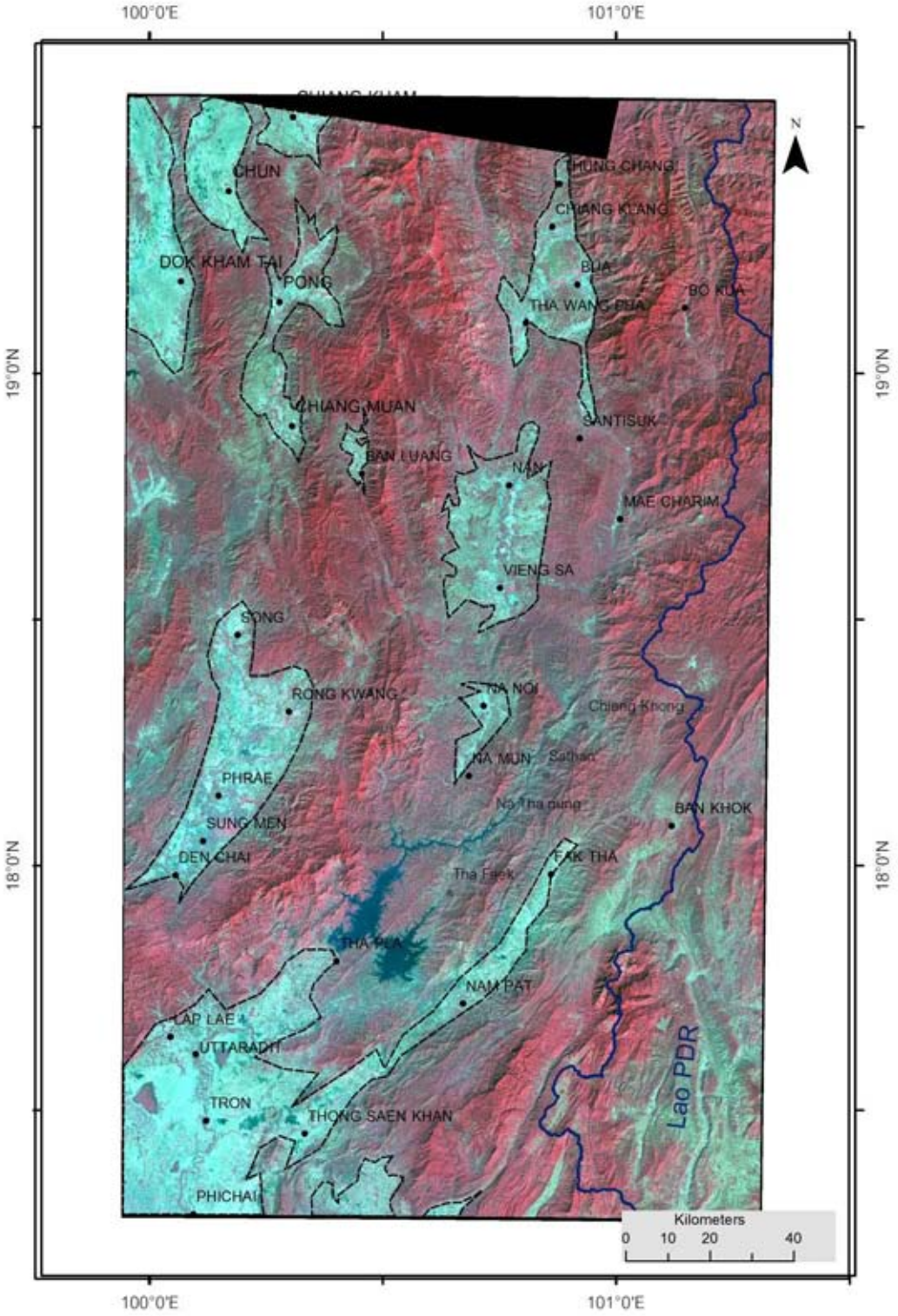

Figure 5.5b Landsat TM5 image data with composite bands 4,3,2, showing orientation and distribution of Cenozoic basins (basin boundary in black) in the Nan-Uttaradit and nearby areas.

3. Lineaments from Landsat TM5 data Map

Figure 5.6 displays lineaments interpreted from PCA technique. An insert box displays a rose diagram that major lineaments are in NE-SW direction. Noted that some lineaments bound the basins. Such lineaments are interpreted as faults, such as those nearby Nam Pat, Pua Basins. Phrae Basin is bounded by NNE-SSW trending lineaments in the western basinal margin and NE-SW trending lineaments in the eastern margin. On the other hand, Nan and Pua Basins are bounded to the east by almost N-S trending faults.

Based on the enhanced Landsat TM5 images, the result also shows that lineaments with somewhat bending and curving are recognized in the north. Their trends are roughly in the NNE to NE-SSW to NW in the north and swing to N-S and NNW-SSE in north of Song and Wiang Sa – Nan areas and deviate back to the NE-SW direction. However the zone dominated by NE-SW trend is obvious from Chiang Khong – Ban Khok towns in the north to Thong Saen Khan and Lap Lae towns in the south. The total length in Thailand is about 10.59 km.

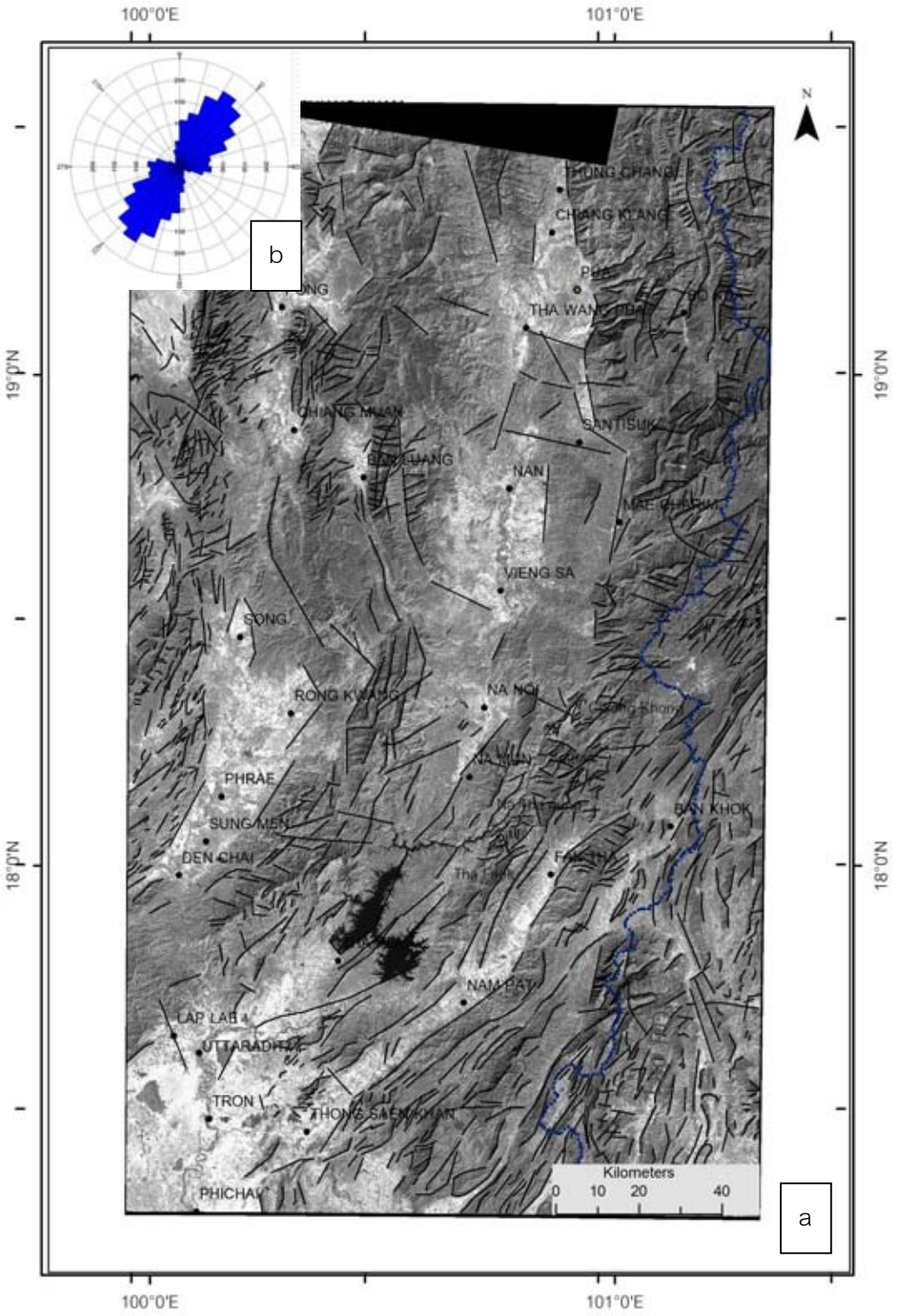

Figure 5.6a Landsat TM5 map with the visually interpreted lineaments from Principle Component Analysis (PCA) technique. (b) An insert box showing a rose diagram from 1,505 points with 2 km./point) showing major lineaments in NE-SW direction.

5.1.2 Result and Interpretation of SRTM DEM data

In this study image of SRTM (Shuttle Radar Topography Mission), operated by NASA and with the resolution of 90 m, is used for interpreting lineaments and associated structures. For the Nan- Uttaradit area, path 57 row 09, with 90x90 m sample spacing have been applied. The result displays 2 major trends similar to those detected by the Landsat TM5 – the more prominent one in the NE-SW direction and the less prominent in the NW-SE direction. Detail description is shown below.

1. SRTM DEM Map

Figure 5.7 illustrates raw data of SRTM digital elevation map in gray scale. There are the clearly observed high-relief area and lineaments from this data, because the SRTM map has higher resolution than Landsat map. So it is clear that lineaments in the eastern area are quite more obvious and extend northeastward to Lao.

2. Lineaments from SRTM DEM Map

Figure 5.8a shows visual interpretation of lineaments derived from SRTM DEM image data using Arc Map 10. The image map clearly displays several low-relief area, such as Nan, Na Noi, Bua, Tha Pla and Phrae Cenozoic basins. The N-S trending lineaments north of Phrae area and the N-S trending ones in the south of study area, in Lao are also obvious.

From the interpretation of the enhanced space-borne image data, several N-S trending Cenozoic basins are determined. These basins are inferred to have been controlled and bounded by several associated faults. Some basins are curvilinear possibly due to subsequence and continuous tectonic stress. Good examples are fault to the west of the Phrae Basin (or Phrae City) and a lineament to the east of Song township. Lineaments seem to be in the N-S direction in the north and become curved and change their direction to the NE-SW direction in area between Amphoe Tron, Fak Tha, Nam Pat and Tha Pla districts. These lineaments become in the approximately NNE-SSW to NE-SW direction again in the south of the Thong Saen Khan and Nam Pat areas. However in Laos area, particularly to the east of Nam Pat and Ban Khok

townships, the prominent lineaments are in the N-S direction. Figure 5.8b display rose diagram with major or long lineaments in the NE-SW direction and minor (short) lineaments in the NNW-SSE direction. They are much more clear in the high relief areas.

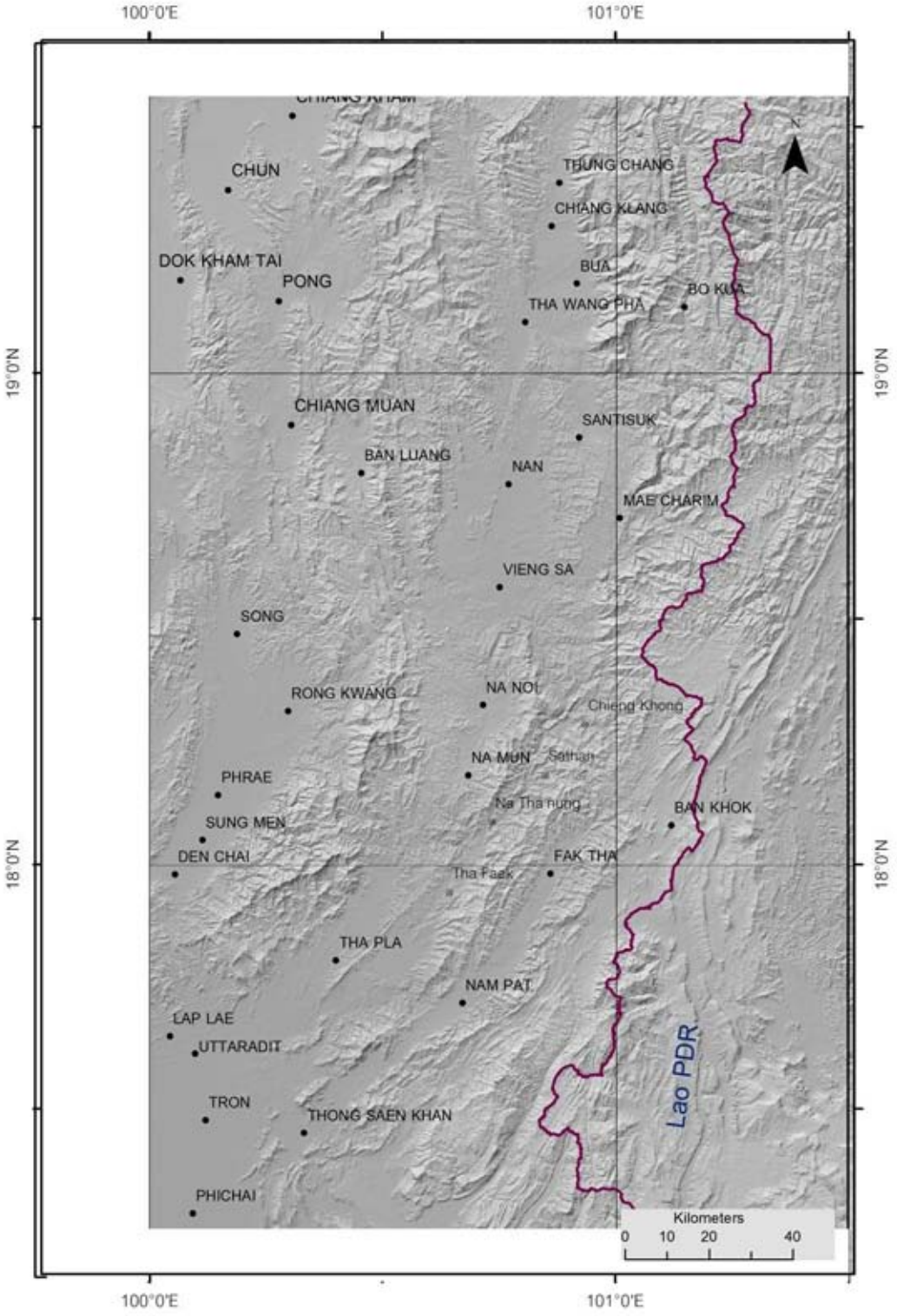

Figure 5.7 Raw data of SRTM DEM image map in grey scale showing location of the Nan-Uttaradit and nearby areas. Noted that there exist prominent lineaments from Ban Khok in eastern most Thai border to west-central Lao PDR.

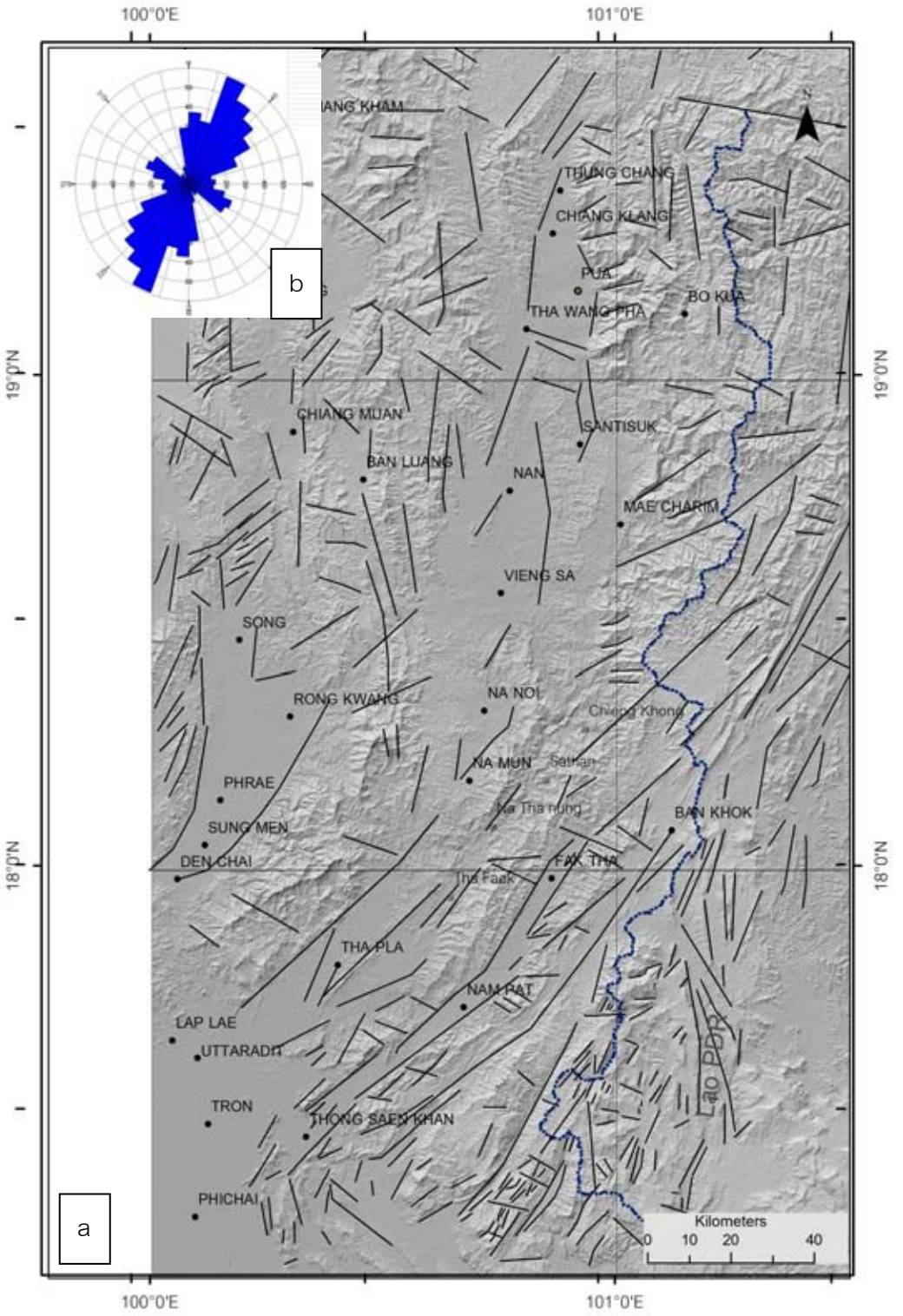

Figure 5.8(a) Visual interpretation of lineaments from SRTM DEM image of Nan-Uttaradit area. (b) rose diagram based upon 443 points (with 2 km/point) showing major lineaments in the NE-SW direction and the minor ones in the NW-SE direction.

5.2 Airborne Radiometric Data

5.2.1 Uranium Content Maps

Figure 5.9 a shows composite color of uranium contents by using ranges of colors. The very low contents on scale bar are in dark blue and blue green colors, the very high content are in red and pink colors. The interpretation of the uranium-content map is shown in Figure. 5.9 b. The map shows various values of uranium contents ranging from 0.49 to 8.34 ppm, which can be divided into 3 different domains.

The Southern domain has obviously low to very low uranium contents, with small, isolated high spots of uranium. No subdomains can be further divided. This domain is located fareast of Thong Sean Khan town. Large part of this domain is located in Laos, but the domain shows faint lineation in the NE-SW direction.

The central domain can be further subdivided into 3 subparallel subdomains (upper, central and lower), all of them are characterized in general by the lowest uranium content incorporated with spots and areas of high uranium content. The narrow band (12 km wide) of the lowest content in the central subdomain (Chiang Khong – Tron zone) trends in the NE-SW direction. This band is sandwiched between the subparallel bands with the higher uranium contents which the width is about 8 to 18km and the length is from 4 to37 km. parallel to the band of high content in the southern area.

The Northern domain shows high to highest uranium contents. At least four subparallel subdomains are recognized. Each subdomain has the length of about 160 km. and the width of 26 to 52 km. The highest content are shown as large spot within the roughly N-S trending arcuate zone in the western part and the rest are the arcuate parallel zones with low to moderate uranium contents. As shown in the interpretation map (Figure 5.9b), some NE to NNE – SW to SSW trending lineaments in the northern domain are interesting. There are the long F1 lineament passing east of Chan and Dok Kham Tai town and the long F2 lineament passing Pong, Song and Den Chai town. The short, NE-SW trending F3 and F4 lineaments cutting high uranium bodies are well defined at SE of Nan city and NE of Uttaradit city, respectively.

The basin in Uttaradit (or Uttaradit Basin) shows high uranium spots in the northern part whereas the Na Noi and the Wiang Sa Basins has low contents of uranium. The Nan Basin has very high contents of uranium in the western side of the basin.

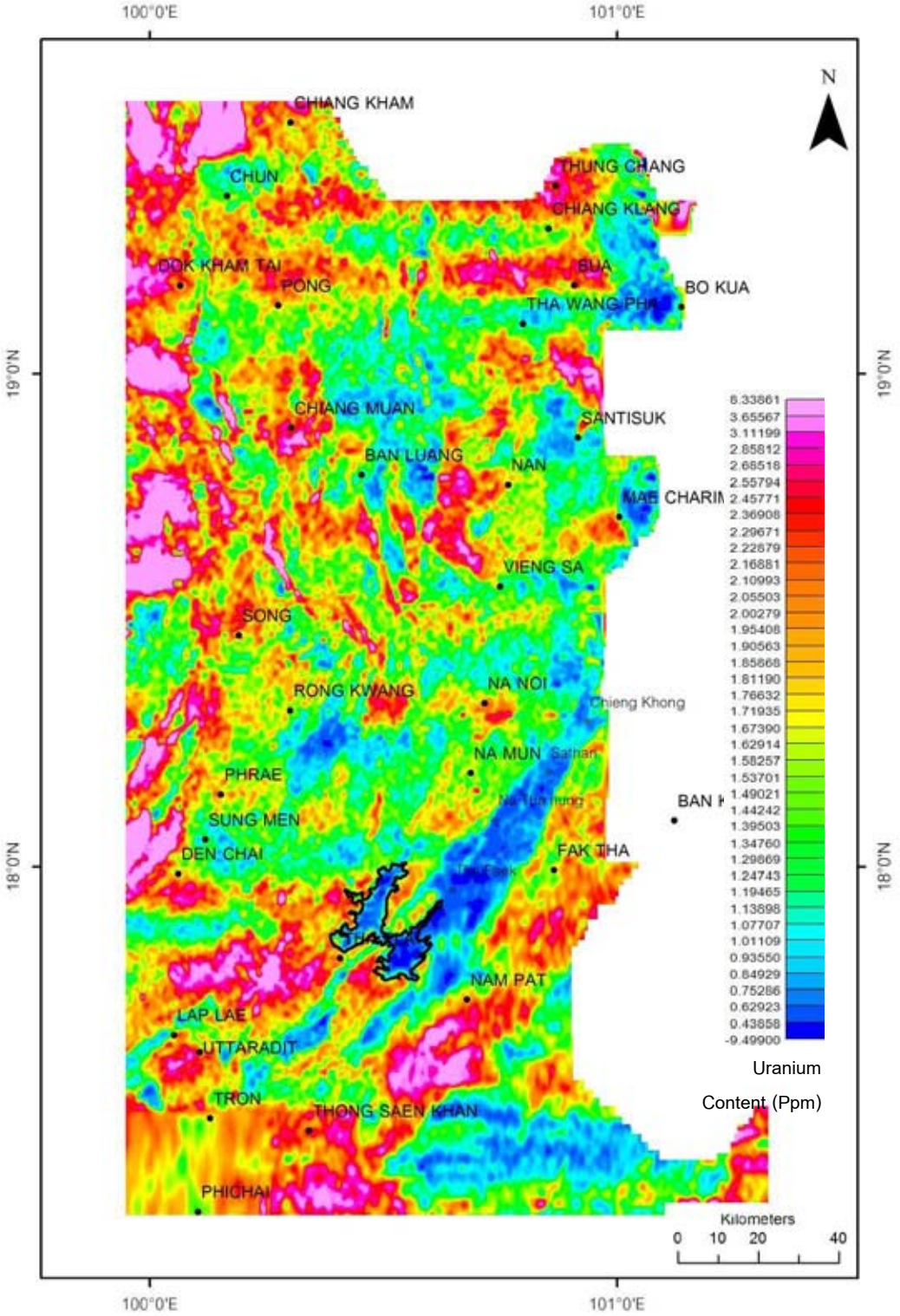

Figure 5.9a. Airborne radiometric map of study area showing the concentration of Uranium (eU). (Sirikit reservoir boundary in black)

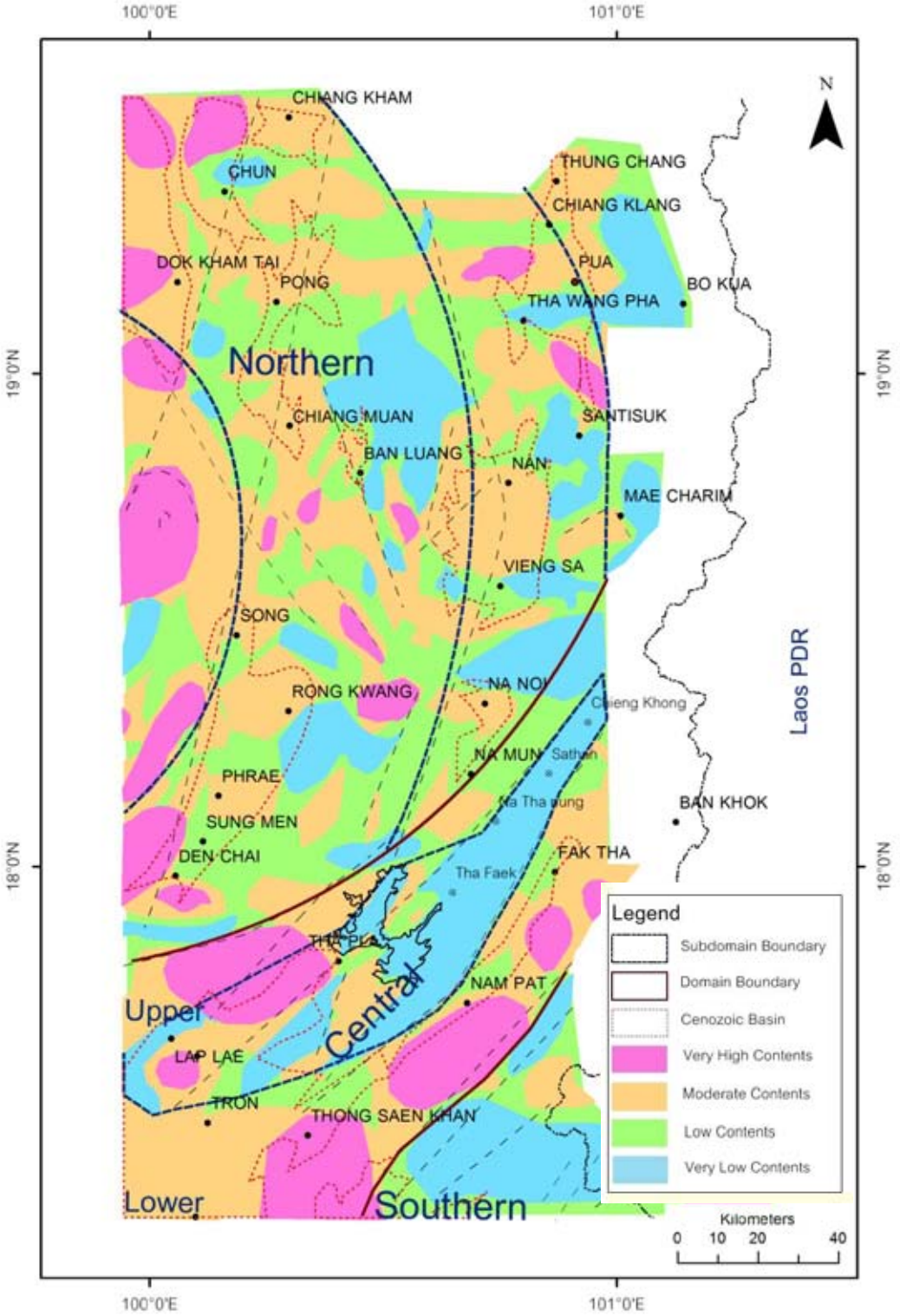

Figure 5.9b Radiometric (Uranium Concentration) data interpretation map showing 3 major domains (north, central and south) and their subdomains in the Nan-Uttaradit area.

5.2.2 Potassium Content Map

Figure 5.10a, illustrates composite colors of potassium contents by applying range of colors. The very low contents on scale bar are in dark blue and blue green colors, and the very high contents are shown in red and pink color. The interpretation of the potassium content map is shown in Figure. 5.10 b. Like that of the uranium contents, the map also shows 3 domains based upon degrees of potassium contents ranging from 0.11 to 3.26 %K.

The southern domain of the potassium map shows low to very low potassium contents. This domain has the clear pattern better than that of the uranium map. The domain has the sharp western boundary with the central domain. Lineations within the domain are less obvious, they are mainly in the NE-SW direction.

The central domain shows the very low to low potassium content incorporated with low potassium content. However when comparing with the uranium map (Figure 5.9b), subdivision into 3 subdomains (upper, central and lower zone) are less clear than those of the uranium map. The central domain has the width of about 50-75 km. It has the NE-SW trend and extend from Chiang Khong to Fak Tha Cities in the north to Phi Chai and Lap Lae Cities in the south. The central subdomain (or the Chiang Khong – Tron zone) is the most obvious and is characterized by the very low content of potassium content. In the central subdomain, lineaments with the NNE-SSW trend are also observed. The upper and lower subdomains which sandwich in the northern and southern boundaries of the central subdomain are less observed. The upper subdomain (20 km. wide) with the cross-cut NNE-SSW lineaments is characterized by the intermediate to low potassium content with somewhat high potassium contents in the central portion. The lower subdomain (20 km. wide) is characterized by the lower potassium content. No cross-cut lineaments are determined in this subdomain. The very low potassium content in central zone are trending in NE-SW direction. Additionally, there are small areas with moderate potassium contents at Fak Tha township.

The northern domain shows high to moderate potassium contents. The highest potassium content are shown as a large spots within the N-S trending arcuate zone in

the western subdomain but show different potassium content at the northern part and southern part of Amphoe Ban Luang. In the eastern part show a parallel band of N-S direction.

Similar to the result from the uranium contents, the northern domain of the potassium content can be subdivided into 3 subdomains, the western subdomain with the high potassium content, the central subdomain with low to intermediate potassium content and with the high potassium content zone between Rong Kwang and Chiang Muan in the central portion. The eastern subdomain contains sporadic spots of the lower potassium content in Nan and Na Noi areas with patches of high potassium content.

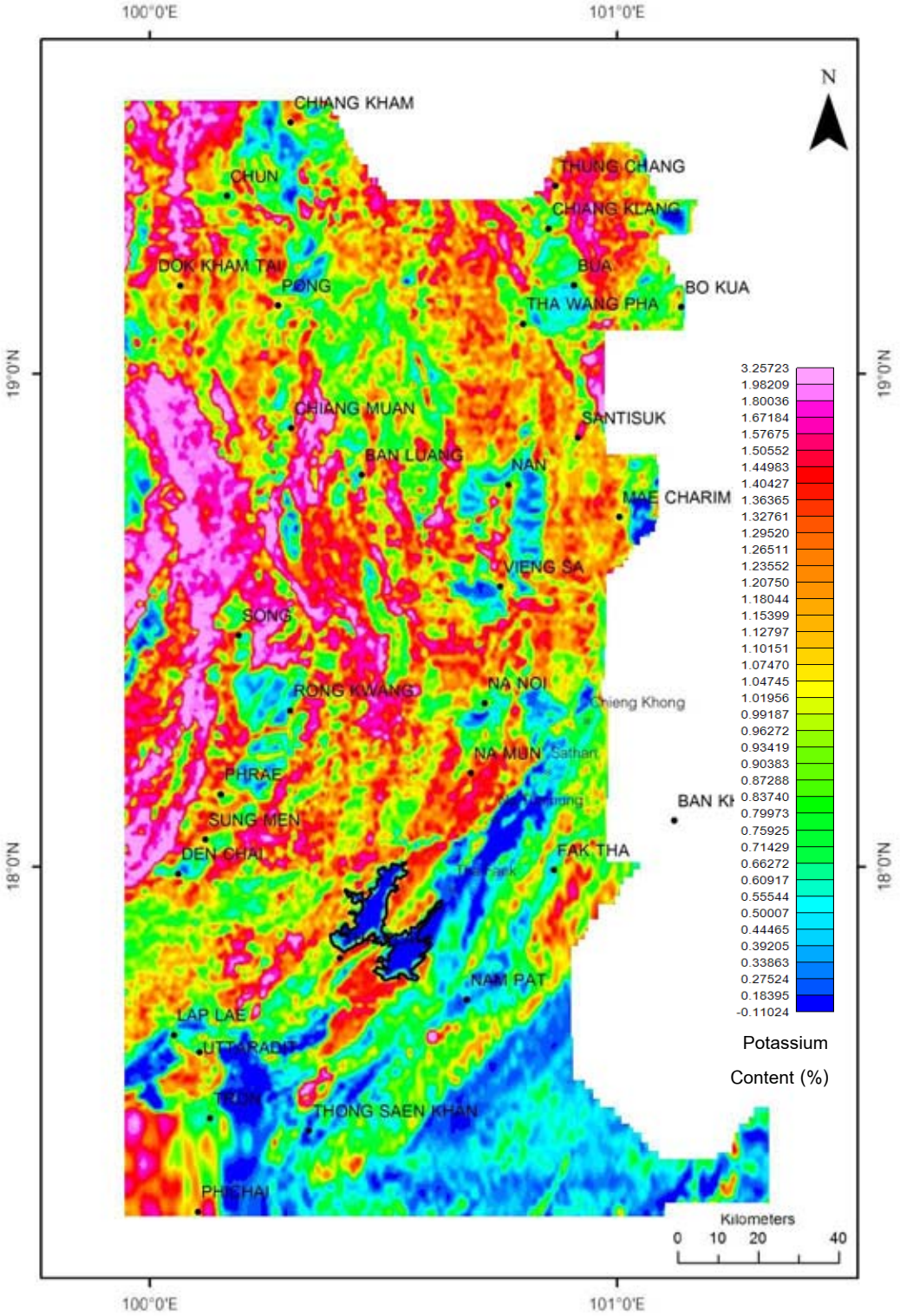

Figure 5.10a Airborne radiometric map of study area showing the concentration of Potassium (%K). (Sirikit reservoir boundary in black).

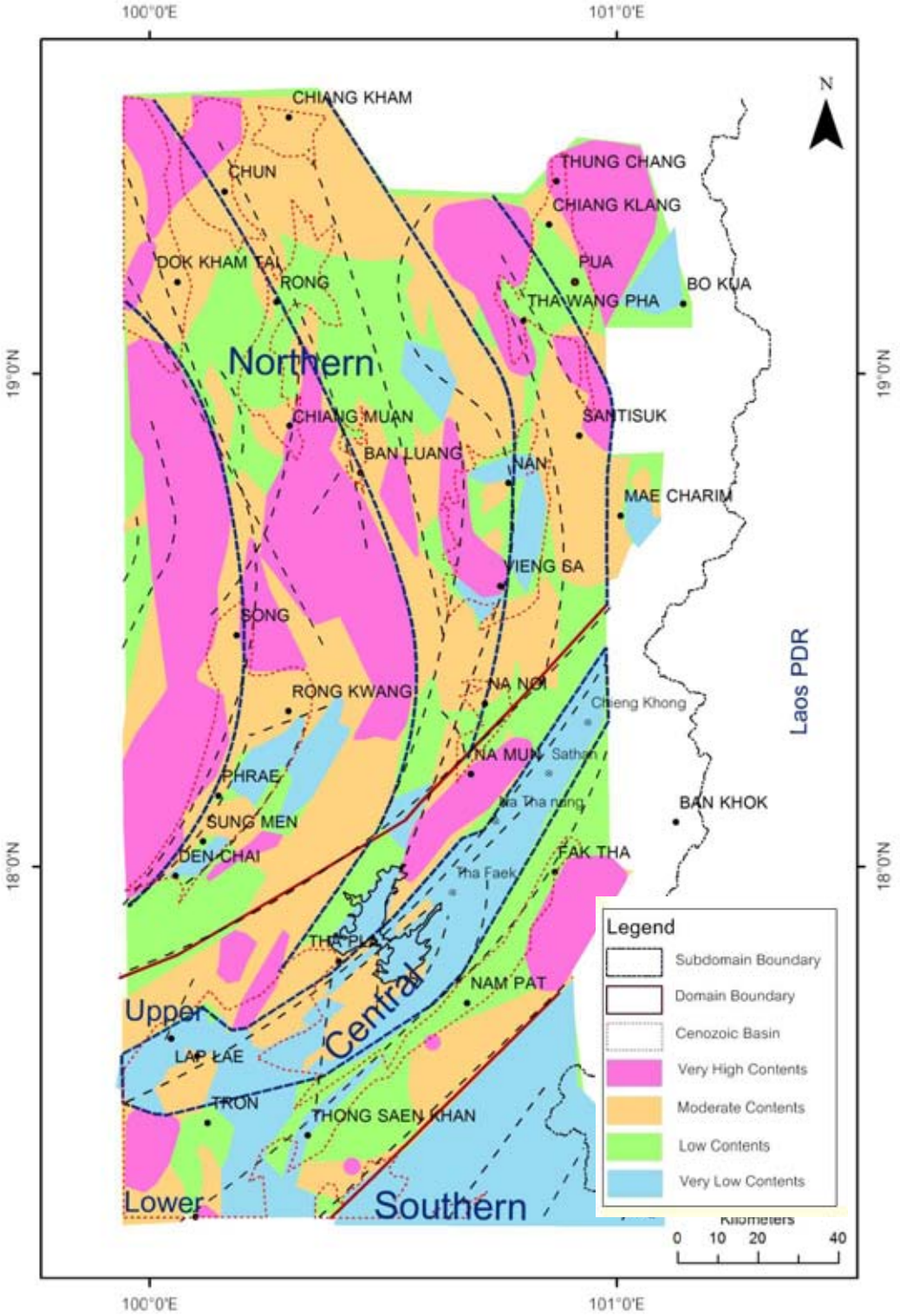

Figure 5.10b Radiometric (Potassium Concentration) data interpretation map showing 3 major domains (north, central and south) and their subdomains in the Nan-Uttaradit area.

5.2.3 Thorium Contents Map

Figure 5.11a shows composite colors of thorium contents by applying ranges of colors. The very low content on scale bar are in dark blue and blue green colors and the very high content are showing in red and pink color. The interpretation of the thorium contents map is shown in Figure. 5.11b.

The map shows various values of thorium content ranging from 1.63 to 40.29 ppm that can be divided into 3 different domains.

The southern domain shows low to very low thorium contents, similar to those of the uranium and potassium maps. In the southern domain, although no subdivision can be made, it show faint lineaments with the NE-SW trend. The unusually high thorium contents occur as a small patch to the easternmost part of the southern subdomain.

The central domain shows very low thorium content incorporated with moderate thorium content. This domain can be further subdivided into 3 subdomains namely upper, central and lower. The very low thorium content in central subdomain trends in NE-SW direction and parallel to the enveloping bands of high thorium contents in the upper and lower subdomains.

The northern domain shows high to very high thorium content. This domain can be further subdivided into 3 main subdomains with the characteristics of curving or arcuate boundaries between them. They are western, central and eastern subdomain. The western subdomain is characterized by large zones of high thorium contents. The central subdomain is denoted by more patches of high thorium contents with deformation zones (foldings) in the west and sporadic and smaller patches of high thorium contents in the east. The eastern subdomain is dominated by low content of thorium with some spots of high thorium contents. The very high thorium content shows in large spots within the N-S trending arcuate area in the western subdomain but shows different thorium contents at the northern and southern parts of Ban Luang township. In the eastern part a parallel band is recognized in the N-S direction.

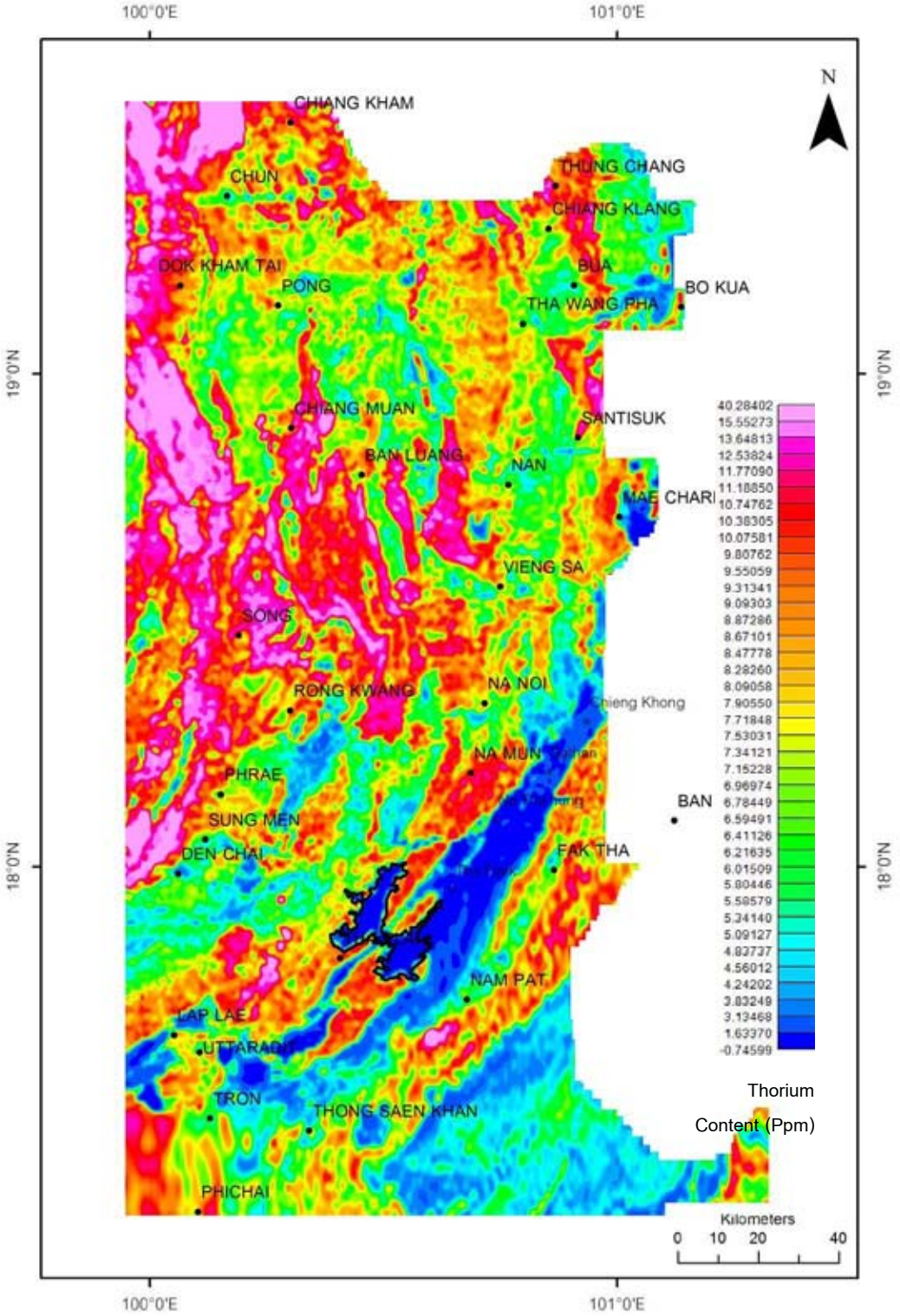

Figure 5.11a Airborne radiometric map of study area showing the concentration of Thorium (eTh). (Sirikit reservoir boundary in black)

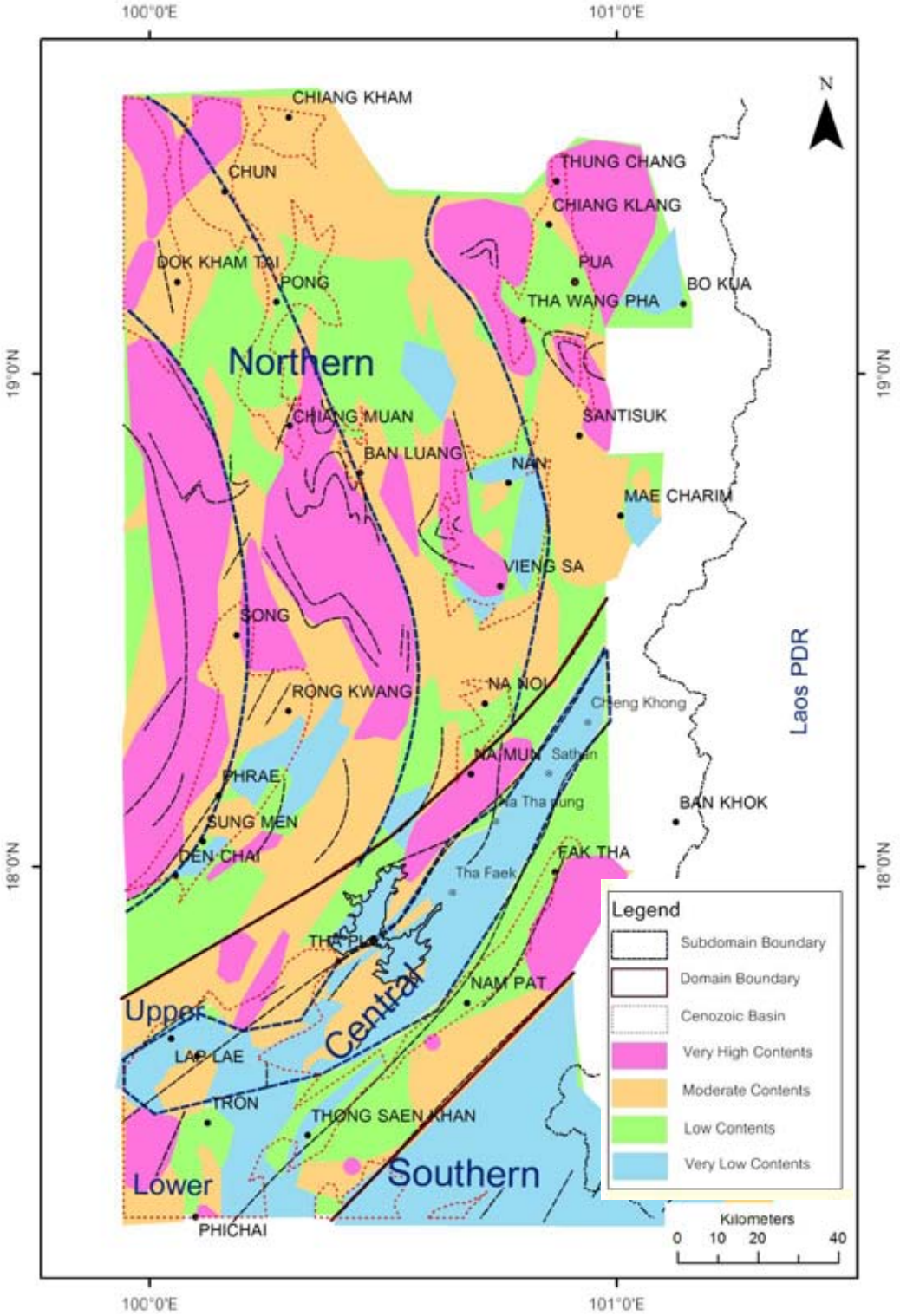

Figure 5.11b Radiometric (Thorium Concentration) data interpretation map showing 3 major domains (north, central and south) and their subdomains in the Nan-Uttaradit area.

5.2.4 Total Counts Map

Figure 5.12 a. displays composite colors of total count contents by ranges of colors, ranging from 2.6 to 34. The very low content on scale bar are in dark blue and blue green colors and the very high content shows in red and pink color. The interpretation of the total counts contents map is shown in Figure. 5.12b.

The map shows various values of total counts content which can divided into 3 different domains.

The southern domain shows low to very low total counts contents, similar to those in Figure 5.9, 5.10 and 5.11.

The central domain shows very low total counts content incorporated with moderate to high total counts content. It can be splitted into 3 subdomains (upper, central and eastern subdomains) with the lineaments similar to those of the other previously shown uranium, thorium and potassium maps. The central subdomain shows outstanding low total count contents.

The northern domain showing high to very high total counts contents. This domain is separated into 3 major subdomains with arcuate boundaries similar to those of the other maps. The high total count contents show as large spots within the N-S trending arcuate zone in the western subdomain. The eastern and central subdomains displays smaller patch of high total counts.

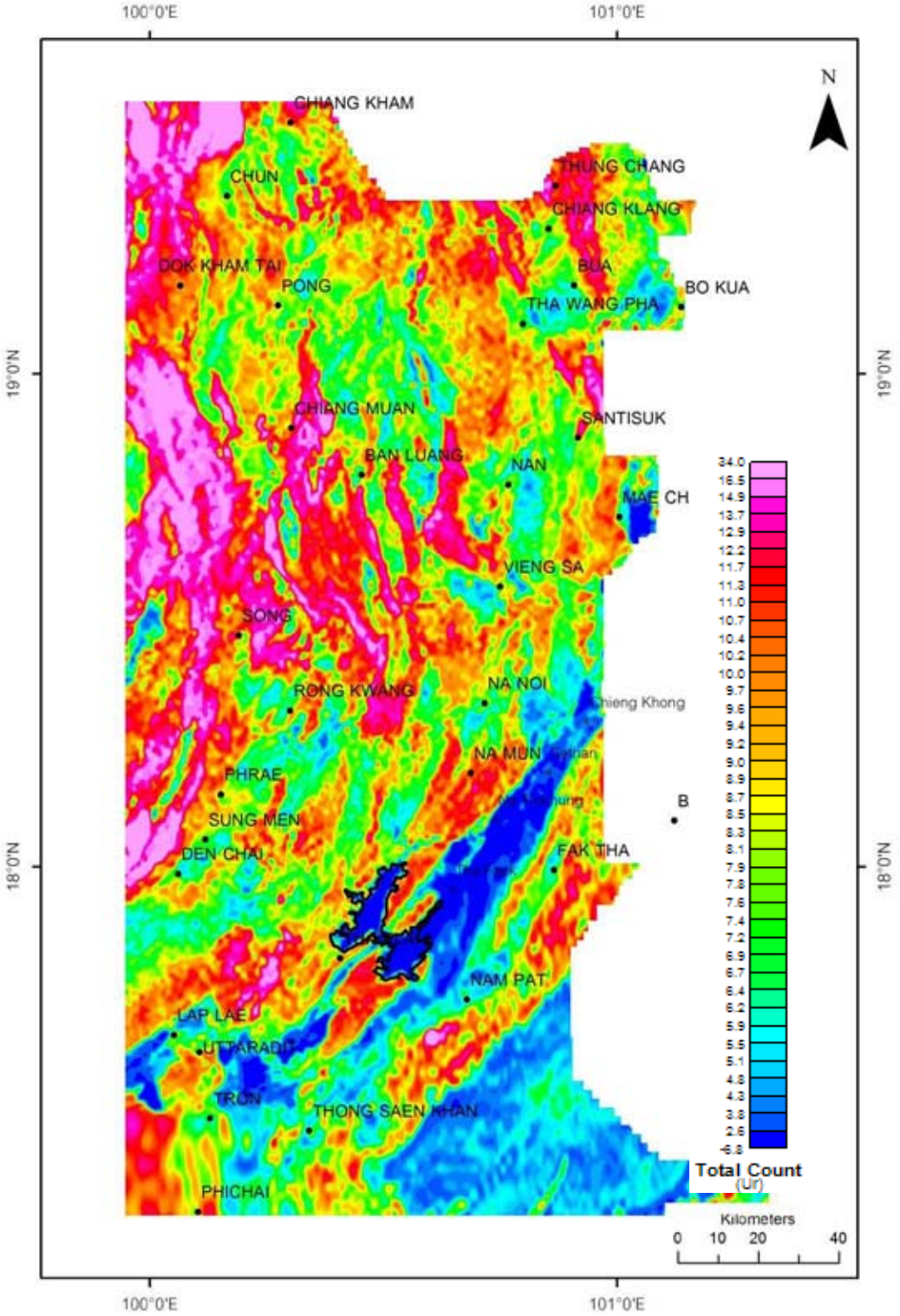

Figure 5.12a Airborne radiometric map of study area showing the Total Count (TC). (Sirikit reservoir boundary in black)

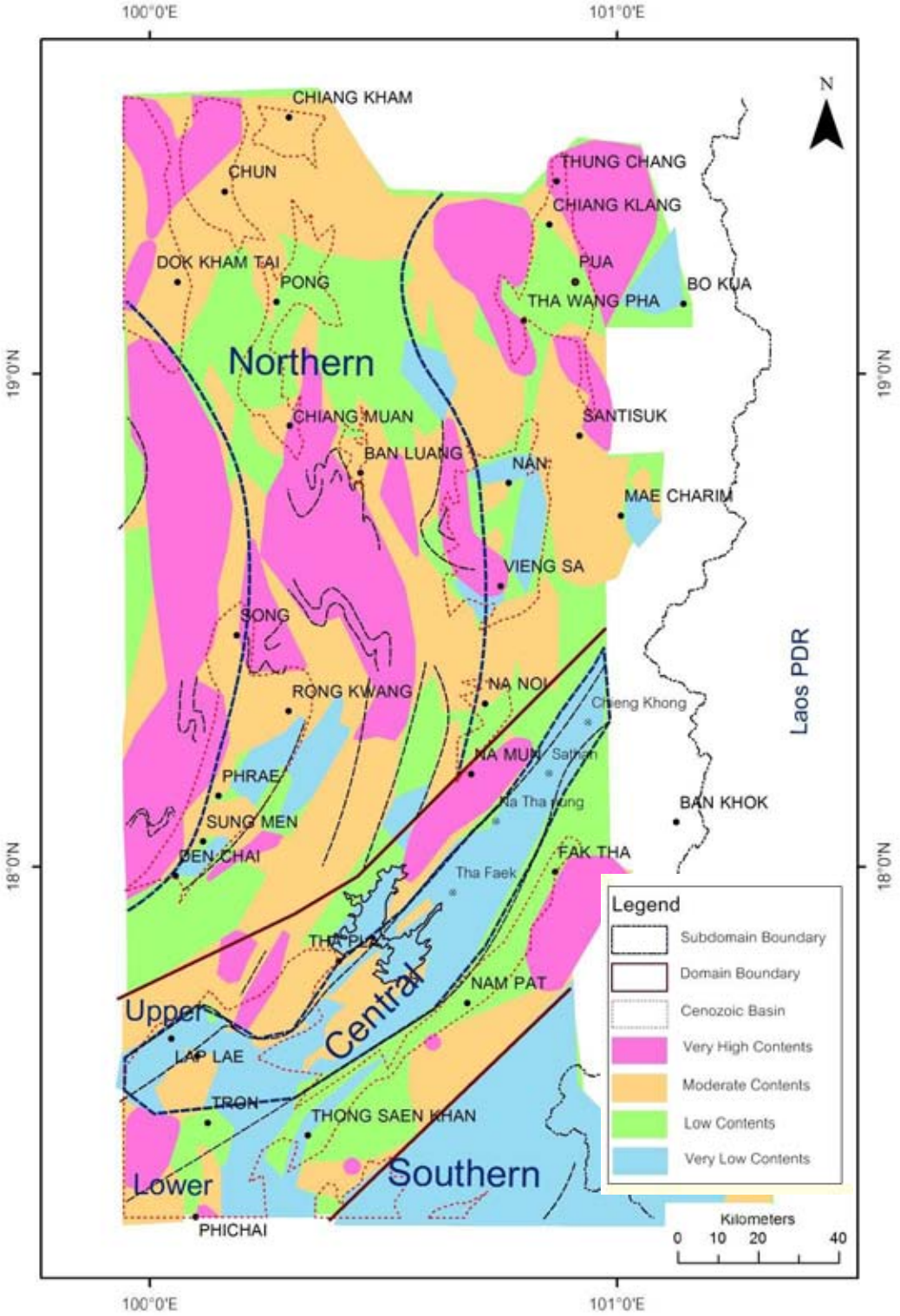

Figure 5.12b Radiometric (Total Count) data interpretation map showing 3 major domains (north, central and south) and their subdomains in the Nan-Uttaradit area.

Individual radioelements (including U, K and Th) for the airborne radiometric survey are shown as in Figure 5.9, 5.10, 5.11 (U, K, Th) respectively. All maps illustrate similar pattern, concentration, and shaped to one another. Quite interestingly is that low and high values of individual elements frequently are shown in the central domain identified as the NE-SW trending belt by RTP magnetic data. It is also displayed by low values of all radiometric elements (K, U and Th) illustrate as dark to black color in ternary map. These low values are interpreted to represent mafic – ultramafic rocks (no. 5,6,7,10 and 11 in table 4.2). On the other hand, the almost white to gray colors, which represent the high values of radio-elements, are likely to indicate the presence of intrusive bodies of felsic composition. It is also visualized that the pattern of radio elements for the northern domain are quite different from those of the southern domain which has higher contents of Th, U and K elements.

Figure 5.12 shows very low contents of total count radio elements within the central domain, but continuous pattern along the central domain (Tha Pla, Tron and Uttaradit) and plutonic belt (Fak Tha, Nam Pat and Thong Saen Khan) respectively.

5.2.5 Uranium and Thorium Composite Map

Figure 5.13a shows composite colors of uranium and thorium contents. Assigned Uranium content as blue color and Thorium content as green color. The interpretation of uranium and thorium composite map is shown in Figure. 5.13 b.

This map shows 3 different domains.

The southern domain shows low to moderate composite content without obvious pattern.

The central domain displays very low composite content incorporated with moderate composite content, the very low composite content in central subdomain trends in NE-SW direction and parallel to the bands of much high contents in the upper and lower subdomains.

The northern domain illustrates high to very high composite contents. The very high composite contents shows in large area in the western part but show different composite contents at the northern part and southern part of Ban Luang town. In the eastern part show a parallel band of N-S direction.

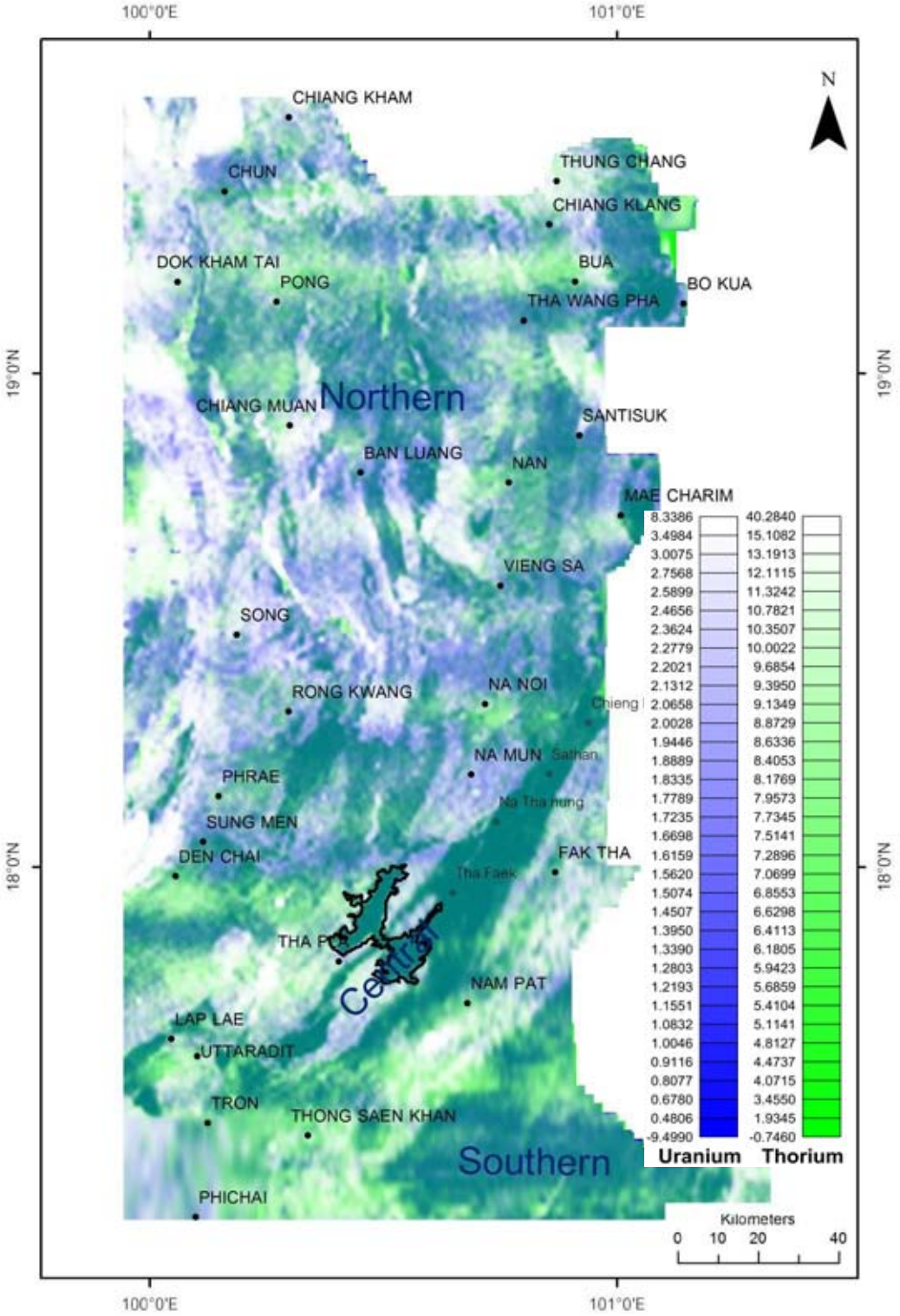

Figure 5.13a Enhanced radiometric map of the Nan-Uttaradit area after using cooking technique (Uranium and Thorium). Noted that Sirikit reservoir is boundary in black.

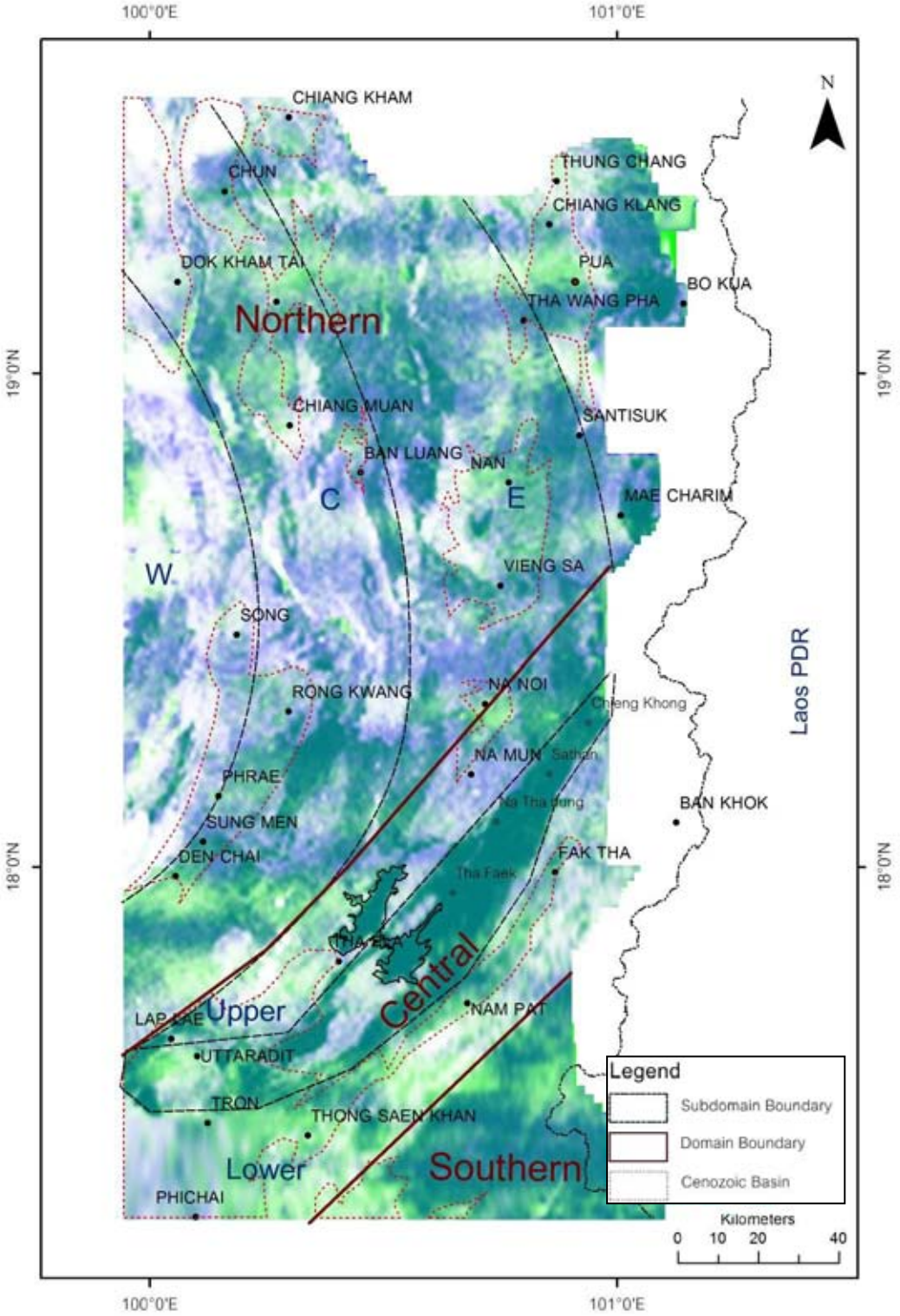

Figure 5.13b Interpreted of uranium and thorium map of the Nan-Uttaradit area showing 3 domains (Northern domain, Central domain and Southern domain) and their subdomains.

5.2.6 Potassium and Thorium Composite Map

Figure 5.14a shows composite color of potassium and thorium contents. Assigned potassium content as red color and Thorium content as green color. The interpretation of potassium and thorium composite map is shown in Figure.5.14b.

This map can be divided into 3 different domains, namely southern, central and northern domains.

The southern domain shows low to moderate composite content.

The central domain shows very low composite content incorporated with moderate composite content. The very low composite content in central zone trends in NE-SW direction and parallel to the band of high content in southern part.

The northern domain shows high to very high composite contents. The very high composite contents are shows as large spot in the western part and show different composite contents at the northern part and southern part of Ban Luang town. In the eastern part show a parallel band of N-S direction.

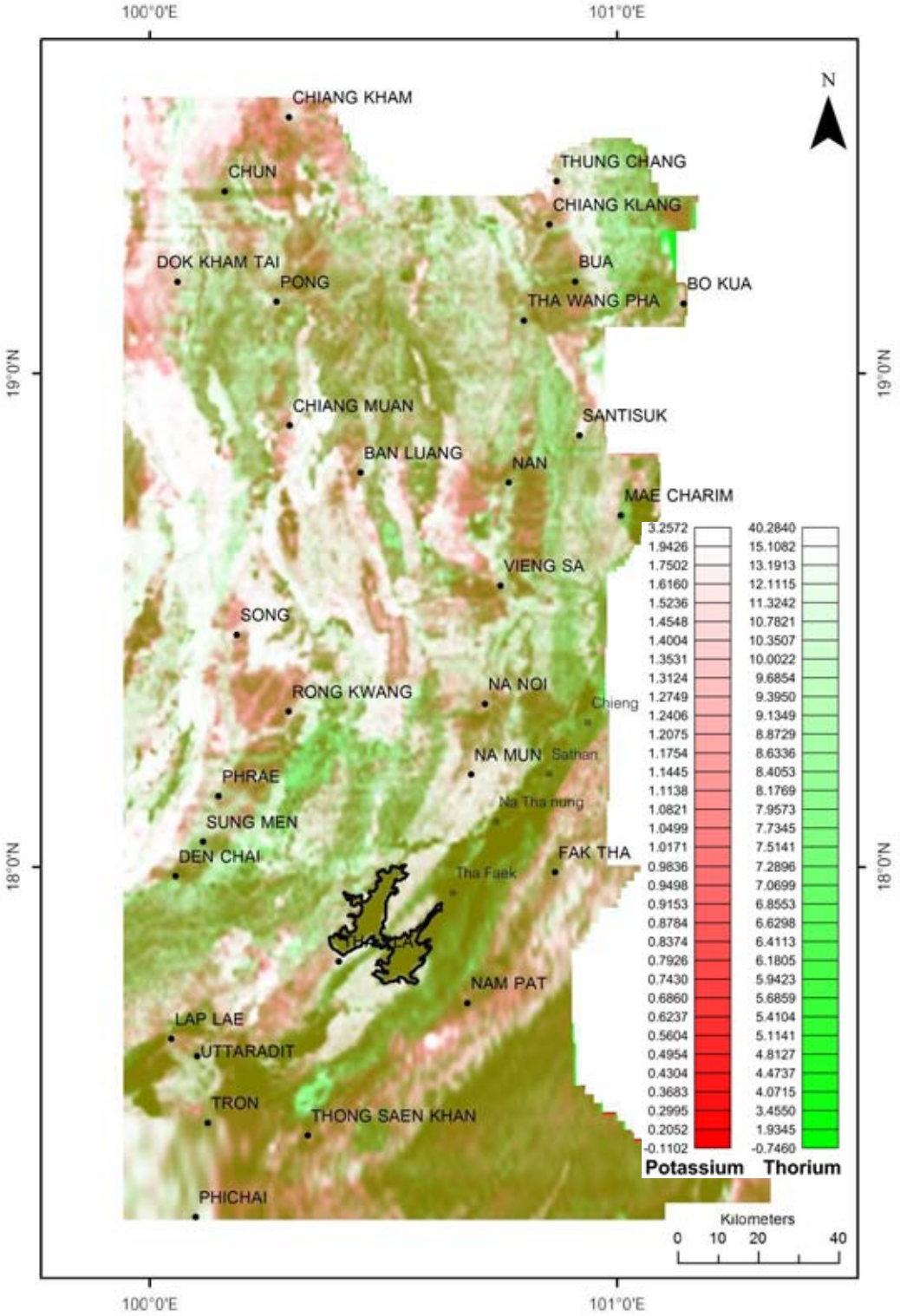

Figure 5.14a Enhanced radiometric map of the Nan-Uttaradit area after using cooking technique (Potassium and Thorium). Noted that Sirikit reservoir is boundary in black.

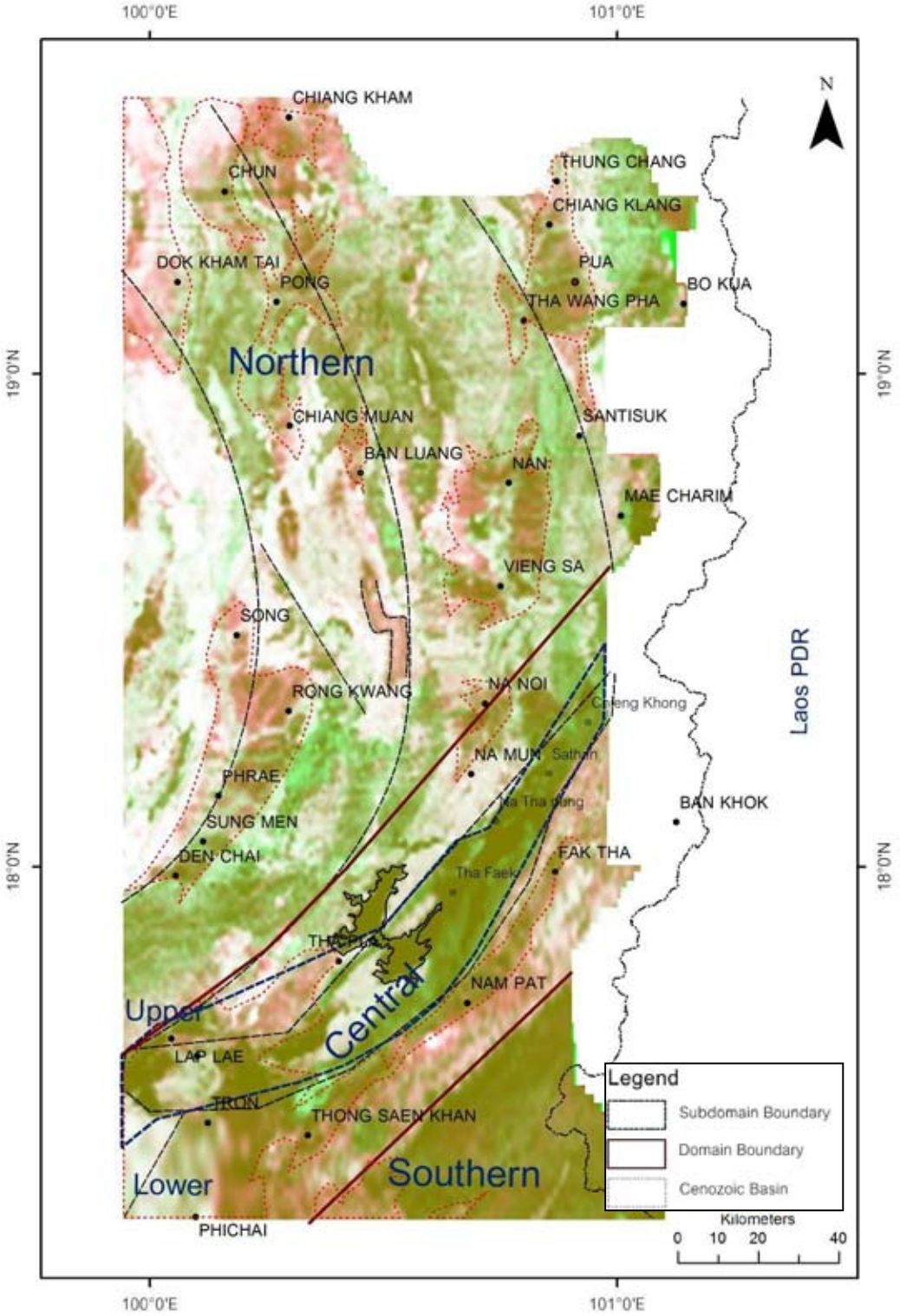

Figure 5.14b Interpreted of potassium and thorium map of the Nan-Uttaradit area showing 3 domains (Northern domain, Central domain and Southern domain) and their subdomains.

5.2.7 Potassium and Uranium Composite Map

Figure 5.15a. shows composite colors of potassium and uranium contents. Potassium contents are assigned as red color and Uranium content as blue color. The interpretation of potassium and uranium composite map is shown in Figure.5.15b.

This map can be divide into 3 different domains.

The southern domain shows low to moderate composite contents.

The central domain shows very low composite content incorporated with moderate composite content, the very low composite content in central zone are trends in NE-SW direction and parallel to the band of moderate content in the southern part.

The northern domain shows very high to high composite contents. The very high composite contents show as large spots in the western part and show different composite contents at the northern and southern parts of Ban Luang town. In the eastern part show a parallel band of N-S direction.

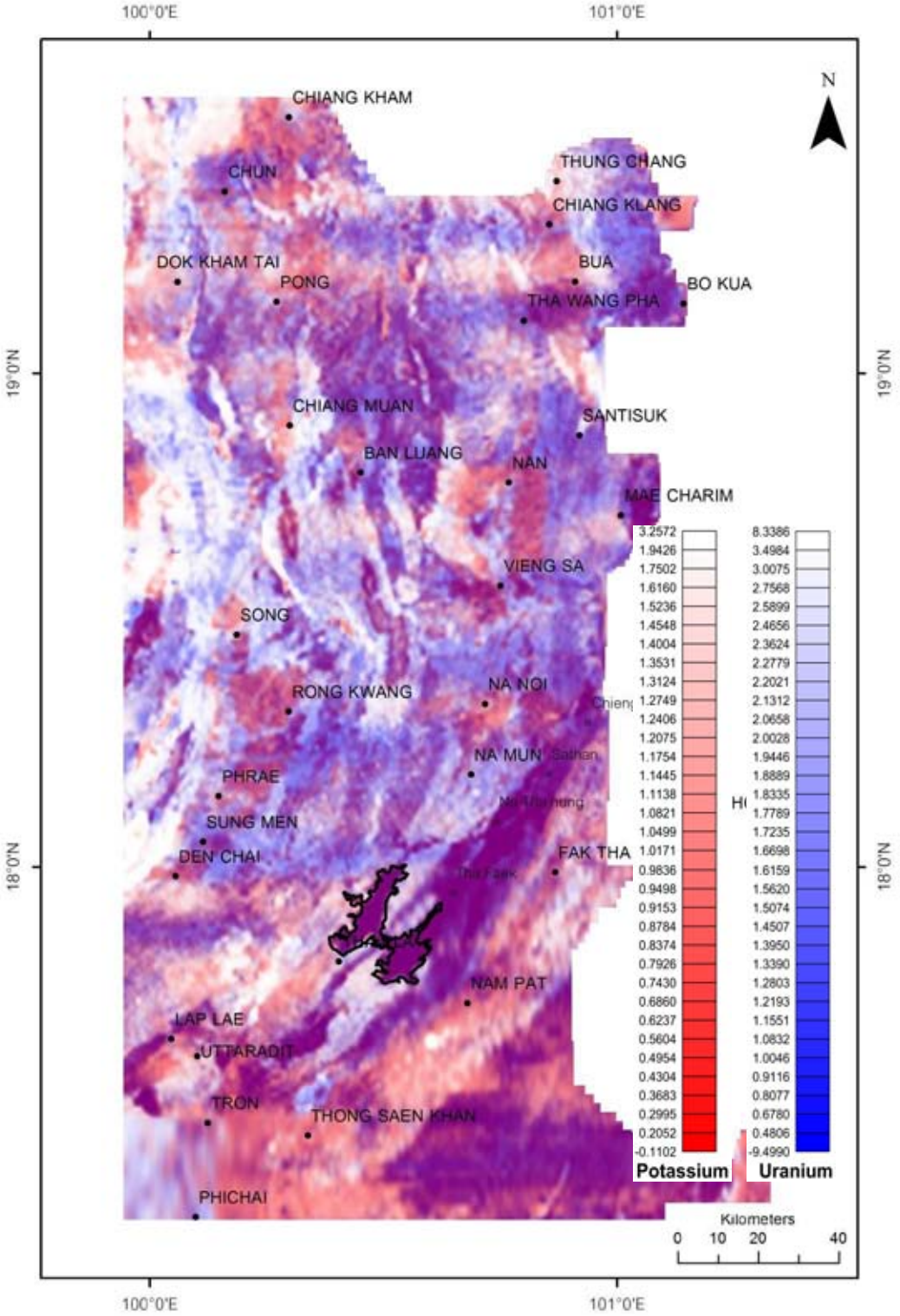

Figure 5.15a Enhanced radiometric map of Nan-Uttaradit area after using cooking technique (Potassium and Uranium). Noted that Sirikit reservoir is boundary in black.

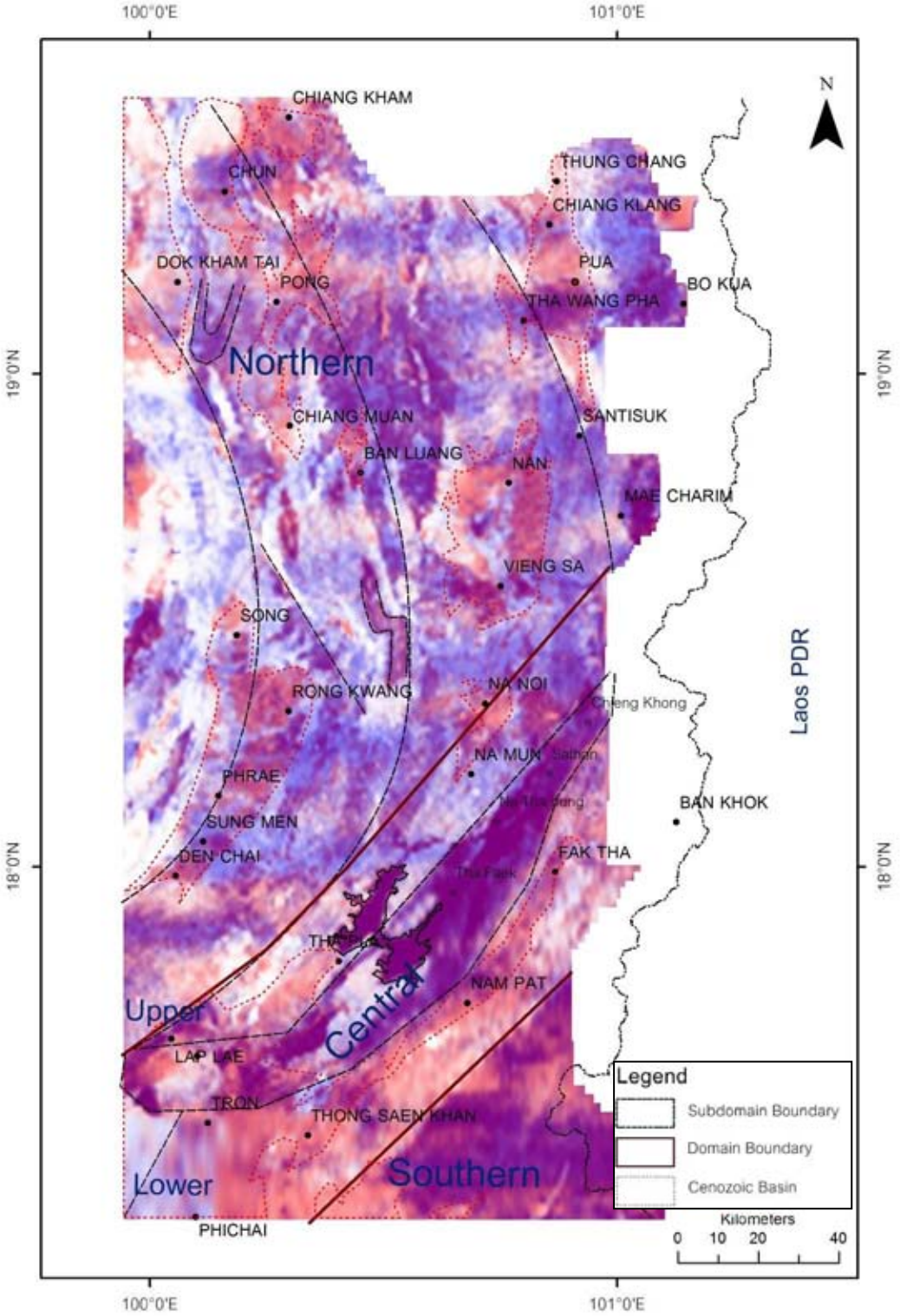

Figure 5.15b Interpreted of potassium and uranium map of the Nan-Uttaradit area showing 3 domains (Northern domain, Central domain and Southern domain) and their subdomains.

5.2.8 Ternary Map

Figure 5.16a shows ternary map of this area. The interpretation of ternary map is shown in Figure.5.16b.

Ternary map can be divided into 3 different domains.

The southern domain shows low to moderate ternary contents.

The central domain shows very low content incorporated with moderate content, the very low content in central subdomain trends in NE-SW direction and parallel to the lower and upper bands of moderate contents.

The northern domain shows high to very high contents with arcuate boundary similar to those of the other concentration maps. The very high contents is show as large spot in the western part but show different composite contents at the northern part and southern part of Ban Luang town. In the eastern part show a parallel band of N-S direction.

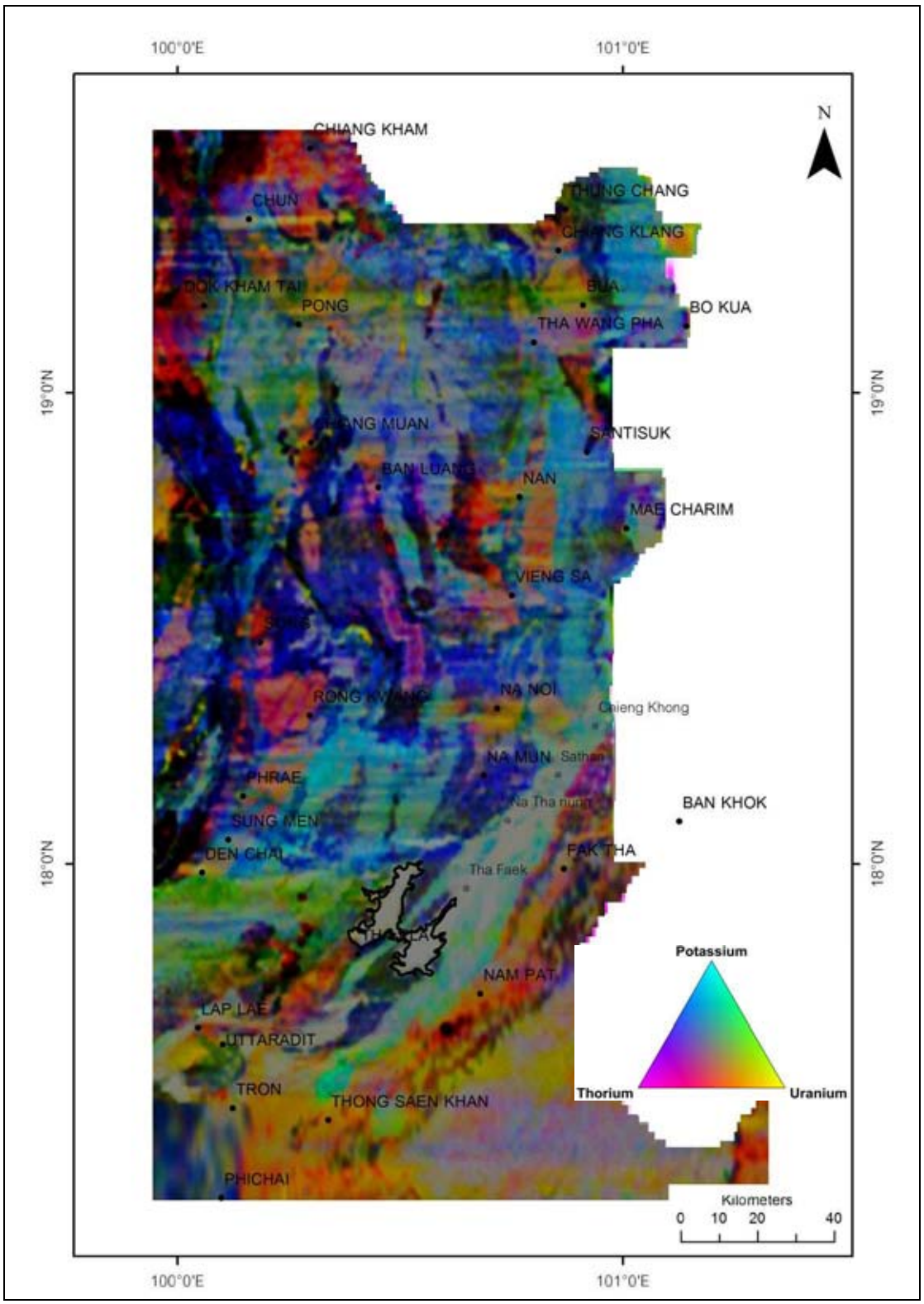

Figure 5.16a Ternary map of the Nan-Uttaradit area. Noted that Sirikit reservoir is boundary in black.

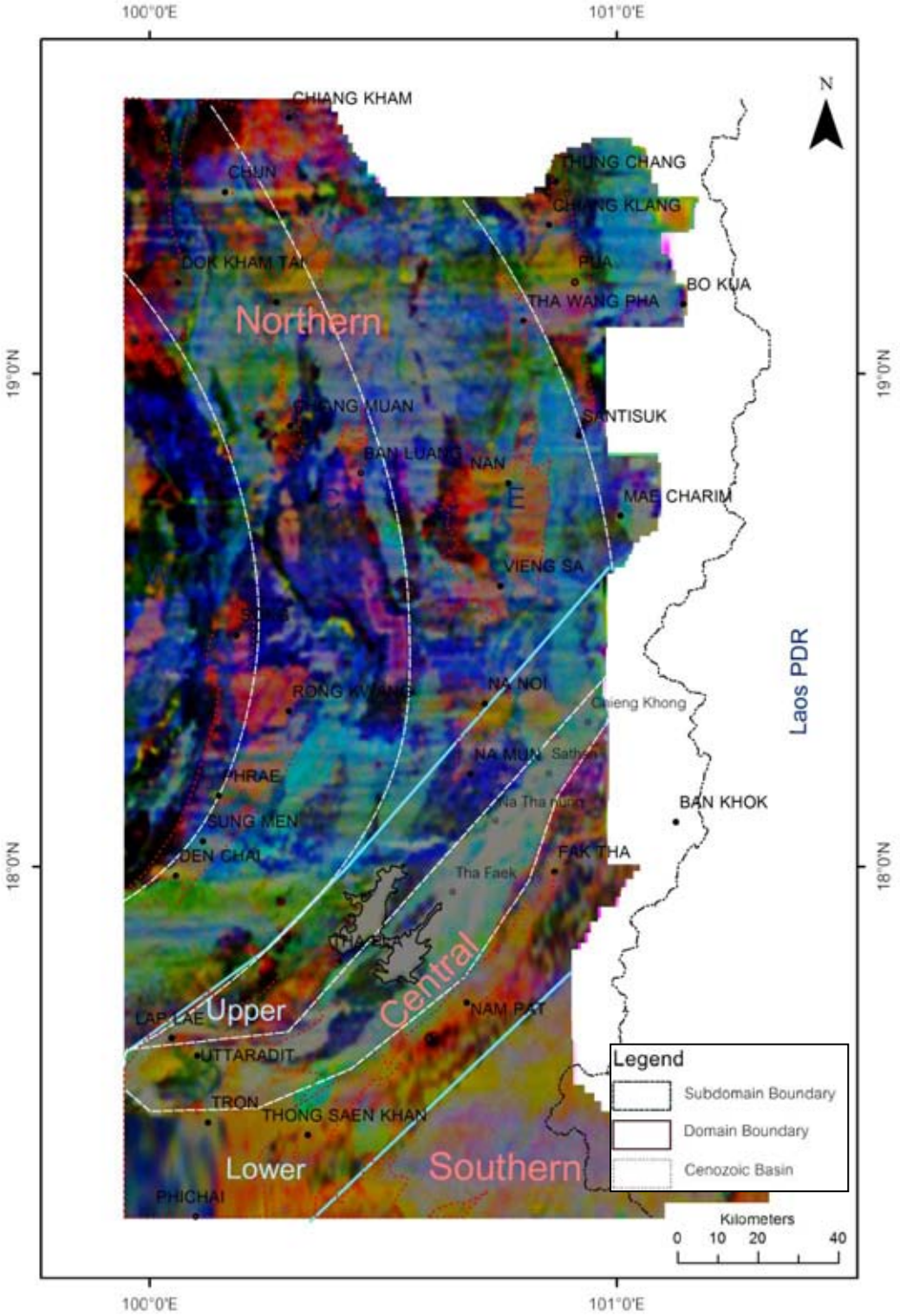

Figure 5.16b Interpreted of ternary map of the Nan-Uttaradit area showing 3 domains (Northern domain, Central domain and Southern domain) and their subdomains.

In addition band composite of the radio elements have also been applied for this interpretation as shown in Figures 5.13, 5.14, 5.15 for U/Th , K/Th and K/U respectively. The result shown similar patterns, shapes and values similar to those of the individual elements. Therefore it is also quite convinced that the occurrence and orientation of the Northern, Central and Southern domains are almost the same as identified herein by both radiometric and magnetic surveys.

It can be concluded that high contents of K, eTh and eU values are recognized in felsic igneous rocks (see table4.2) such as the southern zone almost parallel to the central domain. So the low radioelement contents suggest the presence of mafic to ultramafic rocks, whereas the high radioelement contents suggest the occurrence of the non mafic verities. It is also noted that the northern domain has the radiometric concentration patterns and shapes quite dissimilar to those of the southern domain. Special interest is placed upon the curved boundaries. This implies that the northern domain containing radio-elements corresponding to the surface arcuate structures and the southern domain is the more smooth-shaped domain suggesting that both having contrasting geologic setting and tectonic structures.

5.3 Airborne Magnetic Data

Several enhancement methods have been applied for the airborne magnetic data of the study area. There are reduction to the pole technique, first vertical derivative technique, secondary vertical derivative technique, analytic signal technique automatic grain control technique, upward continuation technique and downward continuation technique. Interpreted maps from these enhancement method are shown, and separated topics are explained below.

5.3.1 The Reduction to the pole map

A map with the enhancement process by reduction to the pole is shown in Figure 5.17 A, by using inclination of 21.6 ° and declination of -0.85° with amplitude correction indicating of 40 °. After using several amplitude values, it is found that 40° can give rise to the maximum positive magnetic field. Fig 5.17 B shows the interpretation map using data from Figure 5.17 A. It is also figured out that the maximum positive and negative magnetic field are 768 nT and minimum field are -683 nT.

As shown in Figures 5.17 A and B, 2 types of anomalies are recognized, the first type occurring as continuous NE-SW trending anomalies extending in the north from east of Na Noi town (Nan) to east of Tha Pla town to Tron town (Uttaradit) and the second type occurring as two discontinuous elongate to circular units with diameter of 10 to 50 km. Based on the interpretation of the enhanced RTP magnetic map, 3 magnetic domains are identified. The northern domain with low to moderate values, the central domain with very high values and the southern domain with low magnetic values.

The anomalies in northern domain can be further subdivided into 3 subdomains, eastern, middle and western subdomain.

The western subdomain extends from Ban Luang town in Nan to Dok Kham Tai town in Phayao. Magnetic values are intermediate, ranging from 10 nT to 15 nT. The boundary is a curve. No signature anomaly is detected in this subdomain.

The middle subdomain also has the intermediate magnetic values (average 20 nT), extends from Ban Luang to Vieng Saand Na Noi town. Magnetic anomalies in this zone are in the N-S direction with smaller cicular bodies than the eastern subdomain. Their bodies vary from xxx km. to xxx km. in diameters. Important anomalies are between Chiang Muan and Song. The more elongate features are located between Chun and Chiang Muan towns. These anomalies do not show significant displacement. But to the east of this subdomain, there are smaller bodies with the diameters of xxx km. to xxx km. These small bodies display obvious left-lateral displacement. These faults are in the NNW-SSE direction.

The eastern sub domain extends from Thung Chang through Vieng sa (Nan) to Na Noi town. There are two large high magnetic bodies with the diameters larger than 50 km locate in this sub domain, the northern one is located in Thung Chang, Chiang Klang, Pua and Tha Wang Pha towns. The anomaly is locate within the Nan Basin. The southern one is located in Mae Charim and Wang Pha town. The radius of magnetic body is about 45 to 50 km. Some small magnetic bodies at Tha Wang Pha town have been recognized.

The anomalies in central domain

The central domain is characterized by small very high magnetic bodies showing an alignment in the NE-SW direction. This zone (or subdomain) with the width of about 10-15 km is sandwiched between the upper and the lower subdomains. These two subparallel subdomains are characterized by very low to low magnetic values. The northern and southern ends of the upper subdomain are shown as the NE-SW trending small elongate bodies. On the other hand, the lower subdomain is characterized by low to very low magnetic values (from -80 to -100 nT). The domain is located from Ban Khok, Fak Tha, Nam Pat towns in the north to Thong Saen Khan and Phi Chai towns in the south. Magnetic features seen to be delineated in the NE-SW trend.

The anomalies in southern domain

The southern domain is a zone with low to intermediated magnetic values. No subduction is determined. This subdomain has two high isolated small bodies to the western and eastern ends.

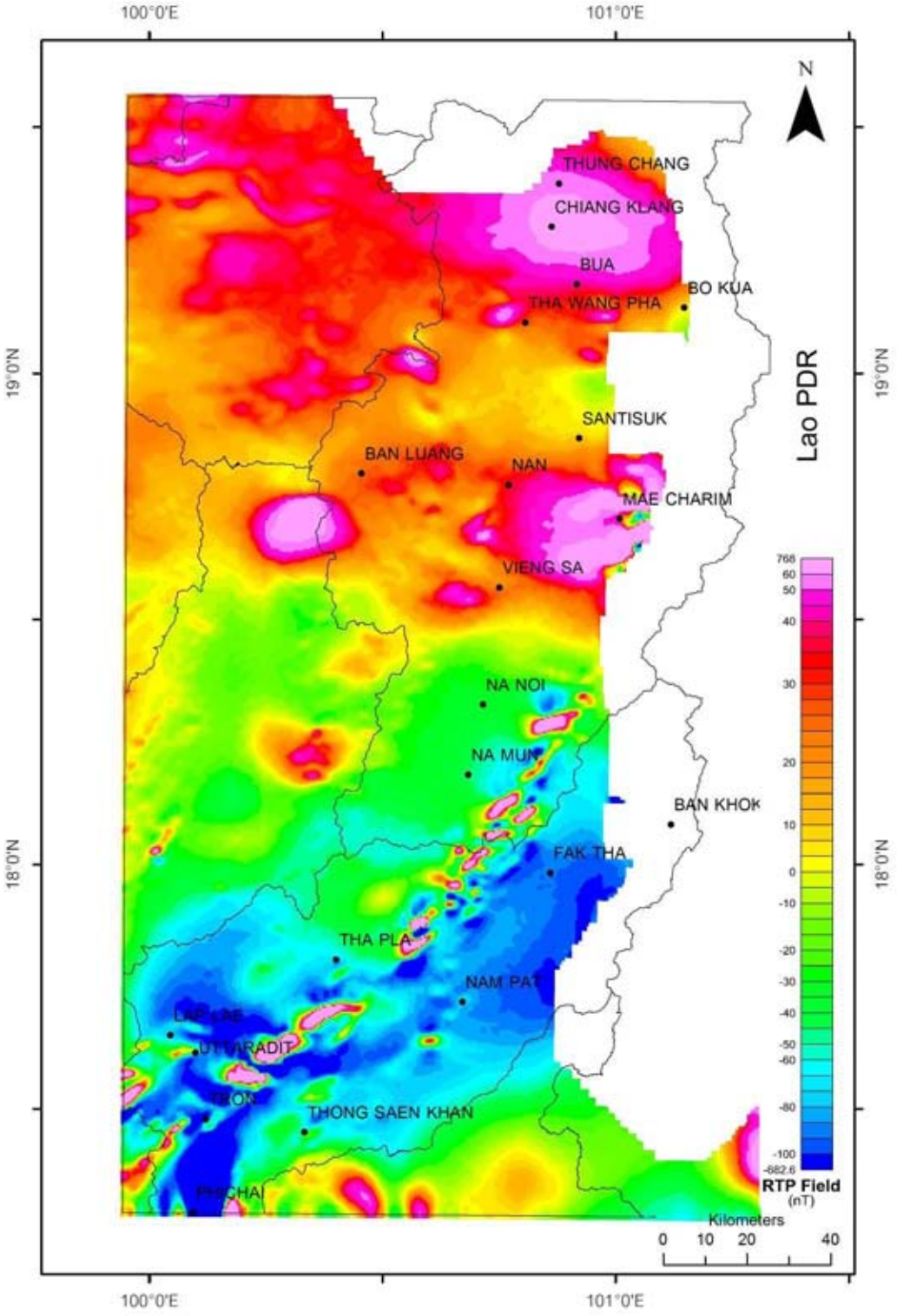

Figure 5.17a Enhanced magnetic map of the Nan-Uttaradit area after applying reduction to the pole technique. (Inclination 21.6˚, declination -0.85˚ and secondary inclination 40˚.)

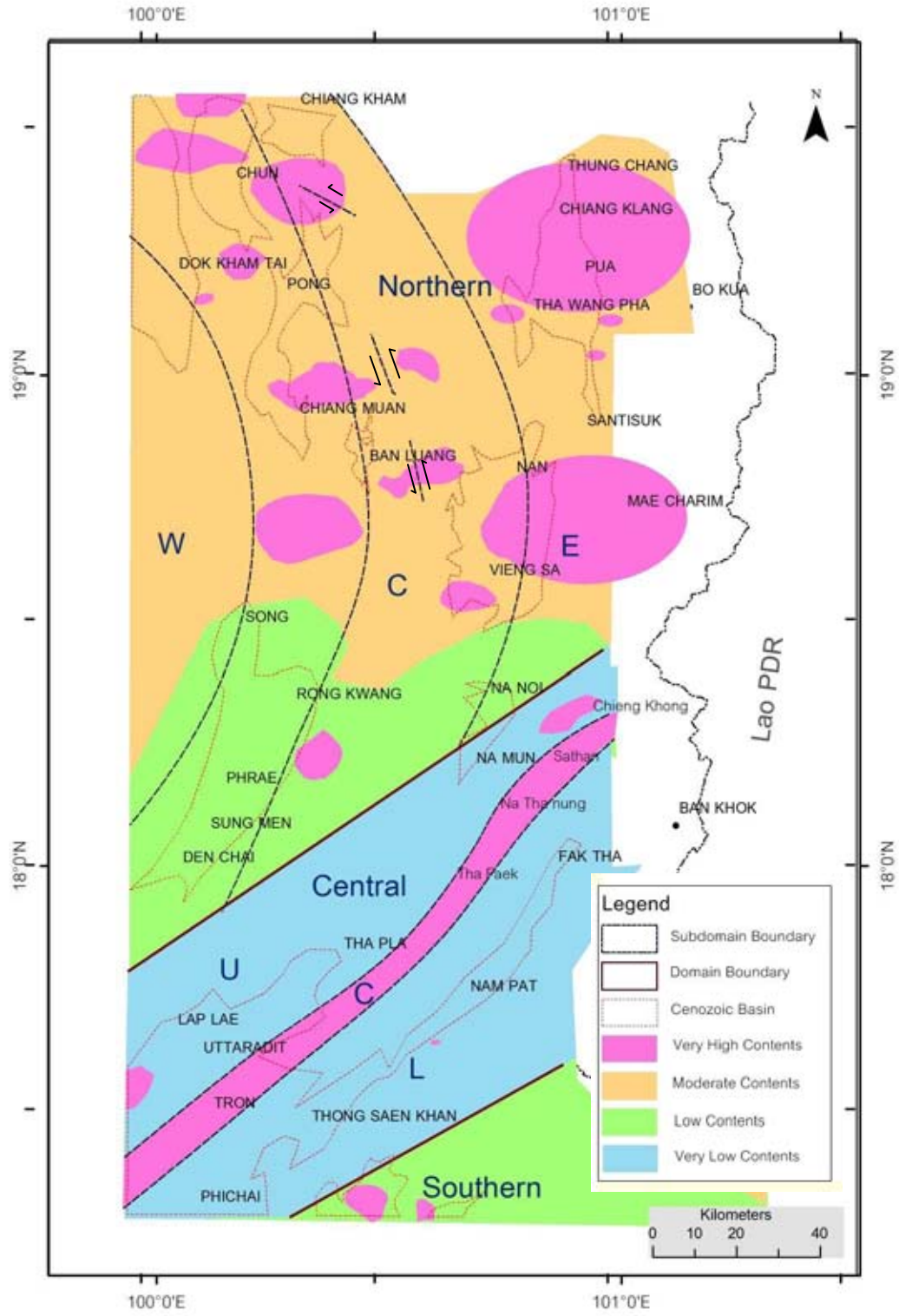

Figure 5.17b Interpreted RTP map of the Nan-Uttaradit area showing 3 magnetic domains (Northern domain, Central domain and Southern domain) and their subdomains (U=Upper, C=Central, L=Lower, W=Western, E=Eastern).

5.3.2 The Analytic Signal map

The map used the enhancement process by analytical signal is shown in Figure. 5.18a. In magnetic interpretation Figure. 5.18b displays the result of interpretation from the enhanced map of Figure. 5.18 A.

The result displays 3 magnetic domains similar to those of the RTP map. However the continuous high magnetic zone of the central domain shows broader domain (about 20-25 km width) than that of the RTP map.

The central zone is therefore splitted into 3 subparallel subdomains, namely the upper, the central and the lower subdomains. Like that of the RTP result, the upper subdomain shows high anomalies at the eastern and western ends. The lower subdomain consists of very low magnetic values in the east whereas in the south the subdomain shows much higher magnetic values. The central subdomain consists of small magnetic bodies with the N to NNE- S to SSW trending faults. Whereas the lower subdomain has the small anomalies with the NE-SW trending right-lateral faults.

Moreover the northern domain shows that high magnetic domain at the Mae Charim town shows a small separated unit from the main lower unit of the northern domain. The other interesting feature for the southern domain is that there exists the high magnetic unit immediate to the central domain from Nam Pat to Thong Saen Khan towns.

The occurrence of N-S sinistral fault at Tha Faek, Na Tha Nung and Sathan towns can indicated that there is compression in NW-SE direction. And the occurrence of dextral fault in NE-SW direction at Thong Saen Khan town can indicated the compression from E-W direction.

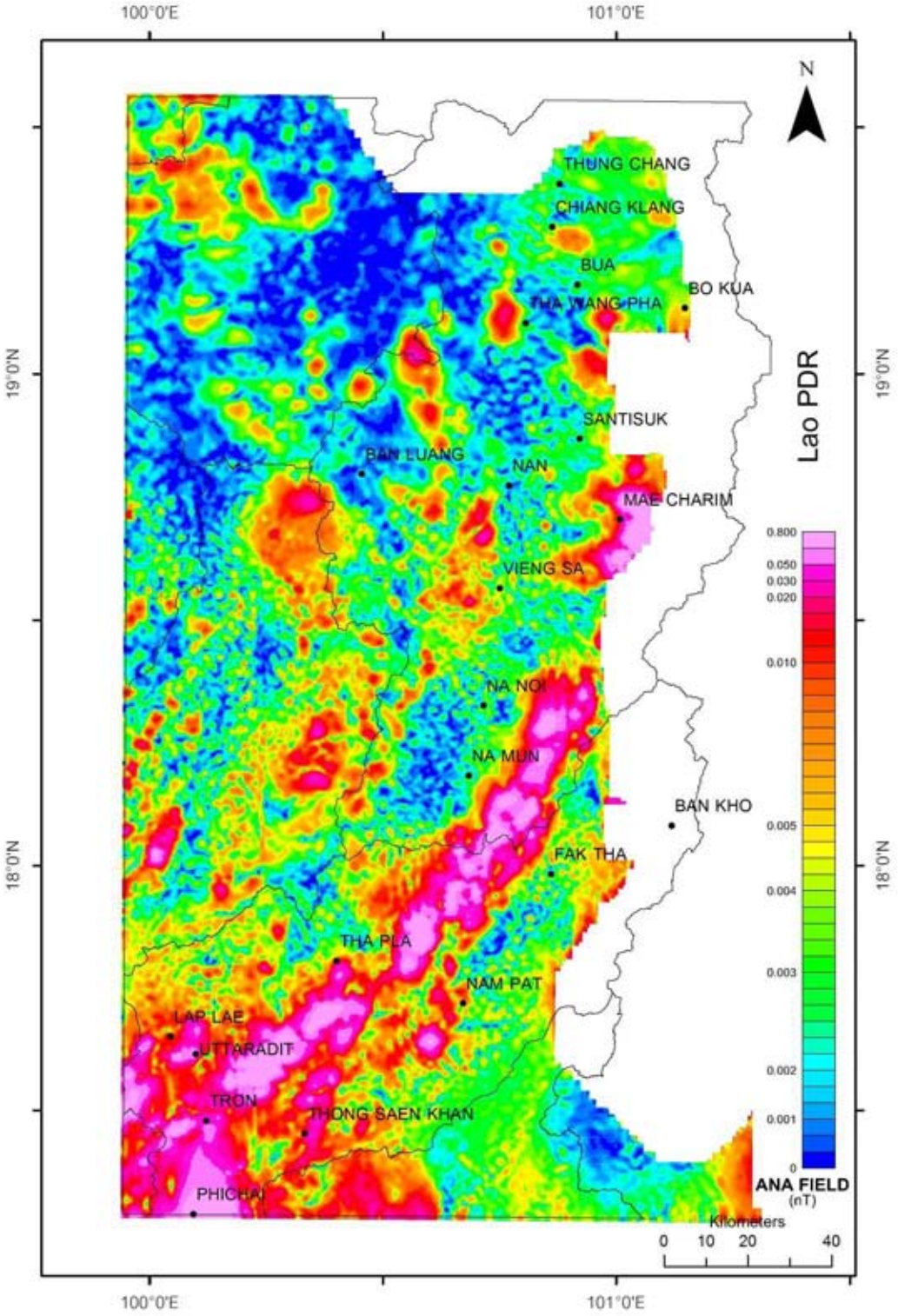

Figure 5.18a Enhanced magnetic map of the Nan-Uttaradit area after applying Analytic Signal technique.

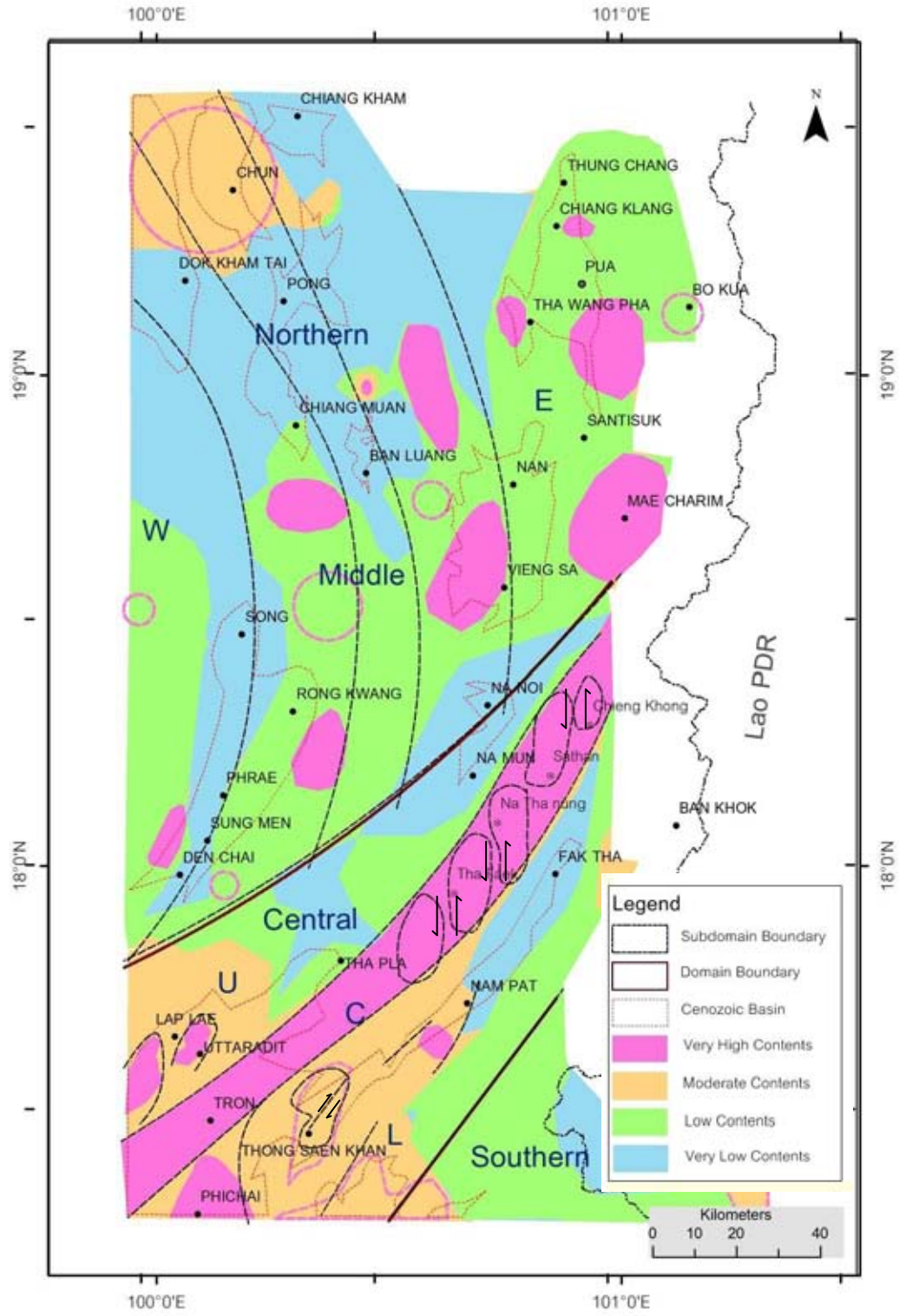

Figure 5.18b Interpreted analytic Signal map of the Nan-Uttaradit area showing 3 magnetic domains (Northern domain, Central domain and Southern domain) and their subdomains (U=Upper, C=Central, L=Lower, W=Western, E=Eastern).

5.3.3 Automatic gain control map

The airborne magnetic map which is enhanced using automatic gain control is shown in Figure. 5.19a. The interpretation map of the enhanced image data is shown in Figure. 5.19b. The result displays 3contrasting magnetic domains similar to those of RTP and analytical maps.

The northern domain consists of 3 subparallel subdomains, namely the western, the middle and the eastern subdomains. The western subdomains show no anomalies and intermediated magnetic values (from 10 to 15 nT). It has the sharp-curve border with the middle subdomain marked by small anomaly in the south and large anomalies in the north and central portions. The middle subdomain is splitted also into 2 zones with the broader circular bodies in the west and the smaller anomaly bodies with folding and faulting. The letter shows left lateral movement. The eastern subdomain show the zone of huge anomalies one in Chiang Klang with the diameter of 46 km and the other in Mae Charim with the diameter of 42 km.

The continuous high magnetic anomaly values in the central domain occurs within a narrower band those with the width of about (ranging from 300-1,400 nT)10-15 km as shown in small bodies in the subdomains align in the E-W direction whereas the lower subdomain has low magnetic values (30 nT) with small anomalies in south of Thong Saen Khan town.

The southern domain has no magnetic pattern and is mashed to the west by the NE-SW trending boundary. One major high magnetic body with circular to oval shaps is recognized. It has the long axis of about 25 km.

Moreover, the occurrences of NW-SE sinistral fault in Ban Laung town and NE-SE dextral fault in Lap Lae town can indicated the compression from E-W direction.

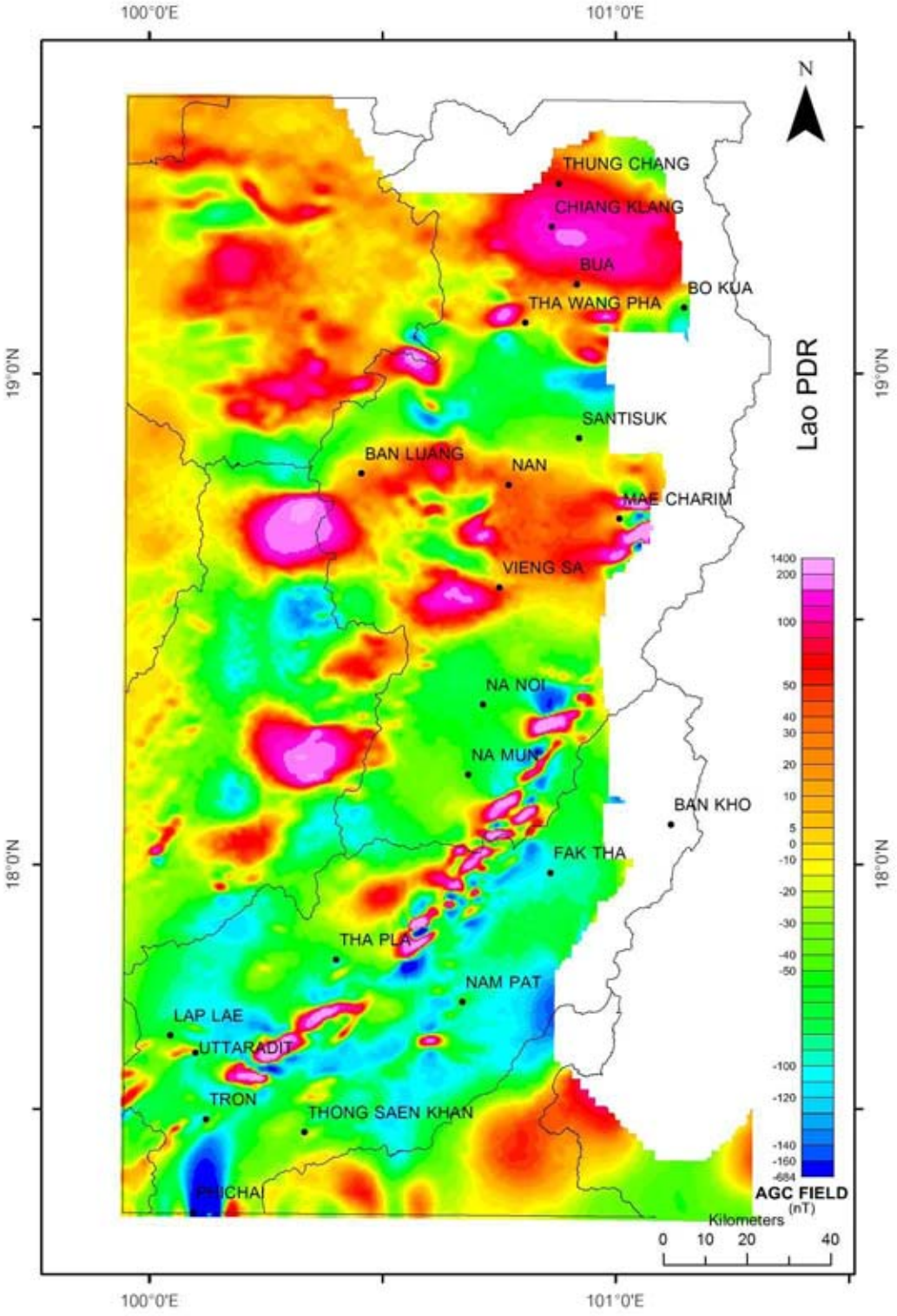

Figure 5.19a Enhanced magnetic map of the Nan-Uttaradit area after applying Automatic gain control technique.

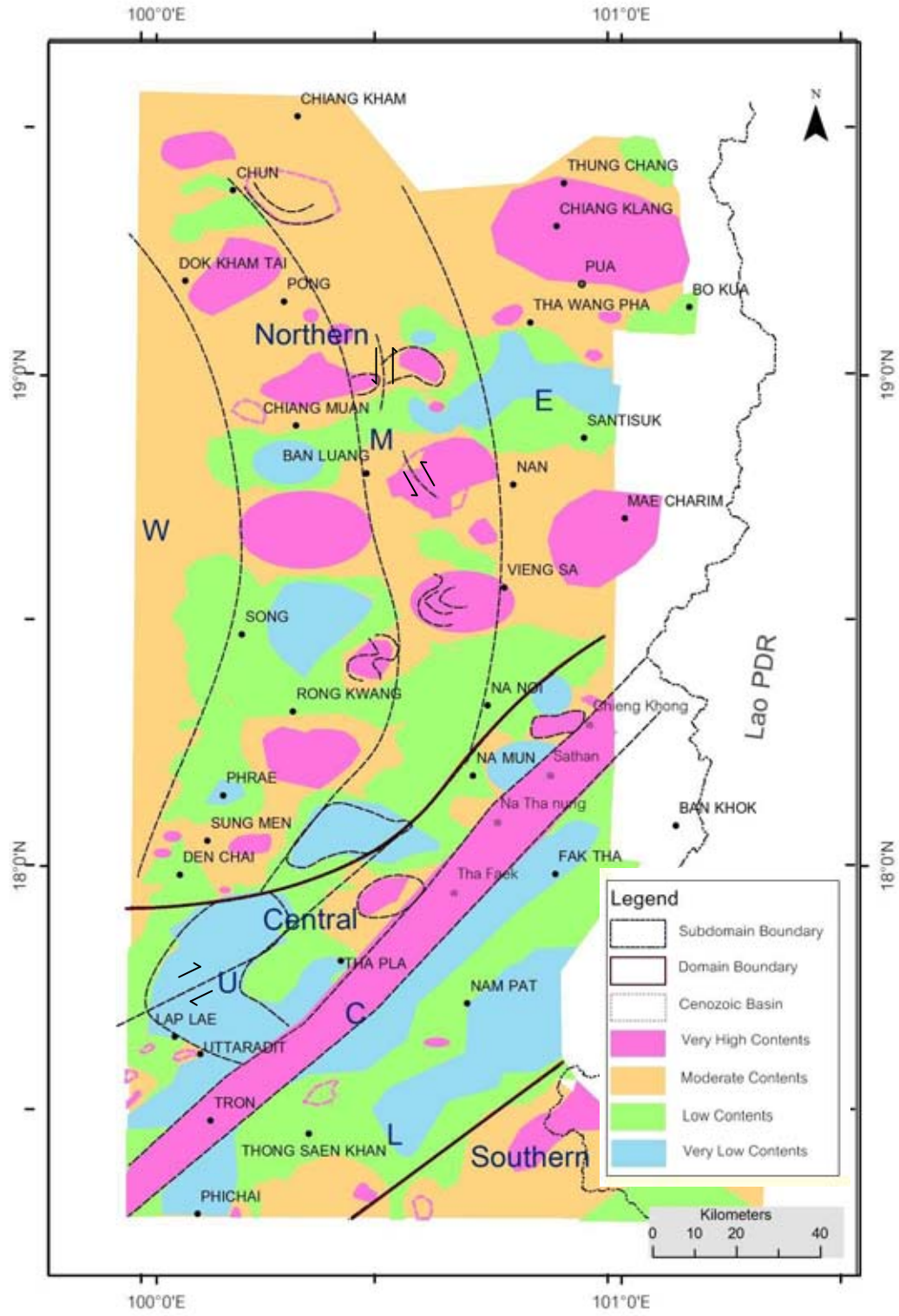

Figure 5.19b Interpreted automatic gain control map of the Nan-Uttaradit area showing 3 magnetic domains (Northern domain, Central domain and Southern domain) and their sub domain (U=Upper, C=Central, L=Lower, W=Western, E=Eastern).

5.3.4 The First Vertical Derivative map

The airborne magnetic map which is enhanced using first vertical derivative is shown in Figure. 5.20 A. The interpretation map of the airborne magnetic data using this kind of enhancement process is shown in Figure. 5.20 B. The result shows similar patterns of 3 magnetic domains to those of the RTP maps.

The northern domain shows the peculiar pattern of subdomains. They are the western, the central and the eastern subdomains. The western subdomain shows discontinuous lineaments in the NE-SW direction whereas the central subdomain shows one large anomaly body between Ban Luang and Song towns and the NW-SE trending linear magnetic bodies near the circular body. Magnetic lineaments are cut by the NW-SE with the sinistral movement and small bodies are cut by the NE-SW trending fault with the dextral movement. The eastern subdomain shows two large semi-circular to irregular bodies (up to 50 km) across in Pua and Nan – Wiang Sa towns.

The central domain is characterized by several small, prominent high magnetic oval bodies of the central subdomain. This subdomain is sandwiched by 2 subparallel subdomains, as the upper and the lower subdomains. The upper subdomain contain some high anomalies with some lineaments similar to the lower subdomain. The central domain shows a clearly defined domain with the NE-SW trend and to the south of the domain, there exists the split of the domain in the Lap Lae and Uttaradit area. This is quite similar to that shown in the analytical signal map of Figure. 5.18b.

In the southern domain 2 anomalous zone are recognized - one between Nam Pat and Thong Saen Khan are and the other to the east of Thong Saen Khan as a large circular unit. The southern domain shows a large circular magnetic body with the diameter of about 40 km and is mashed to the west by NE-SW trending border line.

The occurrences of fold with N-S axis with NW-SE sinistral fault at Chun, Dok Kham Tai and Chiang Muan towns can indicate compression from E-W direction.

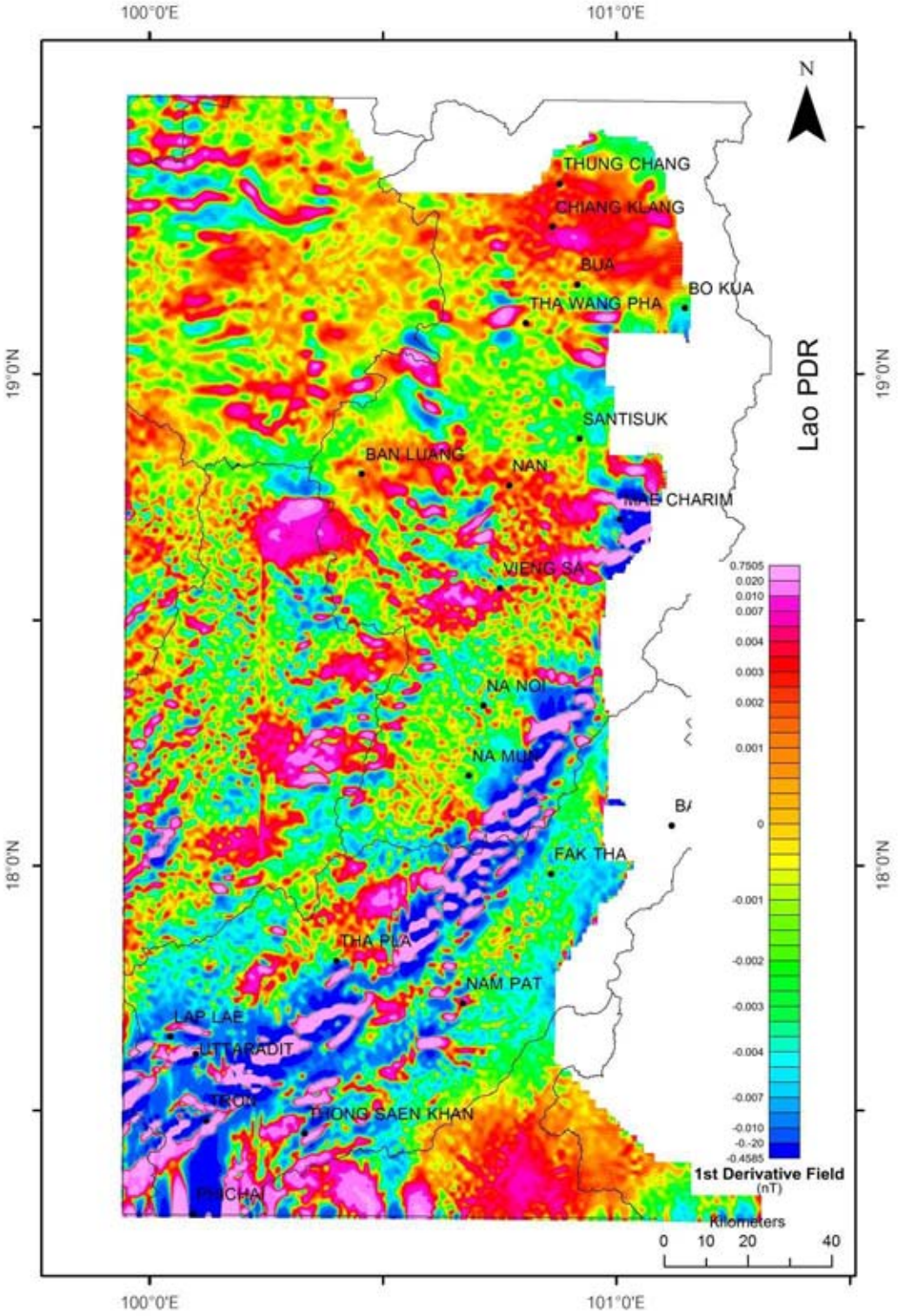

Figure 5.20a Enhanced magnetic map of the Nan-Uttaradit area after applying first vertical derivative technique.

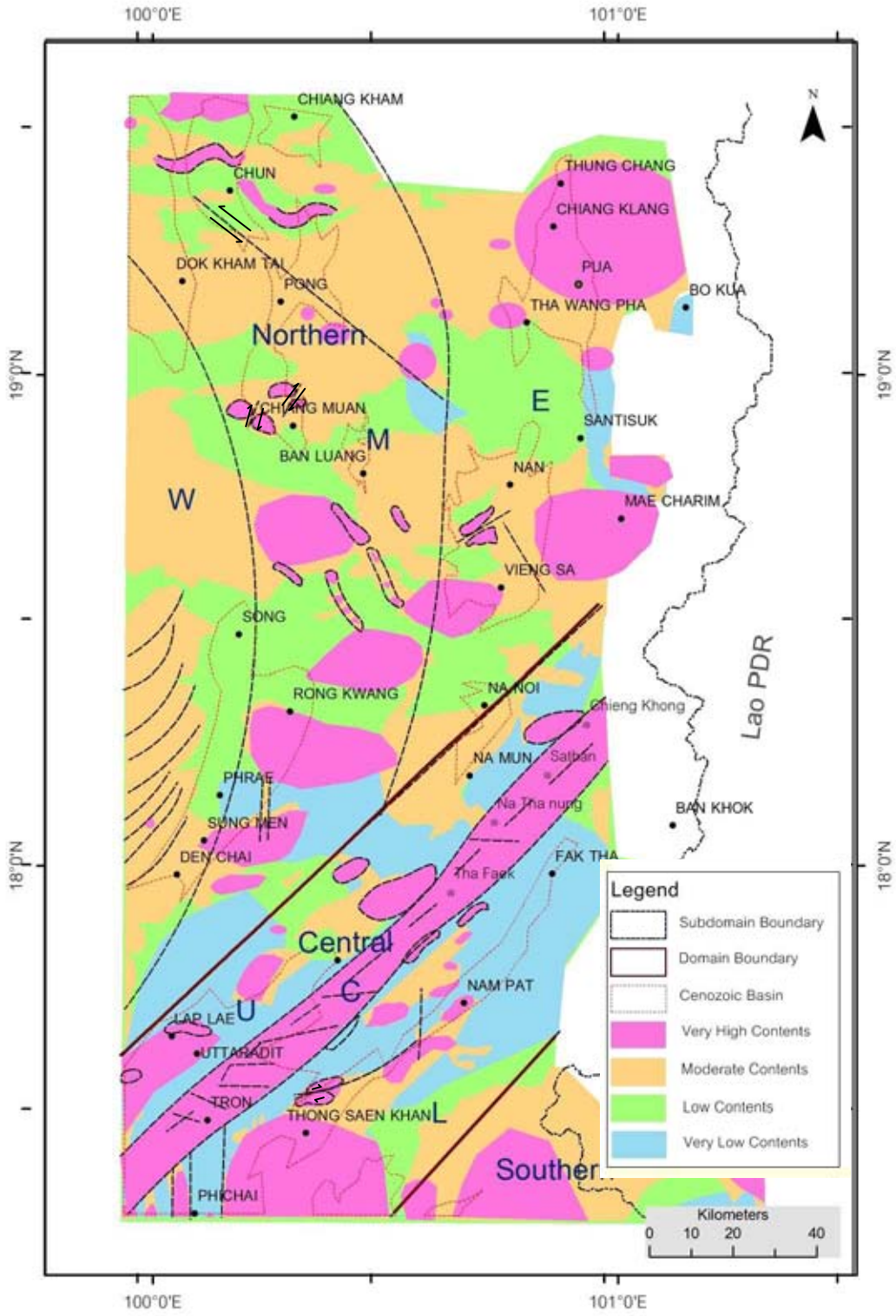

Figure 5.20b Interpreted first vertical derivative map of the Nan-Uttaradit area showing 3 magnetic domains (Northern domain, Central domain and Southern domain) and their sub domain(U=Upper, C=Central, L=Lower, W=Western, E=Eastern).

5.3.5 The Second Vertical Derivative map

The airborne magnetic map which is enhanced using second vertical derivative is shown in Figure. 5.21a. The interpretation map of the airborne magnetic date using this kind of enhancement process is shown in Figure. 5.21b. The result displays 3 similar magnetic domains (northern, central and southern), but with quite more contrasting signatures than those of the other enhancement method. The northern domain shows an obviously high magnetic values except at the Mae Charim town. However, the central domain denotes quite similar trend and value to the other previously mentioned interpretation maps. The other significant features of the southern domain is that there are two small high magnetic units in Nam Pat (north) and Thong Saen Khan (south). The other feature of the southern domain is that with the 2^{nd} derivative enhancement. The higher value of the previous interpretation maps.

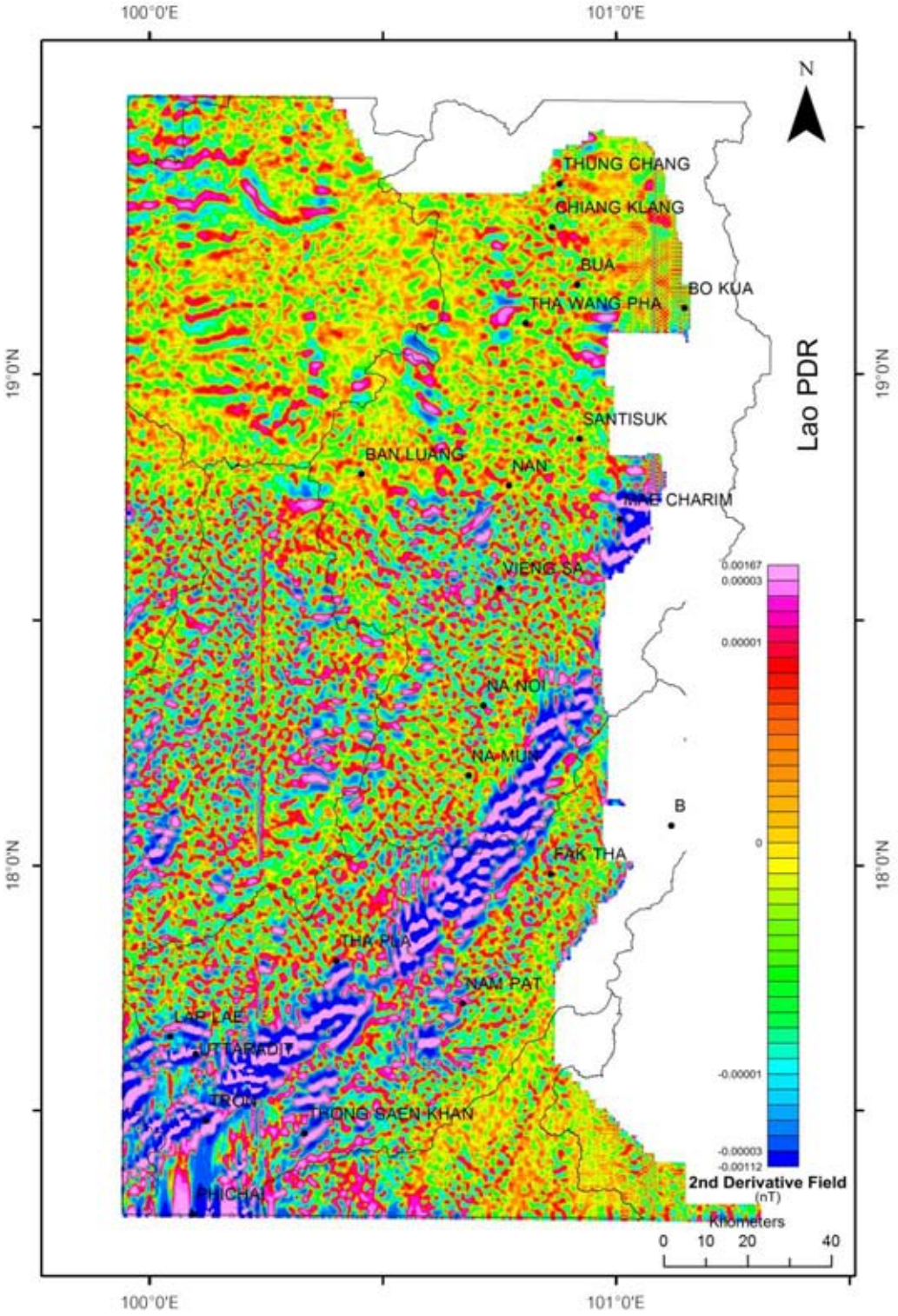

Figure 5.21a Enhanced magnetic map of the Nan-Uttaradit area after applying second vertical derivative technique.

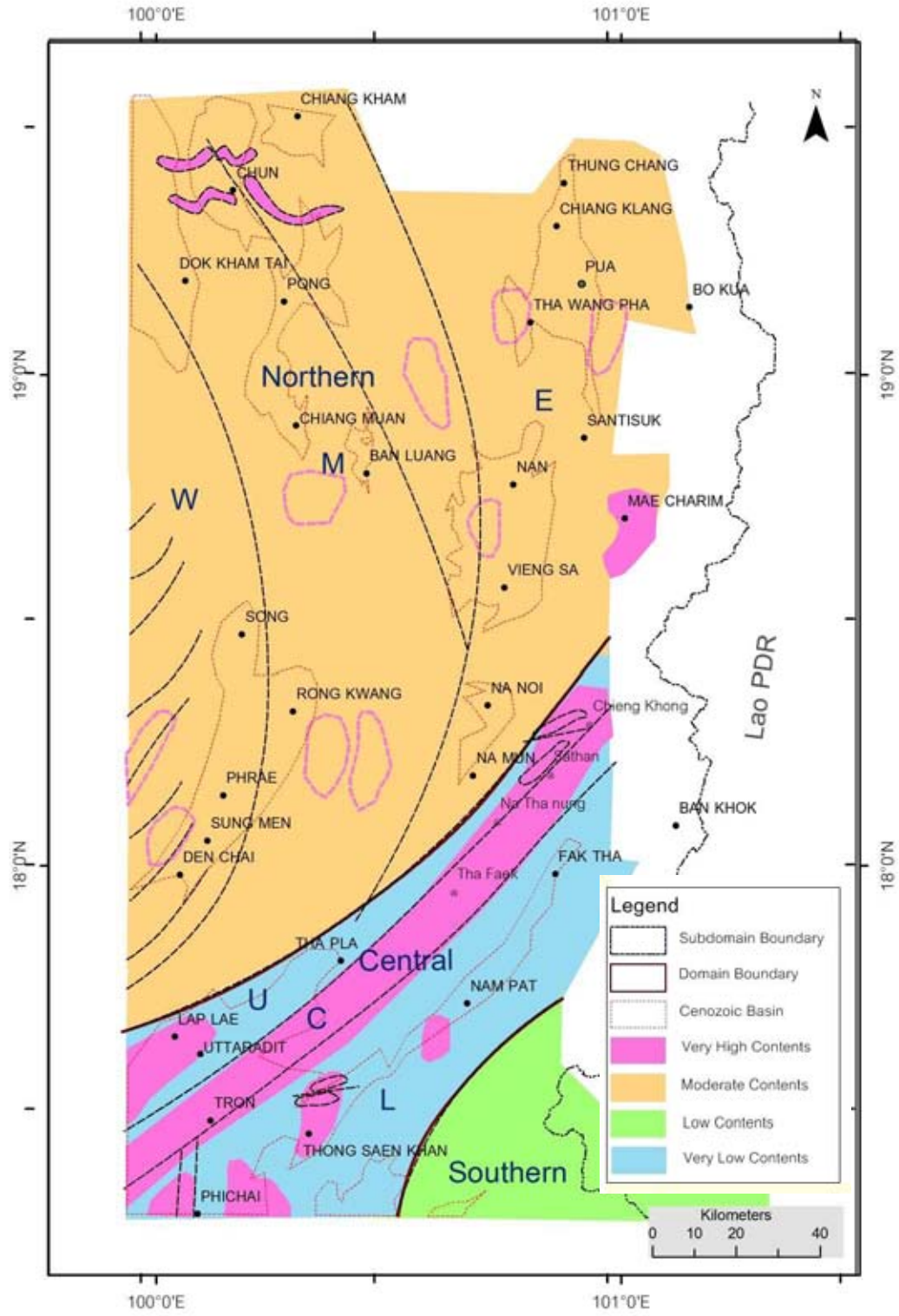

Figure 5.21b Interpreted second vertical derivative map of the Nan-Uttaradit area showing 3 magnetic domains (Northern domain, Central domain and Southern domain) and their sub domain(U=Upper, C=Central, L=Lower, W=Western, E=Eastern).

5.3.6 The Upward continuation map

The airborne magnetic map which is enhanced using upward continuation is shown in Figures. 5.22a at 500 m, 5.23a at 1,000 m, 5.24a at 1,500m and 5.25a at 2,000 m.

The interpretation map of the airborne magnetic data using this kind of enhancement process is shown in Figures. 5.22b to 5.25 b.

The results after applying the upward continuation enhancement support the existence of the central continuous high magnetic domain and the other domain of low value. For the northern domain, two separating zone of the lower and upper units are also present. In the southern domain, two small narrow high magnetic unit at Thong Saen Khan and Nan Pat towns are clearly shown similar to those of the 2^{nd} derivative field map (Figure. 5.21b).

However, as shown in the interpretation maps at 1000 – 2000m, anomalies in the central subdomain of the central domain have been obliterated.

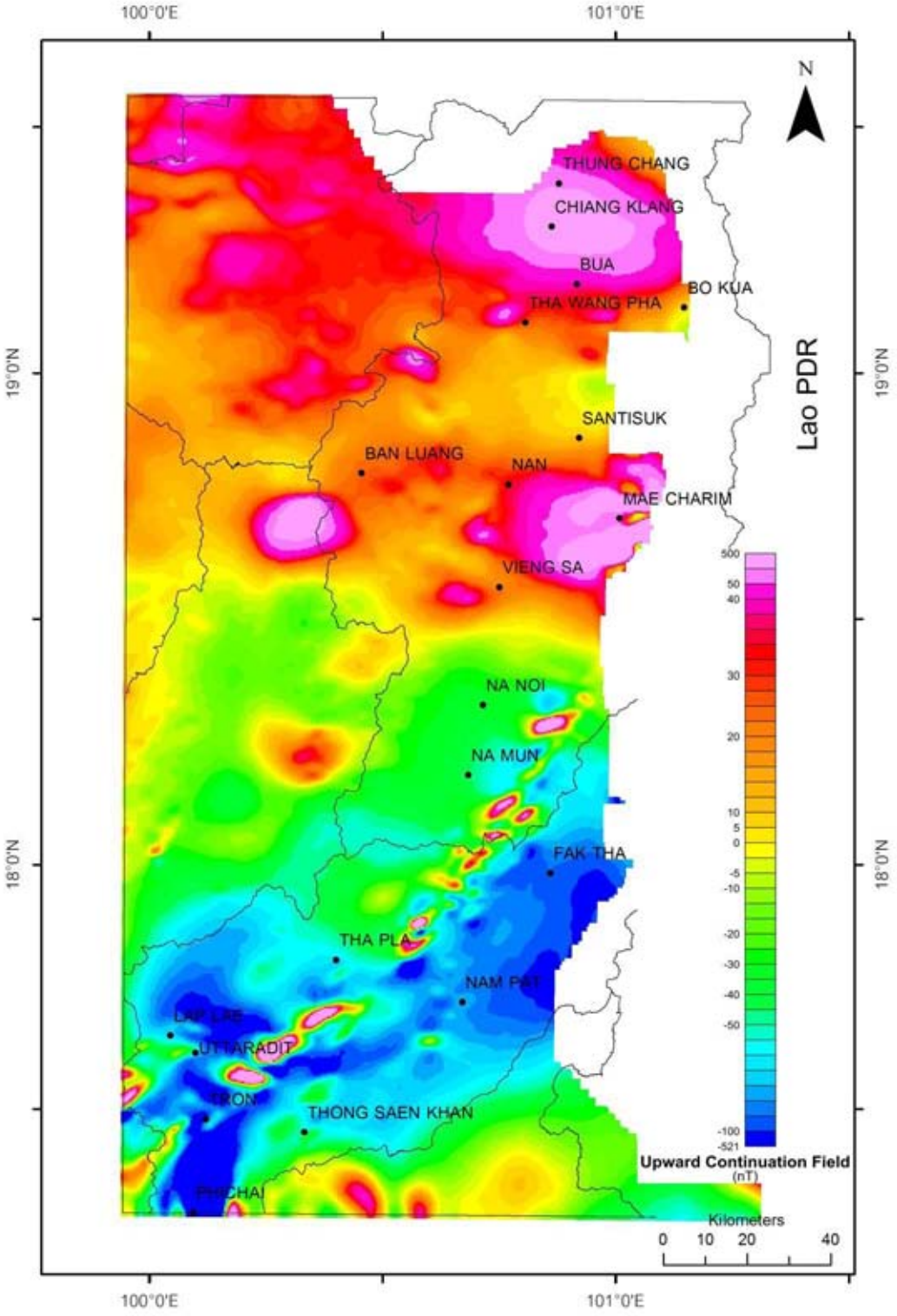

Figure 5.22a Enhanced magnetic map of the Nan-Uttaradit area after applying upward continuation technique. (500m)

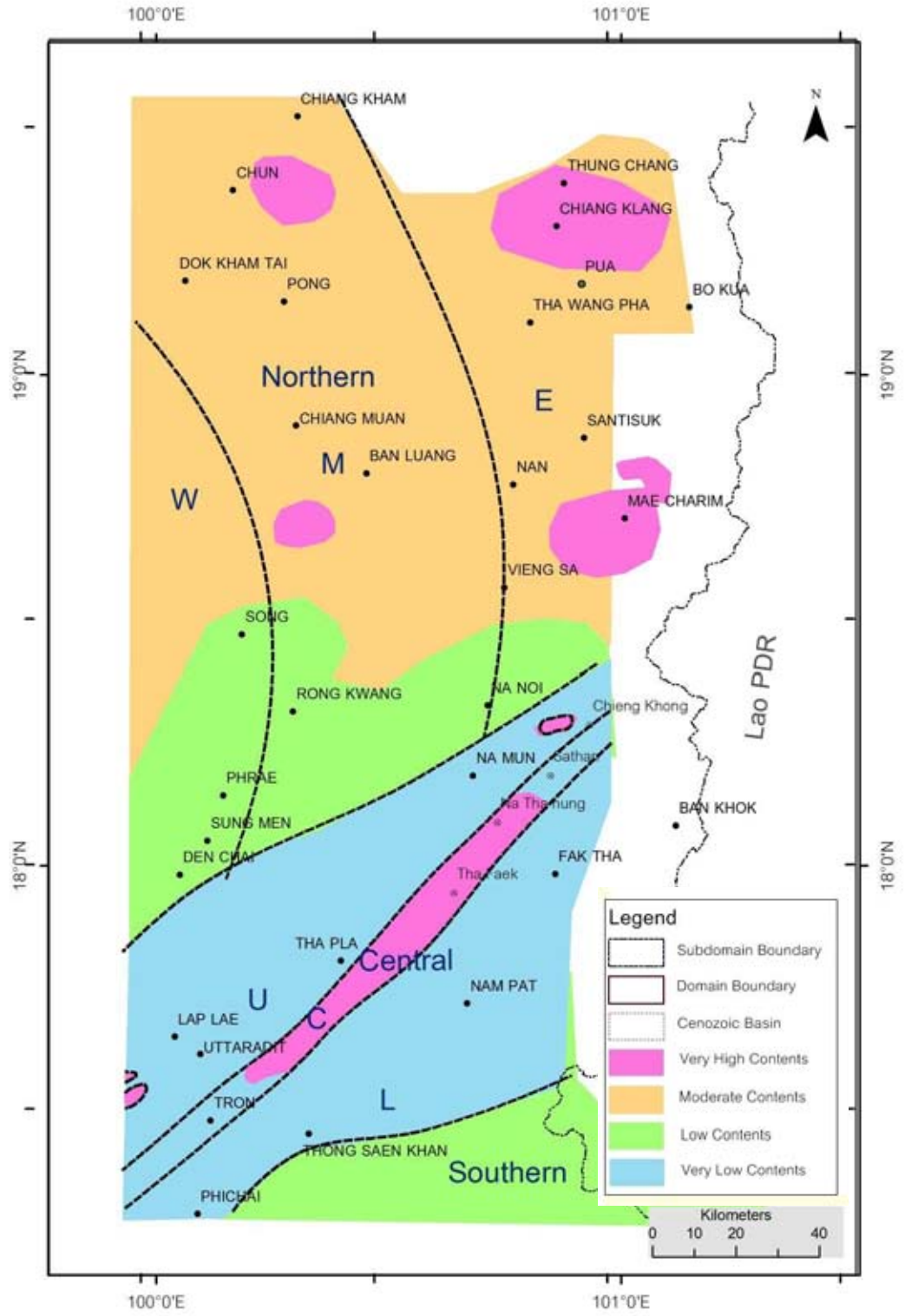

Figure 5.22b Interpretation upward continuation (500m) map of the Nan-Uttaradit area showing 3 magnetic domains (Northern domain, Central domain and Southern domain) and their sub domain(U=Upper, C=Central, L=Lower, W=Western, E=Eastern).

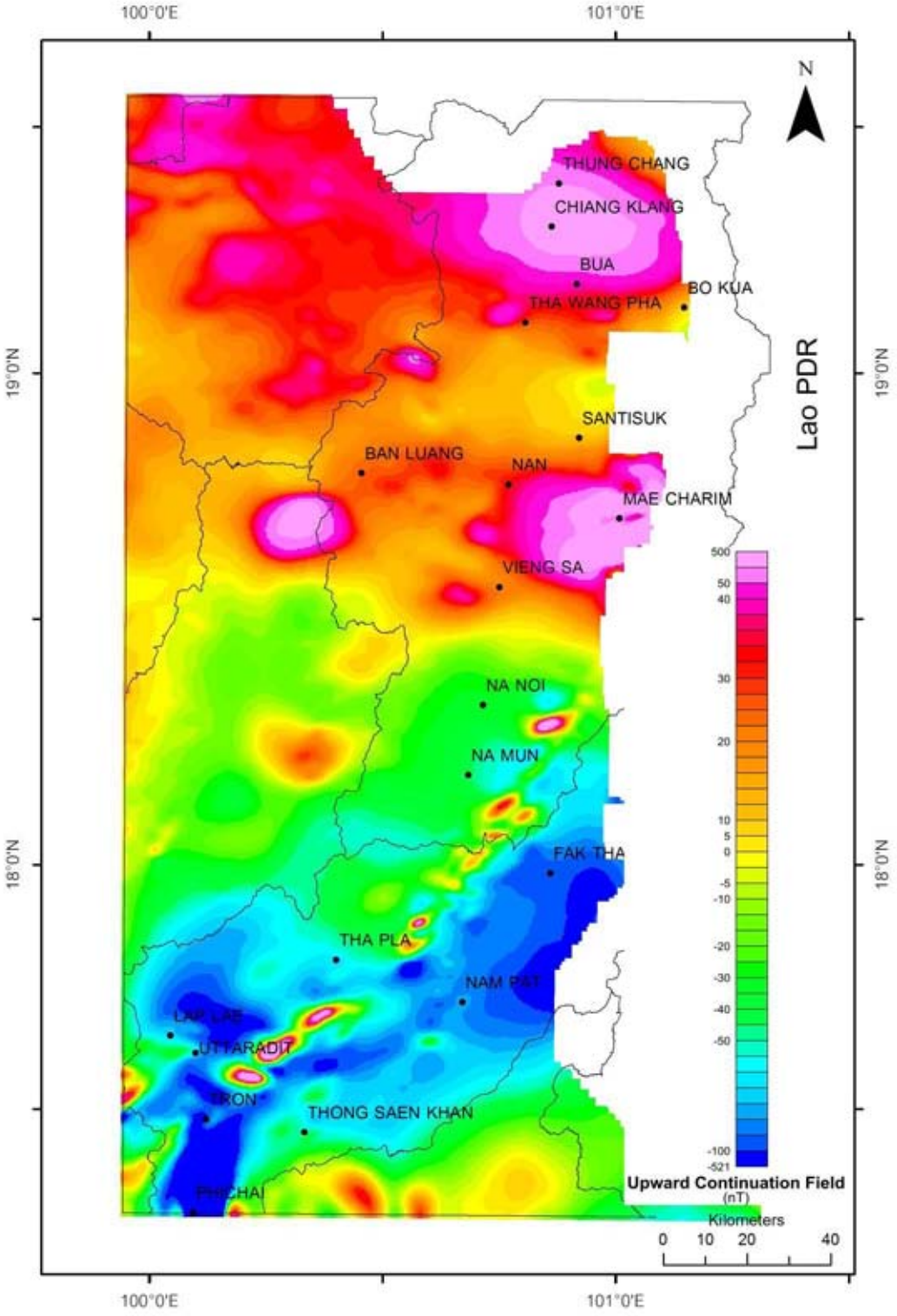

Figure 5.23a Enhanced magnetic map of the Nan-Uttaradit area after applying upward continuation technique. (1000m)

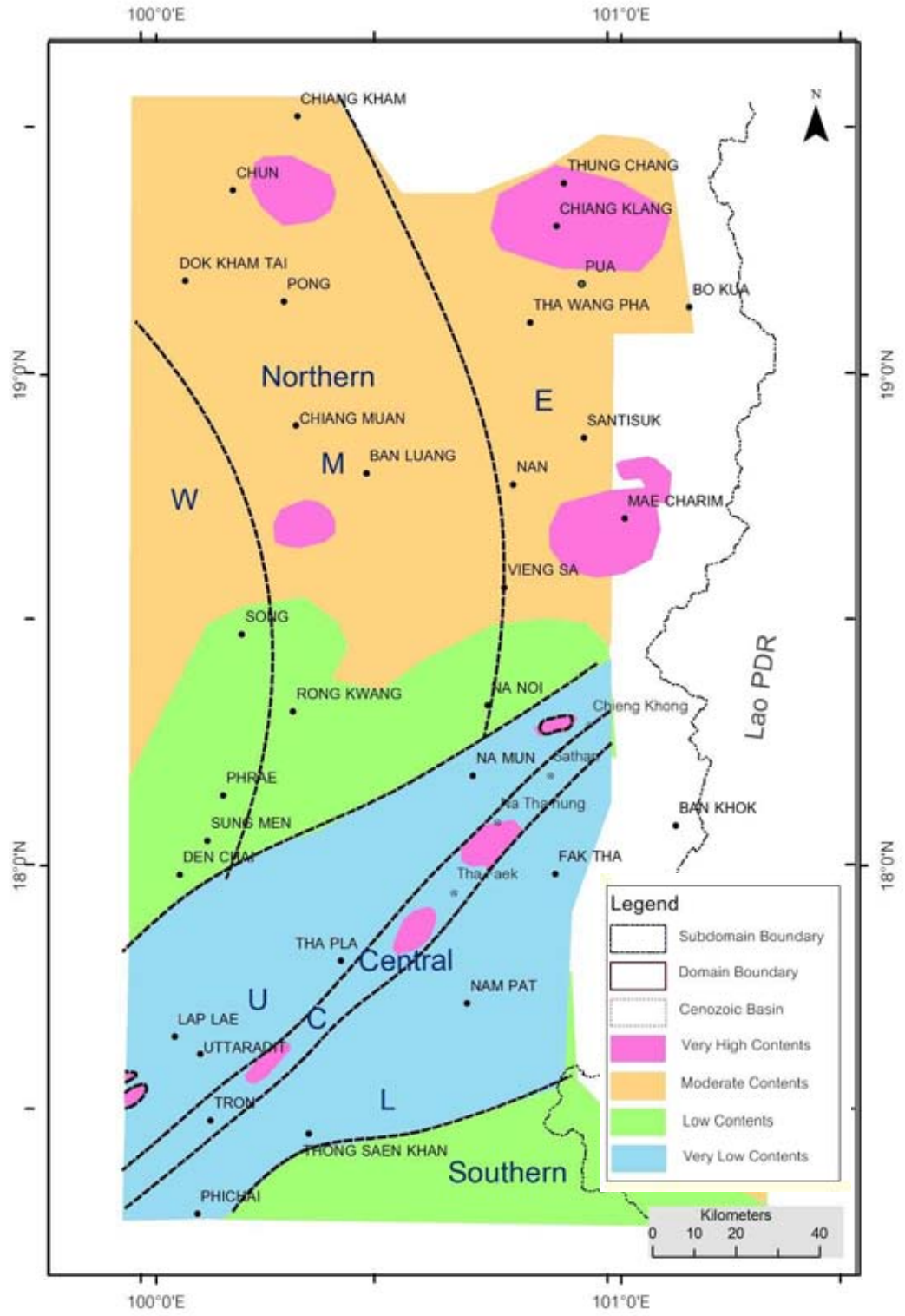

Figure 5.23b Interpreted upward continuation (1000m) map of the Nan-Uttaradit area showing 3 magnetic domains (Northern domain, Central domain and Southern domain) and their sub domain (U=Upper, C=Central, L=Lower, W=Western, E=Eastern).

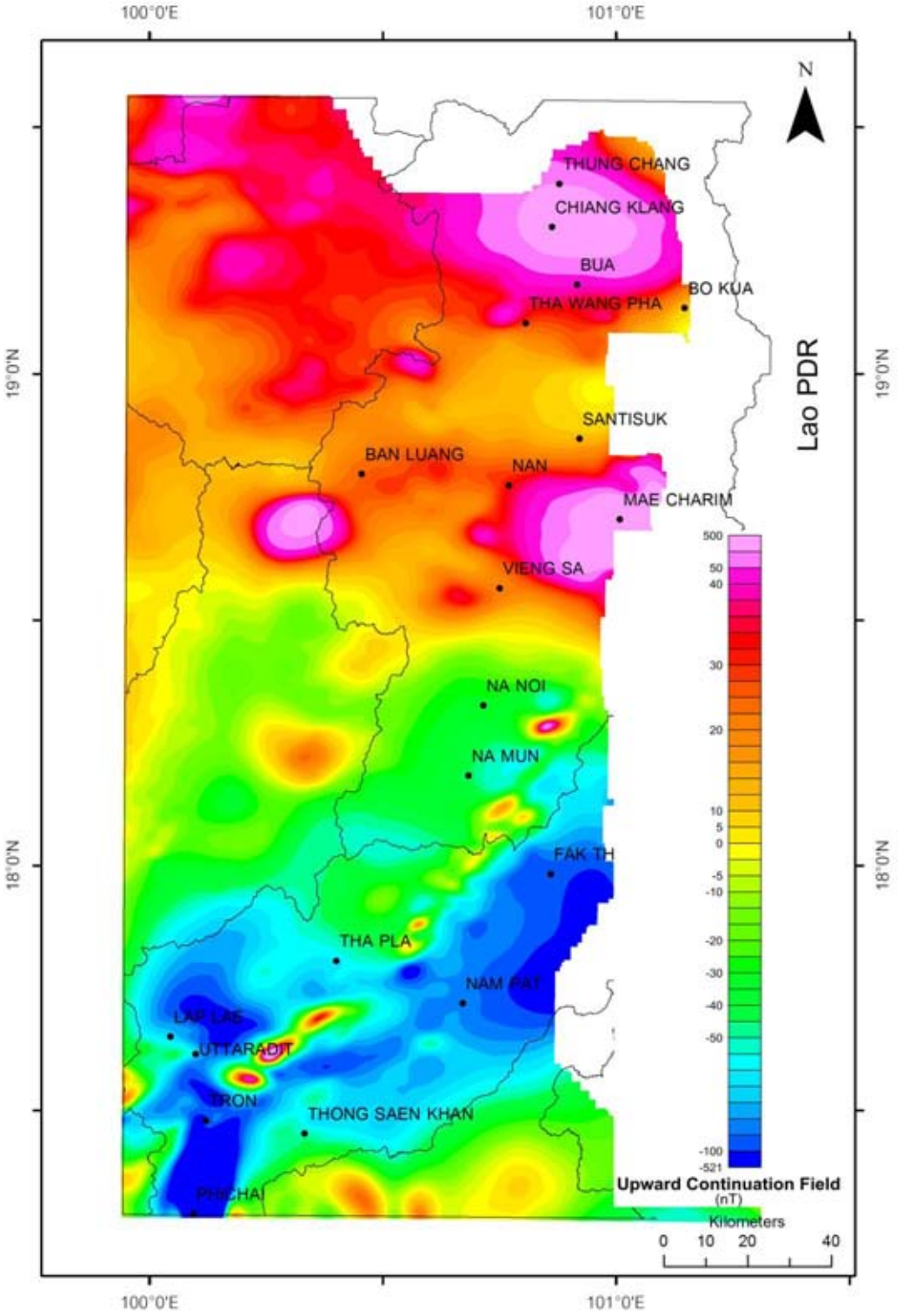

Figure 5.24a Enhanced magnetic map of the Nan-Uttaradit area after applying upward continuation technique (1500m).

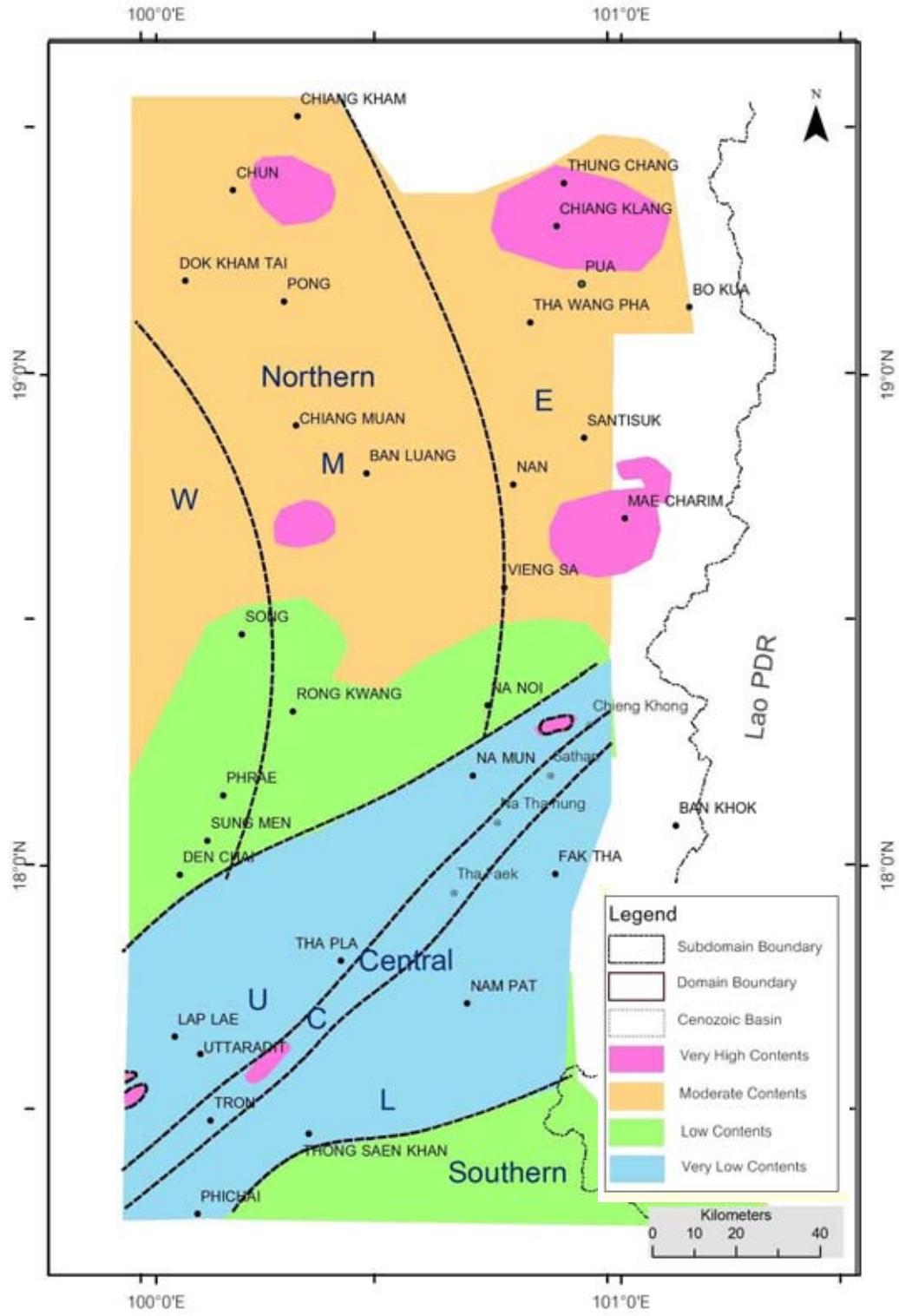

Figure 5.24b Interpreted upward continuation (1500m) map of the Nan-Uttaradit area showing 3 magnetic domains (Northern domain, Central domain and Southern domain) and their sub domain (U=Upper, C=Central, L=Lower, W=Western, E=Eastern).

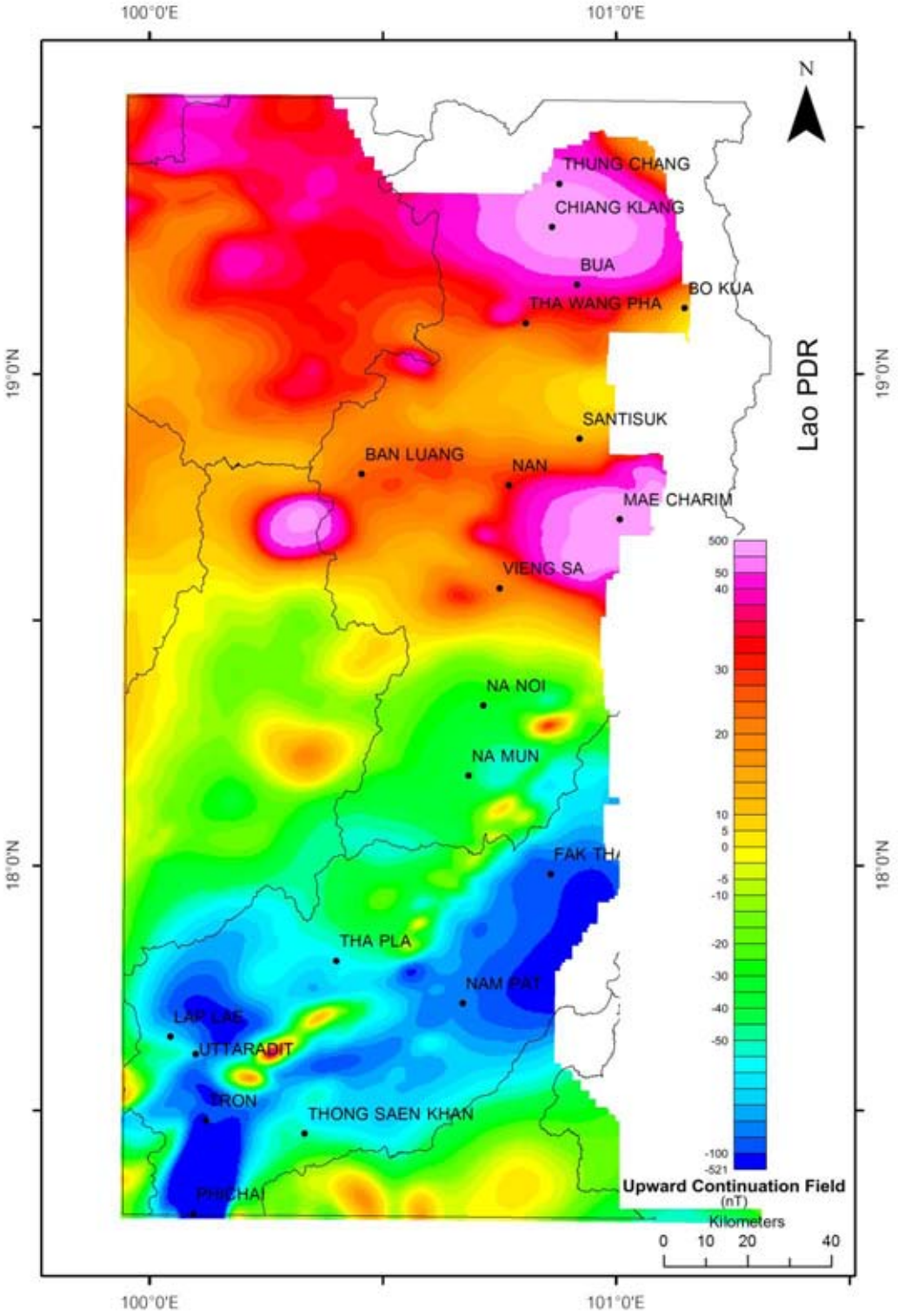

Figure 5.25a Enhanced magnetic map of the Nan-Uttaradit area after applying upward continuation technique (2000m).

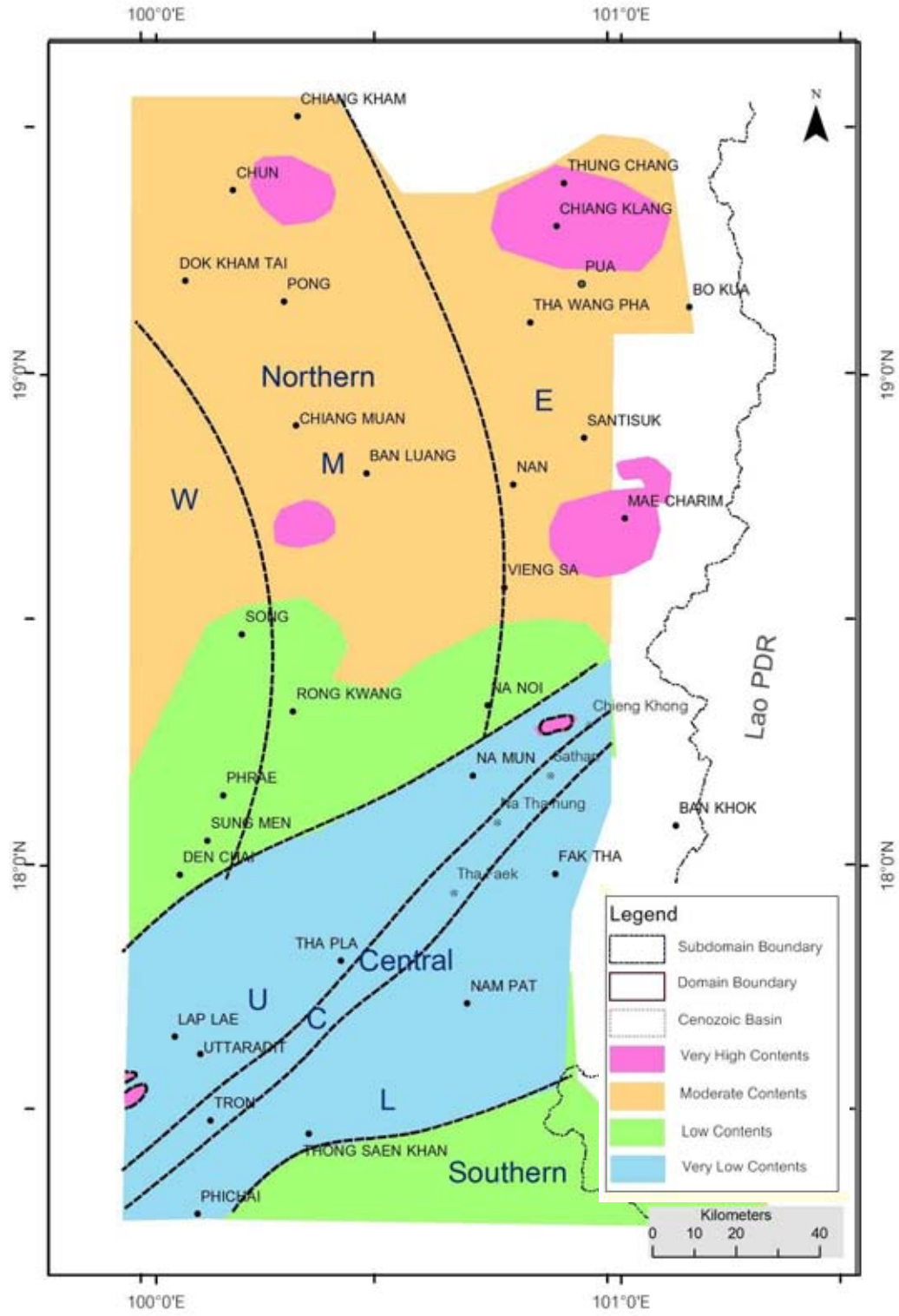

Figure 5.25b Interpreted upward continuation (2000m) map of the Nan-Uttaradit area showing 3 magnetic domains (Northern domain, Central domain and Southern domain) and their sub domain (U=Upper, C=Central, L=Lower, W=Western, E=Eastern).

5.3.7 The Downward continuation map

The airborne magnetic map which is enhanced using downward continuation is shown in Figures. 5.26a at 800 m, 5.27a at 500m, 5.28a at 300m and 5.29a at 100 m.

The interpretation map of the airborne magnetic data using this kind of enhancement process is shown in Figures. 5.26b to 5.29b.

The results after applying the downward continuation enhancement shows 3 subparallel magnetic domains (namely northern, central and southern). The central continuous high magnetic band in the central domain is clearly well-defined. The other two zones of low values are denoted by the occurrence of very low magnetic zone. The northern domain show moderate to high magnetic value with large circular magnetic bodies. In the southern domain, two small narrow high magnetic unit at Thong Saen Khan and Nan Pat areas are clearly shown similar to those of the 2^{nd} derivative field map (Figure. 5.21b)

The occurrences of fold in Chun, Dok Kham Tai and Chiang Muan towns can indicated the compression in E-W direction.

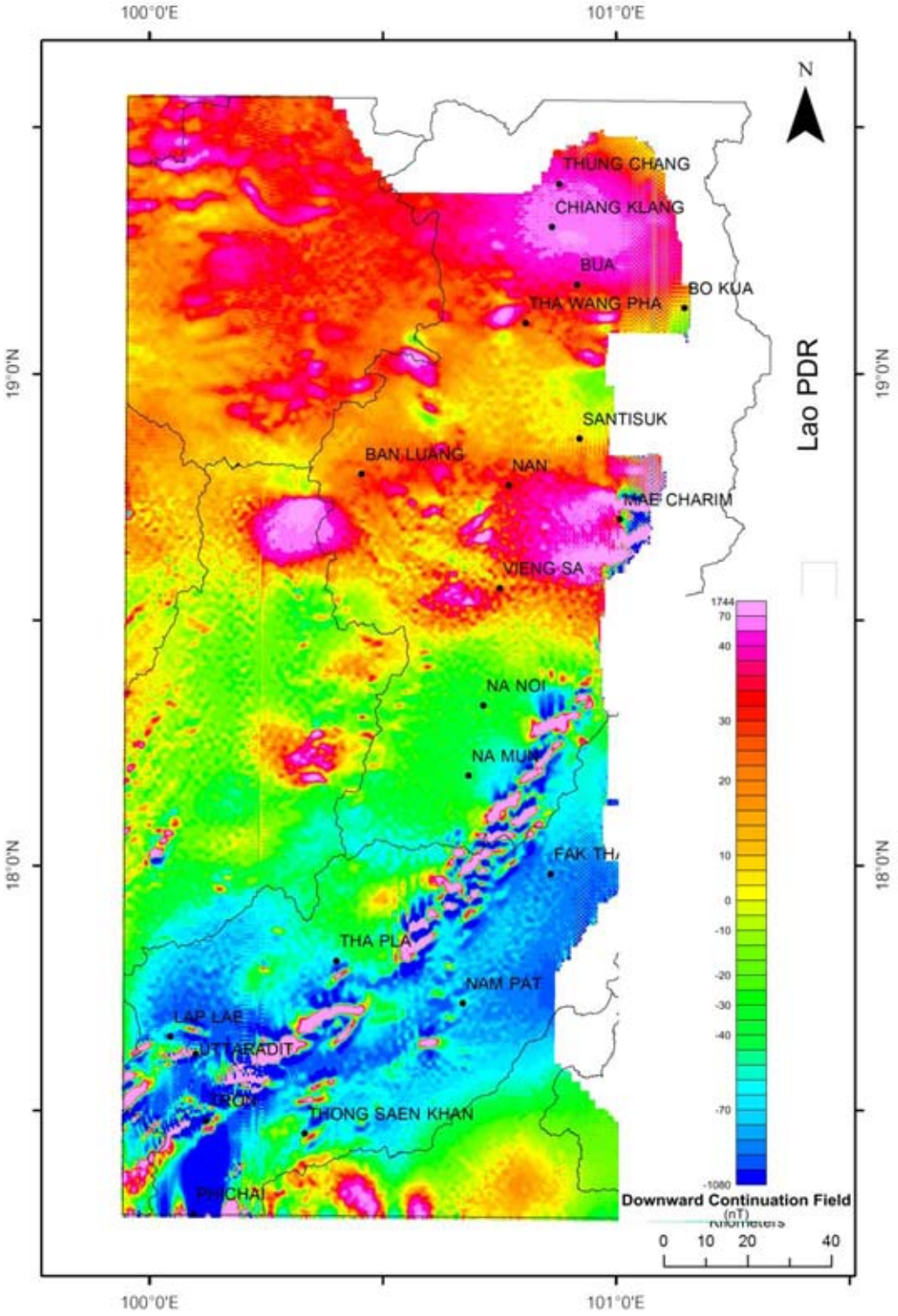

Figure 5.26a Enhanced magnetic map of the Nan-Uttaradit area after applying downward continuation technique (800m).

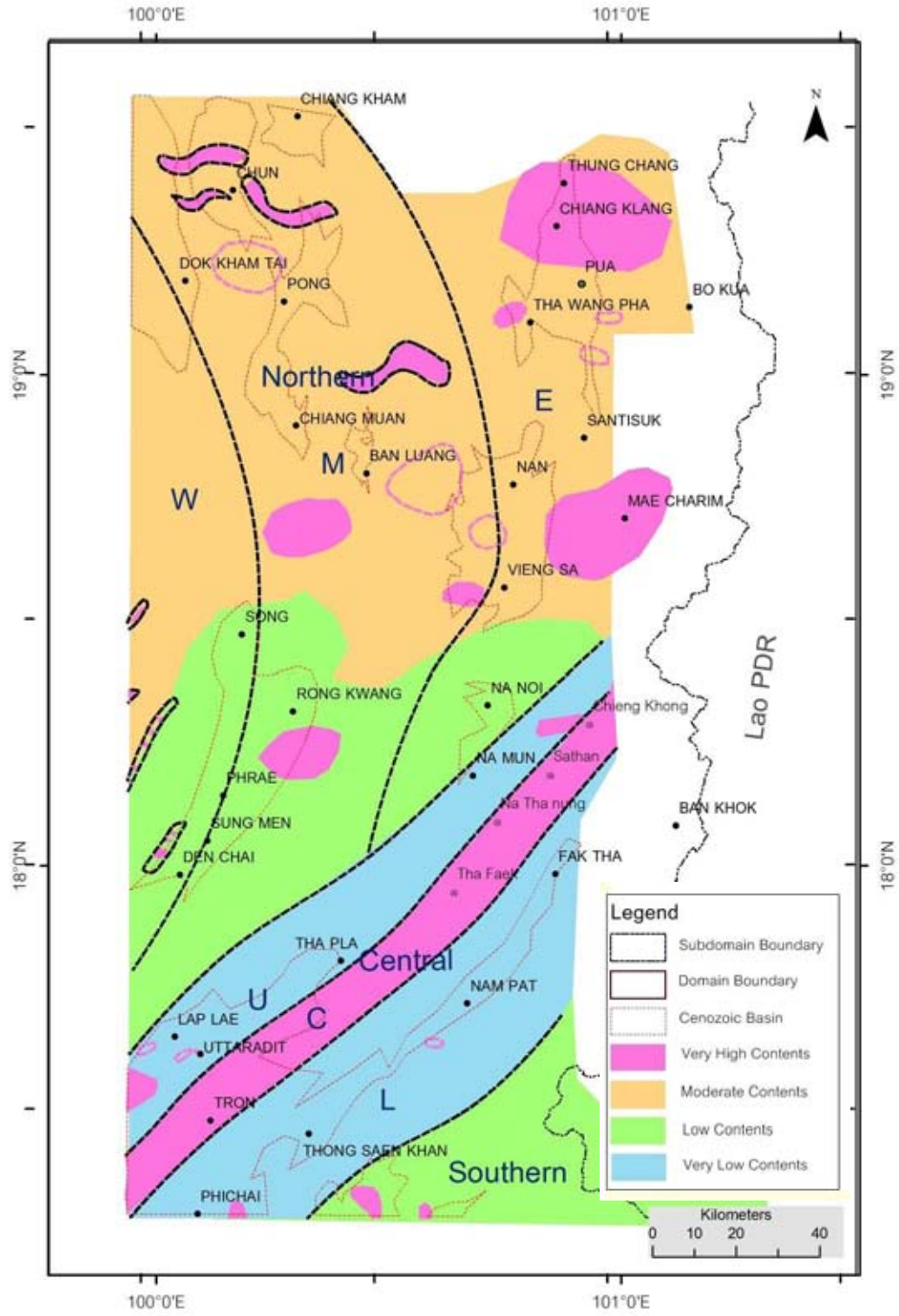

Figure 5.26b Interpreted downward continuation (800m) map of the Nan-Uttaradit area showing 3 magnetic domains (Northern domain, Central domain and Southern domain) and their sub domain (U=Upper, C=Central, L=Lower, W=Western, E=Eastern).

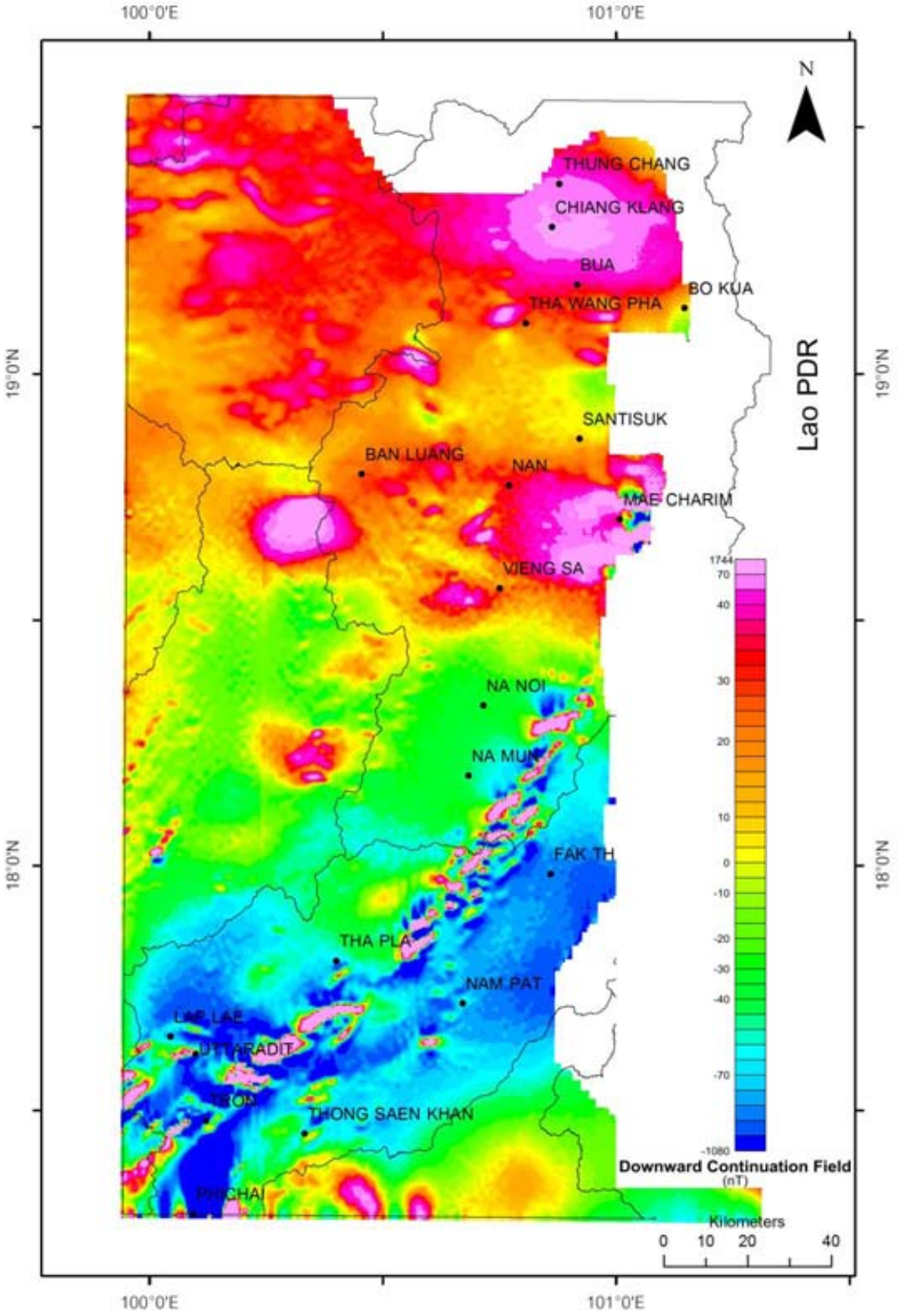

Figure 5.27a Enhanced magnetic map of the Nan-Uttaradit area after applying downward continuation technique (500m).

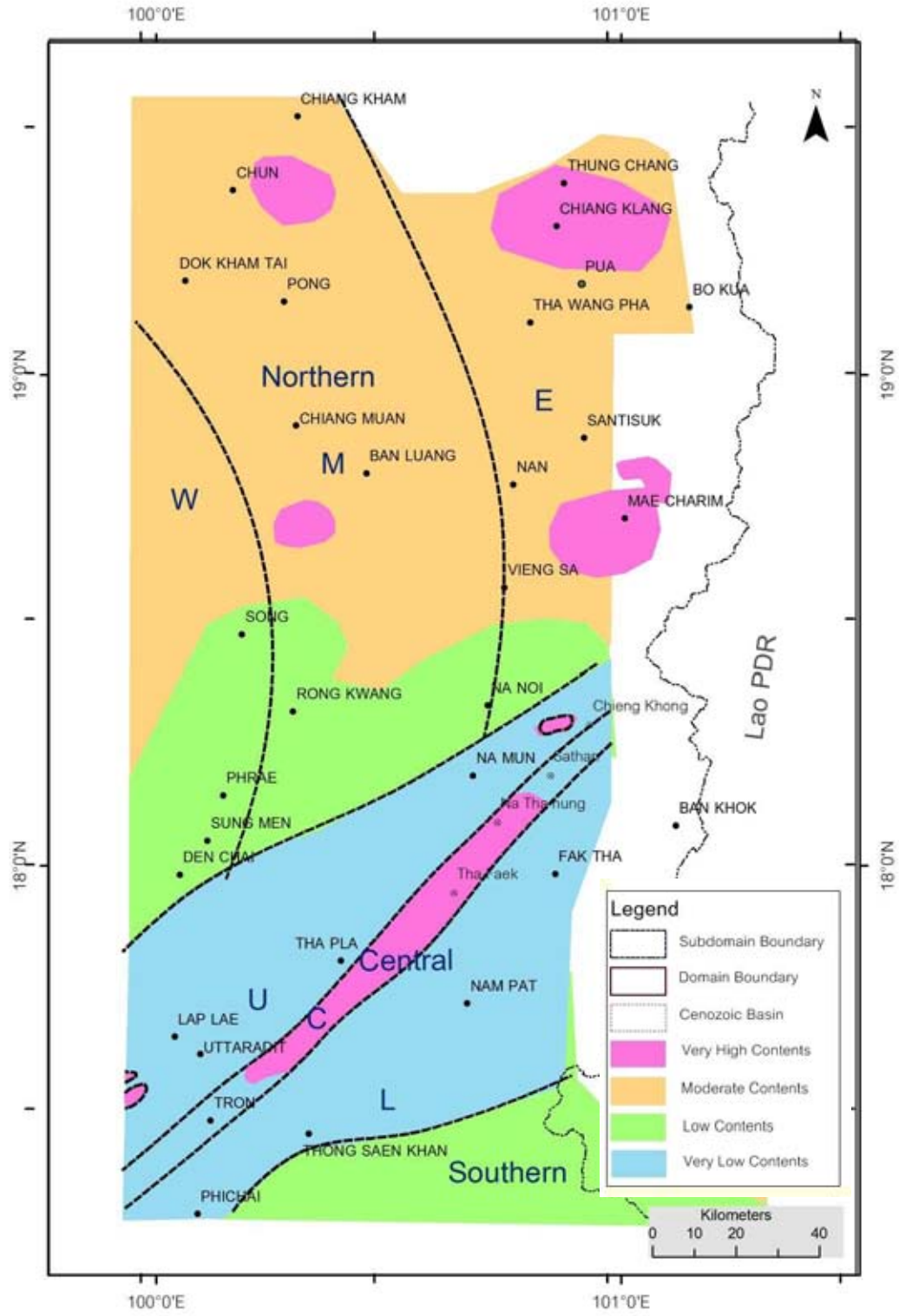

Figure 5.27b Interpretation downward continuation (500m) map of the Nan-Uttaradit area showing 3 magnetic domains (Northern domain, Central domain and Southern domain) and their sub domain (U=Upper, C=Central, L=Lower, W=Western, E=Eastern).

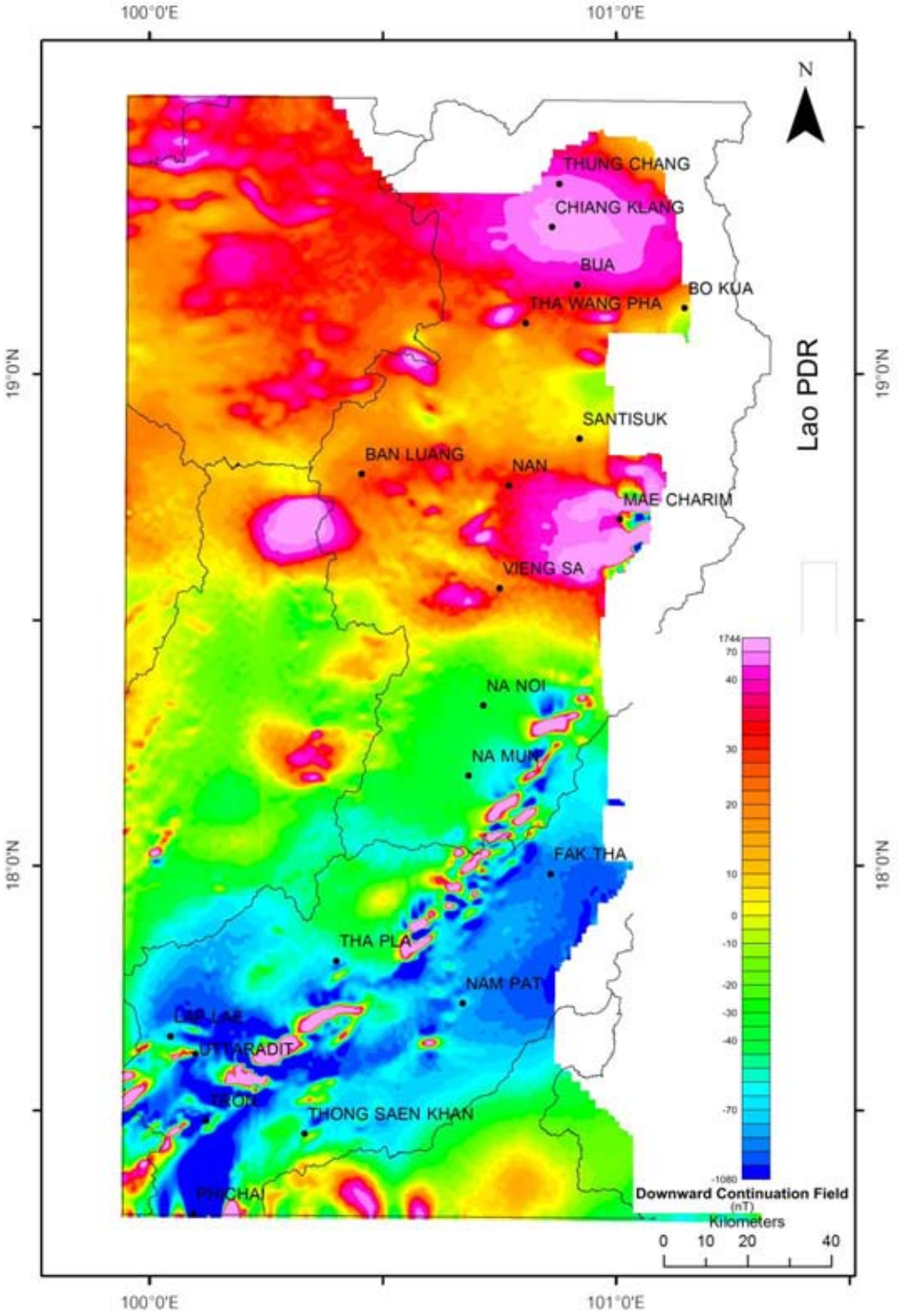

Figure 5.28a Enhanced magnetic map of the Nan-Uttaradit area after applying downward continuation technique (300m).

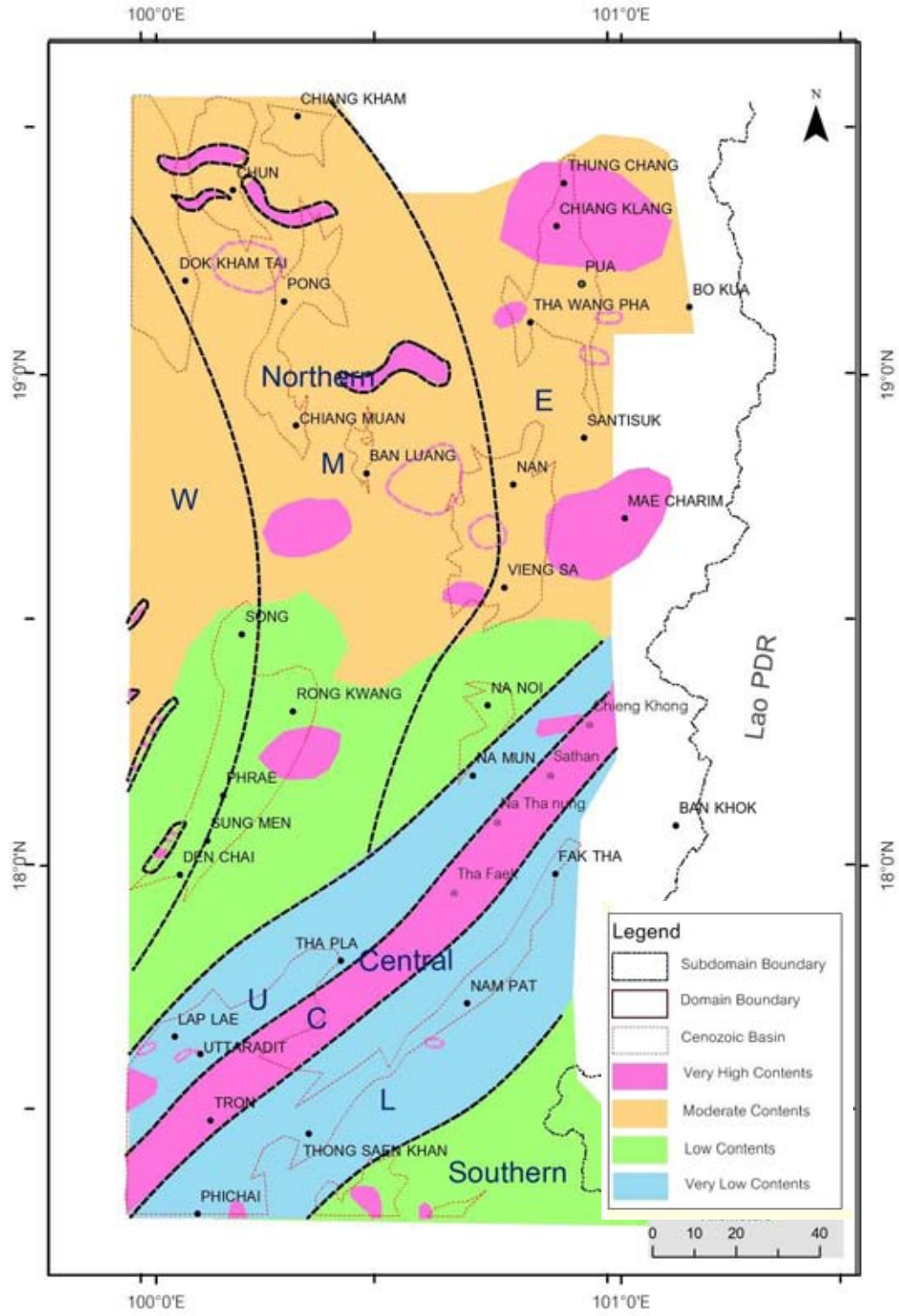

Figure 5.28b Interpreted downward continuation (300m) map of the Nan-Uttaradit area showing 3 magnetic domains (Northern domain, Central domain and Southern domain) and their sub domain (U=Upper, C=Central, L=Lower, W=Western, E=Eastern).

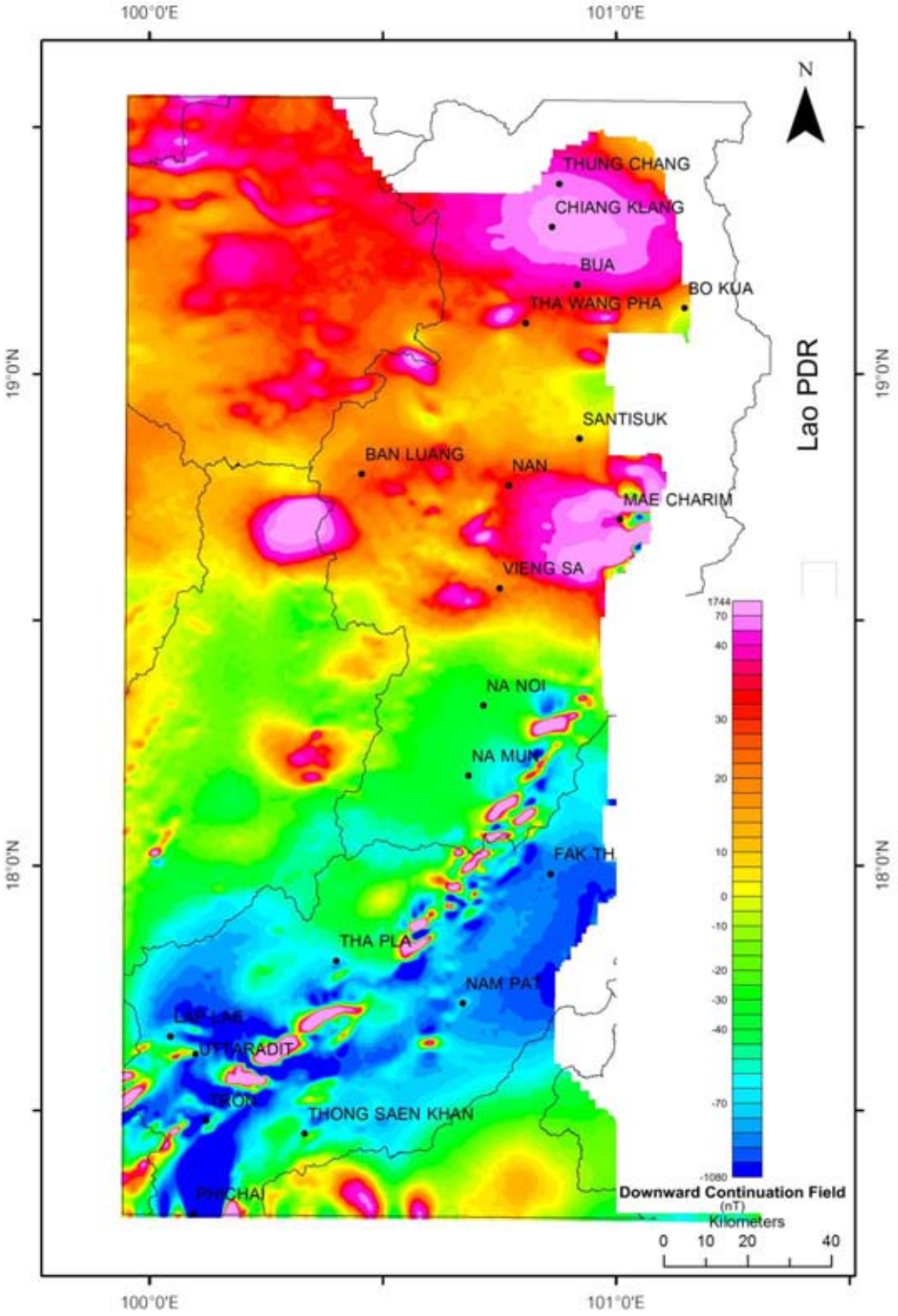

Figure 5.29a Enhanced magnetic map of the Nan-Uttaradit area after applying downward continuation technique (100m).

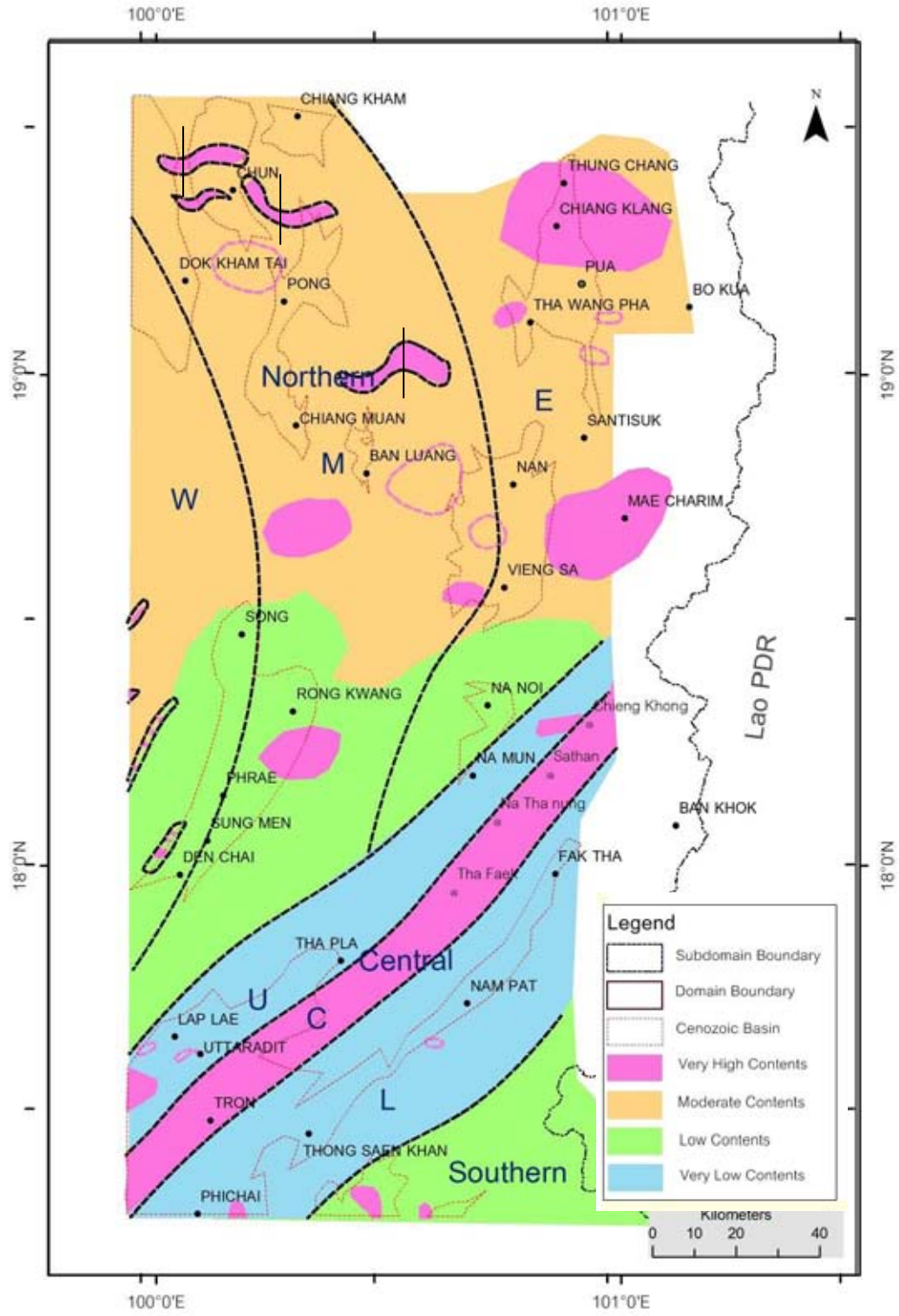

Figure 5.29b Interpreted downward continuation (100m) map of the Nan-Uttaradit area showing 3 magnetic domains (Northern domain, Central domain and Southern domain) and their sub domain (U=Upper, C=Central, L=Lower, W=Western, E=Eastern).

5.3.8 Magnetic Subdivision

The results displayed in Figure 5.17 to 5.29 lead to the conclusion that the central domain of the Nan-Uttaradit area is the most import domain to be ascribed and can be easily subdivided into 3 subparallel subdomains based on the interpretation of the enhanced airborne radiometric and magnetic image data. This NE-SW trending domain follows the regional structures mapped by previous workers. However, as depicted in earlier sections that the central domain shows the contrasting geophysical features to the northern and southern domains. It is also note that the northern domain is quite different from the southern domain because the former displays well-defined NE-SW trending zones of the upper and lower parts and the latter shows unusually high value of immediate to the central domain.

5.3.9 Geophysical cross section

After the division of magnetic domains, cross-sections of the magnetic data were made in the NW-SE direction as shown in Figure 5.30a. Special attention is focused on the central domain where structures and geology are much outstanding (see earlier section). Nine lines of sections were constructed from Na Noi in the north to Phi Chai in the south perpendicular to the main or regional trend of the central domain (see Figure. 5.30b).

The results of the sections are shown in Figure 5.31. Both observed and calculated values with the orientation and shape of the anomalies are illustrated in Figures 5.31a to5.31i. Figure 5.31a is a section along line A (north of Na Noi) showing a large body with a width of about 2.78 km and moderately high angle SE dipping. Figure 5.31b is a section along line B (north of Na Mun) displaying a small (thin) body with the width of about 1.17 km and vertical dipping. A NW-SE section along line C was made through Fak Tha Town (Figure 5.31d) showing 2 separated bodies- a larger body with the width of about 5.09 km. and the other small body with the width of about 1.78 km., But show high angle dipping to SE direction. Figure 5.31D illustrates 3 dike-like bodies between Nam Pat and Fak Tha Town with a width of about 0.8 to 13 km and the large body of about 13 km thickness with almost vertical dipping. Figure 5.31E is line E section showing 3 bodies in Nam Pat Town with moderate dip to the SE and a body with high-angle dip. Similar scenario is seen in the section of Line F through Tha Pla town (Figure 5.31F) with the large bodies of about 3.34 to 16.99 km thickness. Section of line G is shown in Figure 5.31G. It displays 2 small bodies of anomaly dike with the thickness of 2.44 to 2.50 km. and dip at high angle to the SE direction. Line H section in Figure 5.31H shows a large body of about 11.50 km thick, dipping to SE at high angle. Line I section in Figure 5.31 I illustrates 2 small bodies, both dipping SE and as thick as 3.68-5.25 km. It is quite interesting to note that all the sections show quite similar orientation of anomalous bodies in that they are dipping to the east. The details of parameter that use to run these models are showing in Appendix A.

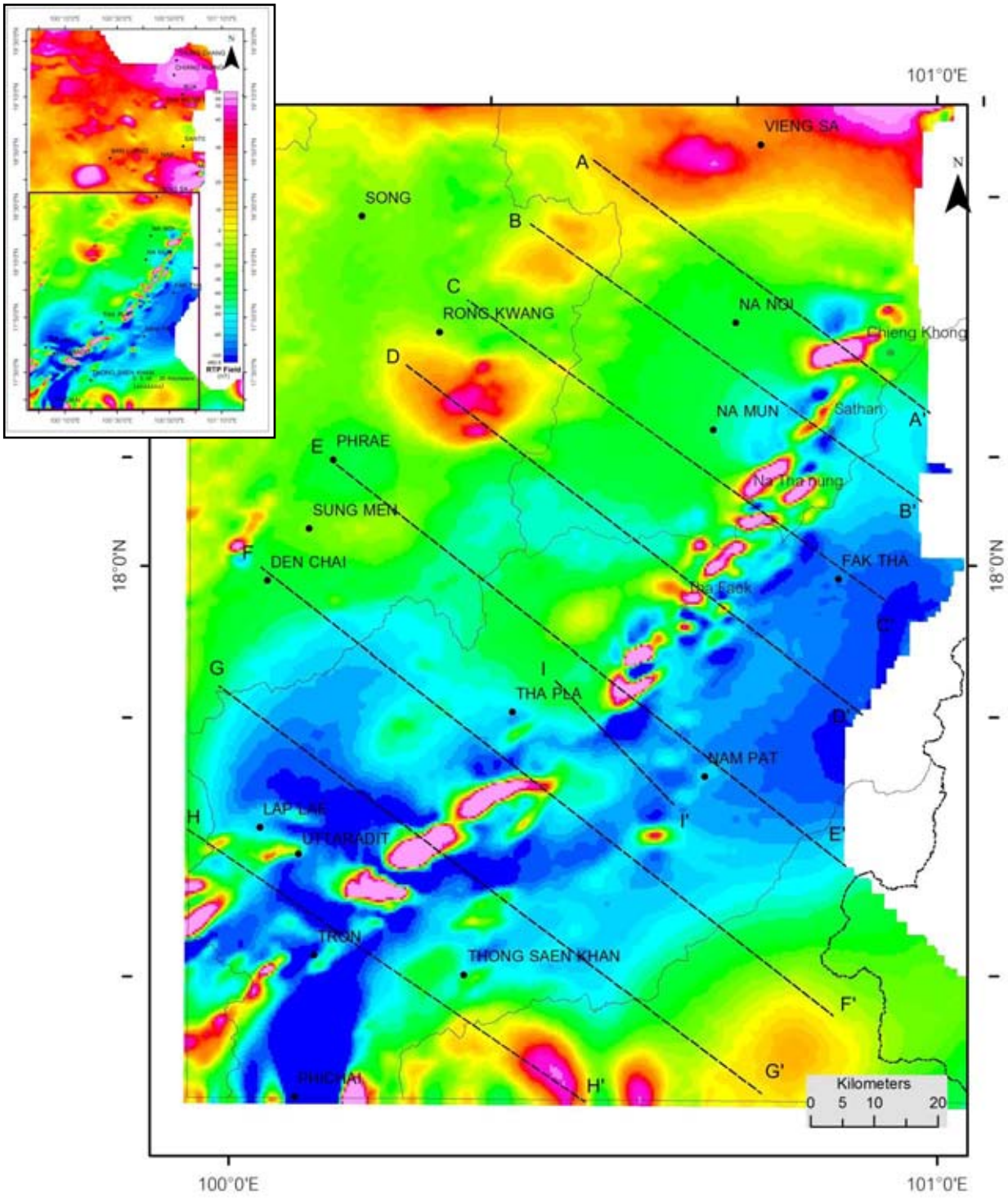

Figure 5.30 The aeromagnetic RTP map of the Nan-Uttaradit area showing selected areas for cross-section. (B) Lines of cross sections used for interpretation shown in Figure. 5.31.

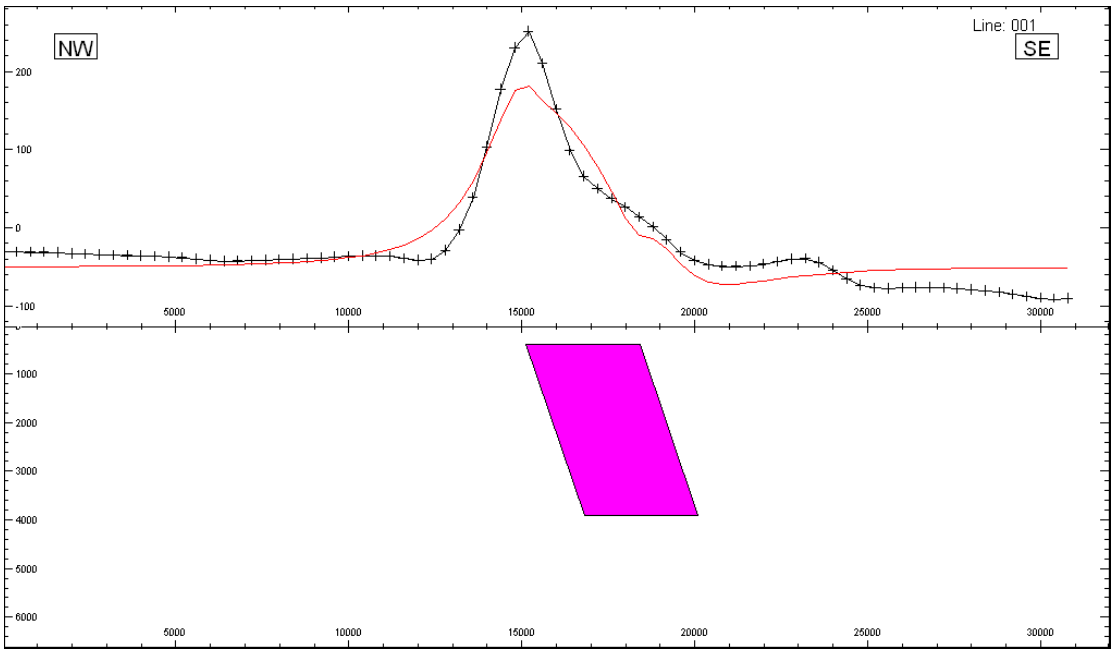

Figure 5.31a Airborne magnetic cross section of the Nan-Uttaradit area showing the observed and calculated value and interpreted magnetic anomaly bodies of line A-A'.

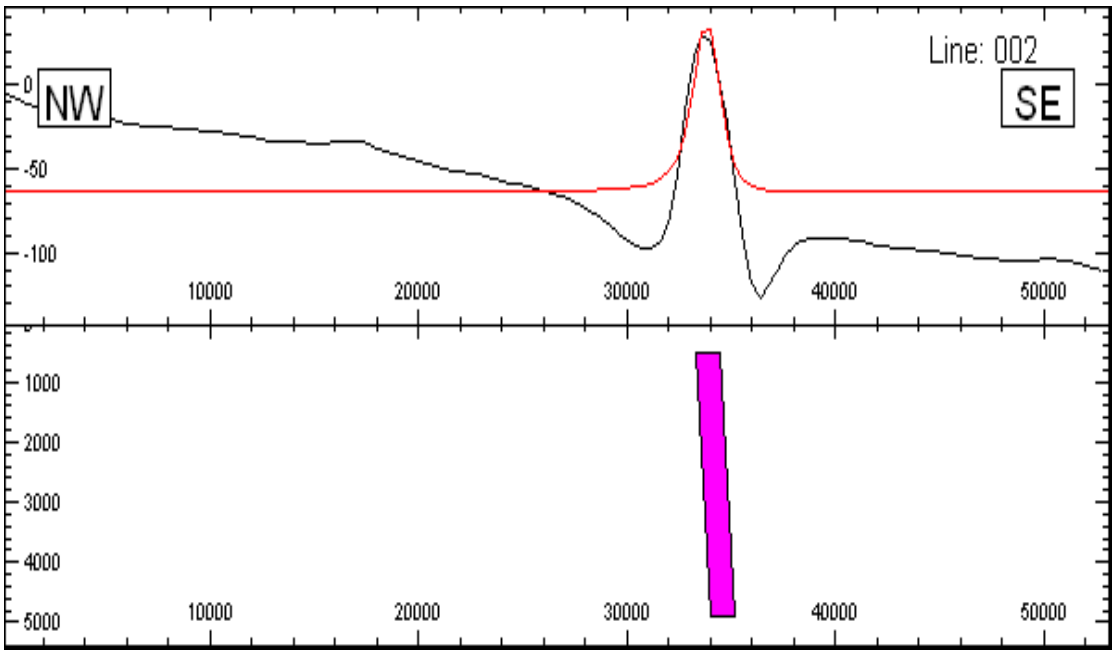

Figure 5.31b Airborne magnetic cross section of the Nan-Uttaradit area showing the observed and calculated value and interpreted magnetic anomaly bodies of line B-B'.

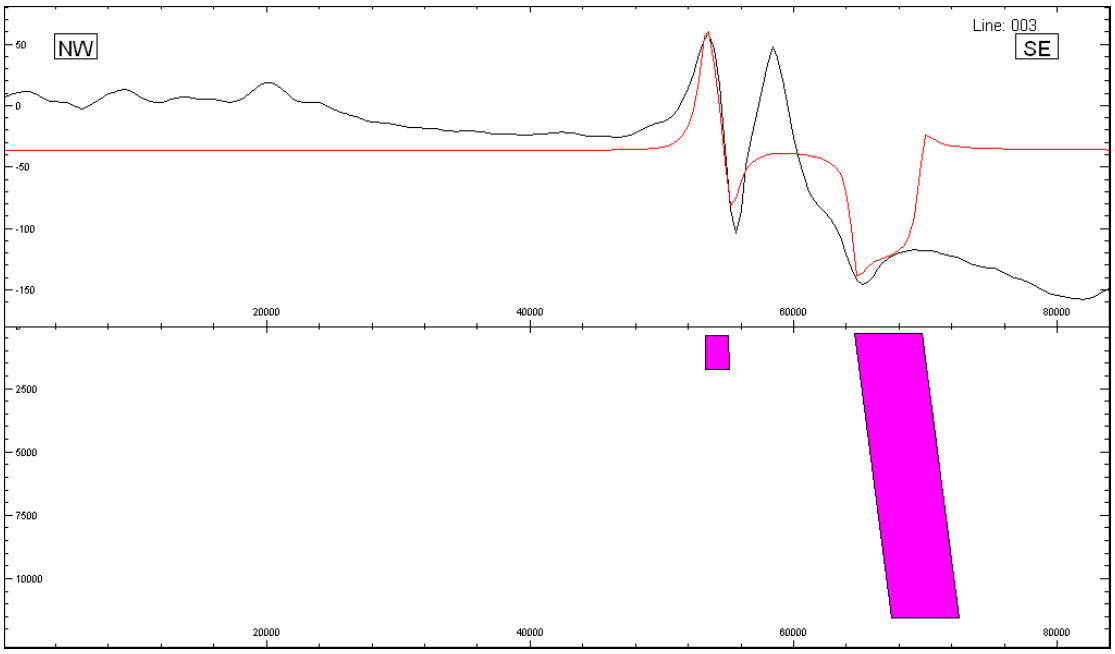

Figure 5.31c Airborne magnetic cross section of the Nan-Uttaradit area showing the observed and calculated value and interpreted magnetic anomaly bodies of line C-C'.

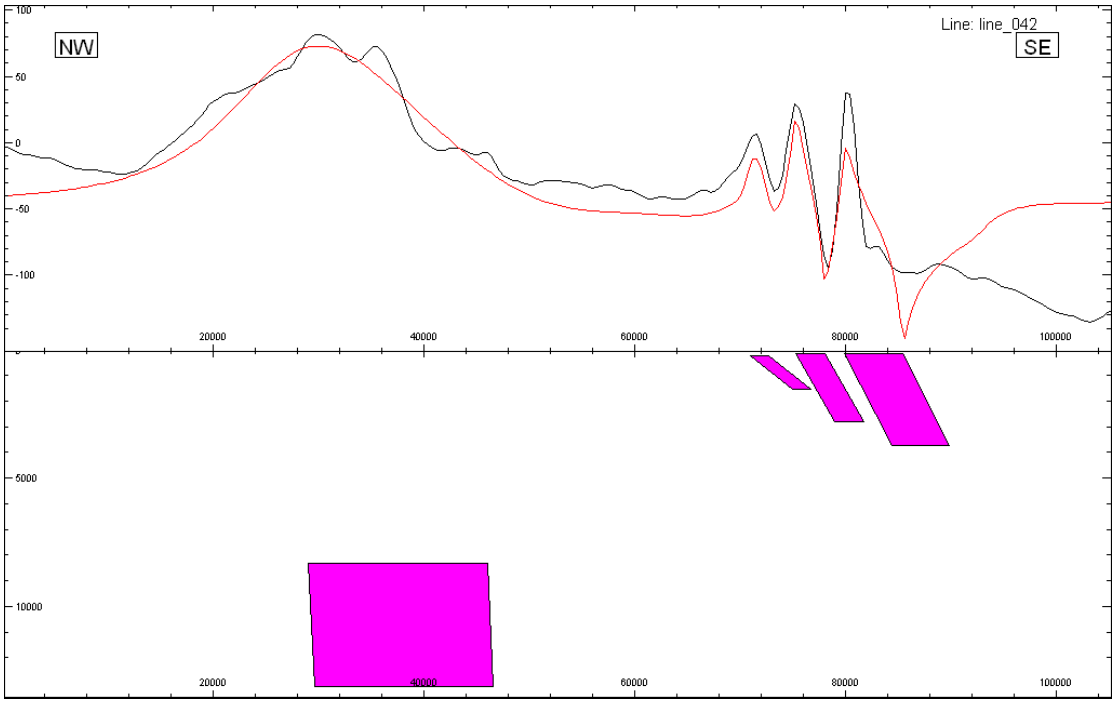

Figure 5.31d Airborne magnetic cross section of the Nan-Uttaradit area showing the observed and calculated value and interpreted magnetic anomaly bodies of line D-D'.

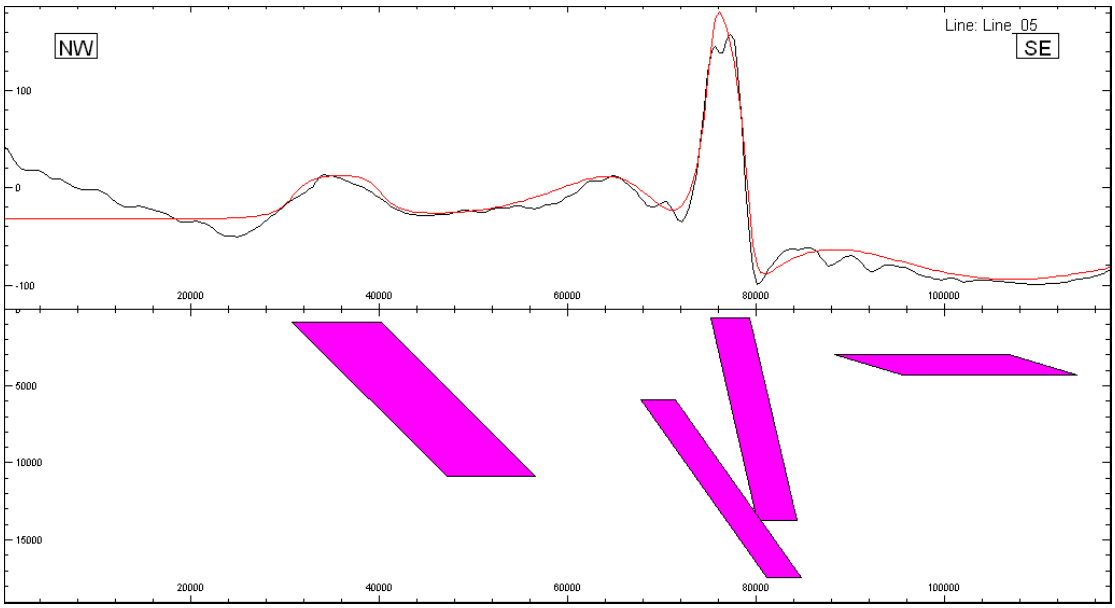

Figure 5.31e Airborne magnetic cross section of the Nan-Uttaradit area showing the observed and calculated value and interpreted magnetic anomaly bodies of line E-E'.

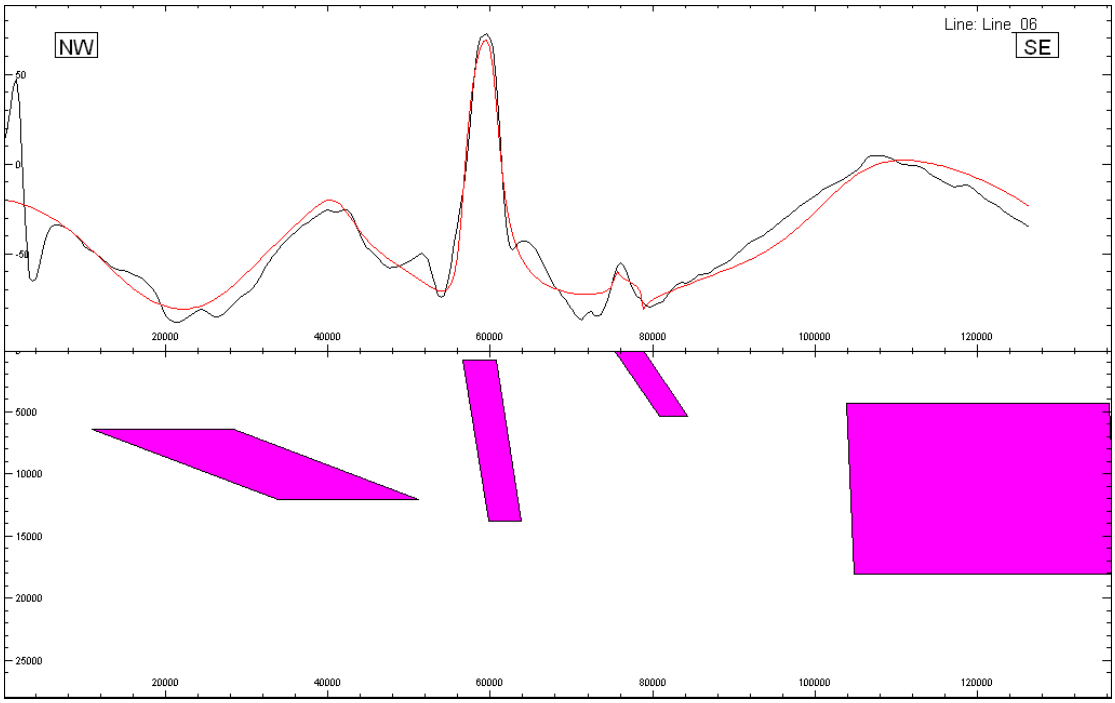

Figure 5.31f Airborne magnetic cross section of the Nan-Uttaradit area showing the observed and calculated value and interpreted magnetic anomaly bodies of line F-F'.

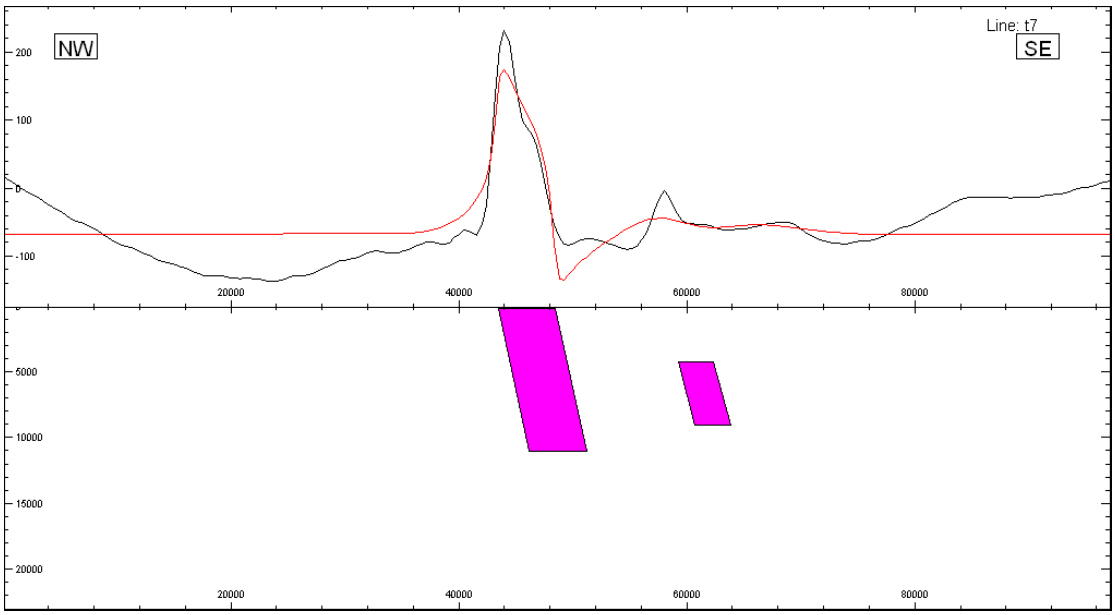

Figure 5.31g Airborne magnetic cross section of the Nan-Uttaradit area showing the observed and calculated value and interpreted magnetic anomaly bodies of line G-G'.

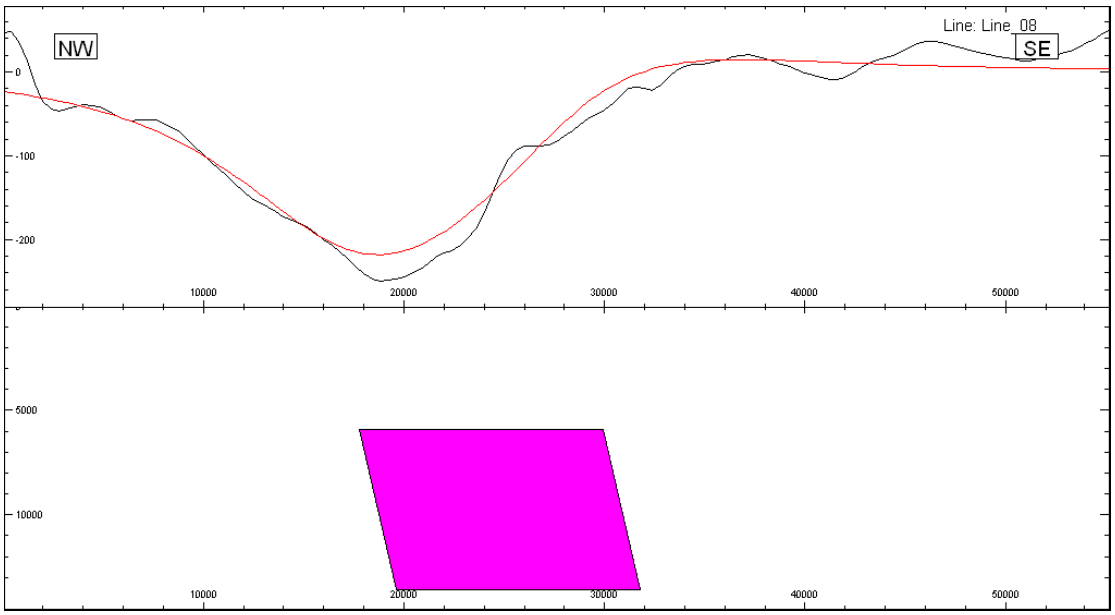

Figure 5.31h Airborne magnetic cross section of the Nan-Uttaradit area showing the observed and calculated value and interpreted magnetic anomaly bodies of line H-H'.

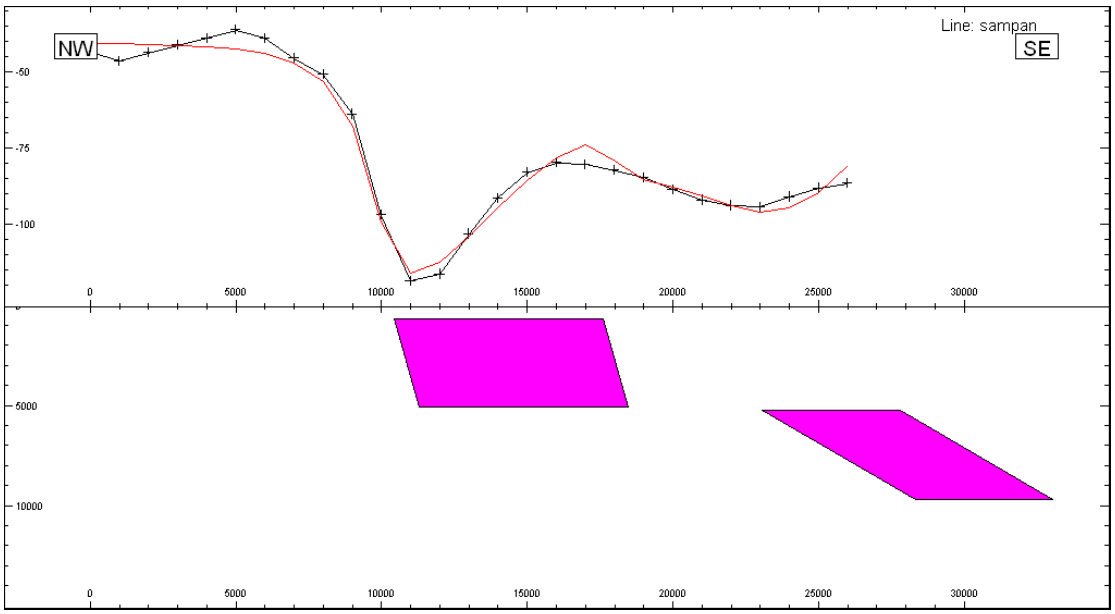

Figure 5.31i Airborne magnetic cross section of the Nan-Uttaradit area showing the observed and calculated value and interpreted magnetic anomaly bodies of line I-I'.

5.4 Field work and EM Verification

5.4.1 Field Verifications

In order to test interpretation on air-borne geophysical results, a ground truth survey is required. Subsequently, in this study, certain rock types have been identified in the field as visual verification whether or not the interpreted geophysical results are similar to or the same as the geologic evidence. Selected locations are shown onto the interpreted NE-SW trending central domain in Figure. 5.32 (Munyou et al., 1986). The enlarged map of these locations is shown in Figure.5.33.

Three groups of rocks are shown in this thesis report, namely the Mesozoic rocks of the Nakhon Thai (Charusiri et al, 2006), the Permian to Triassic rocks of the Phrae Group, and the Pha Som ophiolite suite. Additionally, to the north of the central belt where major ophiolite and mélange rocks are exposed. Outcrop of Permian to Triassic rocks are also added to support geologically the geophysical interpretation. They are illustrated in the Appendix B.

Figures. 5.34 A to D display outcrops of the Jurassic to Cretaceous non marine clastic rocks of the Nakhon Thai Group ranging from conglomerate and conglomeratic sandstone to siltstone and mudstone.

Figures. 5.34 E to O show outcrops of ophiolite and mélange rocks with some deformation structures. Outcrop with rock deformation are also shown in Figures.5.34P to 5.34 T.

The occurrence of the deformation structures is quits essential to geophysical model because its represents either the back thrust of the trend slope or the thrust fault at the back side of the couple subduction system (Plajim, 1997).

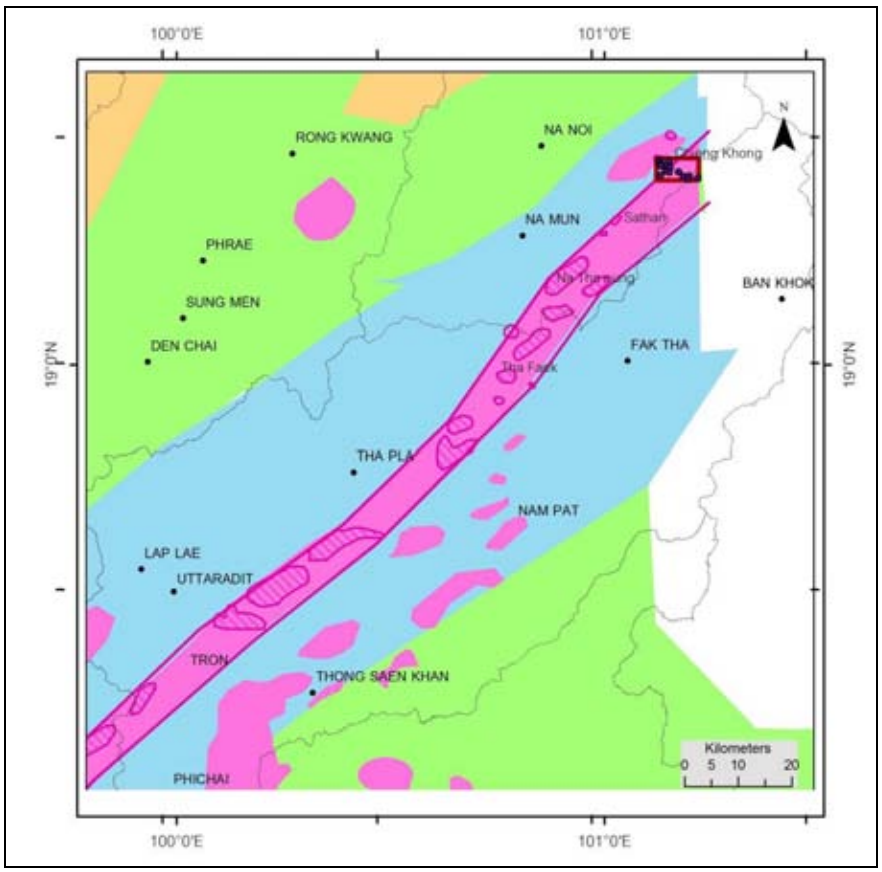

Figure 5.32 Location of field data (red box) on interpreted NE-SW trending central domain.

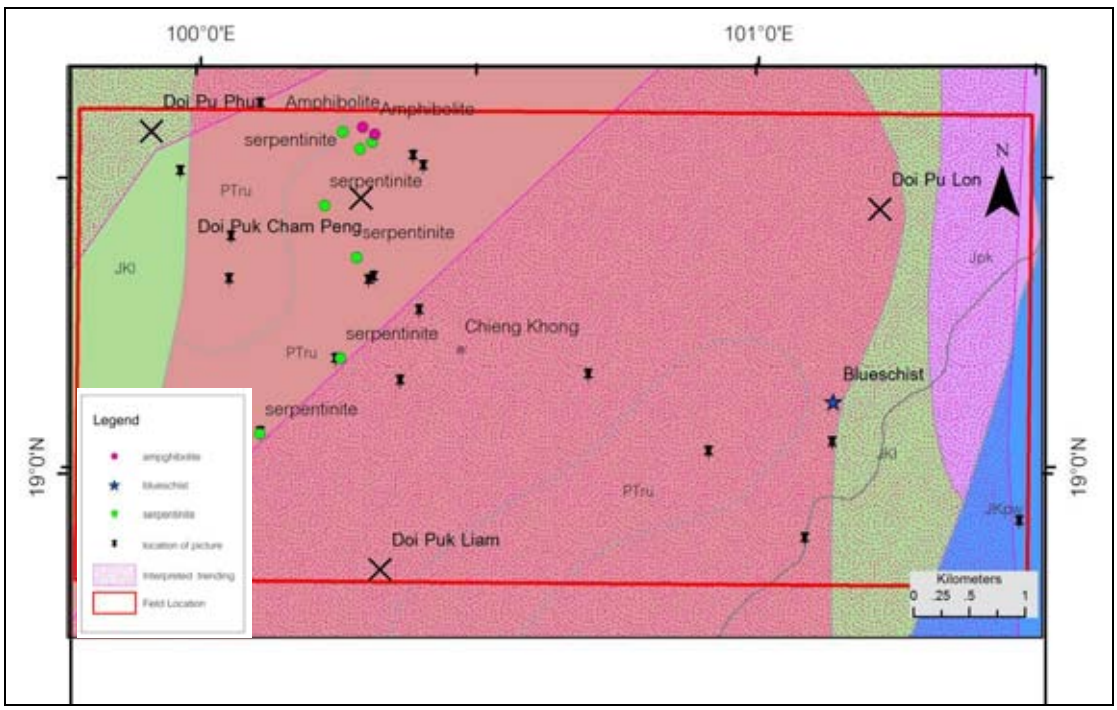

Figure 5.33 The enlarged map of these field locations.

(A)

(B)

Figure 5.34 (A) Outcrop of reddish brown conglomeratic sandstone (with abundant Permian Rong Kwang limestone clast) of Jurassic Cretaceous Nakhon Thai Group (grid no. 702525E 2023733N)

(B) Outcrop of reddish brown coarse grain sandstone showing cross - bedding, the Jurassic-Cretaceous Nakhon Thai Group, (grid no. 702584E 2024208N)

(C)

(D)

Figure.5.34 (C) Outcrop of reddish brown siltstone of Jurassic-Cretaceous Nakhon Thai Group, showing movement along the fault plane (grid no. 702079E 2024461N)

(D) Outcrop of reddish brown siltstone of the Nakhon Thai Group with clasts of "older" sandstone, interpreted to be derived from flysd. Type sequence of the Permo-Carboniferous , Mae Sai Formations. (grid no. 702451E 2024847N)

(E)

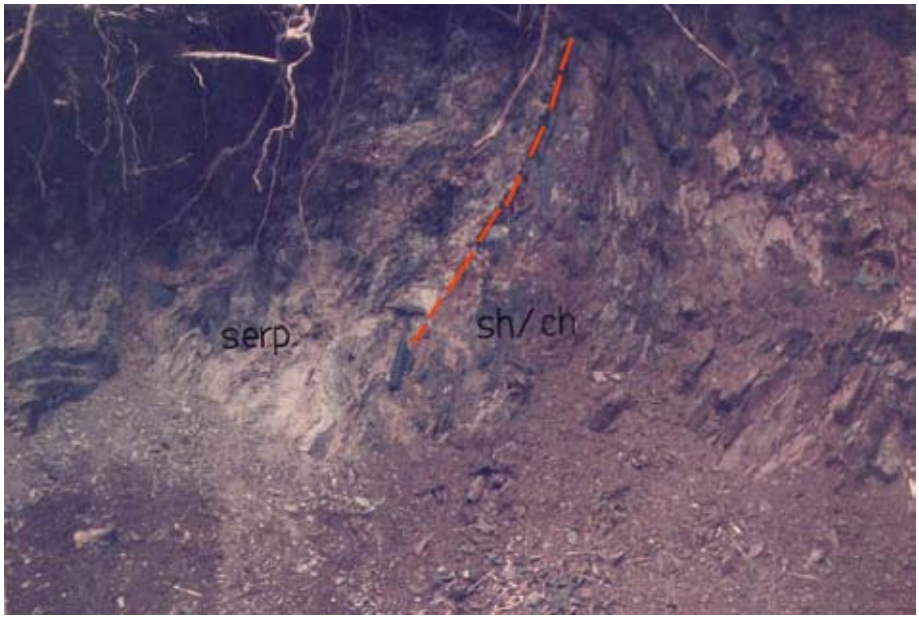

(F)

Figure.5.34 (E) An outcrop of serpentine containing a large remnant block of serpentinized peridotite belonging to the Permo-Carboniferous Pha Som ophiolite suite. (grid no. 703411E 2024625N)

(F) An outcrop of laminated shale and chart showing a sharp fault contact with the serpentinite rocks. (grid no. 703568E 2022172N)

(G) (H)

Figure. 5. 34 (G) A thrust fault contact between serpentinite of the Pha Som ophiolite (older) and conglomerate of the Nakhon Thai Group (younger) (grid no. 702998E 2024371N)

(H) A large outcrop of Permo-Carboniferous deformed chert block in the green sandstone of the Mélange zone (grid no. 706562E 2021973N)

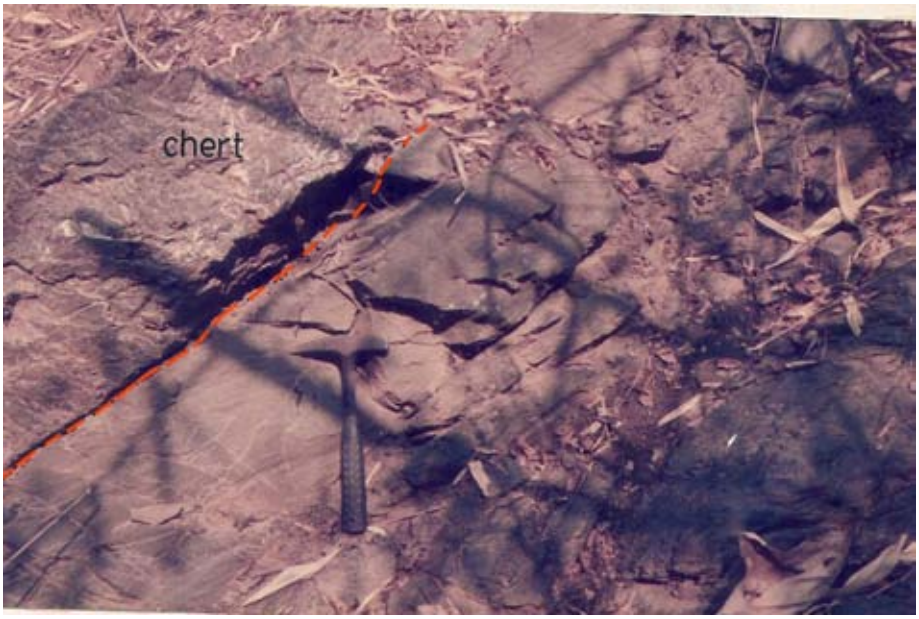

(I)

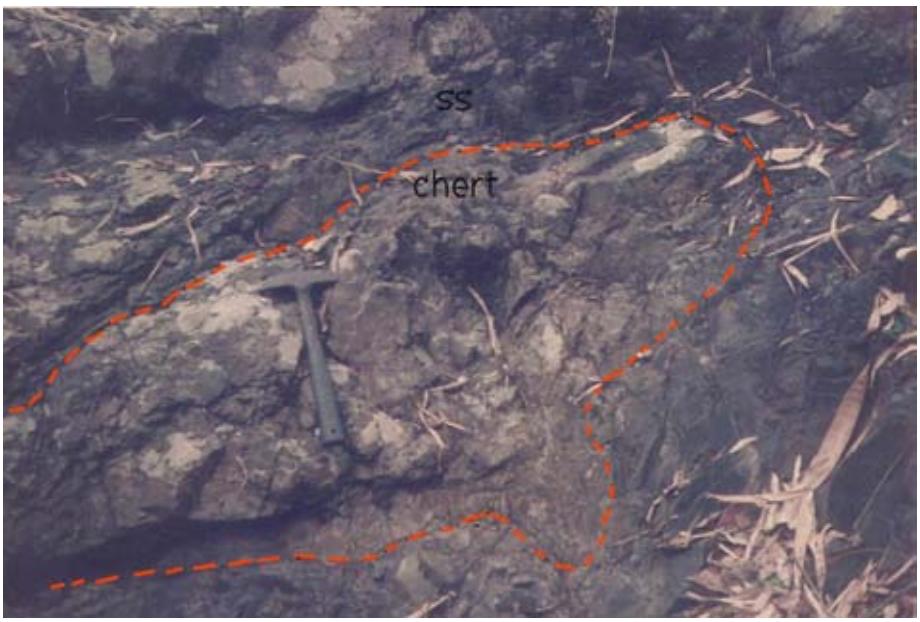

(J)

Figure. 5. 34 (I) A large brown chert block in the green sandstone within the Mélange zone of the Pha Som ophiolite (grid no. 703387E 2022870N)

(J) A large brownish green chert block in the green sandstone within the Mélange zone (grid no. 704141E 2023458N)

(K)

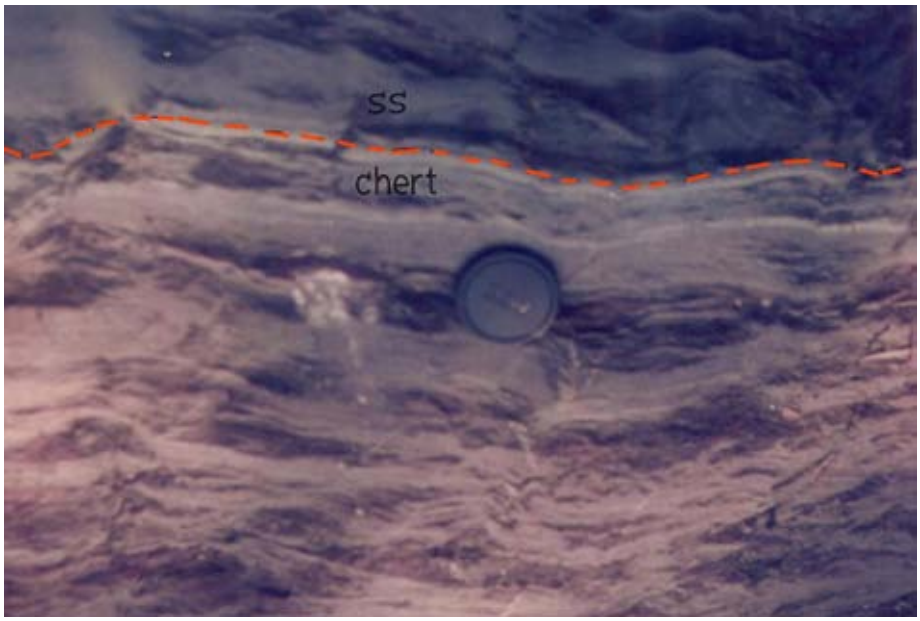

(L)

Figure. 5. 34 (K) and (L) A large brownish green chert block in the green sandstone within the Mélange zone (grid no. 704062E 2022656N and 707380E 2021418N)

(M)

(N)

Figure. 5. 34 (M) A large brownish green chert block in the green sandstone within the Mélange zone (grid no. 703967E 2024561N)

(N) Sandstone blocks in the chert/shale matrix of the mélange rock (grid no. 703586E 2023712N)

(O)

(P)

Figure. 5.34 (O) Conglomeratic sandstone of Jurassic -Cretaceous Nakhon Thai Group with abundant chert pebble clasts (grid no. 709166E 2021696N)

(P) A natural exposure of thinly bedded chert with overturned fold at Huai Sua Khao, view locking to the Northeast (grid no. 707650E 202207)

(Q)

(R)

Figure. 5. 34 (Q) An exposure of thinly bedded chart with overturned fold, view looking almost to the north (grid no. 703721E 2023775N)

(R) A small overturned fold developed in the Permo- carboniferous laminated chart, (grid no. 704022E 2024513N) now looking to the North.

(S) (T)

Figure. 5. 34 (S) A Z-shape fold developed in the alternating fine-grained and siltstone of the Permo-Carboniferous Mae Sai Formation (grid no. 702371E 2025561N)

(T) An outcrop of Carboniferous to Permian ribbon chert green and red bands showing fold structure (grid no. 702729E 2022727N)

5.4.2 EM Verifications

Verify the interpreted lineament of Landsat data by overlay the inphase and quardrature of the HLEM data on to a lineament map. From the map showing the interpreted lineaments are conformed to the peak of data as show in Figure 5.35 a to 5.35 d

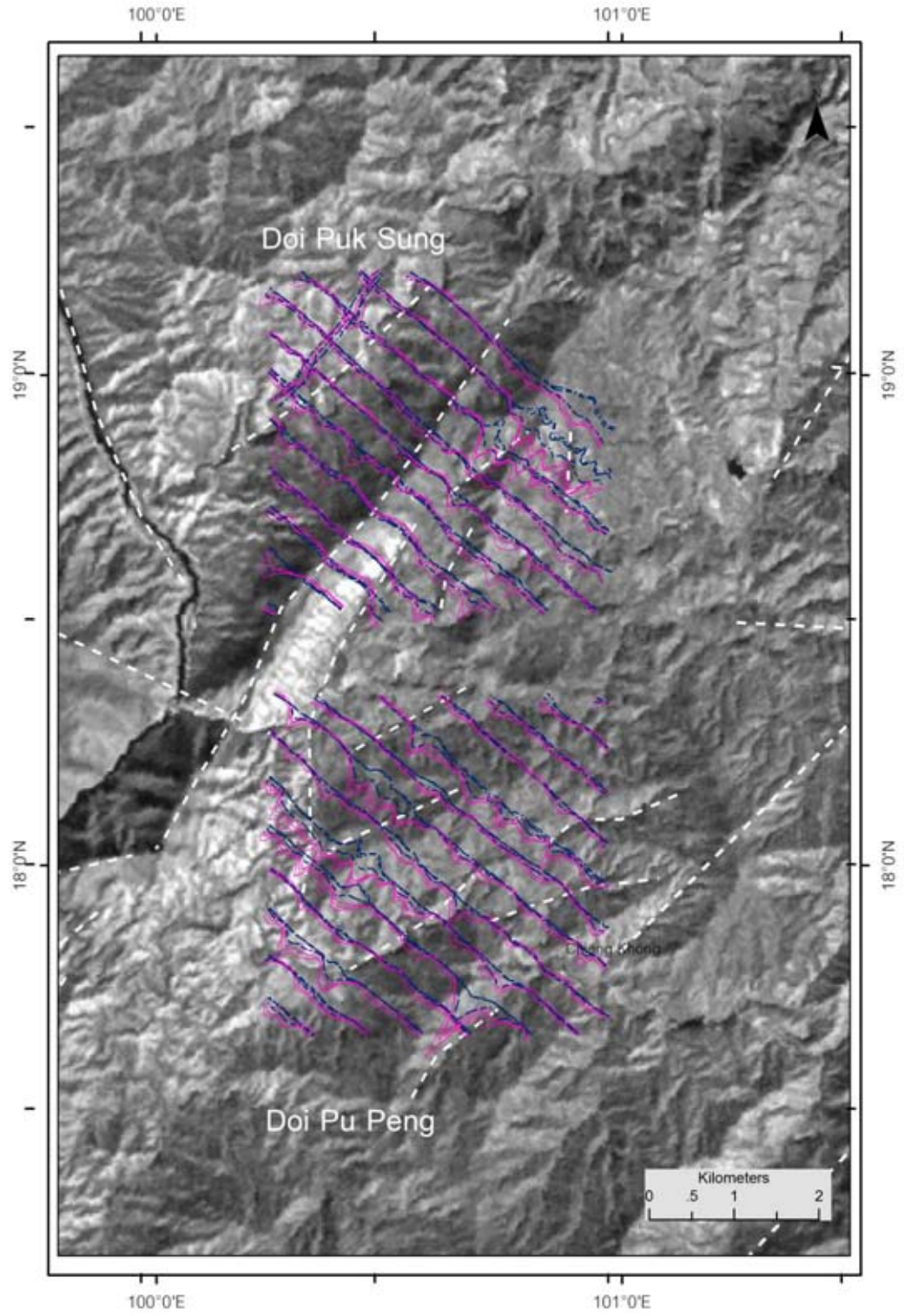

Figure 5.35a Interpreted lineaments of Landsat PCA data overlay with HLEM data of Nan-Uttaradit area (Doi Pu Peng and Doi Puk Sung) showing conform data of lineaments and peak of anomalies.

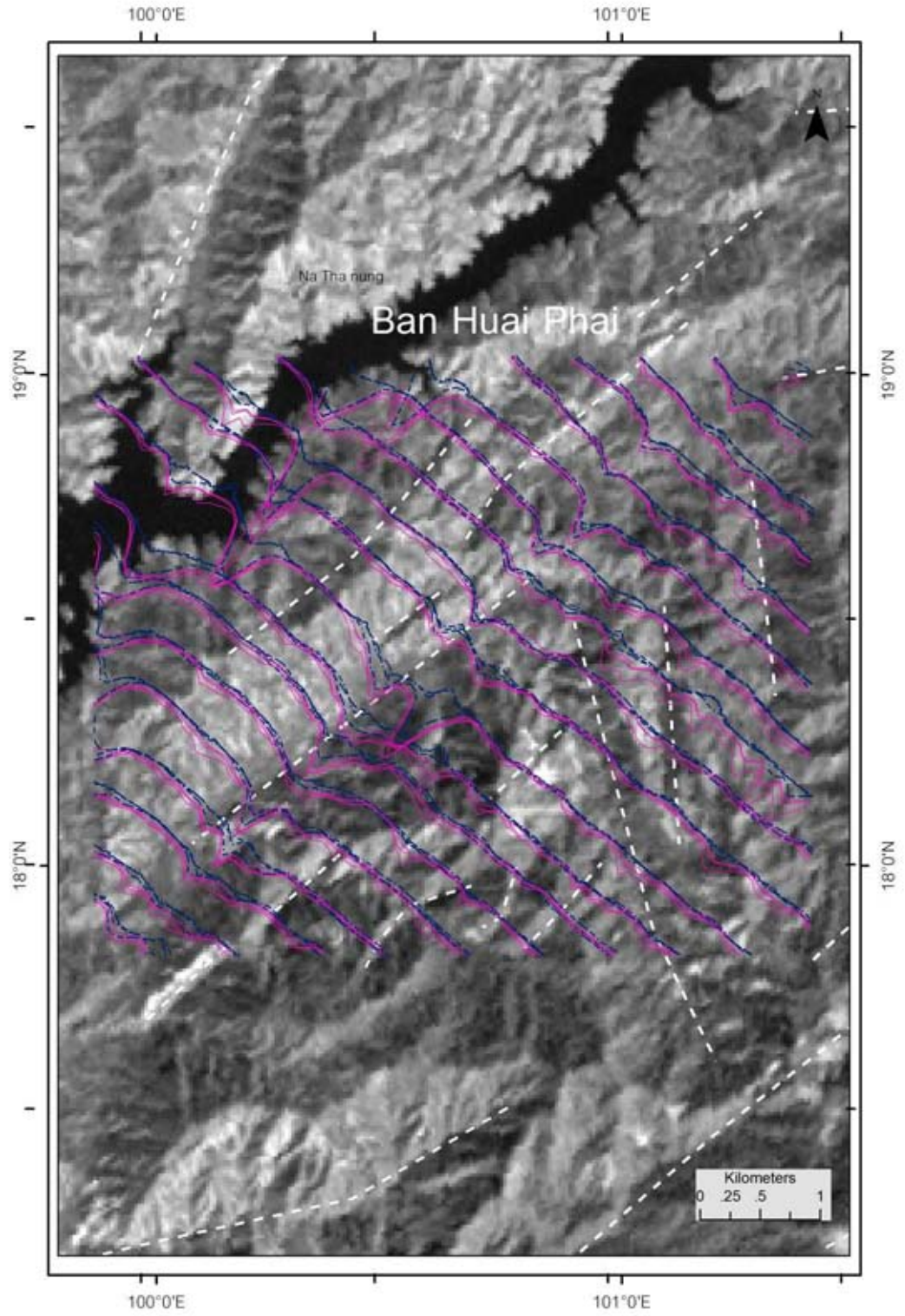

Figure 5.35b Interpreted lineaments of Landsat PCA data overlay with HLEM data of Nan-Uttaradit area (Ban Huai Phai) showing conform data of lineaments and peak of anomalies.

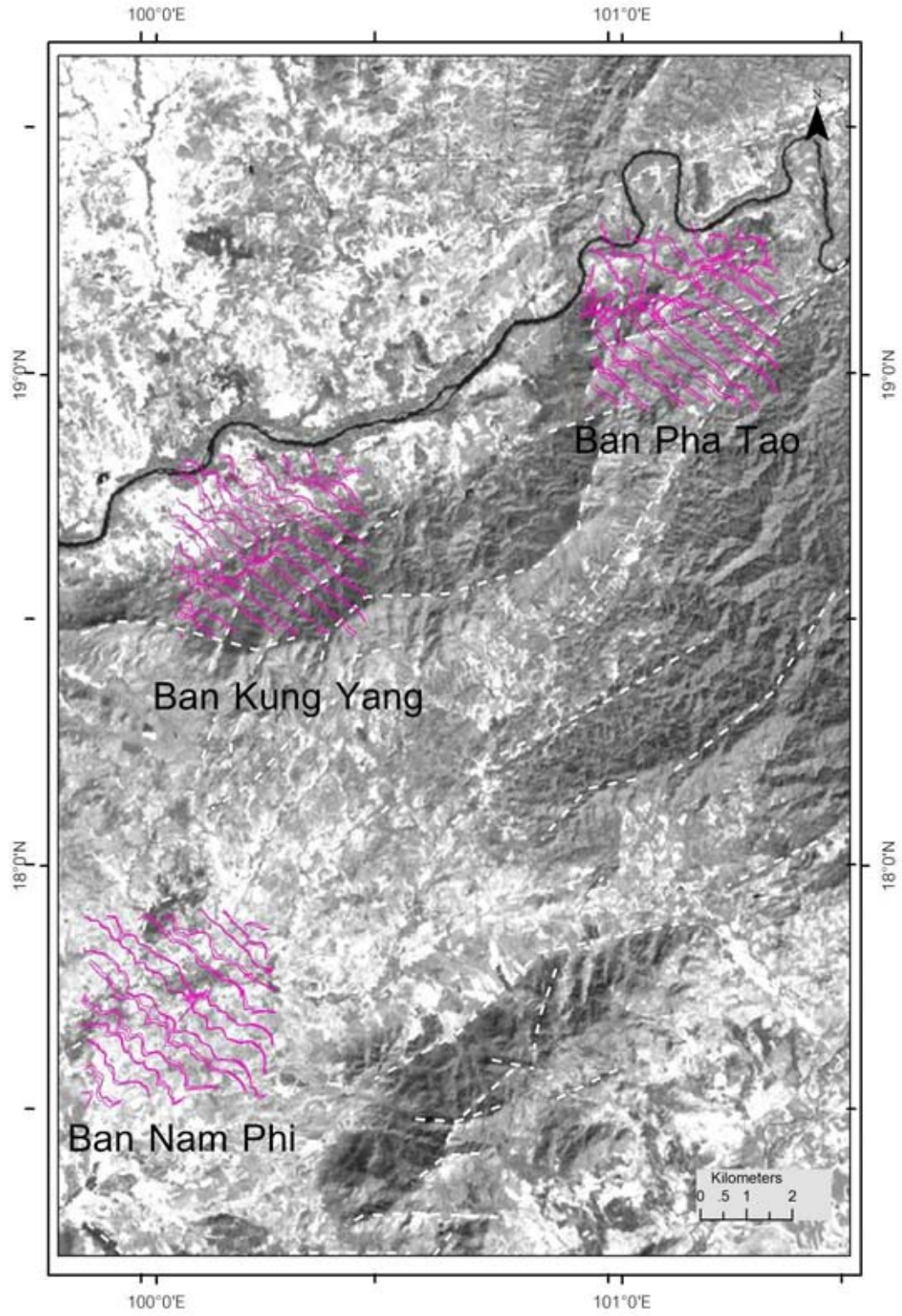

Figure 5.35c Interpreted lineaments of Landsat PCA data overlay with HLEM data of Nan-Uttaradit area (Ban Pha Tao, Ban Kung Yang and Ban Huai Nam Phi) showing conform data of lineaments and peak of anomalies.

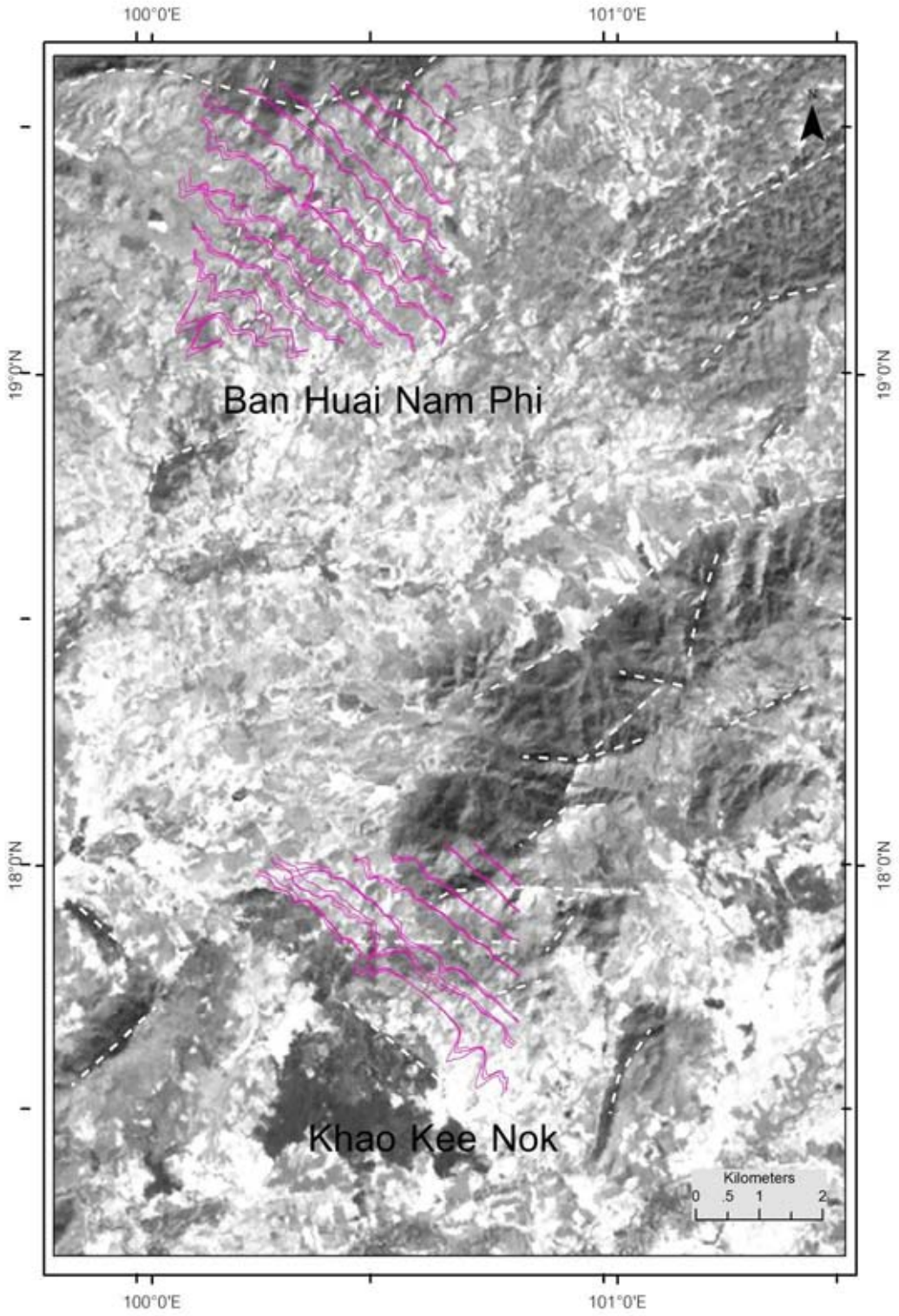

Figure 5.35d Interpreted lineaments of Landsat PCA data overlay with HLEM data of Nan-Uttaradit area (Ban Huai Nam Phi and Khao Kee Nok) showing conform data of lineaments and peak of anomalies.

And for the interpreted lineament of SRTM data overlay the HLEM data are shown in Figure 5.36 a to 5.36 d

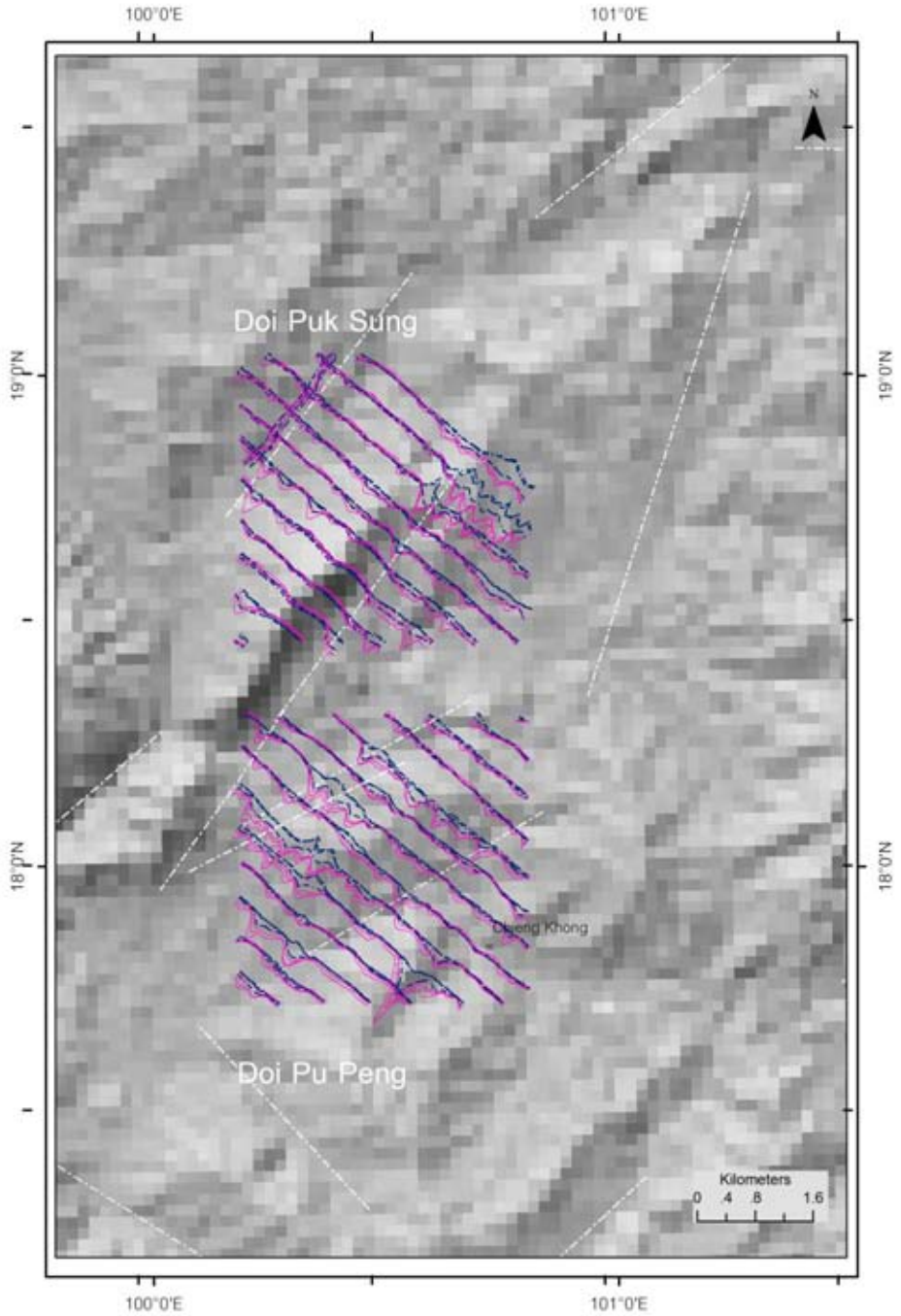

Figure 5.36a Interpreted lineaments of SRTM DEM data overlay with HLEM data of Nan-Uttaradit area (Doi Pu Peng and Doi Puk Sung) showing conform data of lineaments and peak of anomalies.

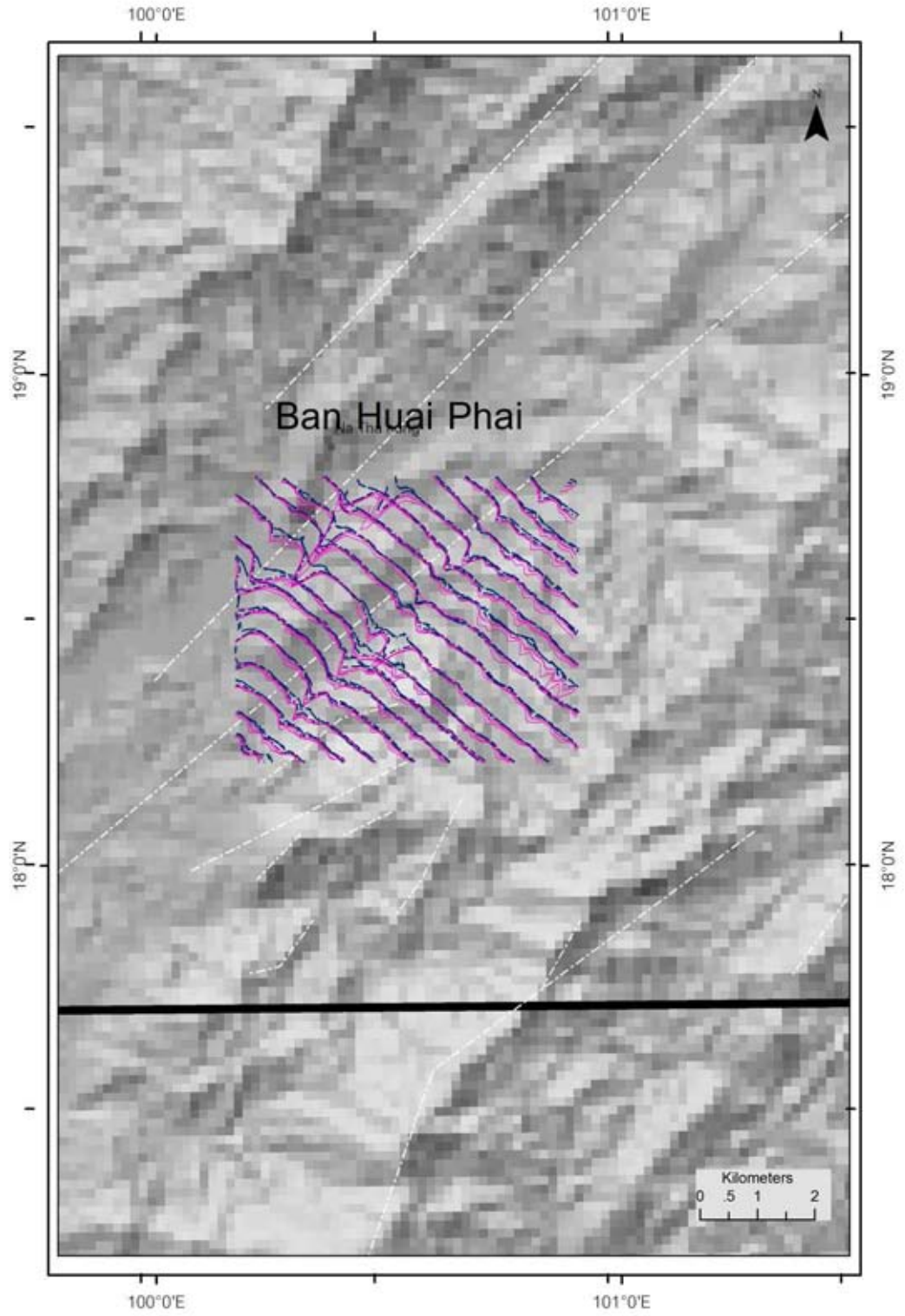

Figure 5.36b Interpreted lineaments of SRTM DEM data overlay with HLEM data of Nan-Uttaradit area (Ban Huai Phai) showing conform data of lineaments and peak of anomalies.

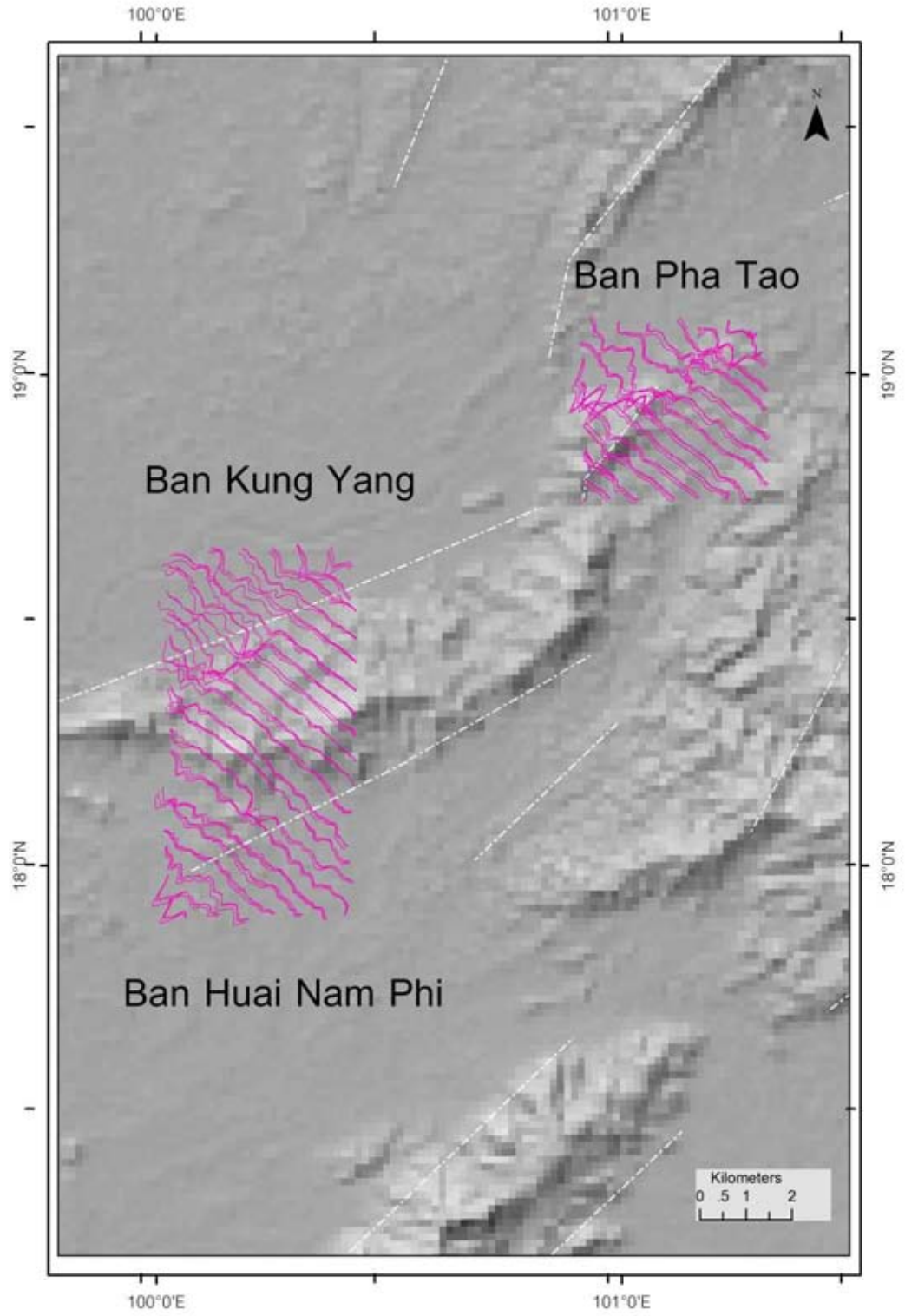

Figure 5.36c Interpreted lineaments of SRTM DEM data overlay with HLEM data of Nan-Uttaradit area (Ban Pha Tao, Ban Kung Yang and Ban Huai Nam Phi) showing conform data of lineaments and peak of anomalies.

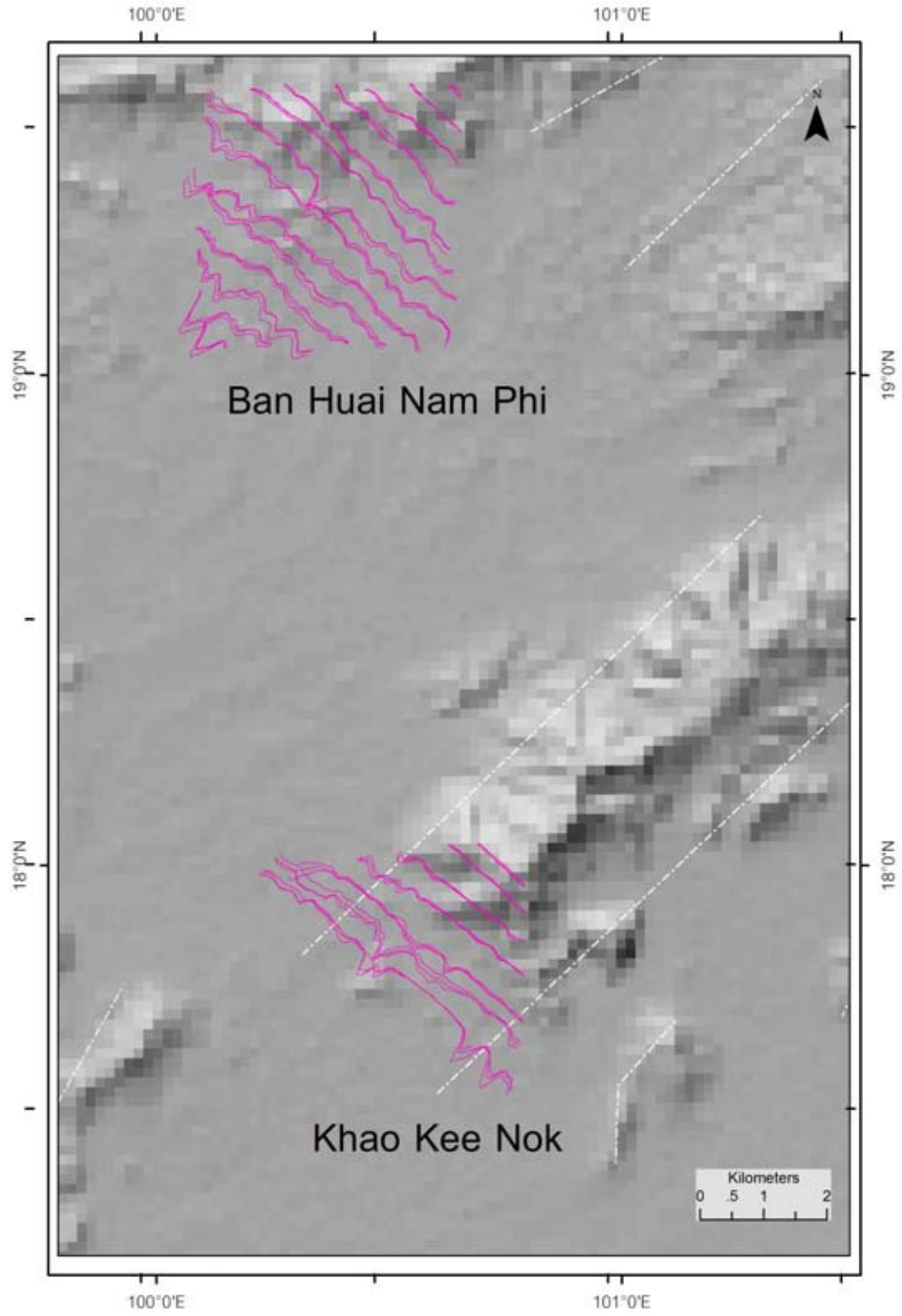

Figure 5.36d Interpreted lineaments of SRTM DEM data overlay with HLEM data of Nan-Uttaradit area (Ban Huai Nam Phi and Khao Kee Nok) showing conform data of lineaments and peak of anomalies.

5.5 Type and Sequence of Lineament Fault

5.5.1 Type of Lineament Fault

The lineaments detection of magnetic data can be done by several methods as listed below

1. Lineaments Fault from Shaded Relief Method

Lineaments Fault is always facilitated by the presence of shadows. This study applied RTP magnetic map, treated like topographic data to illuminate from any azimuth. Shaded relief analysis is focusing on lineament that perpendicular to the direction of the illumination and the strongest contrast illumination will be observed, whereas those lineaments that align parallel to the illumination direction have no shadows. In this study various illuminations will be applied to observe the lineaments of magnetic data.

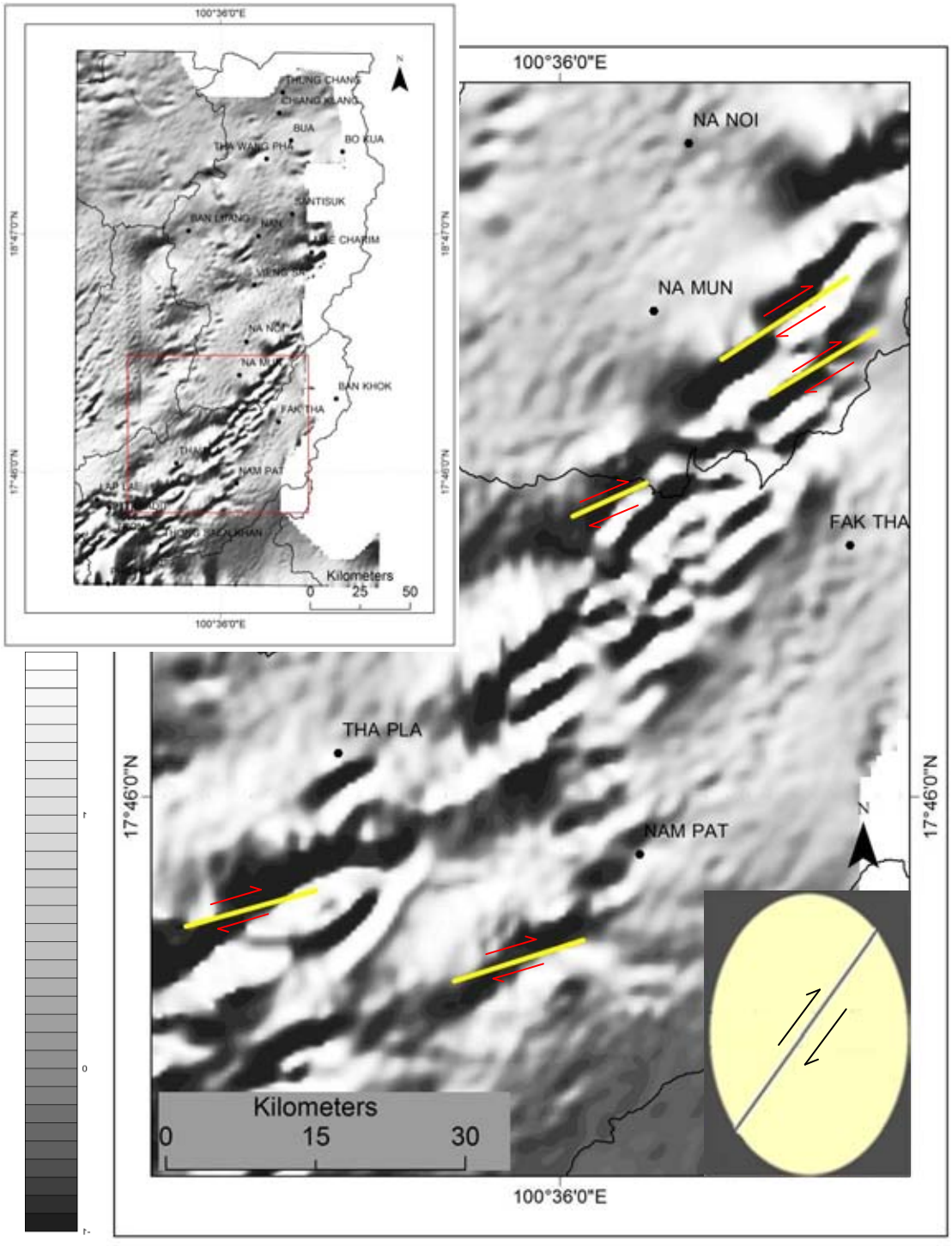

Figure 5.37 Interpreted fault from shaded relief map of 135 degree in Nan-Uttaradit area are showing dextral fault in NE-SW direction. Noted that the ellipsoid fault model are shown in the insert box.

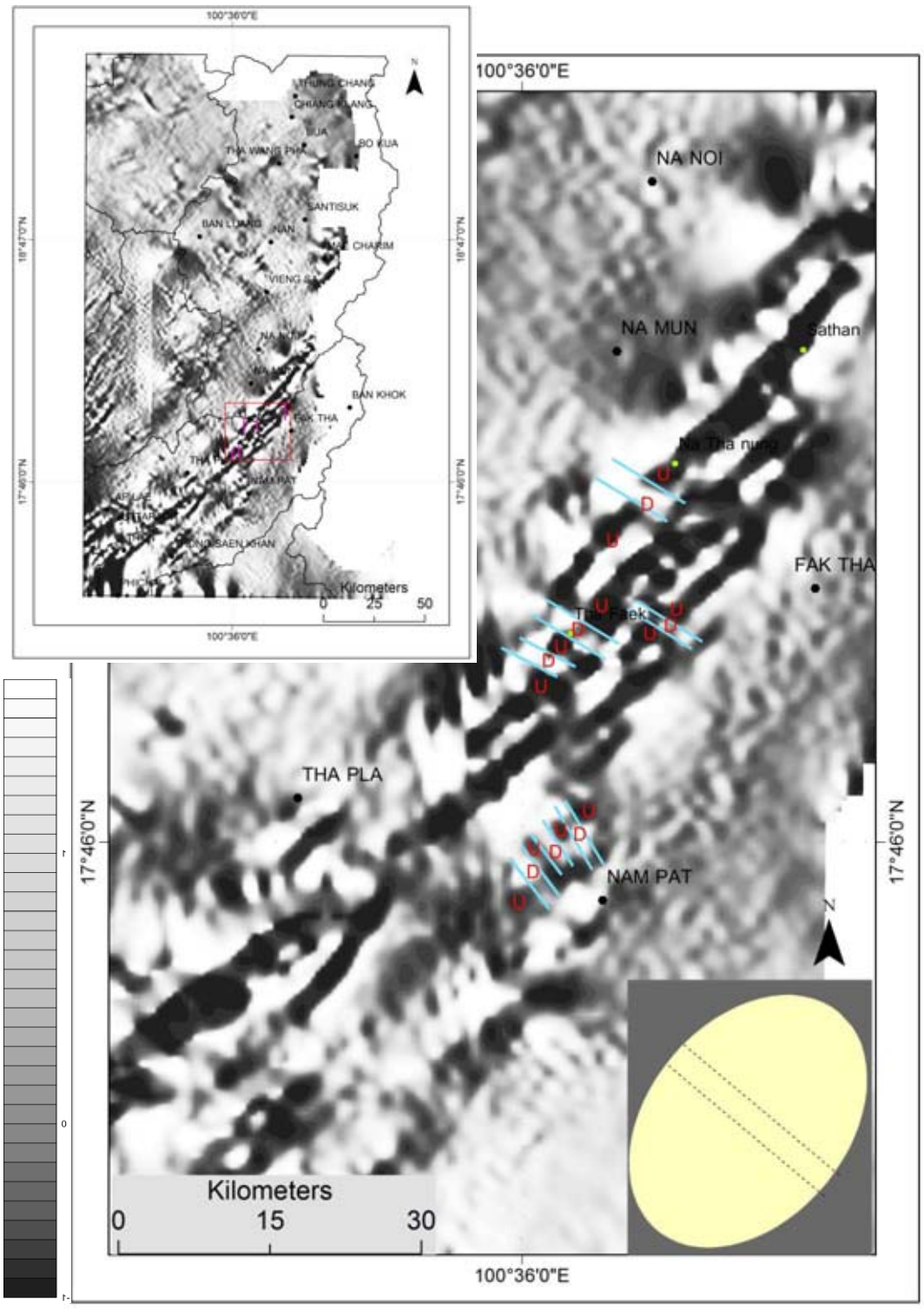

Figure 5.38 Interpreted open fracture from shaded relief map of 270 degree in Nan-Uttaradit area are showing the open fracture in NW-SE direction. Noted that the ellipsoid fault model are shown in the insert box.

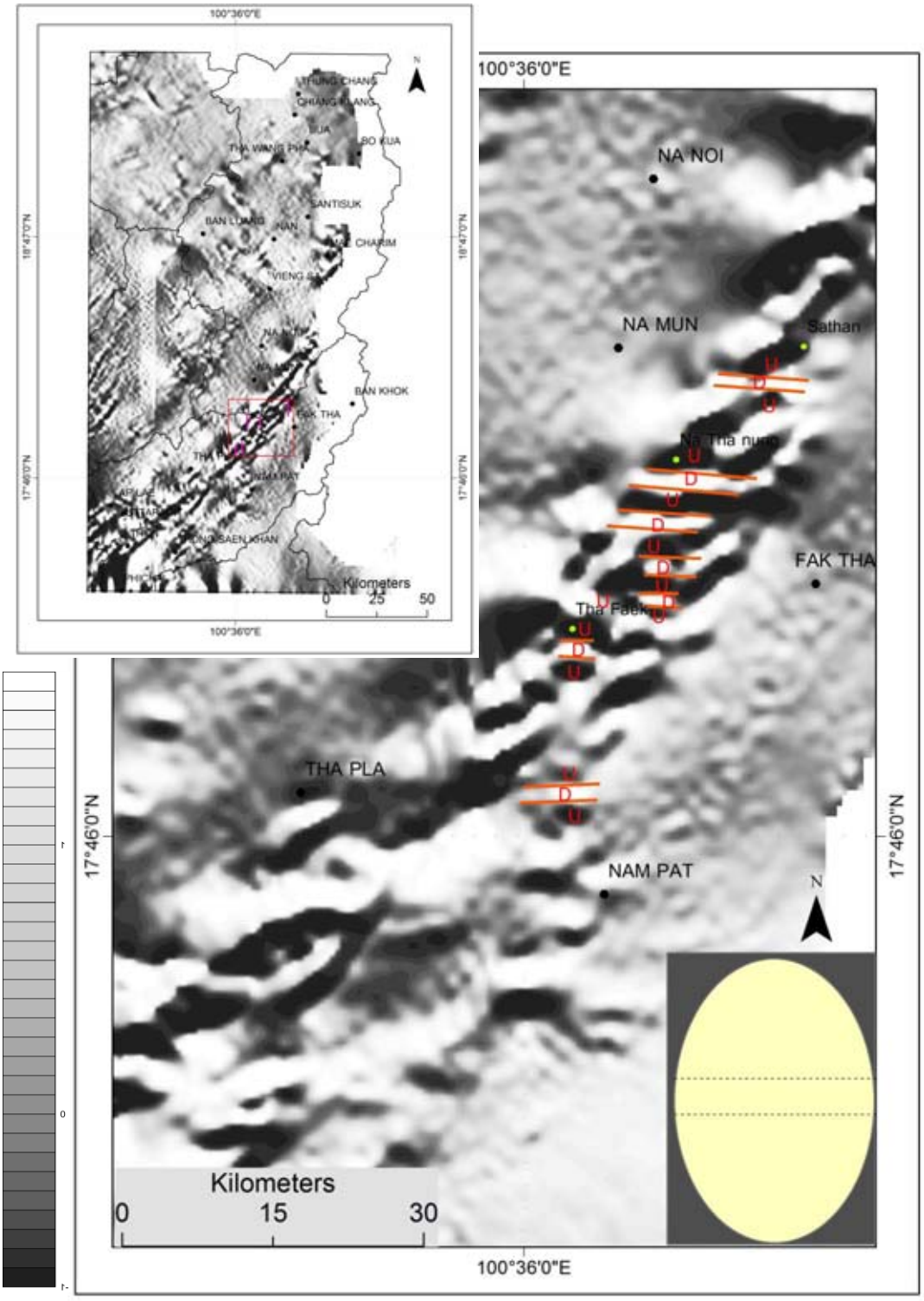

Figure 5.39 Interpreted open fracture from shaded relief map of 360 degree in Nan-Uttaradit area are showing the open fracture in E-W direction. Noted that the ellipsoid fault model are shown in the insert box.

2. Lineaments Fault from Vertical Derivative Method

Lineaments Fault is facilitated by the presence of shadows. These study uses enhanced magnetic data of secondary vertical derivative methods, convert into gray scale and visual interpret the lineament fault.

3. Lineaments Fault from Directional Cosine Filter Method

Lineaments Fault is facilitated by the filter data from any azimuth and focusing on lineament that perpendicular to the direction of the illumination and the strongest contrast illumination will be observed.

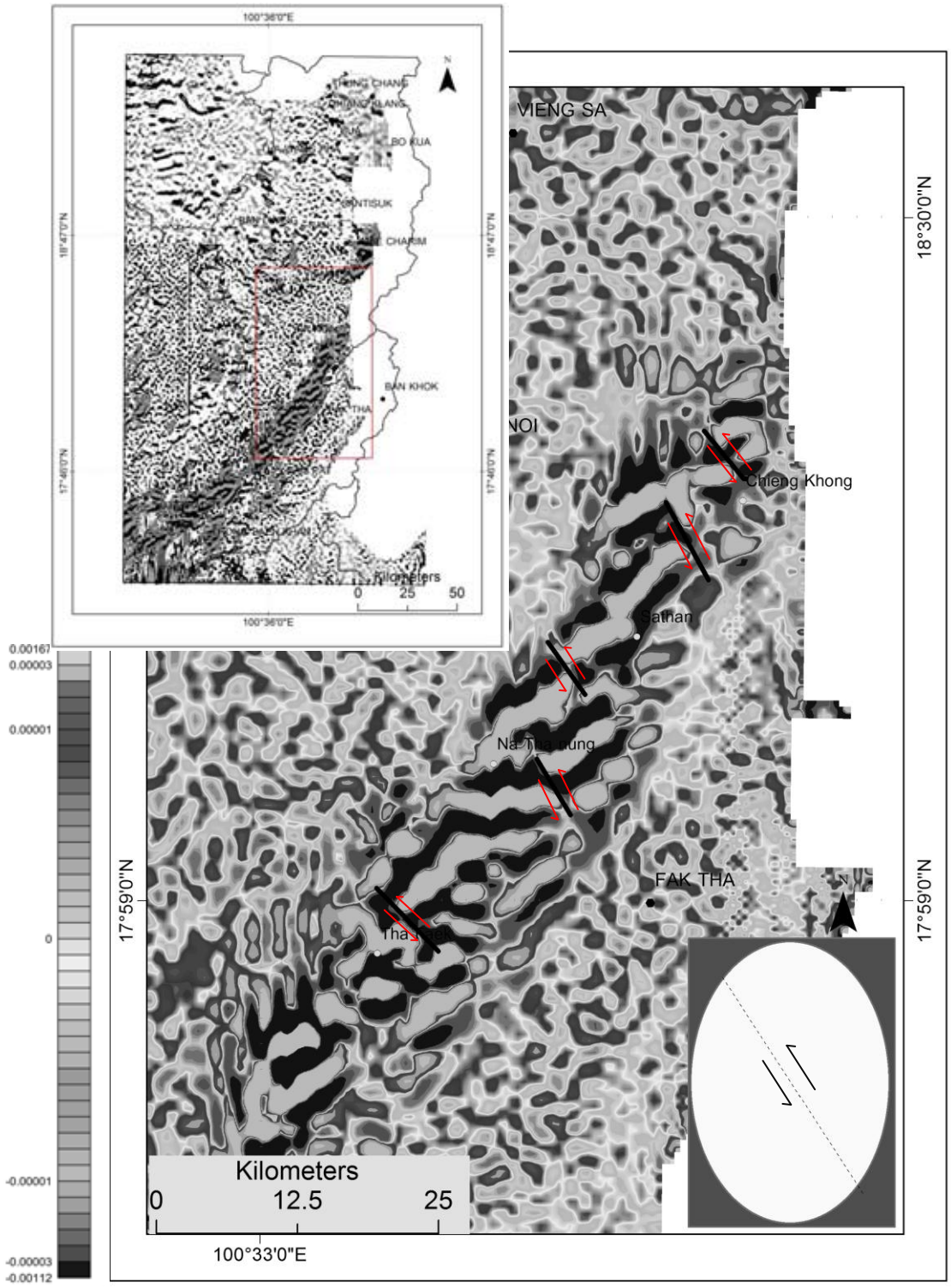

Figure 5.40 Interpreted fault from from 2nd vertical derivative map in Nan-Uttaradit area are showing the sinistral fault in NE-SW direction. Noted that the ellipsoid fault model are shown in the insert box.

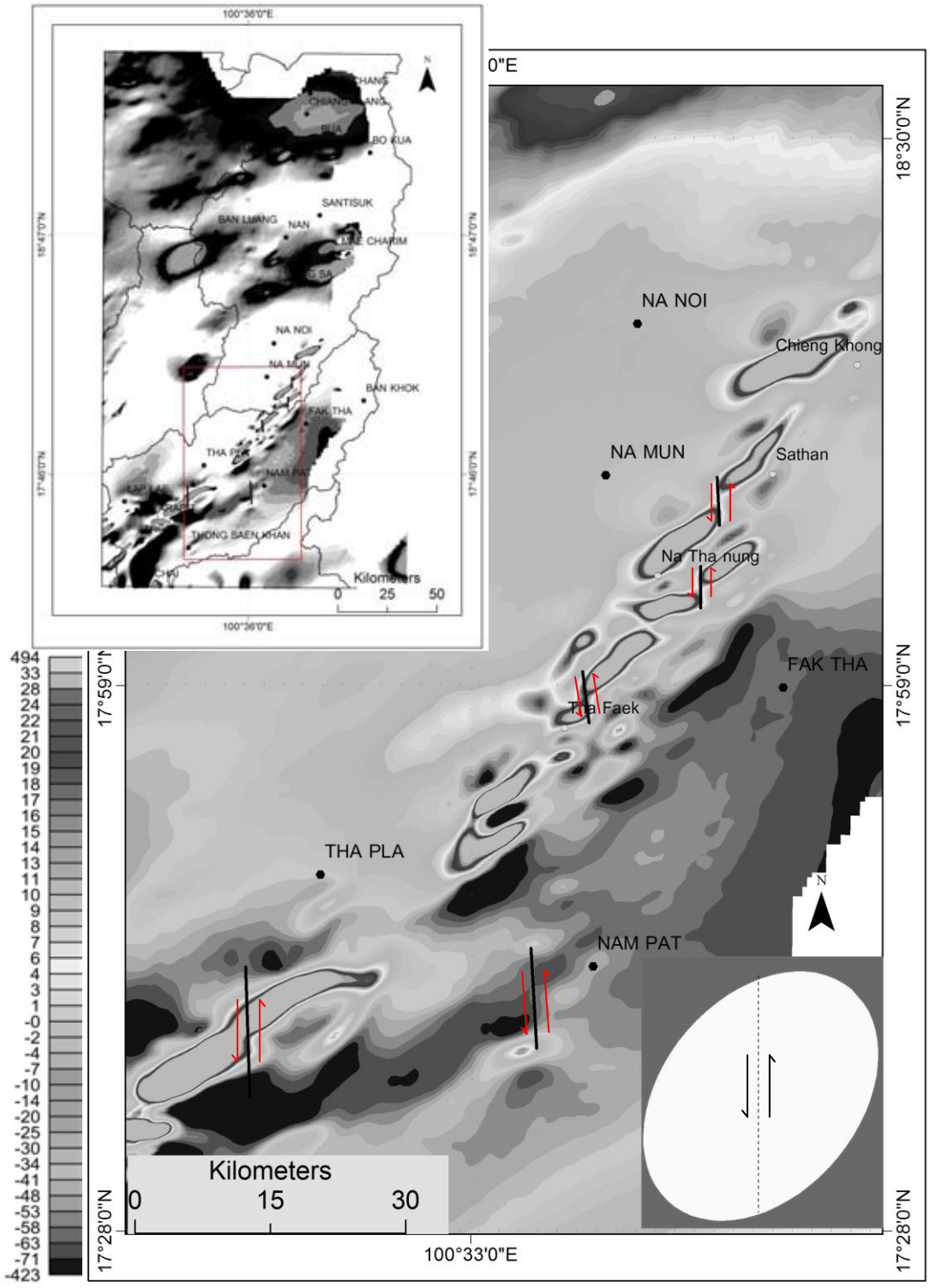

Figure 5.41 Interpreted fault from directional cosine filter map of 315 degree in Nan-Uttaradit area are showing the sinistral fault in N-S direction. Noted that the ellipsoid fault model are shown in the insert box.

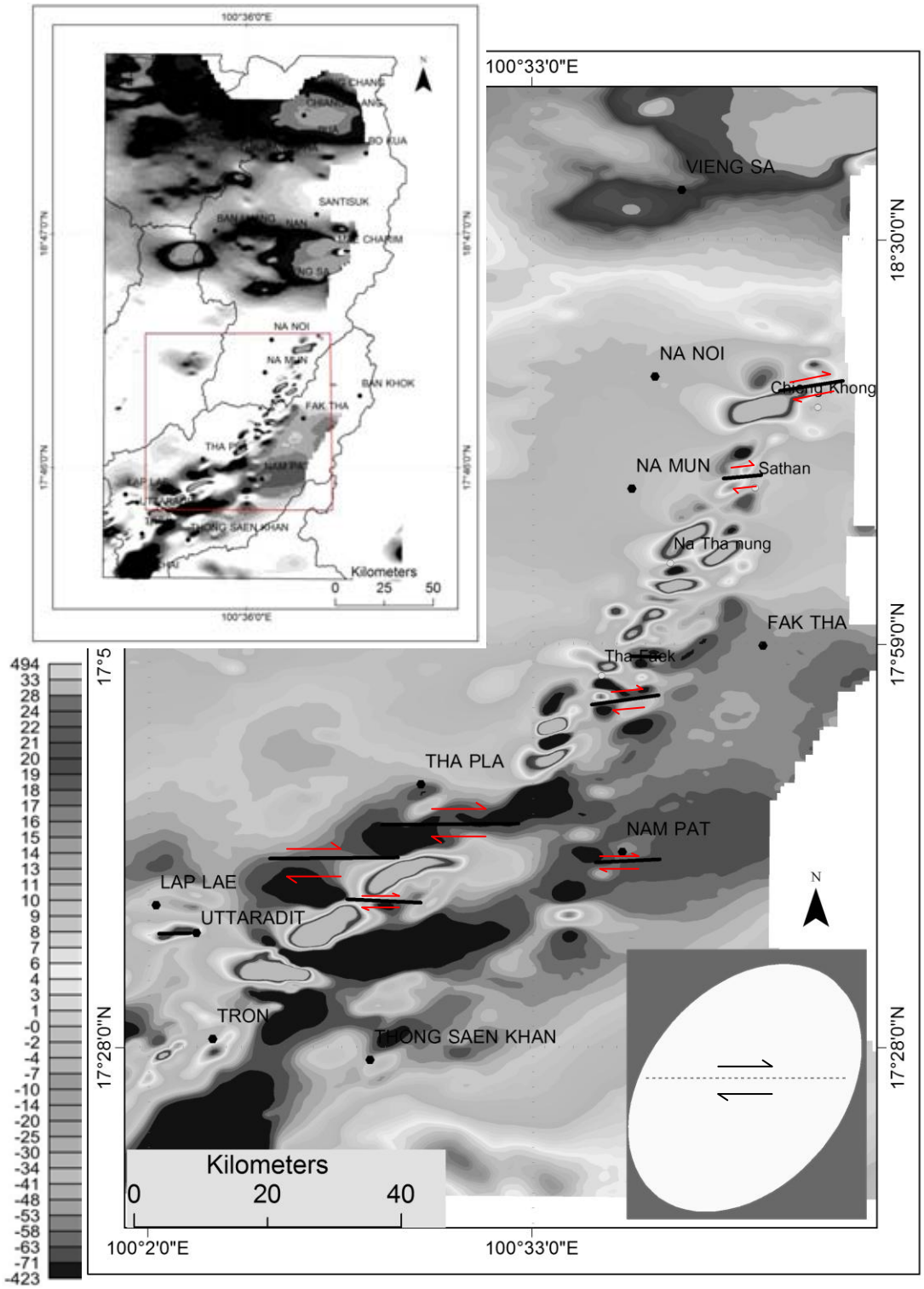

Figure 5.42 Interpreted fault from directional cosine filter map of 180 degree in Nan-Uttaradit area are showing the dextral fault in E-W direction. Noted that the ellipsoid fault model are shown in the insert box.

From interpreted fault and ellipsoid of fault model in Figure 5.38, 5.41 and 5.42 we can combine the interpreted ellipsoid to explain the tectonic machanism in this area as show in Figure 5.43

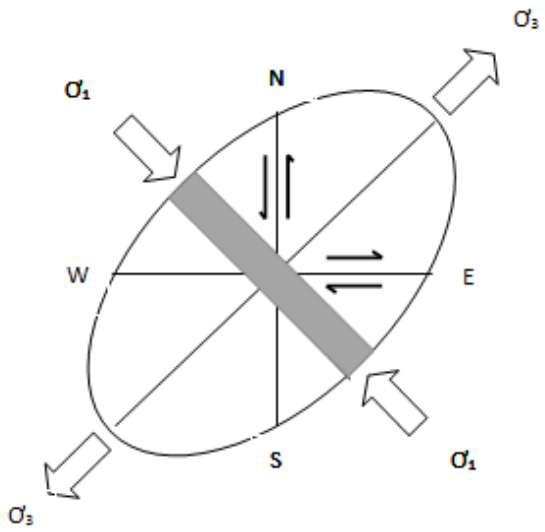

Figure 5.43 Extensional Ellipsoid from Interpreted fault in Nan-Uttaradit area are showing that, there are a compression force in NW-SE direction and extension force in NE-SW direction.

From interpreted fault and ellipsoid of fault model in Figure 5.37, 5.39 and 5.40 combine the interpreted ellipsoid to explain the force in this area as show in Figure 5.44.

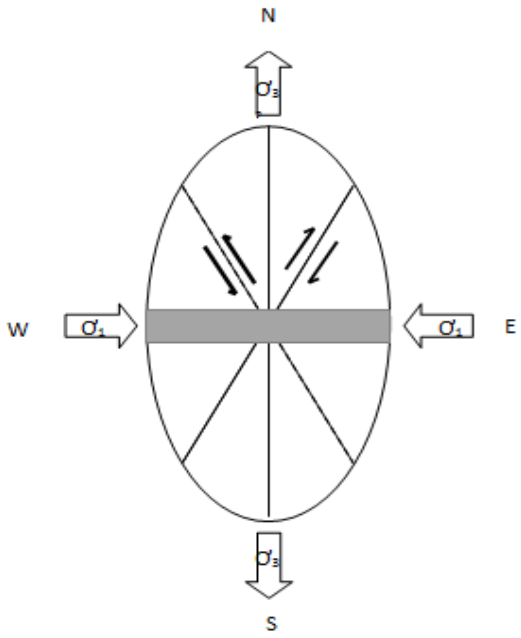

Figure 5.44 Compression Ellipsoid from Interpreted fault in Nan-Uttaradit area are showing that, there are a compression force in E-W direction and extension force in N-S direction.

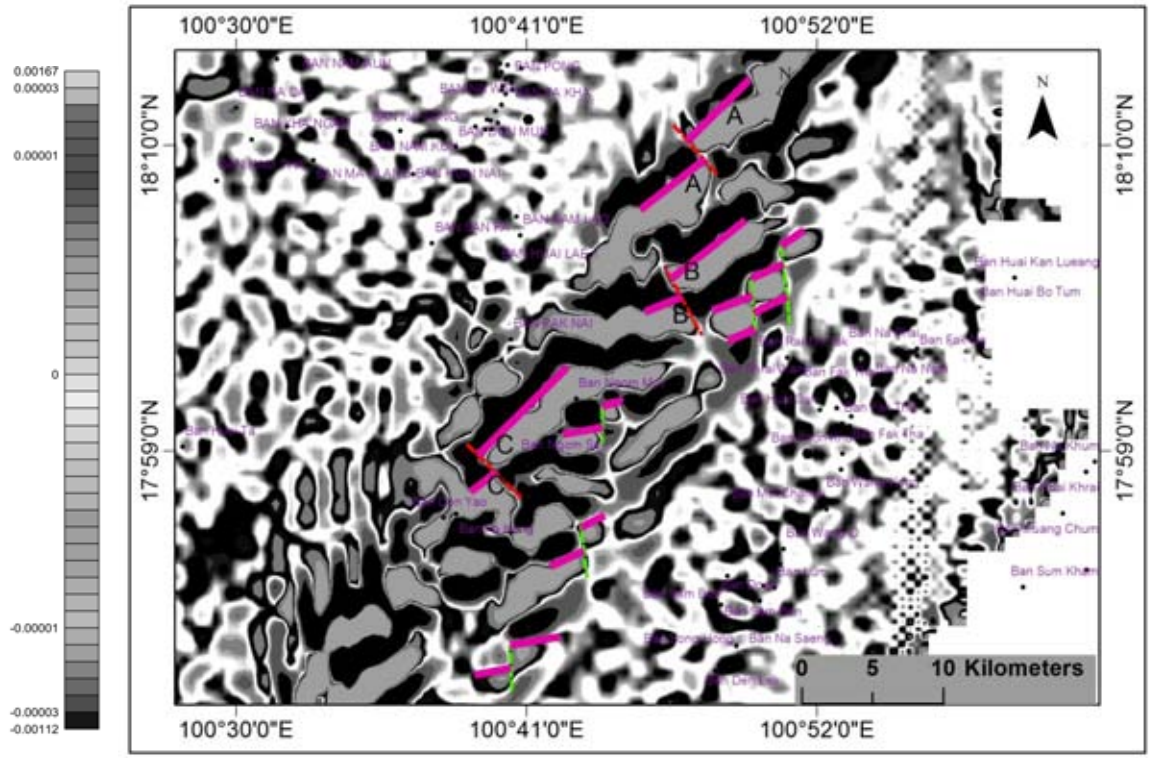

Figure 5.45 Interpreted fault from 2nd vertical derivative map of Nan-Uttaradit are showing the sequence of fault cross cut to another fault. Noted that the pink color represent the major thrust fault in NE-SW direction, the red color represent the sinistral fault in NW-SE direction and the green color represent the sinistral fault in N-S direction.

5.5.2 Sequence of fault

1. <u>Strain Ellipsoid</u>

The strain ellipsoid has shown the sinistral movement in N-S direction and the major structure in NE-SW Direction. From figure 5.45 shows that the sinistral fault in N-S direction are obviously cross cut to the NE-SW major structure.

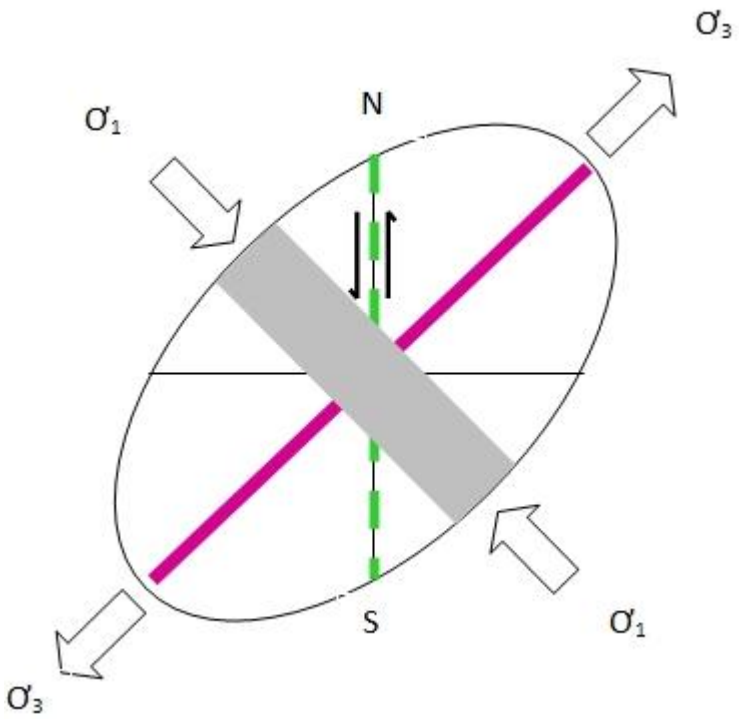

Figure 5.46 Interpreted fault on the strain ellipsoid are showing that the sinistral fault in N-S direction are cross cut through the major thrust fault in NE-SW direction.

2. Stress Ellipsoid

The stress ellipsoid has shown the sinistral movement in NW-SE direction. From figure 5.45 shows that the sinistral fault in NW-SE direction are obviously cross cut to the NE-SW major structure of the strain ellipsoid. It is clearly defined that the major structure are and the strain ellipsoid are occurred first and the stress ellipsoid are developed later.

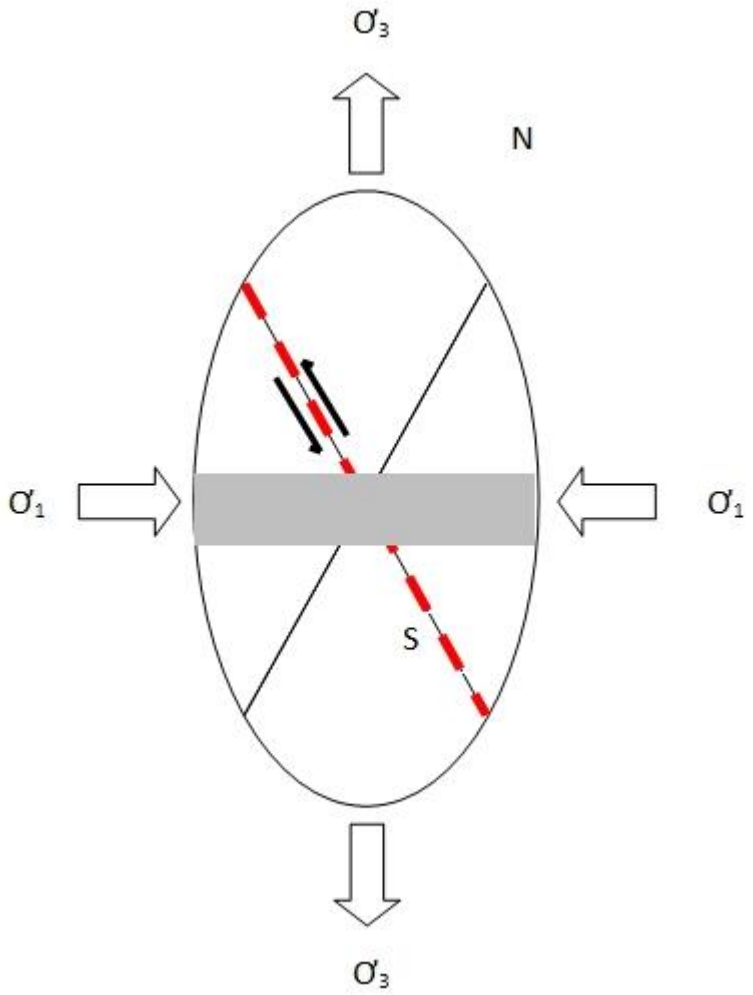

Figure 5.47 Interpreted fault on the stress ellipsoid are showing that the sinistral fault in NW-SE direction are cross cut through the major thrust fault in NE-SW direction(from the strain ellipsoid in Figure 5.46).

From the strain and stress ellipsoid in Figure 4.6 and 4.7 showing the sequence of force mechanism Nan-Uttaradit area. From the fault sequence can summary that the strain ellipsoid occurred before the stress ellipsoid. So, the tectonic mechanism in Nan-Uttaradit area are occurred by compression in NW-SE direction and after that the compression are changing direction into E-W direction.

Chapter 6 Discussion

In this chapter, the focus is made on the occurrences of Nan Suture based upon the previous viewers in comparison with the present researcher. Additionally, with the application of the other data on the suture, its origin can be delineated. Orientation, polarity and definition of the suture are also discussed.

6.1 Related Previous work

Nan suture has been first mentioned by Bunopas (1981) in his thesis entitled "Paleogeographic History of Western Thailand and Adjacent parts of Southeast Asia". The location of Nan-Uttaradit Geosuture in his idea is shown in Fig 6.1a. At that time his geosuture is very approximate, and Tha Pla ophiolite is regarded as a continental-continental collision between Shan Thai block in the west and Indochina block in the east (See Figure 6.2b). Additionally in his map (Figure 6.1a.) the Nan Suture also connected with South China Block in the northern part and extend southward to eastern Thailand and central part of Malay Peninsula.

Barr and Macdonald (1987) study "Nan river suture zone in northern Thailand" and suggested that Nan River Suture Zone consists of ophiolite and ultramafic rocks, forming in a back arc or inter arc setting in Pre-Permian age. They conclude that Nan River Suture is a continent-continent collision between Shan Thai block and Indochina block which is the same concept as previous thought. Figure 6.2 shows the approximate location of Nan River Suture identified by them, but still unconnected to the upper belt in Laos and Bentong Ruab Zone in Malaysia. Moreover, Barr et al. (1985) discovered the blue-schist rock outcropped in the river of Nan, (now inundated by the Sirikit reservoir). Such a blue-schist outcrop is considered to indicate the Nan Suture as subduction-relate tectonic setting. Similarly, their Nan Suture is only approximate.

Subsequently, Panjasawatwong (1991) studies "Petrography, Geochemistry and Tectonic Implication of Igneous rocks in Nan Suture Thailand. With the geochemistry of the Chromian spinel as well as those of the mafic/ultramafic rocks. He summarizes that

the Nan suture is a mélange zone with magma being crystallized from highly refractory melt, and generated in a suprasubduction zone. Figure 6.3 shows the approximate location of Nan suture identified by using exposures of mafic-ultramafic igneous association.

After that, Singharajwarapan and Berry (2000) study “Tectonic Implication of Nan Suture zone and its relationship to Sukhothai fold belt, Northern Thailand”. They conclude that Nan Suture is a serpentinitic mélange zone with thrust slices or accretionary complex that occurred during Late Permian. The Nan Suture zone is a subduction zone of oceanic crust with west dipping direction. Fig 6.4 shows the location of Nan suture which is attached to Sukhothai Fold Belt in Northern Thailand. In their map the more well defined suture is constructed. However, in the cross-section, they interpreted that the suture dips to the west : Such scenario is different from the present study.

Tulyatid and Charusiri(1999) first applied the result of aeromagnetic survey data to delineate the location of the Nan Suture zone. They also relate this Suture to the Srakaew- Chantaburi Suture in southern Thailand based upon the extension of high magnetic anomaly, which was later cut by the major NW-SE trending strike slip fault.

Lunwongsa (2004) and Charusiri et al. (2004) reported regional geology of the Nan area and first locate the Pha Som ophiolite as the Nan Suture. They also recognized the difference in geology to the east and the west of the Nan Suture. However, the geometry of the Nan Suture has not been analyzed, or interpreted. Additionally, the dip of the subduction-related suture is to the east.

From those mentioned studies of the Nan Suture, not many geoscientist described and delineated the location of the Nan suture correctly. There are still unclear to locate the boundary of Nan Suture. But in this study the location and boundary by magnetic data of anomalies zone is more well-defined. Figure 6.5 show the “Real” location and Boundary of Nan Suture.

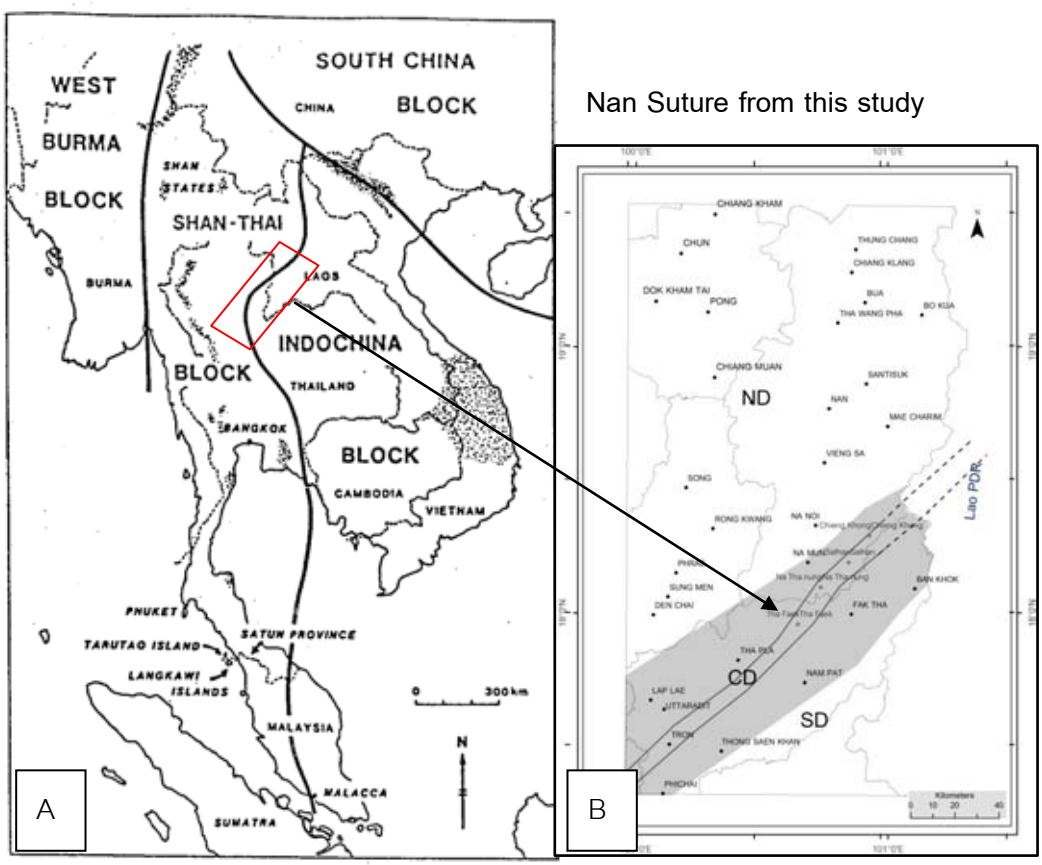

Figure 6.1A- A map of main land SE Asia showing major suture (Bunopas,1981) including Nan Suture (in (A) box) where the study area is located, in comparison with the interpreted Nan suture identified from this study (B)

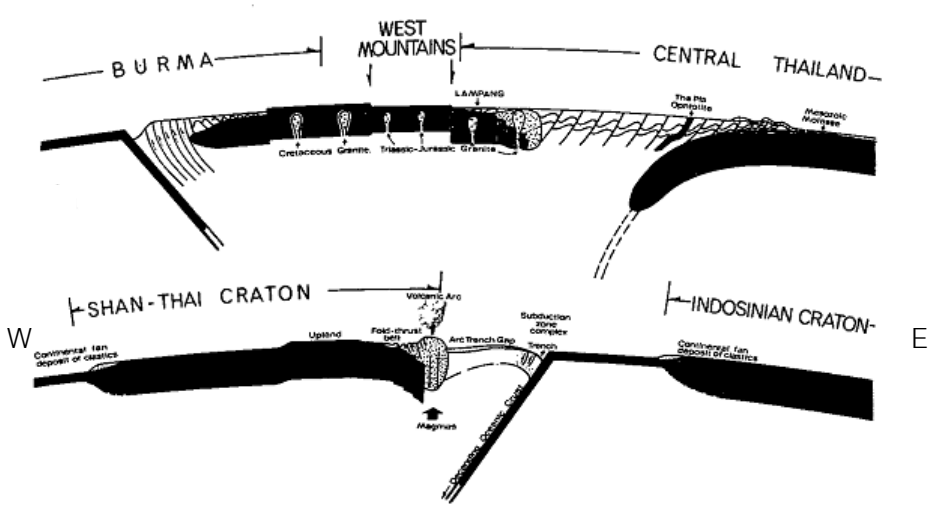

Figure 6.1B- A west-east cross section ofthe plate tectonic models of Northern Thailand (a) Tha Pla ophiolite (ultramafic) marking the approximate position of Nan Suture which result from continent-continent collision in Permo Triassic time. (B) Middle Paleozoic structure with, westward dipping subduction below Shan Thai craton. (Bunopas 1981).

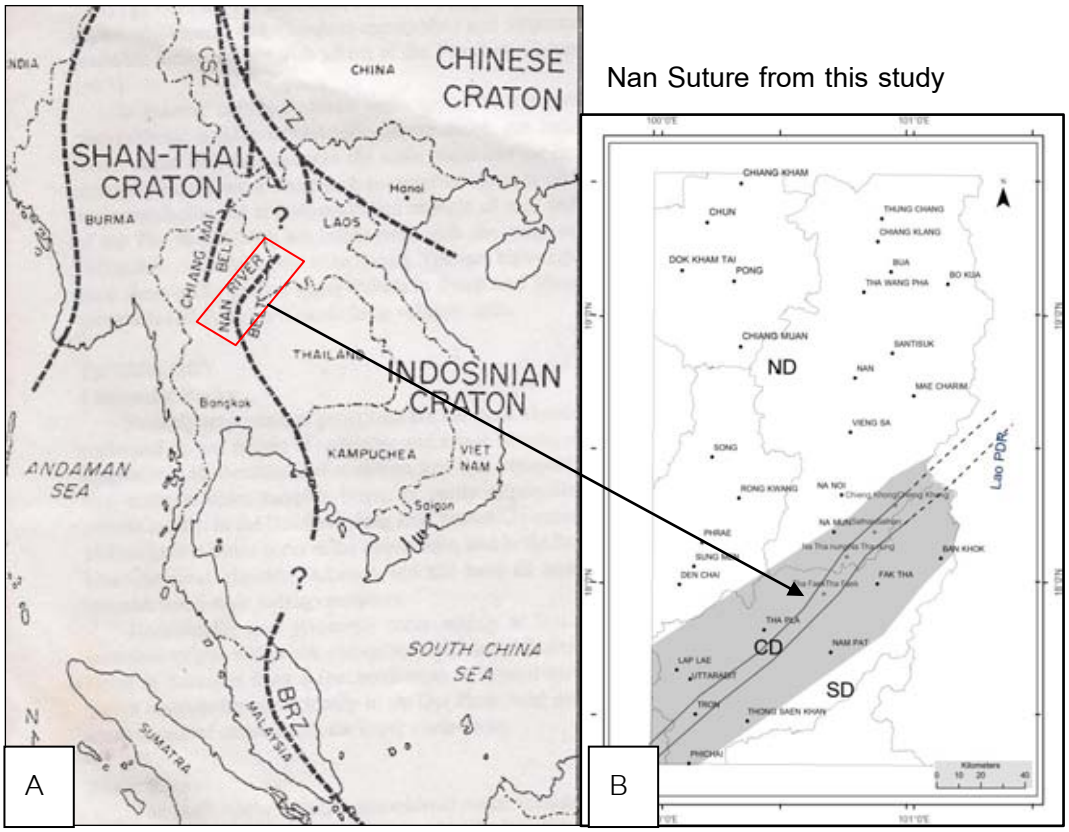

Figure 6.2A- An outline map of Southeast Asia showing location of Nan river belt and major tectonic elements (CSZ = Changning-Shuanging zone, TZ = Tengiaohe zone, BRZ = Bentong Ruab Zone) , (Barr and Macdonald 1987)(in (A) box) where the study area is located, in comparison with the interpreted Nan suture identified from this study (B).

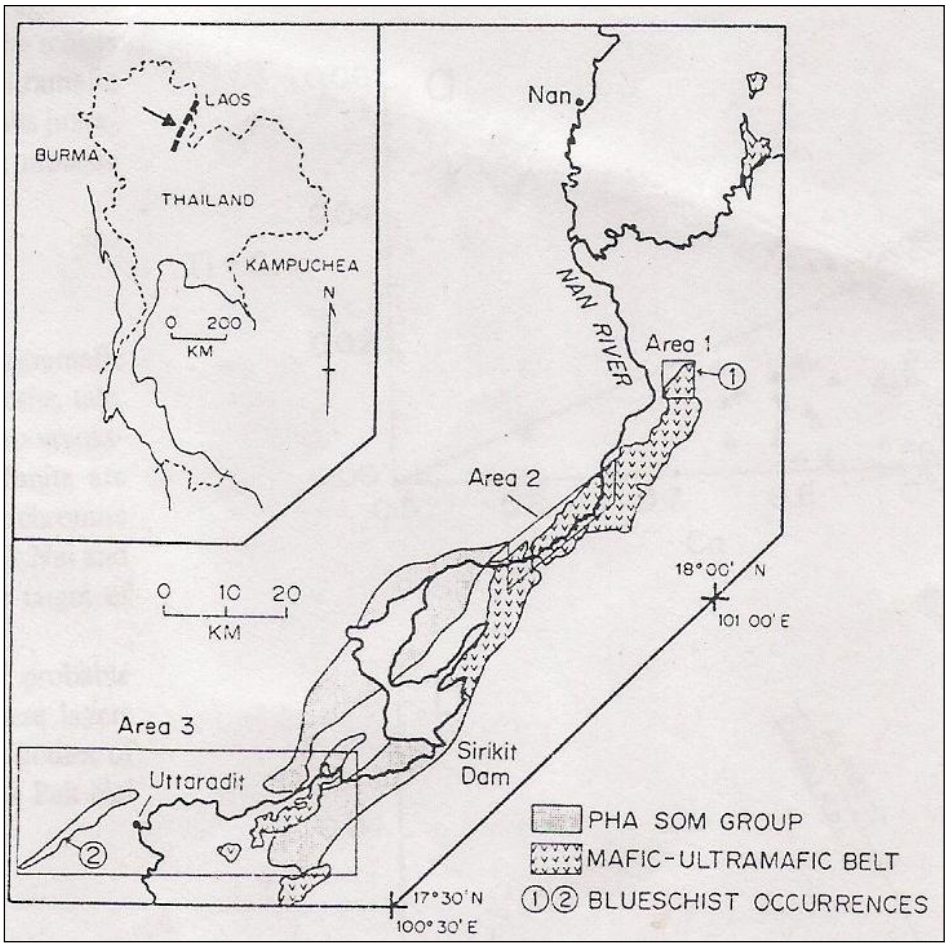

Figure 6.2B- Simplified geologic map of Nan River showing distribution of mafic and ultramafic rocks, Pha Som Group, and known blueschist localities. (Area 1 = Doi Puk Sung ; area 2 = Ban Pak Nai ; Area 3 = Uttaradit) (Barr and Macdonald, 1987)

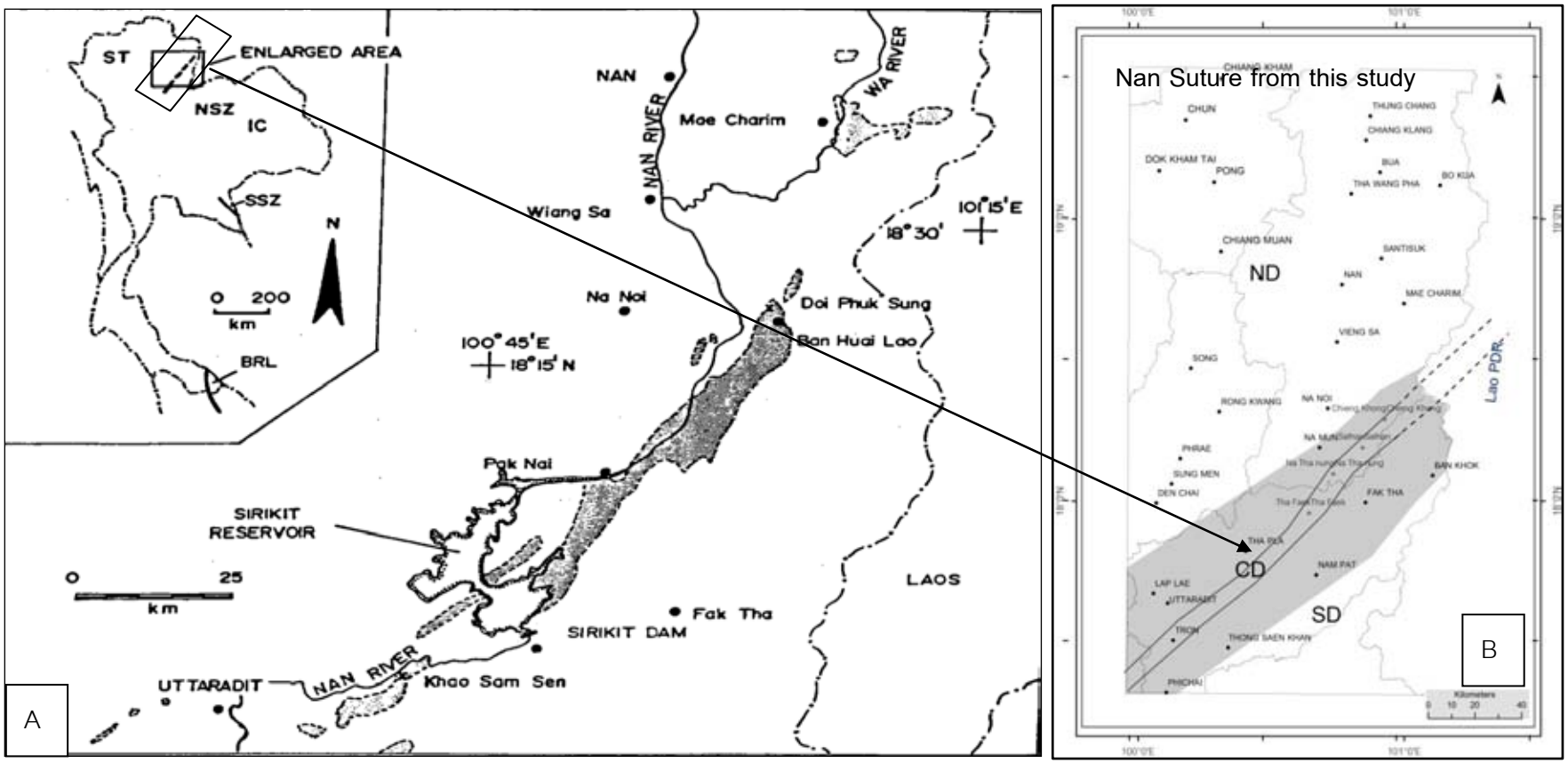

Figure 6.3 Generalized map (A) displaying distribution patterns of mafic-ultramafic igneous rocks along the Nan suture zone as defined by Panjasawatwong (1991) in comparison with (B) Nan Suture zone as defined from this study. (NSZ = Nan Suture Zone, SSZ = Sra Kaew Suture Zone, BRL = Bentong Ruab Line, SC = Shan Thai Craton, IC = Indo China Craton)

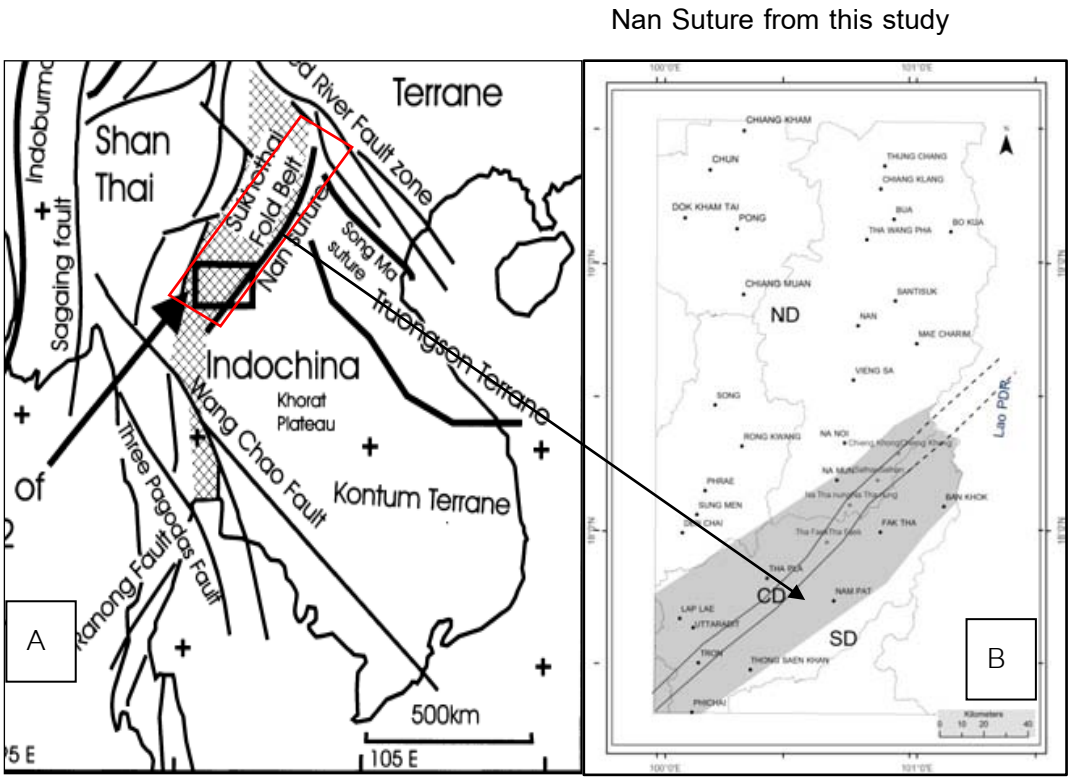

Figure 6.4A Approximate boundary of Nan Suture by Singharajwarapan and Berry (2000) (A) in comparison with the Nan Suture zone determined from this study (B).

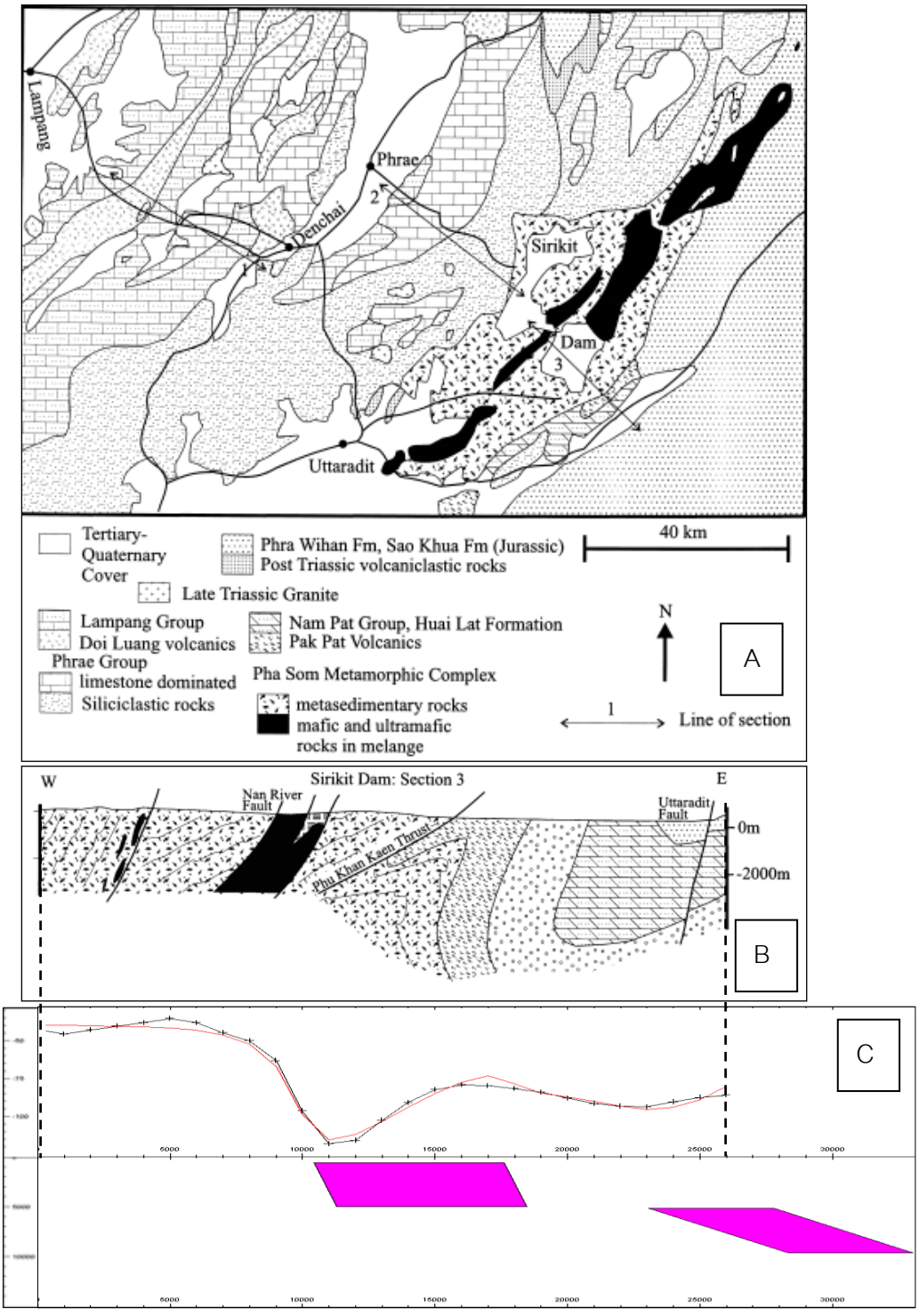

Figure 6.4B Geologic setting of Nan Suture and Sukhothai fold belt (A) and structural section of line 3 (through Sirikit Dam, B), as compiled by Singharajwarapan and Berry, (2000). Noted that the dipping direction of mélange zone is to the west. (C) Geophysical cross- section from this study, on the contrary, show dipping direction to the east.

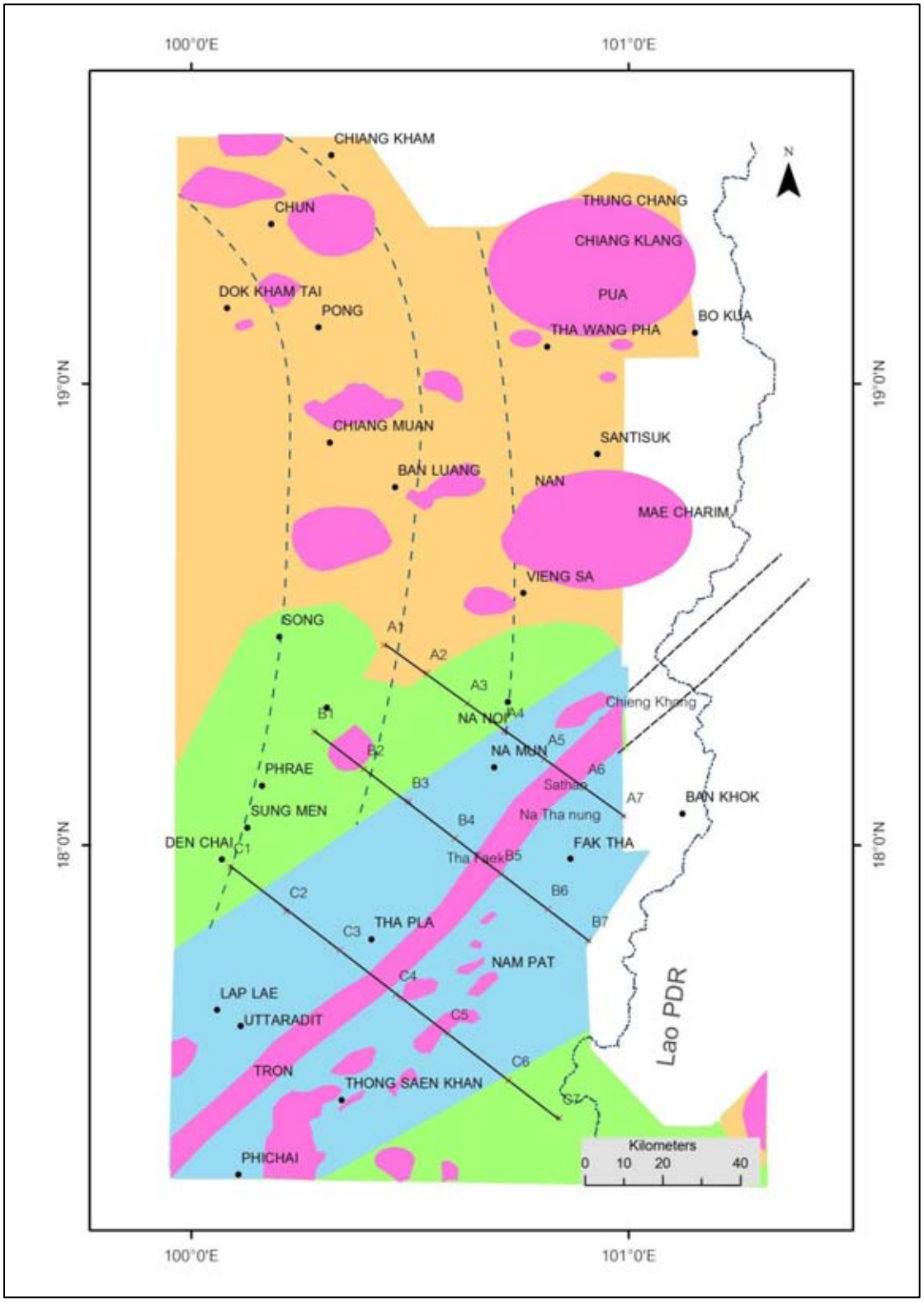

Figure 6.5A- A more-well-defined boundary of the Nan suture (or tectonic line) identified from this study (pink zone). Noted that the more suitable technical term is “the Nan tectonic line”.

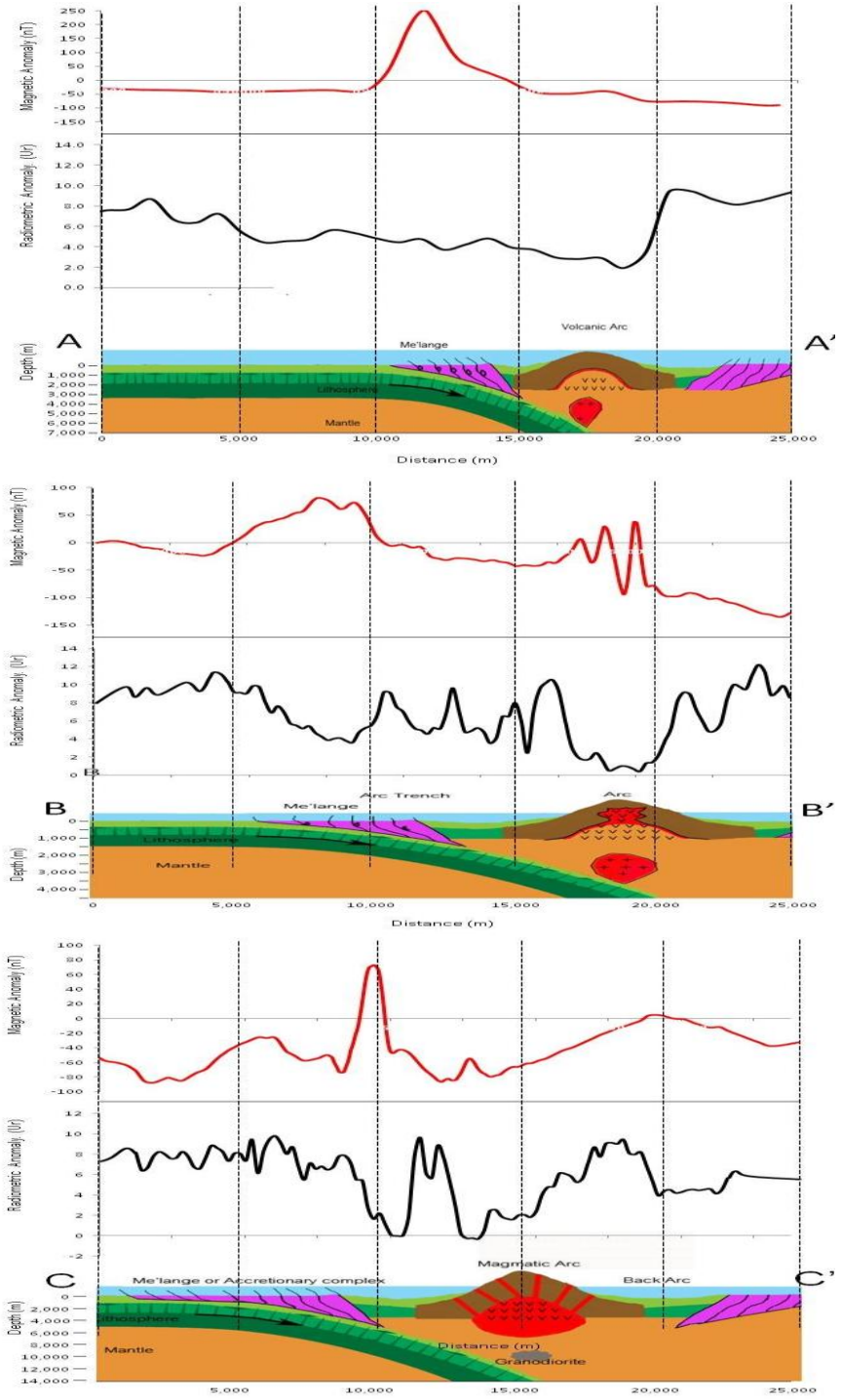

Figure 6.5B Schematic geologic cross section interpreted from the result of geological and geophysical results.

6.2 Geochemical data of igneous rocks and their associated minerals.

6.2.1 Igneous rocks by Panjasawatwong (2000)

Mafic and Ultramafic rocks along the Nan suture zone interpreted by Panjasawatwong (2000) consist of dismembered ophiolite suite occurring in the mélange zone. Fig 6.6 is a geologic map showing distribution patterns of serpentinitic mélange with a mappable gabbroic block. Metavolcanics and post-Triassic basaltic lavas are also shown in his study. It has been shown that the Nan Suture which is a serpentinitic mélange zone, Comprising mafic and ultramafic igneous rocks which are made up in ocean island basalt, back arc basin basalt and andesite, island arc basalt and andesite, island arc basalt/andesite ,supra subduction cumulate and continental intraplate basalts. Those are cumulated and generated during Carboniferous to Permo-Triassic times. The mélange is partly overlain by basaltic lavas of Nan volcanic rocks which erupted in post Triassic.

6.2.2 Chromian Spinel by Lunwongsa (2004)

Lunwongsa (2004) studied petrochemistry of chromian spinels in ultramafic rocks. His result was compared with those of spinel geochemistry of the well known tectonic settings. From his study, two types of tectonic setting are recognized, the first occurring in the suprasubduction zone setting and the second is associated with island-arc setting. suggesting no subsequent metamorphism. Figure 6.7 shows tectonic setting based upon spinel chemistry in Nan-Uttaradit zone as proposed by Lunwongsa, However based on his work, the Nan suture is related to subduction zone with west dipping slab.

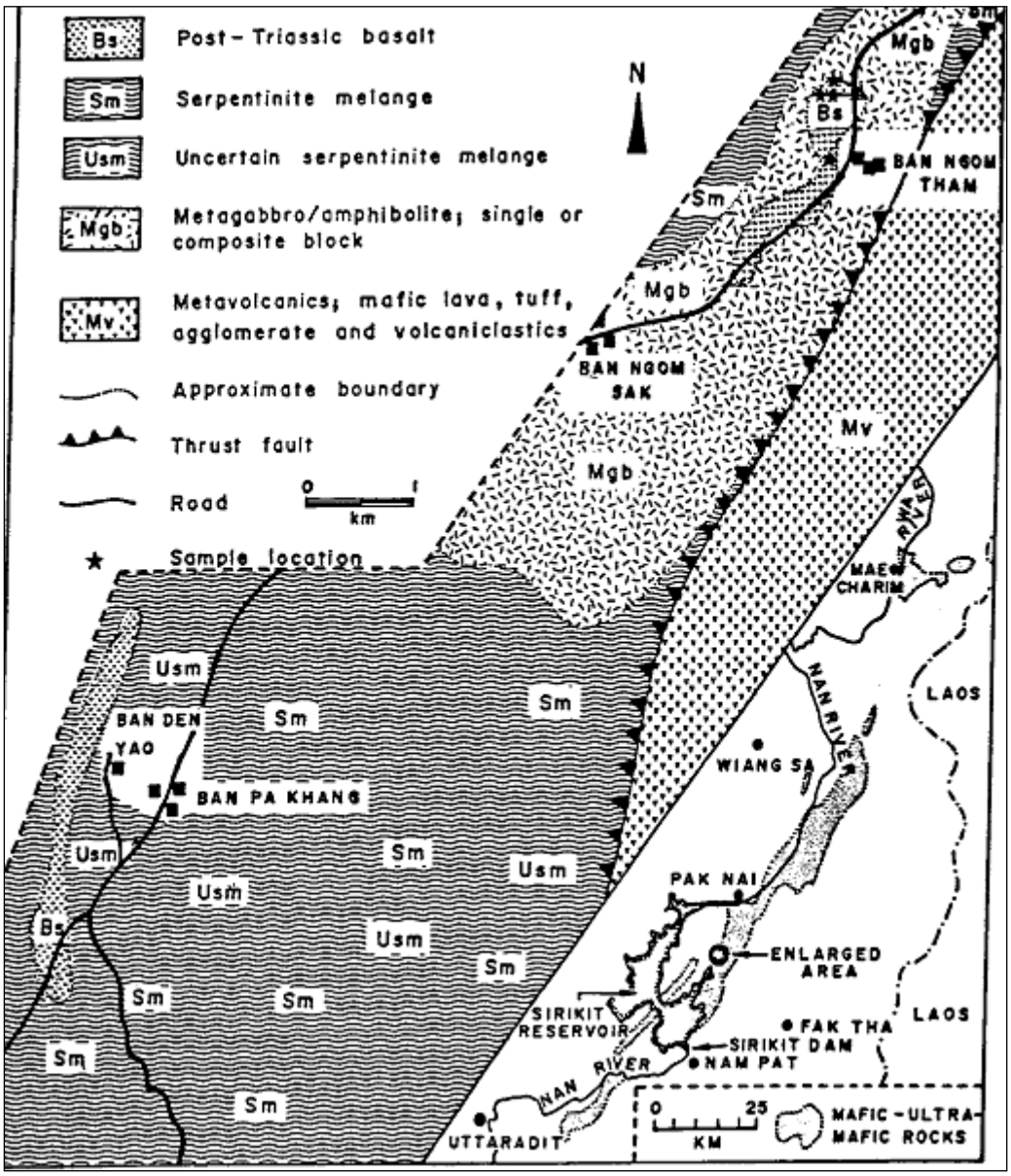

Figure 6.6 Geologic Map of Ban Den Yao-Ban Ngam, in Nan province showing distribution patterns of mélange and the thrust zone serpentinitic mélange (Sm, USm) metagabbro (Mgb) metavolcanic (Mv), and basalt (Bs) (Panjasawatwong,2000).

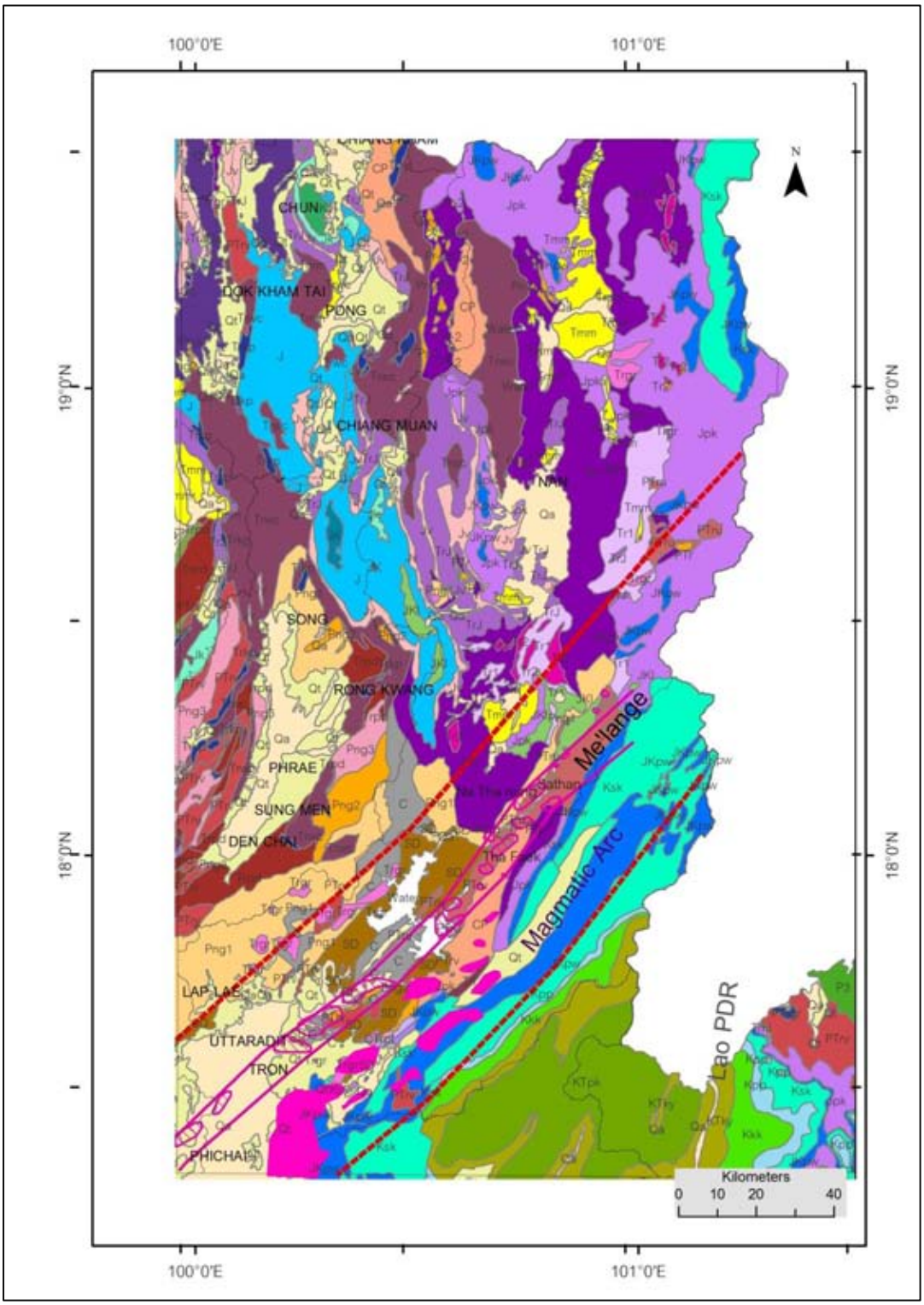

Figure 6.7 Map showing the suture zone and its associated structure band on this study overlain on to the geologic map (DMR, 2007).

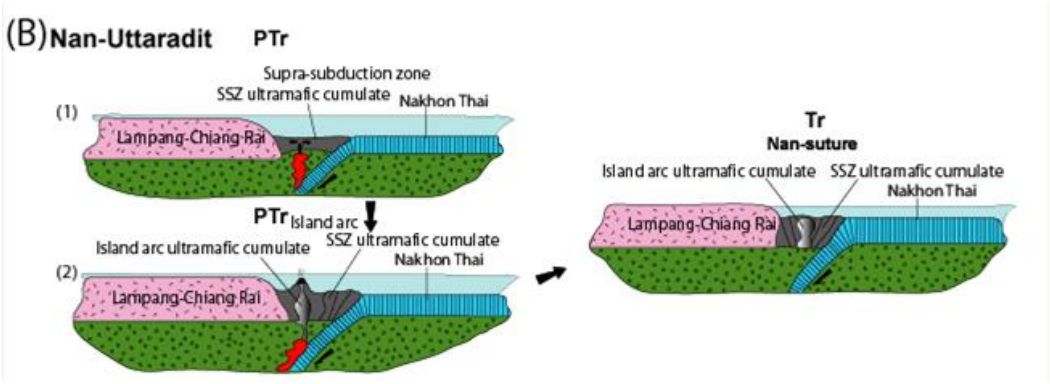

Figure 6.8 Tectonic setting from spinel chemistry in the Nan-Uttaradit zone with the west dipping subduction (Lunwongsa,2004).

6.3 Definition of suture

Based upon the result of this study and the geochemistry of chromian spinel and mafic ultramafic rocks, tectonic setting of the Nan-Uttaradit area in northern Thailand is largely controlled by compression or regarded as collisional tectonics which oceanic-oceanic plate subduction is dominated. However, mélange zone and accretionary complex due to this tectonic setting correspond well with the anomalous EM, high magnetic and low radiometric signatures and is shown as the NE-SW trending central domain.

Such a domain (or mélange zone) is sandwiched between two contrasting geophysical domains in the northern and southern parts, as identified not only by the result of airborne geophysical interpretation but also those of remote-sensing and field investigations. However, the central domain proposed in this study shows opposite polarity of subduction (Figure 6.5) (west dipping) to those earlier reported by Singharajwarapan and Berry (2000) and Lunwongsa (2004). Field evidence as shown in this study (see figure of several outcrops) advocate the possible westward up-thrusting associated with overturned folds occurring in the eastt dipping subduction. However not all thrusting in the accretionary complex is necessarily toward the oceanic trend, as noted by Pluijm (1997), are-verging thrust occur close to the arc in some wedges. As shown in Fig. 6.5 the central domain corresponds well with those recently reported by Department of Mineral Resources (2007). However the present map shows the location

of the zone as a continuous zone (see Fig.6.7) indicating the subsurface continuation of the zone associated with mélange and accretionary complex dominated by high magnetic and low radiometric intensities.

It is also argued that such a suture is better defined as a “tectonic line” recognized by subduction-related (or suprasubduction by Panjasawatwong, 1991) tectonic setting. This tectonic line does not represent the (Shan Thai) continent - (Indochina) continent collision as previously thought (see Bunopas,1981, Mitchell et al,1977). However, if the scenario proposed from this study is correct, then the present tectonic line is caused by ocean -ocean subduction, which fit very well with the tectonic setting proposed as Nakhon Thai overriding plate by subduction underlying Lampang Chiang-Rai oceanic plate during Late Triassic reported by Charusiri et al. (2002)

6.4 Orientation and Polarity of Nan Suture

The airborne geophysical survey result implies that the central domain of high magnetic and low radiometric intensities has been identified clearly. However, if the enhanced RTP and analytical signal maps have been applied, then the central domain can extend extensively southwestward and northeastward. To the south, the possible extrapolation is that this tectonic line appears along the Sukhothai River and is later obscured by the disturbance of the Mae Ping Fault movement. The suture zone of Thailand earlier reported by Tulyatid &Charusiri (1993) can help to define this suture after using the present enhancement process. It is also seen from the interpretation map of the enhanced SRTM Landsat image that lineaments may extend northeastward to western Laos. The high magnetic and low radiometric intensities in the Mae Cha Rim district may be due to the branching of the central domain “a tectonic line” due to the effect of up thrusting similar to the southern part of the central domain.

. 6.5 New Model for Nan Suture

Figure 6.9 From shows a tectonic map of Thailand proposed by Charusiri et al. (2000) and new micro plate between Shan Thai and Indochina plates, namely Nakhon Thai in the east and Lampang Chiangrai plate in the west separated by Nan suture (or

tectonic line) and the associated arc-trend and back-thrust unit.. With this study one a new model of tectonic setting and evolution in Nan Suture is proposed and shown in Figure 6.10

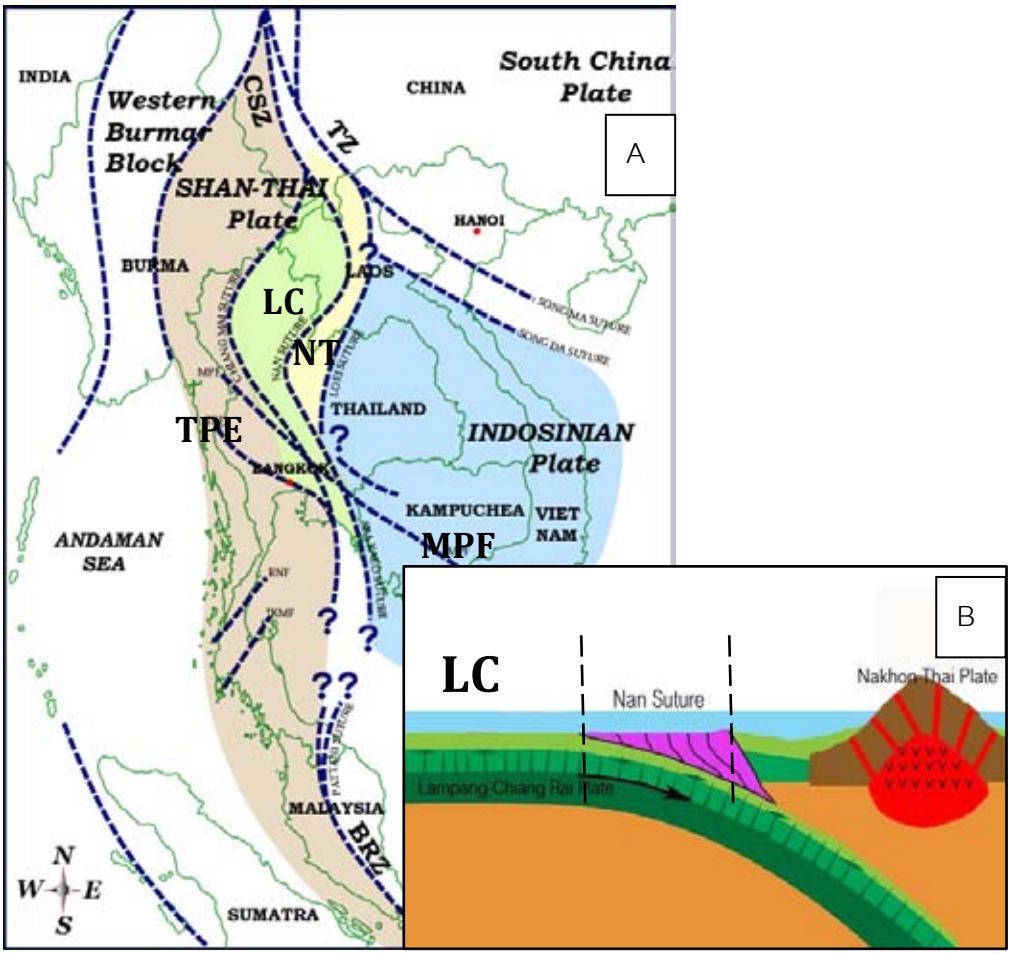

Figure 6.9 Tectonic map of mainland Southeast Asia (modified from Lunwongsa, 2004 and Charusiri et al, 2002) (a) showing new micro plates between Shan Thai and Indochina plates (modified from Charusiri et al.,2002) The inset map (B) shows the tectonic model (cross section) for the Nan Uttaradit area based on the present author's idea. (LC = Lampang Chiang Rai Plate, NT = Nakhon Thai Plate, CSZ = Changning-Shuangjiang Zone , TZ = Tengiaohe Zone, BRZ = Bentong Raub Zone, TPF = Three Pagoda Fault and MPF = Mae Ping Fault.).

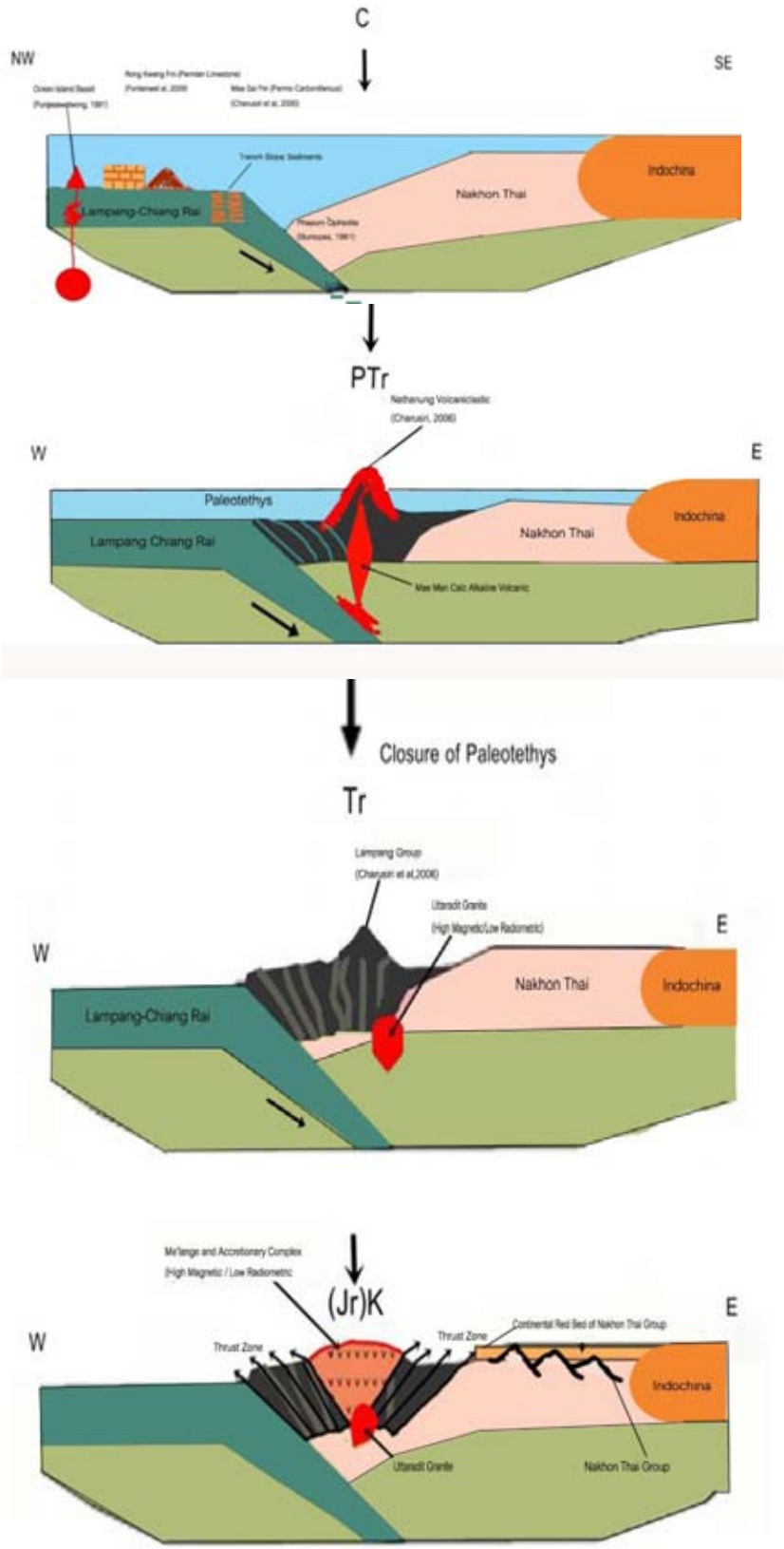

Figure 6.10 New model of tectonic setting in Nan Suture.

Chapter 7
Conclusion and Recommendation

Airborne geophysical interpretation along with remote sensing and field survey data of the Nan-Uttaradit reveal 3 contrasting domains, namely Northern, Central and Southern domains.

The Northern domain is characterized by low magnetic intensities with sporadic high circular anomalies of various size (5 – 50 km radius). The largest anomaly is on the eastern domain in Chiang Klang district and Mae Charim district. They align in the N-S direction.

The central domain consists of 3 sub parallel zones with the high magnetic spots in the inner zone and the other zones are the upper and lower zones, which show weak magnetic and high radiometric intensities. The high magnetic bodies have the average radius of 5.6 km. They align in the NE-SW direction; correspond with the result of remote sensing interpretation. The inner zone of the central domain extends northeastward to Lao and southeastward to Sukhothai area.

The southern domain generally shows low magnetic responds with the N-S trending pattern and few bodies (3-5 km radius) of high magnetic signatures.

Folds and faults have been detected by enhanced remote sensing, field and EM data in the central domain. 3 episodes of fault movements are recognized, they are the NE-SW, NW-SE, N-S and E-W trending faults. Such faulting events can give rise to a change in directional stress ellipsoids from the NW-SE to E-W compressive stress. Compressive stress corresponds well with an eastward subduction of oceanic slap which leads to the generation of the earlier calc-alkaline island arc and the subsequent I-type felsic plutonic rocks.

This research is mainly focused on the result from airborne geophysical and remote sensing interpretation to solve the tectonic settings of the Nan-Uttaradit area. Further work should be placed on the field evidence to verify the real structure which can be validated the geology more clearly.

REFERNCES

Barr, S.M., Macdonald, A.S. 1987. Nan river suture zone, northern Thailand. Geology 15: 907-910.

Brown, G.F., Buravas, S., Charajavanaphet, J., Jalichandra, N., Johnston, W.D., Sresthaputra, V., and Taylor, G.C. 1951. Geological reconnaissance of mineral deposits of Thailand. Bulletin .U.S. Geological Survey 984 (1953): 183.

Bunopas, S. 1981. Paleogeographic history of western Thailand and adjacent part of Southeast Asia-a plate tectonic interpretation. Doctoral dissertation, Victoria University of Wellington, New Zealand. 811pp.

Bunopas, S., and Vella, P. 1983. Tectonic and geologic evolution of Thailand. Workshop On Stratigraphic Correlation of Thailand and Malaysia. 1 (September 8-10) : 307-323.

Chaodumrong, P., Bumroongsong, P. 1994. Stratigraphy of AEM Area, Nan-Uttaradit. Proceedings of The Annual Geologic Conference- Department of Mineral Resources : 117-124.

Charusiri P., Chonglakmani, C., Daorek, V., Supananthi, S., and Imsamut, S. 1994. Detailed Stratigarphy of the Ban Thasi, Lampang, Northern Thailand: Implications for Paleoenvironments and Tectonic History. Proceedings of the International Symposium on Stratigraphic Correlation of Southeast Asia, IGCP 306 (Nov.15-20) : 226-224.

Charusiri, P., Kosuwan, S., and Imsamut, S. 1997. Tectonic Evolution of Thailand: From Bunopas 1981's to a New Scenario. In Dheeradilok, P. et al., editors, Proceedings of the International Conference on Stratigraphy and Tectonic Evolution of SE Asia and the South Pacific-Department of Mineral Resources (Aug.19-24) : 414-420.

Charusiri, P., Imsamut, S., Clark, A.H., Archibald, D. and Hisida, K .1989. Thailand, new suture and new terranes; a new geology synthesis. GEOSEA 9 : 46-47.

Dechawan, S., Surinkhum, A. and Siripongsathian. 1992. Ground Follow Up of Airborne Geophysical Data in Nan-Uttaradit Area. Economic Geological Section, Department of Mineral Resources, Bangkok, 87pp.

Gunn, P.J., Maidment, D., and Milligan, P.R. 1997. Interpreting aeromagnetic data in area of limited outcrop. JGSO Journal of Australian Geology and Geophysics 17 : 115-132.

Hinthong, C., Raksaskulwong, L. and Khositanont, S. 1999. A reconstruction of geology of the Nan area and its vicinities, Northern Thailand. Proceedings of the Symposium on Mineral, Energy, and Water Resources of Thailand: Toward the Year 2000. 178-196. Bangkok

Hutchison, C.S.1989. Geology Evolution of South-East Asia. Oxford, Clarendon Press, 368 pp.

Kuttikun et al., 1988 Preliminary Interpretation of Airborne Geophysical Data In Nan-Uttaradit Area. Economic Geological Section, Department of Mineral Resources, Bangkok, 22pp.

Lunwongsa, W. 2004. Cromian Spinel from Some Ultramafic Igneous Rocks in Northern and Eastern Thailand. Master's Thesis, Department of Geology, Faculty of Science, Chulalongkorn University, Bangkok, Thailand,142pp.

Macleod, I.N., Jones, K., and Ting Fan Dai. 1993. 3-D analytic signal in the interpretation Of total magnetic field data at low magnetic latitude. Exploration Geophysics 24: 679-688.

Metcafe, I., 1995, Gonwana Dispersion and Asian accretion, Proceedings of the IGCP Symposium of Geology of SE Asia, Hanoi, (1995) : 233-266.

Munyou,C., Jongsathaworn, P., Pothisat, S. 1991. Ground Follow up of AEM area, Nan-Uttaradit, Economic Geological Section, Department of Mineral Resources, Bangkok, 125pp.

Neawsuparp, K. 1997. Image processing of Landsat TM and integration with aeromagnetic data for structural interpretation of the Nan suture zone.

Proceedings of a conference on geophysics in prospection for natural resources, engineering and environmental problems, Hat Yai, Thailand, 139-148.

OASIS, 2002. User manual. OASIS Montaj, Toronto, Canada.

Panjasawatwong, Y., 1991, Petrology, Geochemistry and Tectonic Implications of Igneous Rocks in the Nan Suture Thailand and an Empirical Study of the Effects of Ca/Na, Al/Si and H_2O on Plagioclase – Melt Equilibria at 5 – 10 Kb Pressure. Doctoral Dissertation, University of Tasmania, 239 pp.

Panjasawatwong, Y. 1993. Petrochemical study of post-Triassic basalts from the Nan Suture, Northern Thailand. Journal of Southeast Asian Earth Sciences 8: 147-158.

Pintawong, C. 1998. Geology of Mineral Resources in Nan-Uttaradit Area, Geological Research and Development Section, Department of Mineral Resources, Bangkok, 57pp.

Plijm, B.A., and Marshak, S. 1997. Earth Structure, an introduction to structural geology And tectonic. WCB/McGraw-Hill, 495 p.

Salyapongse, S., and Putthapiban, P. 1997. A reconsideration of Nan Suture. Proceedings of the International Conference on Stratigraphy and Tectonic Evolution of Southeast Asia and the South Pacific, 403-411. Bangkok, Thailand.

Sekthera, S., Yaemniyom, .S., Kunawat, P., and Yaemniyom, N. 1978. Regional geochemical survey in Uttaradit, Sheet NE 47-11, scale 1:250,000. Economic Geology Bulletin 24: 1-61.

Singharajwarapan, S. 1993. Structural analysis of the Accretionary complex in Sirikit Dam area, Uttaradit, Northern Thailand. Journal of Southeast Asian Earth Sciences 8: 233-245.

Singharajwarapan, S., Berry, R. 2000. Tectonic implications of the Nan Suture Zone and its relationship to the Sukhothai Fold Belt, Northern Thailand. Journal of Asian Earth Sciences : 18 663–673

Sukvattananunt, P., and Assavapatchara, S. 1987. Geology of map sheets Amphoe Sa and Ban Nam Muap, scale 1:50,000. Annual Report of Geological Survey Division, Department of Mineral Resources : 121-124.

Surinkham, A. 2006. Evaluation of Mineral Deposit Potential in Nan-Uttaradit Suture Zone Using Geophysical Data. Doctoral dissertation, Department of Geology, Faculty of Science, Chiang Mai University, Chiang Mai, Thailand. 251pp.

Surinkum, A. and Siripongsatian, S. 1992. Khao Khee Nok (KKN) AEM anomaly: A gigantic graphite deposit in Thailand. Proceedings of a National Conference on Geologic Resources of Thailand: Potential for Future Development, 407-419. Department of Mineral Resources.

Tulyatid, J., and Charusiri, P., 1999. The Ancient Tethys in Thailand as indicated by the Nationwide Airborne Geophysical Data. Proceedings of an International Symposium: Shallow Tethys(ST) 5 , 335-352. 1- 5 February, Chiang Mai, Thailand.

Tulyatid, J. 1995. Reduction of Nationwide Aeromagnetic Reduction to the Pole, Reduction to the Equator, and Its Derivative Grids of Thailand, Mineral Resources Development Division Repot, No. 3/1995, Department of Mineral Resources, Thailand.

Yensabai, S. 2002. Mineral resources potentials map, scale 1:250,000, sheet (Changwat Nan). Economic Geology Division. Department of Mineral Resources. Geology Division, Department of Mineral Resources, Bangkok, 42pp.

APPENDIX A

Table 1 Parameter of geophysics cross section

Line	Parameter	Body 1	Body 2	Body 3	Body 4
Line A	Susceptibility (SI)	0.063			
	Thickness (m)	2780			
	Dip Angle	112			
	Depth (m)	3499			
	Strike (m)	4726			
Line B	Susceptibility (SI)	0.063			
	Thickness (m)	1171			
	Dip Angle	99			
	Depth (m)	4359			
	Strike (m)	945			
Line C	Susceptibility (SI)	0.063	0.063		
	Thickness (m)	1783	5092		
	Dip Angle	88	76		
	Depth (m)	1328	11231		
	Strike (m)	4477	1086		
Line D	Susceptibility (SI)	0.063	0.063	0.063	0.063
	Thickness (m)	13070	839	1157	2320
	Dip Angle	85	33	59	118
	Depth (m)	4781	1288	2657	3589
	Strike (m)	22000	22000	23000	20000
Line E	Susceptibility (SI)	0.063	0.063	0.063	0.063
	Thickness (m)	5737	31470	2729	2814
	Dip Angle	135	138	76	50
	Depth (m)	10000	11580	13160	1334
	Strike (m)	48000	48000	52000	49920

Line F	Susceptibility (SI)	0.063	0.063	0.063	0.063
	Thickness (m)	1044	3341	3388	16996
	Dip Angle	157	101	45	88
	Depth (m)	5654	12994	5321	13772
	Strike (m)	52000	53000	51000	52801
Line G	Susceptibility (SI)	0.063	0.063		
	Thickness (m)	2442	2508		
	Dip Angle	97	76		
	Depth (m)	10829	4791		
	Strike (m)	20011	19000		
Line H	Susceptibility (SI)	0.063			
	Thickness (m)	11504			
	Dip Angle	103			
	Depth (m)	7640			
	Strike (m)	19000			
Line I	Susceptibility (SI)	0.063	0.063		
	Thickness (m)	5255	3681		
	Dip Angle	98	47		
	Depth (m)	4367	4502		
	Strike (m)	9000	11000		

APPENDIX B

Outcrop of Permian to Triassic

Figure1. Road-cut outcrop of shale with quartz lenses on highway from Ban Pha Sing to Ban Had Pha Khon (looking North) (grid no. UTM 684800E, 2088300N).

Figure 2. Outcrop of Meta-shale with dipping west , interbeded with serpentinite at Ban Lap Muen Phruan. (grid no.UTM 692200E, 2063200N)

Figure3. Outcrop of volcaniclastic rock, weathered with Geyserites and Tuff. At Ban wang Muang (grid no. UTM 685300E, 2063000N)

Figure 4. Outcrop of artificial pond at Ban Thung Setthi showing gravel bed interbeded with sand particle, evidence of terrace deposite. (grid no.UTM 687300E, 2080200N)

Figure 5. Stream sediment of Nan River nearby Nan Hospital, Granule-Cobble with poor sorting, no rounded and found matrix in sand size (grid no.UTM 688700E, 2078300N)

BIOGRAPHY

Name:	Rawiwan Rittisit
Place of birth:	Nakhon Rtchasima
Year of birth:	1982
Education and Degree:	Suranaree University of Technology, Nakhon Ratchasima, Thailand, B.Eng.(Geotech.)
Related work experience:	Geologist, Department of Groundwater Resources